UNIVERSIDADE FEDERAL DE MINAS GERAIS

ESCOLA DE ENGENHARIA

PROGRAMA DE PÓS-GRADUAÇÃO EM

ENGENHARIA DE ESTRUTURAS

RELIABILITY OF SHORT CIRCULAR RC COLUMNS CONFINED BY FRP

JUSCELINA ROSIANE FERREIRA

2017

Ferreira, Juscelina Rosiane.
F383r Reliability of short circular RC columns confined by FRP [manuscrito] / Juscelina Rosiane Ferreira. - 2017.
xvi, 153 f., enc.: il.

Orientadora: Sofia Maria Carrato Diniz.

Tese (doutorado) - Universidade Federal de Minas Gerais, Escola de Engenharia.

Anexos: f. 131-141.

Bibliografia: f. 123-130.

1. Engenharia de estruturas - Teses. 2. Plástico reforçado com fibra - Teses. 3. Colunas - Teses. 4. Confiabilidade (Engenharia) - Teses. I. Diniz, Sofia Maria Carrato. II. Universidade Federal de Minas Gerais. Escola de Engenharia. III. Título.

CDU: 624(043)

UNIVERSIDADE FEDERAL DE MINAS GERAIS
ESCOLA DE ENGENHARIA
PROGRAMA DE PÓS-GRADUAÇÃO EM ENGENHARIA DE ESTRUTURAS

RELIABILITY OF SHORT CIRCULAR RC COLUMNS CONFINED BY FRP

Juscelina Rosiane Ferreira

Tese apresentada ao Programa de Pós-Graduação em Engenharia de Estruturas da Escola de Engenharia da Universidade Federal de Minas Gerais, como parte dos requisitos necessários à obtenção do título de "Doutor em Engenharia de Estruturas".

Comissão Examinadora:

Prof. Dra. Sofia Maria Carrato Diniz (orientadora)
DEES - UFMG -

Prof. Dr. José Márcio Fonseca Calixto
DEES - UFMG -

Prof. Dr. Américo Campos Filho
DECIV- UFRGS

Prof. Dr. André Teófilo Beck
EESC- USP

Prof. Dr. Marcílio da Rocha Souza Freitas
Escola de Minas - UFOP

Belo Horizonte, 05 de Maio de 2017.

AGRADECIMENTOS

À Deus por ter me iluminado, abençoado e conduzido toda minha vida. Por me dar paciência, fé e sabedoria. Por não me deixar desistir. Por permitir a conclusão deste doutorado sem me abater e sem enlouquecer. Obrigada Senhor, por esta vitória.

À profª Drª Sofia, pela orientação, paciência, amizade, otimismo e pela confiança depositada em mim ao longo de todo o curso do doutorado.

À minha família pelo apoio constante, pelo incentivo e pela confiança. Aos meus irmãos, Luis Fernando e Júlio César, pelo cuidado, afeto e compreensão. Aos meus pais, José e Aparecida, pelo imenso amor dedicado a mim. Apesar de todas as dificuldades, sempre valorizaram os meus estudos e nunca mediram esforços para a realização dos meus sonhos. Muitíssimo obrigada, pai e mãe!

Às amigas Alessandra, Eliane e Erica, pela convivência, pela alegria e por me apoiarem em vários momentos importantes da minha vida.

A comunidade Santa Inês, por ter me acolhido tão carinhosamente. Ao Grupo de Oração CRESIN, especialmente ao Álvaro, Geraldo, Jorge, Leone, Luciana, Lucidalva, Marta, Renato, Valda, Vanessa Castro, Vanessa Simão e Welington, pelo carinho, pela fé e pelas orações. Aos amigos David, Eduardo, Milton, Roberto, Ilda, Maria, Silvestre, Lúcia, e Ivana pelas canções, pelas orações e e pelos momentos divertidos que passamos juntos. À Cláudia e às crianças da catequese por tornarem minha vida mais alegre.

À Cleude pelas diversas vezes que recebeu minhas encomendas quando eu estava estudando na UFMG. Por ser muito mais do que uma síndica, mas uma amiga.

Ao Departamento de Engenharia de Estruturas da UFMG, aos professores e funcionários, pela amizade, e pelos ensinamentos transmitidos. A todos colegas da pós-graduação, em especial aos meus amigos Anderson, Anelize, José, Laura, Laura Paes, Rodrigo Sernizon, Samuel, pelo carinho, pelas conversas, pela motivação e torcida na conclusão desta tese.

À CAPES pelo apoio financeiro e à UFMG pela oportunidade e pela estrutura oferecida.

A todos que direta ou indiretamente contribuíram para a concretização deste doutorado. Deus os abençoe!

RESUMO

A utilização de plástico reforçado com fibras (PRF) para reforçar pilares de concreto armado (CA), através do confinamento, tem provado ser uma alternativa viável, especialmente no caso de pilares circulares de pontes. O PRF é um material compósito que apresenta alta resistência à tração, baixo peso específico e alta durabilidade, propriedades importantes para o reforço de estruturas de CA. Apesar dessas vantagens, um grande esforço de pesquisa ainda é necessário para selecionar modelos analíticos que estimem adequadamente a resistência e a deformação última de pilares de CA confinados por PRF. Diferentes modelos com diferentes níveis de conservadorismo têm sido propostos numa tentativa de descrever os efeitos do confinamento. Neste estudo cinco modelos para pilares confinados por PRFC foram avaliados em termos do comportamento tensão-deformação e das condições últimas. Uma vez que a maioria das grandezas envolvidas no projeto de reforço do pilar (propriedades mecânicas, características geométricas, cargas, erro de modelo, etc.) são variáveis aleatórias, a avaliação da resistência e dos níveis de segurança implícitos no projeto do reforço de pilares de CA-PRF deve ser feita através de métodos de confiabilidade estrutural. Nesta pesquisa especial atenção é dada às variáveis aleatórias "erro de modelo" associadas à resistência última e à deformação última do concreto confinado. Um banco de dados experimental abrangendo pilares circulares de CA com aço longitudinal e transversal (estribos ou espirais) confinados por plástico reforçado com fibras de carbono (PRFC) foi compilado a partir da literatura, o que permitiu a obtenção das estatísticas das variáveis aleatórias, "erro do modelo”. Os níveis de confiabilidade implícitos no projeto de reforço segundo a ACI 440.2R (2008), de 144 pilares foram obtidos através da simulação de Monte Carlo. Foi observado que os correspondentes índices de segurança estão em consonância com os valores “objetivo” sugeridos na calibração da norma norte-americana ACI 318.

ABSTRACT

The use of fiber reinforced polymers (FRP) to strengthen reinforced concrete (RC) columns through concrete confinement has proven to be a viable alternative, especially in the case of circular bridge piers. FRP is a composite material that has high tensile strength, low specific weight and high durability, important properties for strengthening RC structures. In spite of these advantages, a large research effort is still necessary to select analytical models to estimate the ultimate stress and strain of RC columns confined by FRP (FRP-RC). Different models with different levels of conservatism have been proposed in an attempt to describe the effects of confinement. In this study five models for FRP-RC columns are evaluated in terms of the stress-strain behavior and ultimate conditions. Since most of the quantities involved in the design of the column strengthening (mechanical properties, geometry, model error, loads, etc.) are random variables, evaluation of the column resistance and implicit safety levels resulting from the assumed design procedures should be performed via structural reliability methods. In this research, special attention is given to the random variables "model error" associated to the ultimate stress and strain of the confined concrete. An experimental database including circular RC columns with longitudinal and transverse steel (stirrups or spirals) confined by carbon fiber reinforced polymers (CFRP) was compiled from the literature, which allowed to obtain the statistics of the random variables “model error”. The reliability levels implicit in the strengthening procedures suggested by ACI 440.2R (2008) were assessed. To this end, the probability of failure (and corresponding reliability indexes) of 144 FRP-RC columns were obtained by Monte Carlo simulation. It was observed that the corresponding reliability levels are in line with the target values suggested in the calibration of the American code ACI 318.

INDEX

List of Figures

List of tables

Notation

ROMAN LETTERS

A^*, B^*, C^*, D^* parameters of stress-strain curve type IIIc;

A_{cc}: area of concrete confined core, excluding the longitudinal steel area;

A_e: area of effectively confined concrete core, according to Mander *et al.* model;

A_f: cross sectional area corresponding to the fibers in the FRP;

A_F: cross sectional area corresponding to the FRP;

A_g: gross area of concrete section;

A_{g_R}: random variable associated to the concrete gross area;

A_m: cross sectional area corresponding to the resin (matrix) in the FRP;

A_{sL}: total area of longitudinal reinforcement;

$A_{s\phi}$: stirrup or spiral steel area;

c: concrete cover;

$c_{\_R}$: random variable associated to the concrete cover;

C_E: environmental reduction factor given by ACI 440.2R (2008);

D: column diameter;

$D_{\_R}$: random variable associate to diameter;

D_c: diameter of the confined concrete core;

D_{c_R}: random variable associated to confined core;

D_n: nominal diameter of the column;

E'_2: tangential slope of the stress-strain curve taken immediately after the initial peak stress f_{c1};

E_1: slope of the first branch of the stress-strain curve of confined concrete;

E_2: slope of the second branch of the stress-strain curve of confined concrete;

E_c: elasticity modulus of concrete;

E_{cc}: parameter of the stress-strain curve proposed by Chastre & Silva (2010);

E_f: elasticity modulus of FRP fibers;

E_F: elasticity modulus of the FRP;

E_m: elastic modulus of the resin (matrix);

E_{s_R}: random variable associated to the Young's modulus of steel;

E_{sL}: elastic modulus of the steel longitudinal reinforcement;

E_{sw}: elastic modulus of the steel transversal reinforcement;

f^*_F: ultimate tensile strength of FRP as reported by the manufacturer;

f'_c: unconfined cylinder compressive strength of concrete; specified concrete compressive strength;

f'_{c_R}: random variable associated to the concrete compressive strength;

f_0: point corresponding to the intersection between the line defined by the second branch and the vertical axis, in the stress-strain curve of confined concrete;

f_c and ε_c: compressive axial stress and corresponding strain in the confined concrete;

f_{c0}: compressive strength of unconfined concrete in the column;

f_{c1} and ε_{c1}: transition point between the first and second branch of the stress-strain curve of confined concrete;

f_{cc} and ε_{cc_A}: ultimate compressive stress of confined concrete and corresponding strain;

f_{cc_A} and ε_{cc_A}.: ultimate conditions adjusted by the corresponding model

f_{cc_up} and ε_{cc_up}: ultimate conditions upgraded by the compatibility strain between confined concrete and longitudinal steel;

f_{cc_R}: Random variable associate to the ultimate confined stress of the concrete;

f_{cm}: required average concrete compressive strength of standard cylinders;

f_{cs} and ε_{cs}: stress and strain corresponding to the start of steel yield according to Lee model;

f_{cu}: ultimate compressive stress of confined concrete;

f_F: tensile strength of FRP;

f_f: tensile strength of the fibers of FRP;

f_{F_R}: random variable associated to the ultimate tensile strength of fibers in the FRP composite;

f_{Fu}: design ultimate tensile strength of FRP, according ACI 440.2R (2008);

f_ℓ: lateral confining pressure provided by the confinement;

$f_{\ell F}$: lateral confining pressure provided by the FRP;

$f_{\ell Fe}$: effective lateral confining pressure due to FRP action;

$f_{\ell s}$: lateral confining pressure due to the action of transversal steel;

$f_{\ell se}$: effective lateral confining pressure due to steel action;

f_m: strength of the resin (matrix);

f_{sL}: stress in the steel longitudinal reinforcement;

f_{sL_R}: random variable associated to the stress in the longitudinal of the steel;

f_{su_R}: random variable associated to the ultimate strength of the steel;

f_{sw}: stress in the steel transversal reinforcement;

F_u: ultimate force resisted by FRP in axial tensile test;

f_y: specified yield strength of the steel longitudinal reinforcement;

f_{y_R}: random variable associated to the yield strength of the steel;

f_{yL}: yield strength of the steel longitudinal reinforcement;

f_{yt} : specified yield strength of the steel transversal reinforcement;

f_{yw}: yield strength of the steel transversal reinforcement;

G^*: gradient vector in the design point

H: height of the column;

I_F: confinement index due to FRP;

I_{Fe}: effective confinement index due to FRP;

I_s: confinement index due to steel;

I_{se}: effective confinement index due to steel;

k_1 and k_2: coefficients related to confinement efficiency;

k_F: effectiveness coefficient of FRP confinement;

k_s: effectiveness coefficient of steel confinement;

n: number of layers of FRP or number of simulations;

N: parameter related to the curvature of the transition between the two branches of the stress-strain curve of confined concrete;

n_L: number of longitudinal bars;

P_F: failure probability;

P_n: nominal axial resistance of the FRP-strengthened concrete member;

P_R: axial resistance of the column;

P_A: acting load in the column

r and x: parameters of stress-strain curve proposed by Mander *et al.* (1988);

R: resistance of structural component;

S: load effect in the structural component;

s': internal vertical spacing of spiral or stirrups (face-to-face);

s: vertical spacing from center-to-center between stirrups or spirals;

t: thickness of each layer of FRP;

T_g: glass-transition temperature;

V_f: volumetric fraction of fibers in the FRP;

V_m: volumetric fraction of resin (matrix) in the FRP;

GREEK LETTERS

α: coefficient in the Chastre and Silva (2010) model that takes into account size effects;

β: reliability index

ε^{*}_{F}: ultimate rupture strain of FRP as reported by the manufacturer;

ε'_c: maximum strain of unconfined concrete corresponding to f'_c; may be taken as 0.002;

ε_{c0}: axial compressive strain of unconfined concrete corresponding to f_{c0};

ε_{cc}: axial compressive strain of confined concrete corresponding to f_{cc};

ε_{cc_R} : Random variable associate to the ultimate confined stress of the concrete;

ε_{cu}: axial compressive strain of confined concrete corresponding to f_{cu};

ε_f: fibers ultimate tensile strain;

ε_F: FRP ultimate tensile strain;

ε_{Fu}: design rupture strain of FRP, according ACI 440.2R (2008) ;

ε_{hF}: FRP hoop strain;

ε_{sh_R}: random variable associated to the strain at the onset of the strain-hardening ;

ε_{su_R}: random variable associated to the ultimate strain of the steel;

ε'_t: transition strain in stress-strain curve of FRP confined concrete;

ε_{yw}: yield strain of the steel transversal reinforcement;

ϕ: strength reduction factor;

ϕ_L: diameter of longitudinal steel bar;

ϕ_w: diameter of transversal steel bar;

μ and σ: mean and standard deviation

ρ_{cc}: volumetric ratio of longitudinal reinforcement relative to the confined core;

ρ_F: volumetric ratio of FRP reinforcement;

ρ_{sL}: volumetric ratio of steel longitudinal reinforcement;

ρ_{sw}: volumetric ratio of steel transversal reinforcement;

ξ_f: model error associated to the ultimate stress;

ξ_ε: model error associated to the ultimate strain;

ψ_f: additional reduction factor;

1

INTRODUCTION

1.1. Initial Considerations

Nowadays, many reinforced concrete (RC) structures require strengthening measures for different reasons such as: design and execution errors, increase in the nominal loads, new design code requirements, changes in the nominal loads as a result of changes in the use of the structure, deterioration, accidents, fire and seismic events, and service-life extension. Jacketing with high-strength concrete, bonding of steel plates, addition of prestressed steel cables and bonding of fiber reinforced polymers (FRP) are examples of strengthening techniques.

FRP are non-corrosive composite materials that present high tensile strength, low specific weight, high durability and electromagnetic neutrality, required features for strengthening of RC structures. FRP also present other advantages compared to conventional materials for strengthening. The high mechanical properties and the low specific weight of FRP allow strength increase without change in the dimensions and weight of the structure. The lightweight also facilitates the transport and application of this material. Furthermore, FRP sheets and fabrics are flexible and continuous, making possible their use in places with difficult access, structures of large dimensions and curved surfaces, as in the case of circular bridge piers. Figure 1.1 illustrates the application of a carbon-FRP (CFRP) fabric on a circular column.

Since 1940, composite materials have found important structural applications in the field of aerospace, marine, rail and automobile engineering. However, the use of FRP in the Civil Engineering construction, -- which includes the strengthening of RC structures--, is more recent, starting in the 80’s, with important researches conducted in Japan, Korea, Canada,

United States and Europe. For instance, a sudden increase in the use of FRP was observed in Japan after the 1995 Hyogoken Nanbu (Kobe) earthquake (ACI 440 2R, 2002).

Figure 1.1 - Application a CFRP fabric in a circular column (http://www.sika.com).

According to Meier & Kaiser (1991), in Europe, the utilization of FRP as an alternative to the use of steel plates in the strengthening of RC structures began to be investigated at the Swiss Federal Laboratories for Materials Testing and Research (EMPA) in 1982. The Kattembusch bridge, in Germany, was the first bridge in the world strengthened in bending with laminates of glass-FRP (GFRP), in 1986.

Juvandes (1999) highlights the three main thrusts related to structural rehabilitation that have fostered the utilization of FRP systems: (i) structures subjected to seismic events (as in Japan and West coast of the USA); (ii) structures subjected to deterioration, in particular caused by steel corrosion; and (iii) preservation and rehabilitation of historical buildings and monuments (as in Europe). In Brazil, according to Machado (2002), the first application of FRP for structural strengthening occurred in 1998 in the Santa Teresa viaduct, in Belo Horizonte.

FRP have been successfully used in the strengthening of RC structural components such as slabs, beams, and columns. Special attention shall be given to the strengthening of columns, due to their importance to the structural integrity, since the failure of a column may cause the

collapse of the whole structure. Strengthening of columns through the confinement of the existing column by FRP has proved to be a viable alternative. When the concrete in the column is subjected to compressive axial load, the lateral pressure exerted by FRP creates a triaxial stress state restraining the lateral expansion of concrete. This results in a potential for increasing column strength, energy absorption capacity and ductility of the column, also preventing buckling of longitudinal reinforcing bars and spalling of concrete cover. This is particularly valid in the case of circular cross-sections and uniform confinement along the column height.

Some countries (Canada, Egypt, Italy, Japan, and USA) have already developed codes and guidelines addressing strengthening of RC structures via column confinement by FRP wrapping (ACI 440.2R, 2008; CNR DT 200, 2004; CSA S806 2002; fib, 2001; ISIS, 2001; JSCE, 2001). In Brazil, some studies on the use of FRP in the confinement of columns have already been performed: Silva (2002), Marques *et al.* (2004), Shehata *et al.* (2002, 2007), Carrazedo & Hanai (2006), Rigazzo & Moreno Jr. (2006). A large body of knowledge has already been accrued with respect to FRP material properties and design of FRP strengthening of RC structures; however, the absence of national documents (codes and guidelines) addressing these topics, --as in the brazilian case--, have impaired the utilization of this material.

The development of national documents dealing with the strengthening of RC structures via FRP is not an easy task. More specifically, in the case of RC columns, most of the variables involved (mechanical properties, geometric characteristics, loads, model error, etc.) are random, thus requiring the tools embodied in the structural reliability methods for the assessment of the implicit safety levels in a given design recommendation. To this end, the probability distributions of all random variables involved in the problem and a deterministic relationship for the computation of the resistance of the strengthened column are required. In the computation of the column resistance, a model to predict the strength of the FRP confined concrete is needed. Several FRP confinement models have been suggested; however, most of them were validated by limited experimental test data, and results of cylinders of plain concrete (Ozbakkaloglu *et al.* 2013). As a consequence, these models do not take into account the influence of longitudinal and transversal steel reinforcement, which commonly occurs in the strengthening of existing RC columns.

1.2. Objectives

From the aforementioned facts, it is clear that the reliability of RC columns strengthened by FRP shall be investigated. As such, the main objective of this research is the assessment of the reliability levels of FRP-confined RC circular columns (FRP-RC), subjected to axial loads, according to ACI 440.2R (2008). It shall be emphasized that in circular columns the confinement efficiency is optimum, since the lateral pressure is continuous and uniform along the circumference of the core. As a consequence, the research presented herein has been restricted to circular columns confined by CFRP. Additionally, this study addresses short axially-loaded columns. This limitation is the result of: (i) FRP confinement is more effective where there is no strain gradient along the cross-section; and (ii) in the cases where there is a strain gradient along the cross-section, this effect should be accounted for in the analysis. On the other hand, paucity of data in the case of eccentrically-loaded FRP-RC columns impairs the development and validation of a general FRP confinement model.

In order to assess the reliability levels of RC columns strengthened by FRP, two main steps are required: (i) selection of the model to predict the behavior of FRP-RC columns and generation of the corresponding statistics of the model error; and (ii) implementation of the reliability analysis procedure for FRP-RC columns.

The first step involves the following specific objectives:

- study of the compressive behavior and stress-strain models for concrete confined by steel stirrups (spirals), FRP, or both;
- compile a database of experimental results corresponding to columns confined by both transversal steel and FRP;
- for each model, generate the statistics of the random variable “model error” related to the ultimate stress and ultimate strain;
- based on the statistics of the model error, select the model to be used in the prediction of the behavior of circular RC columns confined by FRP.

For the second step of this study, relative to reliability analysis of FRP-RC circular columns, the following specific objectives are established:

- select representative FRP-RC columns;

- describe the statistics of the basic random variables (column resistance and acting loads) relevant to the problem;
- implement a deterministic procedure for the simulation of the column resistance;
- implement a Monte Carlo simulation procedure for the generation of the statistics of the column resistance;
- implement a Monte Carlo simulation procedure for the generation of the statistics of the acting loads;
- compute probabilities of failure (and attendant reliability indexes), via Monte Carlo simulation, for each of the 144 columns considered in this research, and assess the adequacy of ACI 440.2R recommendations;
- evaluate the influence of the variables: load ratio, column diameter, concrete compressive strength, longitudinal steel ratio, steel and CFRP confinement ratios on the reliability of FRP-RC columns.

1.3. Scope

This thesis is organized in eight chapters and two annexes. Chapter 2, *Fiber Reinforced Polymer (FRP),* is dedicated to the main properties of interest FRP materials with respect to the strengthening problem. It covers the main definitions, and physical and mechanical properties (specific weight, thermal expansion, stress-strain behavior, tensile strength, etc.).

Chapter 3, *Confined Concrete and Confinement Models*, discusses confinement mechanisms related to concrete confined by steel stirrups (spirals), by FRP, or both (steel and FRP). The stress-strain curves and equations of ultimate stress and strain for each case are also presented. Special attention is given to stress-strain models for concrete confined by FRP and transversal steel. Five representative models (Chastre & Silva, 2010; Pellegrino & Modena, 2010; Lee *et al.*, 2010; Shirmohamadi *et al.*, 2015; and Ilki *et al.*, 2008) addressing the behavior of circular RC columns confined by FRP are discussed.

In Chapter 4, *Performance Assessment of Confinement Models for FRP-RC Columns*, the performance of the five models discussed in Chapter 3 is analyzed with respect to the corresponding stress-strain curve and the prediction of both the ultimate stress and strain. Such predictions are checked against a comprehensive experimental database encompassing

151 CFRP-confined RC columns with longitudinal and transversal steel (spirals or circular hoops). The statitistical description of the random variables "model error" ξ (model uncertainty) relative to prediction of the ultimate stress and the ultimate strain is presented.

Chapter 5, *Structural Reliability*, introduces the basic concepts related to this topic (basic variables, performance function, safety margin, reliability index, probability of failure, FOSM, FORM, and Monte Carlo simulation). It starts with a discussion of the basic reliability problem, followed by the formulation of the first order and second moment method (FOSM), the first order reliability method (FORM), and Monte Carlo simulation.

Chapter 6, *Reliability Bases for FRP-RC Columns*, generates and/or collects the basic information required for the implementation of the reliability assessment of FRP-RC columns. The chapter starts with a brief presentation of both ACI 318-14 (2014) and ACI 440.2R (2008) recommendations for column strengthening, followed by a description of the selected 144 FRP-RC confined columns (48 cross-sections and 3 load ratios). In the sequence, the relevant random variables are identified (column diameter, concrete cover, concrete compressive strength, FRP tensile strength, model errors, mechanical properties of steel, dead and live loads), a summary of the corresponding statistics is presented and a performance function is established.

Chapter 7, *Resistance and Reliability of FRP-RC Columns*, presents the procedures involved in the column resistance simulation and the reliability evaluation of FRP-RC columns via Monte Carlo simulation. The chapter starts with the description of the deterministic procedure for the computation of column resistance, followed by the generation of the statistics of the column resistance. The main features of the program RACOL-FRP, for the simulation of the resistance and reliability analysis of FRP-RC columns, are summarized. The influence of some selected parameters on the resulting safety levels is investigated.

Summary, conclusions and suggestions for future research are presented in Chapter 8.

The work is completed with two annexes. Annex A presents a complete worked example of the reliability analysis procedure adopted in this research, featuring the analysis of column 32 (D2F1L2T1C2). Annex B, displays the source code of the program RACOL-FRP for the resistance simulation and reliability analysis of FRP- RC columns.

2

FIBER REINFORCED POLYMER (FRP)

2.1. Definitions

FRP may be considered as an anisotropic and heterogeneous composite material, obtained from high-strength continuous fibers inserted in a polymer matrix. Composite materials have at least two components or two separate phases: a dispersed phase (reinforcement) and a continuous phase (matrix). These phases have different physical and chemical properties, maintaining its characteristics, i.e., they do not dissolve or merge completely into one another (Strong, 2008). Typically, the fibers and the matrix can be physically identified and they exhibit an interface, as shown in Fig. 2.1.

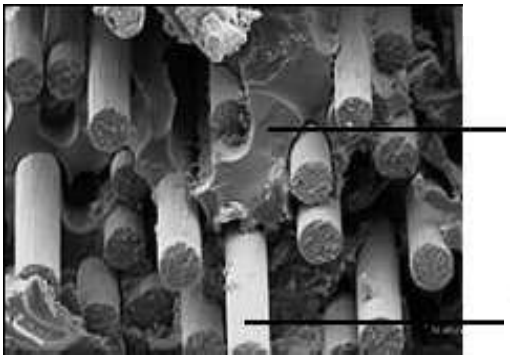

Figure 2.1 - FRP phases: matrix and fibers (Machado, 2002).

Fibers represent 50 to 70% by volume of the FRP material (Jones, 1999). Fibers properties are of great importance in the determination of FRP mechanical characteristics. The major fibers commercialized are carbon, glass and aramid, and the respective reinforced polymers are denoted CFRP (Carbon-FRP), GFRP (Glass- FRP), and AFRP (Aramid- FRP). Compared to glass and aramid, carbon fibers present the best mechanical properties; therefore, CFRP is widely used for structural reinforcement. Glass fibers have the lowest cost; by far the most

widely used grade is E-glass which accounts for almost 95% of total glass fiber production. Aramid fibers are the generic name for aromatic polyamide fibers, a class of synthetic organic fibers (Edwards, 1998).

The matrix shall have excellent durability properties and exhibit a ductile behavior. It shall also ensure the transfer of stresses between the concrete and fibers, keeping them together, and protecting them from damage that may be caused during manufacturing, handling, and along its useful life (Machado, 2002).

According to ACI 440 2R (2008), the externally-bonded FRP systems that are commercially available include:

- Systems of dry unidirectional or multidirectional fiber sheets or fabrics impregnated with a saturating resin on site (wet layup systems). The saturating resin, along with the compatible primer and putty, bonds the FRP sheets to the concrete surface. Wet layup systems are saturated and cured in place and, in this sense, are analogous to cast-in-place concrete;
- FRP systems of partially cured unidirectional or multidirectional fiber sheets or fabrics that are pre-impregnated with a saturating resin in the manufacturer's facility (prepreg systems). These systems are bonded to the concrete surface with or without an additional resin application, depending on specific system requirements. Prepreg systems are saturated off-site and, like wet layup systems, cured in place;
- Systems consisting of a wide variety of composite shapes manufactured off site (precured FRP or laminates). Typically, an adhesive, along with the primer and putty, is used to bond the precured shapes to the concrete surface. The system manufacturer should be consulted for recommended installation procedures. Precured systems are analogous to precast concrete.

Fiber percentage in laminates varies from 65 to 70% of the composite volume. Due to the high fiber concentration, laminates have high rigidity and they cannot be bent. Then, laminates are more suitable for application on plane surfaces, such as in the case RC beams flexural (tensile) reinforcement. Wraps and sheets are flexible and continuous, facilitating the application on curved surfaces, being the most suitable for the confinement of columns (Escobar, 2003).

2.2. Physical and Mechanical Properties

2.2.1. Specific weight

Table 2.1 summarizes information on density of GFRP, CFRP, AFRP and steel. It is noted that FRP presents low specific weights, from 4 to 6 times lesser than steel. The FRP lightweight facilitates the transportation and application of the composite to the column. Moreover, due to its lightweight, the dimensions and weight of the strengthened structure remain practically unchanged.

Table 2.1 - Typical densities of FRP materials (ACI 440 2R, 2008).

Specific weight (g/cm³)			
steel	GFRP	CFRP	AFRP
7,9	1,2 a 2,1	1,5 a 1,6	1,2 a 1,5

2.2.2. Thermal expansion

FRP exhibit different thermal expansion coefficients in each direction. This difference is related to the composition of FRP, where the value of the longitudinal coefficient is defined by the amount of fibers and the transversal coefficient is defined by the matrix. Table 2.2 shows the thermal expansion coefficients for FRP, concrete and steel. The negative value means that the material contracts with the increasing of temperature and the positive value means that the material expands with its decrease. It can be observed that in the longitudinal direction, the GFRP has a thermal expansion coefficient similar to concrete. But, the CFRP and AFRP have lower thermal expansion coefficients than concrete, presenting negative values.

Table 2.2 - Typical coefficients of thermal expansion for FRP materials* (ACI 440.2R, 2008).

Direction	Thermal expansion coefficients ($x10^{-6}$/°C)				
	GFRP	CFRP	AFRP	Concrete	Steel
Longitudinal	6,0 a 10,0	-1,0 a 0,0	-6,0 a -2,0	7,0 a 11,0	11,7
Transversal	19,0 a 23,00	22,0 a 50,0	60,0 a 80,0		

* Typical values for fiber-volume fractions ranging from 0.5 to 0.7

It is interesting to note that, in the case of CFRP and AFRP be used for concrete confinement, when the temperature increases, the concrete expands and FRP contracts, therefore lateral pressure exerted on the FRP jacket is larger, improving the confinement effect. But, when a temperature decreases, the FRP expands and the concrete contracts, having a negative effect on the confinement mechanism. Despite different CFRP and AFRP thermal expansion coefficients from concrete thermal coefficient, for small temperature variations ($\Delta_T = \pm 28°C$), this difference does not affect significantly the bond between concrete and FRP (Juvandes, 1999).

2.2.3. Effect of low temperatures

Two basic effects occur when FRP is exposed to low temperatures: thermal incompatibility and polymer embrittlement. The first causes internal stresses in the fiber-matrix interface and the second increases the strength and stiffness of the polymer, but the failure mode becomes more brittle. The increased stiffness may also reduce the effectiveness of the matrix to transfer stresses between fibers, or between the FRP and the substrate concrete (El-Hacha *et al.* 2010).

Green *et al.* (2006) evaluated the influence of low temperatures on the concrete cylinder strength confined by CFRP. In a first group, with samples kept for 200 days at a temperature of -18 °C and tested at room temperature no strength loss was observed, as compared with samples stored at room temperature. However, in a second group, where samples were maintained at temperatures of -40 °C for 16 days and tested frozen, strength gains of of 14% (on average) were observed. This gain was attributed to freezing of pore water inside the concrete when the cylinders were tested in the frozen state. This effect was not observed in the first set of tests since the cylinders were tested at room temperature.

2.2.4. Effect of high temperatures

The physical and mechanical properties of the resin components of FRP systems are very susceptible to high temperatures. There is a critical temperature named glass-transition temperature T_g that represents the midpoint of the temperature range over which an amorphous material (such as glass or a high polymer) changes from (or to) a brittle, vitreous state to (or from) a plastic state. T_g for FRP systems typically ranges from 60 to 82°C for existing, commercially available FRP systems (ACI 440.2R, 2008).

The decrease of mechanical properties at elevated temperatures is typically governed by the properties of the matrix, since the fibers are much more resistant to thermal effects. In an FRP composite material, the fibers can continue to support some load in the longitudinal direction until the temperature threshold of the fibers is reached. This can occur at temperatures exceeding 1000°C for carbon fibers, and 175°C for aramid fibers. Glass fibers are capable of resisting temperatures in excess of 275 °C. Due to a reduction in force transfer between fibers through bond to the resin, however, the tensile properties of the overall composite are reduced (ACI 220.2R, 2008).

Trapko (2013) performed studies on the influence of high temperatures in the resistance of concrete cylinders (113mm x 300mm) confined by CFRP. Prior to testing, the specimens were exposed for 24h to temperatures 40ºC, 60 ºC, and 80 ºC. Immediately after taking the specimens out of the climatic chamber they were tested until failure. The results demonstrated that the strength drops dramatically with increasing temperature. Load-bearing capacity drops 10% per each 20ºC on average. The cylinders subjected to temperatures of 80°C, had resistance 25% lower than the cylinder kept at 40°C.

Because of the degradation of FRP materials at high temperature, the strength of externally bonded FRP systems is assumed to be lost completely in a fire, unless it can be demonstrated that the FRP temperature remains below its critical temperature (for example, FRP with a fire-protection system). In this way, the structural member without the FRP system should possess sufficient strength to resist all applicable service loads during a fire. The fire endurance of FRP-strengthened concrete members may be improved through the use of certain resins, coatings, insulation systems, or other methods of fire protection (ACI 440.2R, 2008).

Chowdhury (2009) evaluated the response of fire insulation in CFRP confined cylinders. Research showed that despite low resilience of insulation, it is possible to achieve satisfactory load-bearing capacity provided appropriate fire protection is used for reinforced elements. The load bearing capacity of insulated cylinder, after approximately 5h of exposure to fire, was approximately 74% higher compared to uninsulated cylinders. Thickness of insulation deserves special attention, since it is crucial for effective protection of concrete, steel reinforcement and external FRP confinement against high temperature. Chowdhury reports that although the insulation systems used in the research were effective fire protection systems

for the RC columns, the insulation system was not able to maintain the temperature of the FRP system below its glass transition temperature for the entire duration of the fire test. Even though the temperature of the FRP strengthening system exceeded the glass transition temperature during the fire test, the insulated FRP strengthened RC columns were able to resist the applied sustained load under exposure to standard fire for long time (appr. 5h).

2.2.5. Creep and fatigue

Regarding creep, as the ratio of the sustained tensile stress to the short-term strength of the FRP laminate increases, endurance time decreases. The endurance time also decreases under adverse environmental conditions. In general, carbon fibers are the least susceptible to creep rupture; aramid fibers are moderately susceptible, and glass fibers are most susceptible (ACI 220.2R, 2008).

Regarding fatigue, of all types of FRP composites for infrastructure applications, CFRP is the least prone to fatigue failure. An endurance limit of 60 to 70% of the initial static ultimate strength of CFRP is typical. On a plot of stress versus the logarithm of the number of cycles at failure, the downward slope of CFRP is usually about 5% of the initial static ultimate strength per decade of logarithmic life. At one million cycles, the fatigue strength is generally between 60 and 70% of the initial static ultimate strength and is relatively unaffected by the moisture and temperature exposures of concrete structures unless the resin or fiber/resin interface is substantially degraded by the environment (ACI 440 2R, 2008).

In ambient-environment laboratory tests, individual glass fibers demonstrated delayed rupture caused by stress corrosion, which had been induced by the growth of surface flaws in the presence of even minute quantities of moisture. When many glass fibers are embedded into a matrix to form an FRP composite, a cyclic tensile fatigue effect of approximately 10% loss in the initial static strength per decade of logarithmic lifetime is observed. Usually, no clear fatigue limit can be defined. Environmental factors can play an important role in the fatigue behavior of glass fibers due to their susceptibility to moisture, alkaline, and acidic solutions (Mandell & Meier, 1983).

Aramid fibers appear to behave reasonably well in fatigue. Neglecting in this context the rather poor durability of all aramid fibers in compression, the tension-tension fatigue behavior

of an impregnated aramid fiber strand is excellent. Strength degradation per decade of logarithmic lifetime is approximately 5 to 6%. While no distinct endurance limit is known for AFRP, two million-cycle endurance limits of commercial AFRP tendons for concrete applications have been reported in the range of 54 to 73% of the ultimate tensile strength. Based on these findings, Odagiri suggested that the maximum stress be set to 0.54 to 0.73 times the tensile strength. Because the slope of the applied stress versus logarithmic endurance time of AFRP is similar to the slope of the stress versus logarithmic cyclic lifetime data, the individual fibers appear to fail by a strain-limited, creep rupture process. This lifetime-limiting mechanism in commercial AFRP bars is accelerated by exposure to moisture and elevated temperature (Roylance, 1983).

2.2.6. Tensile strength

The tensile behavior of FRP materials is characterized by a linearly elastic stress-strain relationship until failure, which is sudden and can be catastrophic: FRP materials do not exhibit any plastic behavior (yielding), before rupture. Figure 2.2 presents the stress-strain diagram to the FRP with different volumetric fraction of fibers. It can be observed that the increase in the fibers percentage increases the strength and the elastic modulus, but the ultimate strain remains unaffected.

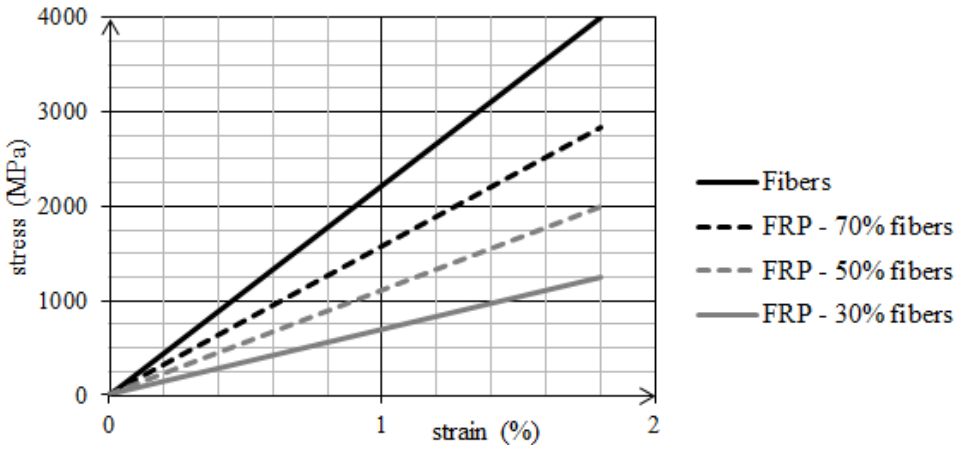

Figure 2.2 - Stress-strain relationship as a function of the volumetric fraction of fibers (CNR DT 200, 2004).

The effect volumetric fraction of matrix and fibers in the mechanical properties of FRP can be evaluated by the relationships known as the *rule of mixtures*. By this rule, the elastic modulus E_F and the strength f_F of FRP can be obtained by Eqs. 2.1 and 2.2, respectively:

$$E_F = E_f V_f + E_m V_m \tag{2.1}$$

$$f_F = f_f V_f + f_m V_m \tag{2.2}$$

where:

E_f and E_m are the elastic modulus of fibers and matrix, respectively;

f_f and f_m are the strength of fibers and matrix, respectively;

V_f and V_m are the volumetric fraction of fibers and matrix, respectively.

The *rule of mixture* is based on the hypothesis of a perfect bond between fibers and matrix; for unidirectional composites it provides accurate assessment of the elastic modulus. The same accuracy cannot be obtained for ultimate strength. For design purposes, it is always preferable to rely upon experimental determination. Table 2.3 presents the effect of fibers volume in the mechanical properties of unidirectional fabric FRP, were A_f, A_m and A_F, are cross sectional area corresponding to the fibers, matrix, and FRP, respectively. In these data, the fibers present f_f = 4000 MPa and E_f = 220 GPa and the matrix present f_m = 80 MPa and E_m = 3 GPa. The properties of FRP, E_F and f_F, were calculated using Eq. 2.1 and Eq. 2.2, respectively.

Table 2.3 - Influence of fiber volumetric fraction on the FRP mechanical properties (CNR DT 200, 2004).

A_f (mm²)	A_m (mm²)	A_F (mm²)	V_f (%)	E_F (GPa)	f_F (MPa)	ε_F (%)	F_u (kN)	$E_F A_F$ (kN)
70	0	70	100	220,0	4000	1,818	280,0	15400
70	30	100	70	154,9	2824	1,823	282,4	15490
70	70	140	50	111,5	2040	1,830	285,6	15610
70	163,3	233,3	30	68,1	1256	1,840	293,0	15890

It can be observed, when the properties are referred to the overall section of the composite (matrix and fibers) both Young modulus and strength at failure decrease as the resin content increases. The same does not apply if one were to look the both ultimate force F_u, and axial stiffness (E_F A_F) whose variations (3-4%) are negligible (CNR DT 200, 2004). This indicates

that the FRP strength is not a good design parameter, because it depends directly of the FRP thickness which can not be obtained with precision after the application of the composite, in the case of confinement columns.

Figure 2.3 presents the stress-strain diagram of various reinforcing fibers and to steel. It can be observed that glass fibers present high ultimate strength, but have elastic modulus smaller than carbon and aramid fibers. Carbon fibers present the highest elastic modulus, even higher than steel.

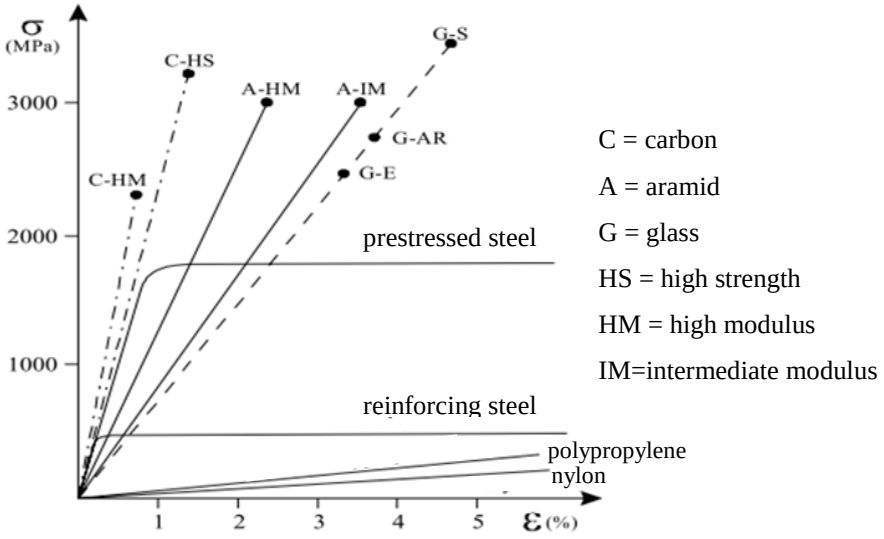

Figure 2.3 - Tensile stress-strain behavior of various reinforcing fibers (ACI 440.R 1996)

3

CONFINED CONCRETE AND CONFINEMENT MODELS

Confinement of RC columns has been seen as an efficient way of improving both column strength and ductility. A large volume of research has been dedicated to columns confined by steel spirals (or ties). In these cases, the occurrence of a non-uniform lateral pressure at the column height and at the cross-sectional level reduces confinement efficiency. On the other hand, confinement of circular cross-sections by FRP wrapping circumvents this problem and a more efficient use of the materials may be attained. In this chapter, concrete confinement mechanisms, concrete confined by steel spirals, concrete confined by FRP jackets, and concrete confined by FRP and steel are reviewed. Special attention is given to stress-strain models for concrete confined by FRP and steel, and five models (Chastre & Silva, 2010; Pellegrino & Modena, 2010; Lee *et al.*, 2010; Shirmohamadi *et al.*, 2015; and Ilki *et al.*, 2008) are discussed.

3.1. Confinement Mechanisms

Plain concrete subjected to longitudinal compression is in a uniaxial state of stress. Longitudinal strains generated by such loading give rise to transverse tensile strains that may result in vertical cracking. As the material approaches its uniaxial compressive capacity, the transverse strains and the vertical cracks reach their limiting values. In the confined concrete, the combination of lateral pressure and axial compression results in a triaxial state of stress. Transverse strains caused by lateral pressure counteract the tendency of material to expand laterally, and result in increased strength (Saatcioglu, 1992).

Confinement may be divided into two types, passive and active. The major difference between both techniques is the lateral confining pressure which is exerted on the section prior to axial loading in the case of active confinement. In the passive confinement technique the

confining pressure is exerted only as a direct result of the lateral dilation of concrete (Shin & Andrawes, 2010). In Fig. 3.1, an FRP-wrapped RC column is used to illustrate both types of confinement. It can be observed that a natural active confinement, induced by the beams and the slab occurs; in the remainder of the column a passive confinement due to the FRP wrapping occurs.

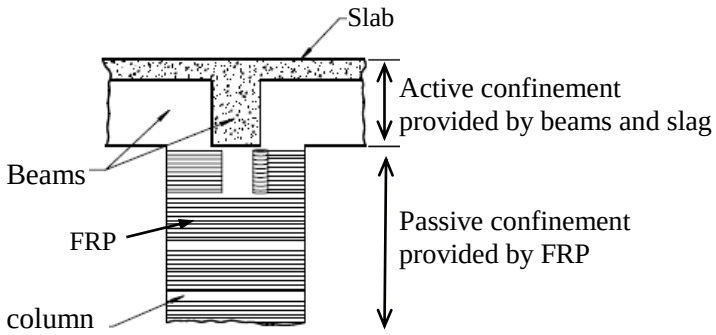

Figure 3.1 - Active confinement in the top column provided by beams and slabs and passive confinement of column provided by FRP (Silva, 2002).

The main factors influencing the behavior of confined concrete are:

- concrete compressive strength: the effect of the confinement in normal-strength concrete is more efficient than in high-strength concrete. This is due to higher lateral dilation presented by normal-strength concrete as compared to high-strength concrete. This higher lateral dilation resulting into a higher lateral pressure on the confined core and, consequently, higher strength gains;
- cross-section geometry: circular cross-sections produce uniform and continuous lateral pressures around the circumference of the core; on the other hand, a non-uniform lateral pressure arises in rectangular cross-sections generating stress concentrations at the corners and low confinement between longitudinal bars. Tie configuration and distribution of longitudinal bars in the cross-section also have an important effect on confinement efficiency
- confining material and geometric properties: strength and elastic modulus, volumetric ratio and spacing of the transverse reinforcement, thickness and number of layers of FRP, etc.

Lateral confinement increases concrete strength and ductility by restraining the dilation of concrete. The positive effect of confinement on the properties of concrete in compression was first studied by Richart *et al.* (1928), on concrete cylinders subjected to lateral fluid pressure; in a later study Richart *et al.* (1929) investigated the effects of confinement provided by steel

spirals on concrete cylinders. In these studies, it was observed that the maximum strength of concrete confined f_{cc} can be assumed as the sum of the unconfined concrete strength f_{c0} and an additional contribution, resulting from the strength gain due to the lateral pressure f_{ℓ}. Several researches have indicated that the compressive strength f_{cc} (peak stress) of confined concrete and the corresponding axial strain ε_{cc} can be expressed by Eqs. 3.1 and 3.2, respectively:

$$f_{cc} = f_{c0} + k_1 f_{\ell} \quad \Rightarrow \frac{f_{cc}}{f_{c0}} = 1 + k_1 \frac{f_{\ell}}{f_{c0}} \tag{3.1}$$

$$\varepsilon_{cc} = \varepsilon_{c0}\left(1 + k_2 \frac{f_{\ell}}{f_{c0}}\right) \quad \Rightarrow \quad \frac{\varepsilon_{cc}}{\varepsilon_{c0}} = 1 + k_2 \frac{f_{\ell}}{f_{c0}} \tag{3.2}$$

where:

f_{c0} and ε_{c0} are axial compressive strength (peak stress) of unconfined concrete and the corresponding axial strain, respectively;

f_{cc} and ε_{cc} are the peak axial compressive stress (peak stress) of confined concrete and the corresponding axial strain, respectively;

f_{ℓ} is the lateral confining pressure provided by the confinement material;

k_1 and k_2 are coefficients of confinement efficiency.

Empirical models for concrete confined by steel (Ilki *et al.* 2004) or FRP (Lam & Teng, 2003), or both (Chastre & Silva, 2010) have been developed based on the above equations with coefficients k_1 and k_2 adjusted by experimental data. As a result, the main problem in dealing with Eqs. 3.1 and 3.2 is the determination of the lateral pressure f_{ℓ} and coefficients k_1 and k_2.

3.2. Concrete Confined by Steel Spirals or Hoops

In the confinement by transversal steel reinforcement (spirals or circular hoops), two distinct regions are noted: the core and the concrete cover. The core is the region effectively confined, defined by the transversal steel. The concrete cover is unconfined and will eventually become ineffective and spall off after the concrete compressive strength is attained, but the core will continue to carry stress at high strains. Furthermore, in the confinement by transversal steel, the lateral pressure increases until the steel yield strength is reached, then the restraining action remains approximately constant.

Figure 3.2 illustrates the pressures acting on the transversal section of a RC circular column confined by circular hoops. The lateral confining pressure provided by steel $f_{\ell s}$ is obtained through the balance of forces, according to Eq. 3.3. This pressure is a function of the pressure f_{sw} in the transversal steel, hoop or spiral area $A_{s\phi}$, diameter of the steel confined core D_c, and vertical spacing s from center-to-center between hoops or spirals. For normal strength concrete columns confined with normal-strength transversal steel, the stress f_{sw} in the steel has been used as the yield strength f_{yw} (Mander *et al.* 1988; Ilki *et al.* 2004).

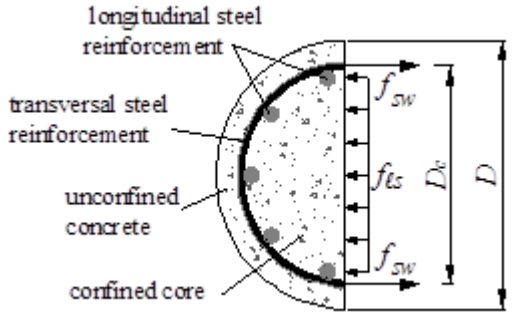

Figure 3.2 - Confined concrete core for circular hoop reinforcement.

$$f_{\ell s} = \frac{2\ A_{s\varphi}}{D_c\ s}\ f_{sw} \tag{3.3}$$

This pressure can also be written as a function of volumetric transversal steel ratio ρ_{sw}:

$$f_{\ell s} = \frac{\rho_{sw}}{2}\ f_{sw} \tag{3.4}$$

where ρ_{sw} is obtained by:

$$\rho_{sw} = \frac{4\ A_{s\varphi}}{D_c\ s} \tag{3.5}$$

The pressure provided by hoops (spirals) $f_{\ell s}$ is not uniform because the stirrups (spirals) do not wrap the whole longitudinal extension of the column. To account for this, most of the models introduces a uniform confinement pressure $f_{\ell se}$ by the effectiveness coefficient k_s, i. e. $f_{\ell se}=k_s f_{\ell s}$.

According to Razvi & Saatcioglu (1992), an important parameter to evaluate the confinement efficiency provided by steel is the confinement index (I_s), measured as the relation between the pressure provided by transverse steel and the concrete cylinder strength f'_c, i. e., $I_s = f_{\ell s}/f'_c$.

However, Cusson & Paultre (1995) propose an effective confinement index (I_{se}), i. e., the relation between effective confinement pressure and the concrete cylinder strength, $I_{se} = f_{\ell se}/f'_c$. These authors classified the efficiency of confinement in three classes according to their effective confinement index: (i) Low confinement: $0 < I_{se} < 0.05$; (2) medium confinement: $0.05 < I_{se} < 0.20$; and (3) high confinement: $I_{se} > 0.20$.

Many studies have been dedicated to the investigation of the confinement effects of transversal steel on concrete columns. To this end a number of models for predicting both the strength and ductility of such columns have been proposed (e.g. Sheikh & Uzumeri, 1982; Mander *et al.*, 1988; Muguruma & Watanabe, 1990; Razvi & Saatcioglu, 1992; Cusson & Paultre, 1995). In what follows, a brief presentation of a representative confinement model is made.

Mander *et al.* (1988) model is based on the active confinement and was calibrated using experimental data on RC columns made with normal-strength concrete. It considers the effectively confined area of the core, i.e. the cross-sectional area excluding arch effects (see Fig. 3.3). An effectiveness coefficient, $k_s = A_e/A_{cc}$, is used, where:

A_e is the area of effectively confined concrete core;
A_{cc} is the area of the core enclosed by the center lines of the perimeter spiral (or hoop), excluding the longitudinal steel area, i.e., $A_{cc} = A_c\left(1-\rho_{cc}\right)$

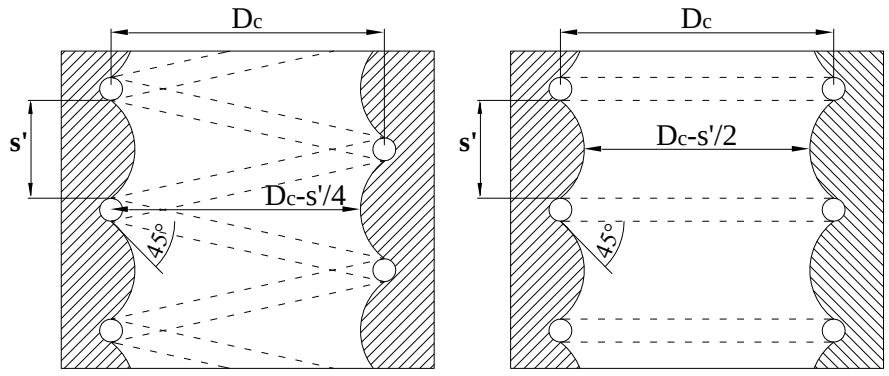

Figure 3.3 - Effectively confined core for spirals and circular hoops reinforcement considering the arching action (Mander *et al.*, 1988).

The steel effectiveness coefficient k_s is given by Eqs. 3.6 and 3.7, for hoops and spirals, respectively:

$$k_s = \frac{\left(1 - \frac{s'}{2D_c}\right)^2}{1 - \rho_{cc}} \tag{3.6}$$

$$k_s = \frac{1 - \frac{s'}{2D_c}}{1 - \rho_{cc}} \tag{3.7}$$

where:

ρ_{cc} is the ratio of longitudinal steel reinforcement area to confined core area;

s' is the internal vertical spacing of spirals or stirrups (see Fig. 3.3);

D_c is the confined diameter (see Fig. 3.3)

The curve proposed by Mander is illustrated in Fig. 3.4 and is based on Eq. 3.8 suggested by Popovics (1973).

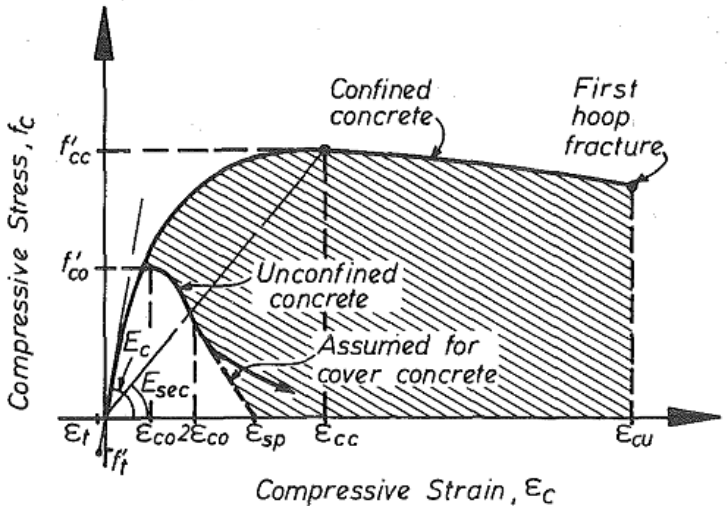

Figure 3.4 - Stress-strain curve proposed for concrete confined by transversal steel proposed by Mander *et al.* (1988).

$$f_c = \frac{f_{cc}\, x.r}{r - 1 + x^r} \tag{3.8}$$

with, $r = \left(\frac{E_c}{E_c - f_{cc}/\varepsilon_{cc}}\right)$ and $x = \varepsilon_c / \varepsilon_{cc}$

where:

f_c is the compressive axial stress in the confined concrete;

ε_c is the compressive axial strain in the confined concrete;

E_c is the tangent modulus of elasticity of the concrete, obtained by:

$$E_c = 5000\sqrt{f_{c0}} \quad (MPa) \tag{3.9}$$

To define the stress-strain behavior of the cover concrete the part of the falling branch in the region where $\varepsilon_{c0} > 2\varepsilon_{c0}$ is assumed to be a straight line which reaches zero stress at the spalling strain, ε_{sp}. To determine the confined concrete compressive strength f_{cc}, a constitutive model involving a specified ultimate strength surface for multiaxial compressive stresses is used. In this way, the confined concrete strength f_{cc} is given by Eq. 3.10:

$$f_{cc} = f_{c0}\left[2{,}25\sqrt{1+7{,}9\frac{f_{\ell se}}{f_{c0}}} - 2\frac{f_{\ell se}}{f_{c0}} - 1{,}254\right] \tag{3.10}$$

The effective lateral confining pressure $f_{\ell se}$ is obtained by Eq. 3.3 multiplied by the coefficient k_s (Eq. 3.6 and Eq. 3.7), and the pressure in the transversal steel reinforcement f_{sw} is adopted as the yield stress f_{yw}. The axial strain ε_{cc} corresponding to the stress f_{cc} can be obtained by:

$$\frac{\varepsilon_{cc}}{\varepsilon_{c0}} = 1 + 5\left(\frac{f_{cc}}{f_{c0}} - 1\right) \tag{3.11}$$

3.3. Concrete Confined by FRP Jackets

3.3.1. General behavior

Confinement action exerted by the FRP on the concrete core is of the passive type, that is, it arises as a result of the lateral expansion of concrete under axial load. As the axial stress increases, the corresponding lateral strain also increases and the confining device develops a tensile hoop stress balanced by a uniform radial pressure, which reacts against the concrete lateral expansion (Benzaid *et al.*, 2010).

The confinement of concrete with FRP jackets can be understood by considering a concrete cylinder wrapped by FRP subjected to axial compression, as shown in Fig. 3.5. After application of the axial force *P*, the FRP restricts the lateral expansion of concrete, developing a lateral pressure f_F which causes a tensile stress f_F in the FRP. The relationship between these pressures can be calculated through the balance of forces in the cylinder section, according:

$$f_{\ell F} = \frac{2nt}{D} f_F \Rightarrow f_{\ell F} = \frac{2nt}{D} E_F \varepsilon_F \tag{3.12}$$

where:

f_F is the tensile stress in the FRP jacket, assumed as the product of the FRP elastic modulus E_F and the ultimate tensile strain ε_F;

n is the number of FRP plies;

t is the thickness of each ply;

D is the cylinder diameter.

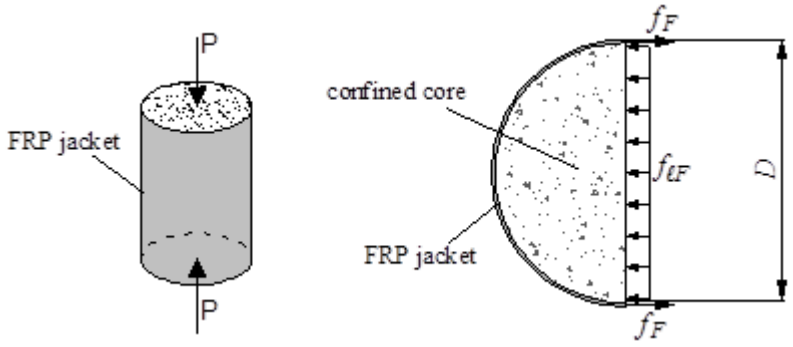

Figure 3.5 - Pressures acting on the cross-section confined by FRP.

The lateral confining pressure $f_{\ell F}$ can also be written as a function of FRP ratio ρ_F:

$$f_{\ell F} = \frac{\rho_F}{2} f_F \tag{3.13}$$

where ρ_F is obtained by:

$$\rho_F = \frac{4.n.t}{D} \tag{3.14}$$

Usually, the confinement models assume that FRP ruptures when the strain in the jacket reaches the FRP ultimate strain ε_F obtained from direct tensile tests. However, experimental

results (Xiao & Wu, 2000; Pessiki *et al.* 2001, Lam & Teng, 2003; De Lorenzis & Tepfers, 2003; Teng & Lam, 2004) show that the ultimate strain measured in the FRP jacket at the time of rupture (the hoop strain ε_{hF}) is lower than the ultimate strain, ε_F. According to Lignola *et al*. (2008), De Lorenzis & Tepfers (2003) and Lam & Teng (2003), the possible reasons for this phenomenon are:

- radius of curvature in FRP jackets on cylinders as opposed to flat tensile coupon;
- presence of voids, protrusions and misalignments of fibers in the FRP;
- non-homogeneous deformations in the FRP jacket due to local stress concentrations in the jacket resulting from internal concrete cracks and the change in geometry in the overlap region of the jacket;
- residual strains or uneven tension during FRP lay-up;
- multiaxial stress state in the FRP: The transfer of axial load through bond with concrete and the radius of curvature in FRP jackets on cylinders leads to multiaxial stress state in the FRP.

Pessiki *et al.* (2001) established a strain efficiency factor k_F that relates the hoop strain ε_{hF} with the FRP ultimate strain ε_F; in this way, the effective lateral confining pressure $f_{\ell Fe}$ is given by $k_F\ f_{\ell F}$. Similarly to confinement by transversal steel, the efficiency of confinement due to FRP can be measured by the confinement index (I_F) obtained by the relation between the pressure provided by the FRP and the strength of unconfined concrete, i. e., $I_F = f_{\ell F}/f'_c$. However, according to Lam & Teng (2003), the confinement efficiency is better evaluated by the effective confinement index (I_{Fe}), considering the relation between effective confinement pressure and the strength of unconfined concrete, i. e., $I_{Fe} = f_{\ell Fe}/f'_c$.

In contrast to steel, the stress-strain curve of FRP composites remains linear-elastic until the final brittle rupture. In this way, the stress-strain curve of FRP-confined concrete features a monotonically ascending bilinear shape. However for low confinement ratios, a post-peak descending branch can be observed, i.e., the specimen is said to be insufficiently confined.

3.3.2. Confinement models

Ozbakkaloglu *et al.* (2013) conducted an extensive review of existing models for concrete confined by FRP for circular sections. Most of these models consist of closed form equations

that were developed through regression analyses and were calibrated from axial compression test results of FRP-confined concrete. Therefore, the accuracy of these models depends greatly on the size and reliability of the test database as well as the parametric range of the test data used in the model development.

3.3.2.1. Stress-strain curve

The stress-strain curve for concrete confined by FRP can be classified into three categories based on their geometries:

Type I curves (parabolic curves): In early studies of FRP-confinement, the models developed for actively confined or steel confined concrete were applied to describe the stress-strain behavior of FRP confined concrete. Hence, the stress-strain curves given by these models feature parabolic curves similar to that of steel or actively confined concrete (Fig. 3.6). As to be expected, these models do not accurately capture the typical bilinear shape of the stress-strain curves of FRP-confined concrete.

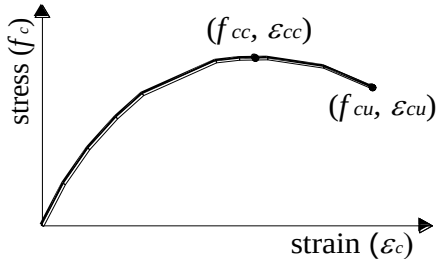

Figure 3.6 - Curve type I: Parabolic stress-strain curve for concrete confined by FRP (Ozbakkaloglu *et al.*, 2013).

Type II curves: Bilinear stress-strain curves appeared more frequently in the subsequent studies on FRP-confined concrete. These early studies recognized that FRP confined concrete developed significantly different stress-strain response than steel or actively confined concrete. Behavior of FRP-confined concrete was simply represented by a bilinear curve defined by a transition point (f_{c1}, ε_{c1}) near the location of the unconfined concrete peak stress and a final point (f_{cu}, ε_{cu}) at the ultimate condition, that coincides with the maximum stress and strain (f_{cc}, ε_{cc}) as shown in Fig. 3.7.

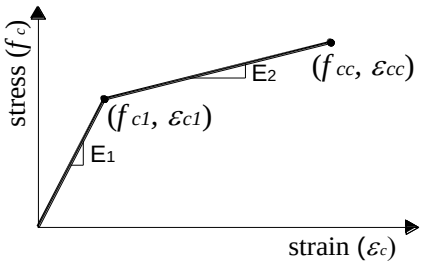

Figure 3.7 - Curve type II: Bilinear stress-strain curve for concrete confined by FRP (Ozbakkaloglu *et al.*, 2013).

Type III curves. In most of the later studies, the stress-strain curves of FRP-confined concrete were further improved by more accurate modeling of the initial ascending portion. These models described the initial ascending region as a parabola, which was followed by a second region that was approximately linear. As noted previously, several different approaches have been used to establish the Type III stress–strain curves, which are further classified herein as Types IIIa, IIIb and IIIc curves.

In the curve Type IIIa, illustrated in Fig. 3.8 and defined by Eq. 3.15, the Hognestad's parabola has been used to model the initial ascending portion. The second branch was obtained by connecting the initial peak with the ultimate condition (f_{cu}, ε_{cu}) or (f_{cc}, ε_{cc}) through a straight line. The parameter E_2 corresponds to the slope of the second branch.

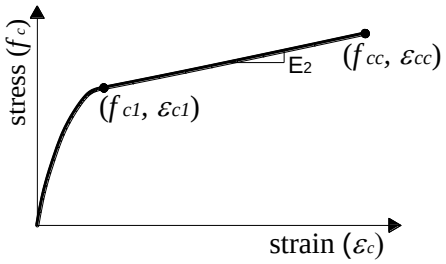

Figure 3.8 - Curve type IIIa: stress-strain curve for concrete confined by FRP with first branch described by the Hognestad's parabola (Ozbakkaloglu *et al.*, 2013).

$$
\begin{aligned}
f_c &= f_{c1}\left[\frac{2.\varepsilon_c}{\varepsilon_{c1}} - \left(\frac{\varepsilon_c}{\varepsilon_{c1}}\right)^2\right]; \text{ for } \varepsilon_c < \varepsilon_{c1} \quad (\text{a}) \\
f_c &= f_{c1} + E_2\left(\varepsilon_c - \varepsilon_{c1}\right); \text{ for } \varepsilon_c \geq \varepsilon_{c1} \quad (\text{b}) \\
E_2 &= \frac{f_{cc} - f_{c1}}{\varepsilon_{cc} - \varepsilon_{c1}} \quad (\text{c})
\end{aligned}
\tag{3.15}
$$

The four parameter (E_1, E_2, f_0 and N) curve proposed by Richard and Abbott (1975), defined by Eq. 3.16, was adopted to describe the first branch of stress-strain curves of type IIIb (Fig. 3.9). In these curves, a polynomial constant N was used to fit a smooth transition curve between the two segments. The slope of the first branch E_1 is the elasticity modulus of the plain concrete E_c, and most of the models adopt the Eq. 3.17 recommended by ACI 318 to calculate its value. The prolongation of the second branch of the curve intersects the axis of axial tension, the value f_0.

$$f_c = \frac{(E_1 - E_2)\varepsilon_c}{\left[1 + \left(\frac{(E_1 - E_2)\varepsilon_c}{f_0}\right)^n\right]^{1/n}} + E_2\,\varepsilon_c \leq f_{cc}$$
$$f_0 = f_{cc} - E_2\,\varepsilon_{cu} \qquad (3.16)$$
$$N = 1 + \frac{1}{(E_1/E_2) - 1}$$

$$E_c = 4730\sqrt{f_{c0}} \qquad (3.17)$$

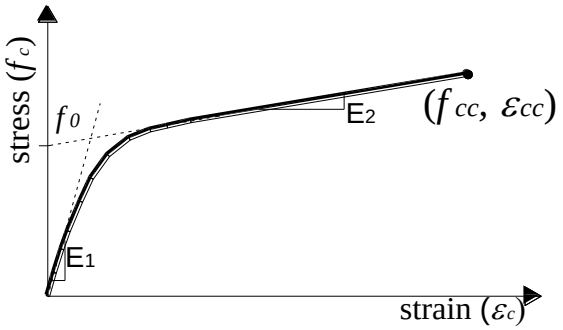

Figure 3.9 - Curve type IIIb: stress-strain curve for concrete confined by FRP with first branch described by the Richart and Abbott equation (Ozbakkaloglu *et al.*, 2013).

Type IIIc curves: Based on the general expression developed by Sargin (1971) and Toutanji (1999) according to Eq. 3.1. These models used the slopes of the initial ascending branch E_1 and the post-peak second branch E'_2 to describe the stress-strain curve. It should be noted that in these models the slope of the second branch E'_2 refers to the tangential slope of the stress-strain curve taken immediately after the initial peak stress f_{c1} is reached (Fig. 3.10). Hognestad's parabola is a specific case of Eq. 3.18 with the parameters A^* and B^* taking values 2 and 0, respectively.

$$\frac{f_c}{f_{c0}} = \frac{\frac{A^*.\varepsilon_c}{\varepsilon_{c0}} + \left(B^* - 1\right).\left(\frac{\varepsilon_c}{\varepsilon_{c0}}\right)^2}{1 + \left(A^* - 2\right)\frac{\varepsilon_c}{\varepsilon_{c0}} + B^*.\left(\frac{\varepsilon_c}{\varepsilon_{c0}}\right)^2} \quad \text{(a)}$$

$$f_c = \frac{E_1.\varepsilon_c}{1 + C^*.\varepsilon_c + D^*.\varepsilon_c^2} \quad \text{(b)} \qquad (3.18)$$

$$C^* = \frac{E_1}{f_{c1}} - \frac{2}{\varepsilon_{c1}} + \frac{E_1.E_2^{'}}{f_{c1}}; \quad D^* = \frac{1}{(\varepsilon_c)^2} - \frac{E_1.E_2^{'}}{f_{c1}} \quad \text{(c)}$$

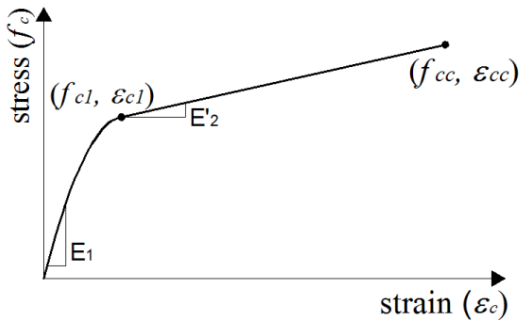

Figure 3.10 - Curve type IIIc: stress-strain curve for concrete confined by FRP with first branch described by the Sargin (1971) equation (Ozbakkaloglu *et al.*, 2013).

In some models, the behavior of FRP-confined concrete at the initial ascending portion of the stress-strain relationship was assumed to be similar to that of unconfined concrete. In this case, the confinement provided by the FRP was insignificant along the initial branch, because the lateral strain of confined concrete and the resulting lateral confinement pressure were low during that stage. Consequently, initial axial strength and strain enhancement were considered negligible by these models. However, other models consider the strengthening effect of FRP confinement on the initial ascending portion of the stress-strain curve.

3.3.2.2. Ultimate conditions

The majority of the models reviewed by Ozbakkaloglu *et al.* (2013) were based on the general format of the expressions proposed by Richart *et al.* (Eq. 3.1 and Eq. 3.2). The adequacy of the proposed models was checked against an experimental database compiled from the literature by Ozbakkaloglu *et al.* (2013). All specimens in the database are FRP-confined concrete cylinders tested under monotonic axial compression, confined by continuous FRP jackets, with fibers oriented in the hoop direction and an aspect ratio H/D (height/diameter) less than 3. This resulted in a final database of 730 datasets collected from 92 experimental studies: 422 of the specimens were confined by CFRP, 52 by HM-CFRP (high- modulus), 198

by GFRP, and 58 by AFRP. The diameters of the specimens *D* varied between 47 and 600 mm, the height *H* varied between 100 and 1200 mm, and the unconfined concrete strength f_{c0} (obtained from concrete cylinder tests) varied from 6.2 to 55.2 MPa.

Ozbakkaloglu *et al.* (2013) observed that models calibrated from relatively small test databases of FRP-confined concrete (e. g. Miyauchi *et al.*, 1997; Toutanji, 1999) and those that were based on active/steel-confined concrete (Saadatmanesh *et al.*, 1994; Fardis & Khalili, 1982; Li *et al.*, 2003) performed relatively poorly in comparison to the rest of the assessed models. The best models were determined among those that were applicable to the complete dataset. The model prediction errors associated with the prediction of ultimate axial strains are significantly larger than those of ultimate stresses. The top performing strength enhancement models were found to be those proposed by Lam & Teng (2003), Bisby *et al.* (2005) and Teng *et al.* (2007). The best performing strain enhancement models were those proposed by Tamuzs *et al.* (2006), Jiang & Teng (2006) and Teng *et al.* (2009).

3.4. Concrete Confined by Steel and FRP

As illustrated in Fig. 3.11, in the strengthening of existing RC columns, the concrete core is simultaneously confined by FRP and transverse steel reinforcement. However, few researchers have developed models for the estimation of the lateral confining pressure f_l, considering contributions of both the FRP and the transverse steel.

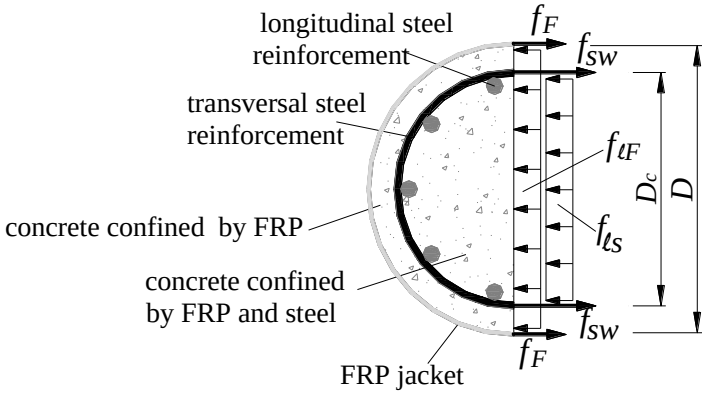

Figure 3.11 - Forces acting on the cross-section of a RC column confined by steel and FRP.

In the research presented herein, five representative models addressing RC columns confined by steel and FRP will be evaluated: Chastre & Silva (2010), Pellegrino & Modena (2010),

Lee *et al.* (2010), Shirmohamadi *et al.* (2015) and Ilki *et al.* (2008). These models are discussed in the following sections.

3.4.1. Chastre & Silva model

Chastre & Silva model (C&S) has been developed specifically for RC columns confined by CFRP. In this model, the proposed stress-strain curve (f_c - ε_c) is based on a four-parameter (E_1, E_2, f_0 and N) curve whose general form is given by Eq. 3.19:

$$f_c = \frac{(E_1 - E_2)\,\varepsilon_c}{\left[1+\left(\frac{(E_1 - E_2)\,\varepsilon_c}{f_0}\right)^N\right]^{1/N}} + E_2\,\varepsilon_c \le f_{cc} \tag{3.19}$$

where:

E_1 is the slope of the first branch of the curve and represents the elastic modulus of the unconfined concrete, $E_1 = 3950\sqrt{f_{c0}}$ (f_{c0} in MPa);

E_2 is the slope of the second branch of the curve, $E_2 = 0.8\,E_{cc}\sqrt{\frac{f_{\ell s} + k_F\,f_{\ell F}}{f_{c0}}}$ (where $E_{cc} = f_{cc}/\varepsilon_{cc}$);

f_0 is the point corresponding to the intersection between the line defined by the second branch and the vertical axis, $f_0 = f_{c0} + 1.28\,(f_{\ell s} + k_F\ f_{\ell F})$;

N is the parameter related to the curvature of the transition between the two branches, $N = 2$.

The four parameters (E_1, E_2, f_0 and N) were calibrated by experimental results; the corresponding stress-strain model is illustrated in Fig. 3.12.

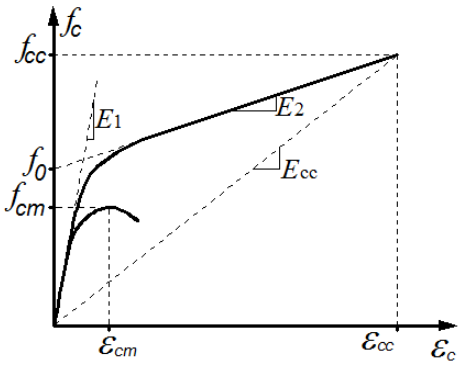

Figure 3.12 - Four-parameter stress-strain curve proposed by Chastre & Silva for concrete confined by steel and FRP.

The ultimate conditions of Chastre & Silva model have been validated by experimental results of 25 RC columns with diameter varying from 150 mm to 400 mm, and height of 750 mm. The ultimate stress f_{cc} and the corresponding strain ε_{cc} can be calculated by Eqs. 3.20 and 3.21, respectively:

$$f_{cc} = f_{c0} + 5.29\,(f_{\ell s} + k_F\ f_{\ell F}) \tag{3.20}$$

$$\varepsilon_{cc} = 17.65\ \varepsilon_{co} \left(\frac{f_{\ell s} + k_F\ f_{\ell F}}{f_{c0}} \right)^{0.7} \tag{3.21}$$

where $f_{c0} = \alpha\, f'_c$.

The coefficient α takes into account scale effects, relating the unconfined concrete strength in the column f_{c0} with concrete strength of standard cylinders f'_c, and it is given by Eq. 3.22, where, D and H are the diameter and the height of the column, respectively :

$$\alpha = \left(\frac{1.5 + D/H}{2} \right) \tag{3.22}$$

The strain of unconfined concrete, ε_{c0}, is adapted from Eurocode 2, given by ε_{c0} = 0.0007 $f'^{\,0.31}_c$ (f'_c in MPa). In this model, the confinement efficiency coefficient k_1 (see Eq. 3.1) is assumed as 5.29; on the other hand, the effectiveness coefficient of the steel confinement k_s is not included. The stress in the lateral steel, f_{sw}, is given by:

$$f_{sw} = \begin{cases} E_{sw}\,\varepsilon_{hF}\,D_c/D & \text{for } \varepsilon_{hF} < \varepsilon_{yw}\,D/D_c \\ f_{yw} & \text{for } \varepsilon_{hF} \geq \varepsilon_{yw} D/D_c \end{cases} \tag{3.23}$$

where E_{sw} is the steel Young's modulus, ε_{yw} is the yield strain of the transversal steel, and other variables as previously defined. The efficiency coefficient associated to the FRP, k_F, is taken as 0.6.

In the prediction of ultimate strain, it can be observed that, for unconfined columns, i.e. $f_{\ell F} = 0$ and $f_{\ell s} = 0$, the proposed equation gives a null value for the strain ε_{cc}. This implies that the model is not applicable to unconfined columns.

3.4.2. Pellegrino & Modena model

Pellegrino & Modena model (P&M) has been developed for RC columns confined by CFRP or GFRP. For circular columns, they also adopted a bilinear four-parameter curve to describe the stress-strain diagram of the confined concrete (Fig. 3.13), with the parameters, E_1, E_2, f_0 and N, given by Eq. 3.24:

$$E_1 = f_{c0}/\varepsilon_{c0}\ ;\ E_2 = \frac{f_{cc} - f_{c0}}{\varepsilon_{cc} - \varepsilon_{c0}};\ f_0 = f_{cc} - E_2\,\varepsilon_{cc}\ ;\ N = 1 \tag{3.24}$$

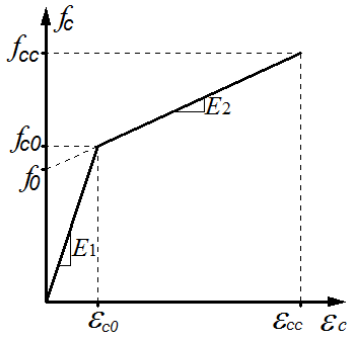

Figure 3.13 - Four-parameter bilinear stress-strain curve proposed by Pellegrino & Modena for concrete confined by steel and FRP.

Pellegrino & Modena validated the ultimate conditions of their proposed model using an experimental database comprising 77 FRP confined circular columns with steel reinforcement. The confined strength f_{cc} and the strain ε_{cc}, for circular RC columns confined by CFRP, are given by Eqs. 3.25 and 3.26, respectively:

$$f_{cc} = f_{c0} + k_1(k_s f_{\ell s} + k_F\ f_{\ell F}), \qquad k_1 = 2.95\left(\frac{k_s f_{\ell s} + k_F\ f_{\ell F}}{f_{c0}}\right)^{0.40} \tag{3.25}$$

$$\varepsilon_{cc} = \varepsilon_{c0}\left[2 + 28\frac{k_s\ f_{\ell s}\ + k_F\ f_{\ell F}}{f_{c0}}\right] \tag{3.26}$$

It is important to mention that, in contrast to C&S model that adopts k_1 as a constant, the confinement coefficient k_1 (see Eq. 3.1), is a function of the ratio $f_{\ell e}/f_{c0}$. The coefficient k_s is calculated as shown previously (see Eqs. 3.6 and 3.7). In the calculation of the lateral steel contribution $f_{\ell s}$, the stress in the lateral steel f_{sw} is taken as the yield strength. The coefficient k_F, i.e. the efficiency factor related to the FRP contribution, is calculated by Eq. 3.27:

$$k_F = 0.7\left(\frac{E_F\ \rho_F}{E_{s\ell}\ \rho_{s\ell}}\right)^{0.7} \leq 0.8 \tag{3.27}$$

where:
E_{sL} and E_F are the Young's modulus of the longitudinal steel and CFRP, respectively;
ρ_{sL} and ρ_F are the ratios of longitudinal steel and CFRP, respectively.

In the calculation of the ultimate strain (Eq. 3.29) it can be observed that, in the case of unconfined columns, i.e. $f_{\ell F} = 0$ and $f_{\ell s} = 0$, the P&M model overestimates ε_{cc}. In this case, the correct value of the ultimate strain is ε_{c0}, however, according to the P&M model a value of $\varepsilon_{cc} = 2\ \varepsilon_{c0}$ is obtained. As such, in the cases of small amounts of FRP and transversal steel reinforcement, and consequently, small lateral confining pressure, it can be expected that the P&M model will return overestimated values of the ultimate strain.

3.4.3. Lee *et al.* model

The stress-strain curve proposed by Lee *et al.* model (Lee) for concrete confined by steel and FRP (regardless of FRP type) is shown in Fig. 3.14. It is characterized by three branches: the first represents unconfined concrete behavior, ending at the point (f_{c0}, ε_{c0}); the second accounts for the simultaneous confining effect of FRP and transversal steel, ending at (f_{cs}, ε_{cs}) which represents the yield strength of transversal steel; in the third branch, the lateral pressure exerted by the transversal steel remains constant while the FRP confining pressure increases

up to the failure of the column represented by the ultimate condition (f_{cc}, ε_{cc}). These three branches are given by the following equations:

$$f_c = E_c\ \varepsilon_c + \left(f_{c0} - E_c\ \varepsilon_{c0}\right)\left(\frac{\varepsilon_c}{\varepsilon_{c0}}\right)^2 \quad \text{for} \quad 0 \le \varepsilon_c \le \varepsilon_{c0} \tag{3.28}$$

$$f_c = f_{c0} + \left(f_{cs} - f_{c0}\right)\left(\frac{\varepsilon_c - \varepsilon_{c0}}{\varepsilon_{cs} - \varepsilon_{c0}}\right)^{0.7} \quad \text{for} \quad \varepsilon_{c0} \le \varepsilon_c \le \varepsilon_{cs} \tag{3.29}$$

$$f_c = f_{cs} + \left(f_{cc} - f_{cs}\right)\left(\frac{\varepsilon_c - \varepsilon_{cs}}{\varepsilon_{cc} - \varepsilon_{cs}}\right)^{0.7} \quad \text{for} \quad \varepsilon_{cs} \le \varepsilon_c \le \varepsilon_{cc} \tag{3.30}$$

where E_c is the elastic modulus of concrete, given by ACI equation, $E_c = 4700\sqrt{f_{c0}}$ (f_{c0} in MPa).

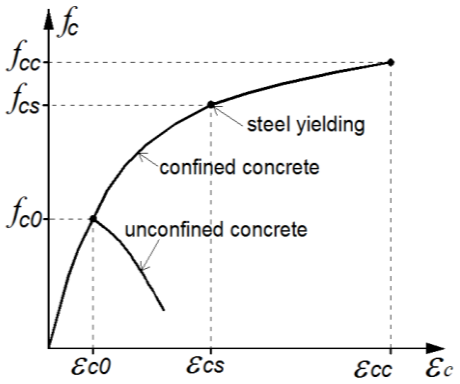

Figure 3.14 - Stress-strain curve proposed by Lee *et al.* for concrete confined by transversal steel and FRP.

The stress f_{cs} and strain ε_{cs}, corresponding to the steel yield, are given by Eqs. 3.31 and 3.32, respectively:

$$\begin{aligned} f_{cs} &= 0.95\, f_{cc} \quad \text{for } f_{\ell F} \ge f_{\ell s} \\ f_{cs} &= f_{cc}\left(\frac{\varepsilon_{cs}}{\varepsilon_{cu}}\right)^{0.4} = 0.867\, f_{cc} \quad \text{for } f_{\ell F} < f_{\ell s} \end{aligned} \tag{3.31}$$

$$\varepsilon_{cs} = \varepsilon_{cc}\left(0.85 + 0.03\,\frac{f_{\ell F}}{f_{\ell s}}\right) \quad \text{for } f_{\ell F} \geq f_{\ell s}$$
$$\varepsilon_{cs} = 0.7\,\varepsilon_{cc} \quad \text{for } f_{\ell F} < f_{\ell s} \tag{3.32}$$

It can be seen from Eq. 3.35 that in the case of $f_{\ell F} \geq f_{\ell s}$ and when $f_{\ell F} \geq 5\ f_{\ell s}$, the parameter ε_{cs} (axial strain corresponding to the steel yield) is greater than or equal the parameter ε_{cc} (ultimate axial strain), what is not appropriate. This implies that in Lee model, the upper limit for the ratio ($f_{\ell F}$ / $f_{\ell s}$) is 5.

The parameters f_{cc} and ε_{cc} were adjusted by experimental results of 24 columns with diameter of 150 mm, height of 300 mm and f'_c of 36.2 MPa. These parameters, required in Eq. 3.33, were based on the Lam & Teng (2002, 2003) models, differing from the latter by the inclusion of the contribution of the transversal steel. According to Lee model, the confined strength f_{cc} and corresponding strain ε_{cc}, are given by Eqs. 3.33 and 3.34, respectively:

$$f_{cc} = f_{c0} + 2\,(f_{\ell s} + f_{\ell F}) \tag{3.33}$$

$$\varepsilon_{cc} = \varepsilon_{c0}\left[1.75 + 5.25\left(\frac{k_s\ f_{\ell s} + f_{\ell F}}{f_{c0}}\right)\left(\frac{\varepsilon_F}{\varepsilon_{c0}}\right)^{0.45}\right] \tag{3.34}$$

where, the coefficient k_s is given by:

$$k_s = 2 - \left(f_{\ell F} / f_{\ell s}\right) \quad \text{for } f_{\ell F} \leq f_{\ell s};$$
$$k_s = 1 \text{ for } f_{\ell F} > f_{\ell s} \tag{3.35}$$

Similarly to P&M, the stress in the lateral steel f_{sw} is taken as the yield strength. Furthermore, in the calculation of ultimate strain (Eq. 3.37) for unconfined columns, the Lee model overestimates the ultimate strain, resulting in ε_{cc} = 1.75 ε_{c0}.

3.4.4. Shirmohammadi *et al.* model

The stress-strain curve proposed by Shirmohammadi *et al.* (2015) model (SH) for concrete confined by steel and FRP (regardless of FRP type) is shown in Fig. 3.15, and the corresponding equation is given by:

$$f_c = \frac{r\, f_{cc}\left(\varepsilon_c / \varepsilon_{cc}\right)}{r - 1 + \left(\varepsilon_c / \varepsilon_{cc}\right)^{0.8r}} \tag{3.36}$$

where $r = E_c / (E_c - f_{cc}/\varepsilon_{cc})$ and E_c is given by equation ACI. This equation is a modified version of the Popovics model.

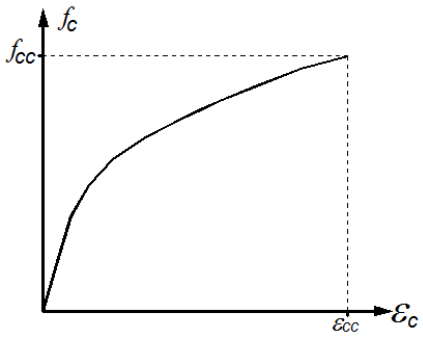

Figure 3.15 - Stress-strain curve proposed by Shirmohammadi *et al.* for concrete confined by steel and FRP.

These ultimate conditions of SH model were validated by experimental results of 22 RC with diameter in the range 150-400 mm and f'_c ranging from 14 to 28 MPa. The stress f_{cc} and the strain ε_{cc} are calculated by Eqs. 3.37 and 3.38, respectively (all variables have been previously defined). Similarly to the P&M and Lee models, SH model overestimates the ultimate strain (Eq. 3.41) for unconfined columns, resulting $\varepsilon_{cc} = 2\varepsilon_{c0}$, and adopts the yield strength f_{yw} in the calculation of the lateral steel contribution $f_{\ell s}$.

$$f_{cc} = f_{c0}\left[1.1 + 2.5\left(\frac{f_{\ell F}}{f_{c0}}\right)^{0.8}\left(\frac{f_{\ell s}}{f_{c0}}\right) + 3.5\left(\frac{f_{\ell s}}{f_{c0}}\right)^{0.2}\left(\frac{D_c}{D}\right)^{8}\right] \tag{3.37}$$

$$\varepsilon_{cc} = \varepsilon_{c0}\left[2.0 + 6.5\left(\frac{f_{\ell F}}{f_{c0}}\right)^{0.7}\left(\frac{f_{\ell s}}{f_{c0}}\right)^{0.7} + 6.0\left(\frac{f_{\ell s}}{f_{c0}}\right)^{0.04}\left(\frac{D}{2s}\right)^{0.8}\left(\frac{E_F}{f_{c0}}\right)^{0.5}\right] \quad (3.38)$$

3.4.5. Ilki *et al.* model

Ilki *et al.* model (Ilki) presented only the equations for the ultimate conditions, that were validated by experimental data of 18 circular RC columns with a diameter of 250 mm and 500 mm in height, with a compressive strength of standard cylinders ranging from 14 to 28 MPa. The strength of confined concrete f_{cc}, and corresponding strain ε_{cc} can be calculated according to Eqs. 3.39 and 3.40, respectively:

$$\frac{f_{cc}}{f_{c0}} = 1 + 4.54\frac{f_{\ell se}}{f_{c0}} + 2.54\frac{f_{\ell Fe}}{f_{c0}} \quad (3.39)$$

$$\frac{\varepsilon_{cc}}{\varepsilon_{c0}} = 1 + 22.7\frac{f_{\ell se}}{f_{c0}} + 19.27\left(\frac{f_{\ell Fe}}{f_{c0}}\right)^{0.53} \quad (3.40)$$

The strength of unconfined concrete is assumed equal to 85% of the strength of standard cylinders f'_c. The coefficient k_s is calculated by Eq. 3.6 and Eq. 3.7. The model considers that the transverse steel yields and adopts the efficiency factor for the FRP k_F equals to 0.85. The strain ε_{c0} is assumed as 0.002.

3.5. Summary of the chapter

In this chapter the stress-strain curve and the ultimate conditions of models for concrete confined by transversal steel (stirrups or spirals), concrete confined by FRP, and concrete confined by transversal steel and FRP were presented. A large number of models for predicting both the strength and ductility of RC columns confined by transversal steel have been proposed (e.g. Sheikh & Uzumeri, 1982; Mander *et al.*, 1988; Muguruma & Watanabe, 1990; Razvi & Saatcioglu, 1992; Cusson & Paultre, 1995).

An extensive review of the confinement models for concrete confined by FRP jackets, for circular sections, was performed by Ozbakkaloglu *et al.* (2013). However, the models presented by those authors were derived based on experimental results of cylinders of plain

concrete. As a consequence, these models do not take into account the influence of longitudinal and transversal steel reinforcement, which commonly occurs in the problem of strengthening of existing RC columns.

In the strengthening of existing RC columns, the concrete core is simultaneously confined by FRP and transverse steel reinforcement. Few researchers have addressed the problem of the estimation of the lateral confining pressure f_ℓ, considering contributions of both the FRP and the transverse steel. In this chapter, five representative models (Chastre & Silva, 2010; Pellegrino & Modena, 2010; Lee *et al.*, 2010; Shirmohamadi *et al.*, 2015; and Ilki *et al.*, 2008) were discussed, presenting the equations to predict the stress-strain curve and ultimate conditions. In the next chapter, the performance of these models is assessed against a database of experimental results corresponding to columns confined by both CFRP and steel, in order to generate the statistics of the random variable "model error".

4

PERFORMANCE ASSESSMENT OF CONFINEMENT MODELS FOR FRP-RC COLUMNS

A large research effort is still necessary in order to select analytical models that properly estimate the ultimate stress and strain of FRP-confined RC columns. Different models with different levels of conservatism have been proposed in an attempt to describe confinement effects, but most of the available models have been validated by experimental results of cylinders of plain concrete. As such, these models do not take into account the influence of longitudinal and transversal steel reinforcement, which commonly occur in the problem of strengthening of existing RC structures.

4.1. Experimental Database

The mechanisms associated to confinement are still not clearly understood and the validation of proposed equations depends heavily on the use of databases. A large number of experimental studies have been conducted; however, most of the studies performed so far correspond to specimens without transversal and/or longitudinal steel. As an example, Ozbakkaloglu & Lim (2013) published an extensive database encompassing axial compression tests on 832 circular specimens of plain concrete confined by FRP. Additionally, even though the models considered herein were developed for different FRP types, most of available experimental data on FRP-confined RC columns are limited to CFRP confinement. Therefore, in this work, an experimental database encompassing RC columns with longitudinal and transversal steel (spirals or circular stirrups) confined by CFRP is compiled from the available literature.

In existing RC columns, i.e. the practical problems requiring FRP strengthening measures, the presence of longitudinal and transversal steel reinforcements shall be taken into account. To

this end, a comprehensive database including 151 experimental results from 8 different experimental programs (Chastre & Silva, 2010; Benzaid., 2010; Abdelrahman & El Hacha, 2012; Carrazedo, 2002; Eid *et al.*, 2009; Ilki *et al.*, 2008; Matthys *et al.*, 2006; Rigazzo & Moreno Jr., 2006) has been compiled. This database encompasses RC columns confined by CFRP under monotonic uniaxial compression; specimens without confinement are used as a reference. All the selected specimens in the database are confined by continuous CFRP jackets with fibers orientated in the hoop direction. A summary of each research program (number of tests, column diameter D, column height H, ratio D/H, cylinder concrete strength f'_c, transversal steel ratio ρ_{sw}, CFRP ratio ρ_F, steel lateral confining pressure $f_{\ell s}$ and CFRP lateral confining pressure $f_{\ell F}$) is presented in Table 4.1.

Table 4.1- Summary of experimental data included in the database (151 columns).

paper	Author	# of tests	D (cm)	H (cm)	f'_c (MPa)	ρ_{sw} (%)	ρ_F (%)	$f_{\ell s}$ (MPa)	$f_{\ell F}$ (MPa)
I	Abdelrahman & El-Hacha (2012)	4	30	120	38-40	0-2.97	0-0.17	0-7.0	0-2.9
II	Benzaid. (2010)	77	16-19.7	32-100	26-62	0-0.93	0-0.99	0-1.3	0-21.6
III	Carrazedo (2002)	9	15	57	32-35	0-1.96	0-0.54	0-7.4	0-9.6
IV	Chastre & Silva (2010)	25	15-25	75	35-38	0-0.57	0-1.34	0-0.9	0-22.7
V	Eid *et al.*(2009)	20	25.3-30.3	120	29-51	0.74-2.5	0-0.68	2.2-7.5	0-11.7
VI	Ilki *et al.* (2008)	10	25	50	15-28	0.69-2.91	0.26-1.32	1.7-4.8	4.5-22.6
VII	Matthys *et al* (2006)	3	40	200	32-34	0.38	0-0.94	0-1.1	0-11.1
VIII	Rigazzo & Moreno Jr. (2006)	3	20	160	16	0.462	0-0.94	0-1.4	0-17.8
	Range	-	15-40	32-200	15-62	0-2.97	0-1.34	0-7.5	0-22.7

The complete characteristics are presented in Table 4.2, namely: specimen geometric properties (diameter D, heigth H and concrete cover c), concrete properties (compressive strength of standard cylinders f'_c and unconfined concrete strength f_{c0}), details of the transversal steel (type, diameter ϕ_w, spacing s, and yield strength f_{yw}) and longitudinal steel (number of bars n_L, diameter ϕ_L, and yield strength f_{yL}) reinforcements, mechanical properties of the fibers in the CFRP composite (type, elastic modulus E_f, tensile strength f_f and ultimate strain ε_f as provided by the manufacturer), and details of the confinement (ply thickness t, number of plies n). It is common to use the mechanical properties of the fibers, in the computation of the lateral confining pressure $f_{\ell F}$, disregarding the contribution of resin (Chastre & Silva, 2010 and Carrazedo, 2002). This is due to the fact that the final thickness of the FRP composite jacket has a considerable variability. In addition, when the thickness of the

ply is increased with the utilization of more resin, a significant increment of the rupture load (direct tensile test) does not occur. Therefore, the information regarding ply thickness t, Young's modulus E_f, tensile strength f_f, and ultimate strain ε_f in Table 4.2 refers to CFRP fibers and is used in the research presented herein.

Table 4.2 - Characteristics of the specimens in the compiled database.

Paper	Geometry				Concrete		Transversal Steel				Longitudinal Steel			FRP Details			Fiber properties		
	Specimen	D (mm)	H (mm)	c (mm)	f'_{cm} (MPa)	$f_{c0\,exp}$* (MPa)	Type	diameter ϕ_t (mm)	spacing s (mm)	f_{yw} (MPa)	# of bars	diameter ϕ_L(mm)	f_{yL} (MPa)	FRP type	# of plies	ply thickness t (mm)	E_f (GPa)	f_f (MPa)	ε_f (‰)
I	1	300	1200	15	40.1	37.0	spirals							Sikawrap Hex 230					
	2	300	1200	15	40.1	37.0		11.3	50	472	6	19.5	444						
	3	300	1200	15	38.3	37.0									1	0.128	230	3450	15.0
	4	300	1200	15	38.3	37.0		11.3	50	472	6	19.5	444		1	0.128	230	3450	15.0
II	5	160	320	15	25.9	25.9								SikaWrap Hex 23 C/45					
	6	160	320	15	25.9	25.9													
	7	160	320	15	25.9	25.9													
	8	160	320	15	25.9	25.9									1	0.13	238	4300	18.0
	9	160	320	15	25.9	25.9									3	0.13	238	4300	18.0
	10	160	320	15	25.9	25.9	stirrups	8.0	140	235	4	12.0	500						
	11	160	320	15	25.9	25.9		8.0	140	235	4	12.0	500						
	12	160	320	15	25.9	25.9		8.0	140	235	4	12.0	500		1	0.13	238	4300	18.0
	13	160	320	15	25.9	25.9		8.0	140	235	4	12.0	500		1	0.13	238	4300	18.0
	14	160	320	15	25.9	25.9		8.0	140	235	4	12.0	500		3	0.13	238	4300	18.0
	15	160	320	15	25.9	25.9		8.0	140	235	4	12.0	500		3	0.13	238	4300	18.0
	16	160	320	15	27.2	27.2	stirrups	8.0	140	235	4	12.0	500						
	17	160	320	15	27.2	27.2		8.0	140	235	4	12.0	500						
	18	160	320	15	27.2	27.2		8.0	140	235	4	12.0	500		3	0.13	238	4300	18.0
	19	160	320	15	27.2	27.2		8.0	140	235	4	12.0	500		3	0.13	238	4300	18.0
	20	160	320	15	49.5	49.5													
	21	160	320	15	49.5	49.5													
	22	160	320	15	49.5	49.5													
	23	160	320	15	49.5	49.5									1	0.13	238	4300	18.0
	24	160	320	15	49.5	49.5									3	0.13	238	4300	18.0

* concrete compressive strength measured in the specimen of plane concrete in the same dimensions of the column

Table 4.2 - Characteristics of the specimens in the compiled database (continued).

Paper	Geometry				Concrete		Transversal Steel				Longitudinal Steel			FRP Details			Fiber properties		
	Specimen	D (mm)	H (mm)	c (mm)	f'_c (MPa)	$f_{c0\,exp}$* (MPa)	Type	diameter ϕ_t (mm)	spacing s (mm)	f_{yw} (MPa)	# of bars	diameter ϕ_L(mm)	f_{yL} (MPa)	FRP type	# of plies	ply thickness t (mm)	E_f (GPa)	f_f (MPa)	ε_f (‰)
II	25	160	320	15	49.5	49.5	stirrups	8.0	140	235	4	12.0	500	SikaWrap Hex 23 C/45					
	26	160	320	15	49.5	49.5		8.0	140	235	4	12.0	500						
	27	160	320	15	49.5	49.5		8.0	140	235	4	12.0	500		1	0.13	238	4300	18.0
	28	160	320	15	49.5	49.5		8.0	140	235	4	12.0	500		1	0.13	238	4300	18.0
	29	160	320	15	49.5	49.5		8.0	140	235	4	12.0	500		3	0.13	238	4300	18.0
	30	160	320	15	49.5	49.5		8.0	140	235	4	12.0	500		3	0.13	238	4300	18.0
	31	160	320	15	61.8	61.8													
	32	160	320	15	61.8	61.8													
	33	160	320	15	61.8	61.8													
	34	160	320	15	61.8	61.8									1	0.13	238	4300	18.0
	35	160	320	15	61.8	61.8									3	0.13	238	4300	18.0
	36	160	320	15	61.8	61.8	stirrups	8.0	140	235	4	12.0	500						
	37	160	320	15	61.8	61.8		8.0	140	235	4	12.0	500						
	38	160	320	15	61.8	61.8		8.0	140	235	4	12.0	500		1	0.13	238	4300	18.0
	39	160	320	15	61.8	61.8		8.0	140	235	4	12.0	500		1	0.13	238	4300	18.0
	40	160	320	15	61.8	61.8		8.0	140	235	4	12.0	500		3	0.13	238	4300	18.0
	41	160	320	15	61.8	61.8		8.0	140	235	4	12.0	500		3	0.13	238	4300	18.0
	42	155	1000	15	27.2			8.0	140	235	4	12.0	500						
	43	155	1000	15	27.2			8.0	140	235	4	12.0	500						
	44	155	1000	15	27.2			8.0	140	235	4	12.0	500		3	0.13	238	4300	18.0
	45	155	1000	15	27.2			8.0	140	235	4	12.0	500		3	0.13	238	4300	18.0
	46	155	1000	15	25.9			8.0	140	235	4	12.0	500						
	47	155	1000	15	25.9			8.0	140	235	4	12.0	500						
	48	155	1000	15	25.9			8.0	140	235	4	12.0	500		1	0.13	238	4300	18.0
	49	155	1000	15	25.9			8.0	140	235	4	12.0	500		1	0.13	238	4300	18.0
	50	155	1000	15	25.9			8.0	140	235	4	12.0	500		3	0.13	238	4300	18.0

* concrete compressive strength measured in the specimen of plane concrete in the same dimensions of the column

Table 4.2 - Characteristics of the specimens in the compiled database (continued).

Paper	Geometry				Concrete		Transversal Steel				Longitudinal Steel			FRP Details			Fiber properties		
	Specimen	D (mm)	H (mm)	c (mm)	f'_c (MPa)	$f_{c0\,exp}$* (MPa)	Type	diameter ϕ_t (mm)	spacing s (mm)	f_{yw} (MPa)	# of bars	diameter ϕ_L(mm)	f_{yL} (MPa)	FRP type	# of plies	ply thickness t (mm)	E_f (GPa)	f_f (MPa)	ε_f (‰)
II	51	155	1000	15	25.9		stirrups	8.0	140	235	4	12.0	500	Sikawrap Hex 230/45	3	0.13	238	4300	18.0
	52	155	1000	15	49.5			8.0	140	235	4	12.0	500						
	53	155	1000	15	49.5			8.0	140	235	4	12.0	500						
	54	155	1000	15	49.5			8.0	140	235	4	12.0	500		1	0.13	238	4300	18.0
	55	155	1000	15	49.5			8.0	140	235	4	12.0	500		1	0.13	238	4300	18.0
	56	155	1000	15	49.5			8.0	140	235	4	12.0	500		3	0.13	238	4300	18.0
	57	155	1000	15	49.5		stirrups	8.0	140	235	4	12.0	500		3	0.13	238	4300	18.0
	58	155	1000	15	61.8			8.0	140	235	4	12.0	500						
	59	155	1000	15	61.8			8.0	140	235	4	12.0	500						
	60	155	1000	15	61.8			8.0	140	235	4	12.0	500		1	0.13	238	4300	18.0
	61	155	1000	15	61.8			8.0	140	235	4	12.0	500		1	0.13	238	4300	18.0
	62	155	1000	15	61.8			8.0	140	235	4	12.0	500		3	0.13	238	4300	18.0
	63	155	1000	15	61.8			8.0	140	235	4	12.0	500		3	0.13	238	4300	18.0
	64	197	1000	15	25.9			8.0	140	235	4	12.0	500						
	65	197	1000	15	25.9			8.0	140	235	4	12.0	500						
	66	197	1000	15	25.9			8.0	140	235	4	12.0	500		1	0.13	238	4300	18.0
	67	197	1000	15	25.9			8.0	140	235	4	12.0	500		1	0.13	238	4300	18.0
	68	197	1000	15	25.9			8.0	140	235	4	12.0	500		3	0.13	238	4300	18.0
	69	197	1000	15	25.9			8.0	140	235	4	12.0	500		3	0.13	238	4300	18.0
	70	197	1000	15	49.5			8.0	140	235	4	12.0	500						
	71	197	1000	15	49.5			8.0	140	235	4	12.0	500						
	72	197	1000	15	49.5			8.0	140	235	4	12.0	500		1	0.13	238	4300	18.0
	73	197	1000	15	49.5			8.0	140	235	4	12.0	500		1	0.13	238	4300	18.0
	74	197	1000	15	49.5			8.0	140	235	4	12.0	500		3	0.13	238	4300	18.0
	75	197	1000	15	49.5			8.0	140	235	4	12.0	500		3	0.13	238	4300	18.0

* concrete compressive strength measured in the specimen of plane concrete in the same dimensions of the column

Table 4.2 - Characteristics of the specimens in the compiled database (continued).

Paper	Geometry				Concrete		Transversal Steel				Longitudinal Steel			FRP Details			Fiber properties		
	Specimen	D (mm)	H (mm)	c (mm)	f'_c (MPa)	$f_{c0\,exp}$* (MPa)	Type	diameter ϕ_t (mm)	spacing s (mm)	f_{yw} (MPa)	# of bars	diameter ϕ_L(mm)	f_{yL} (MPa)	FRP type	# of plies	ply thickness t (mm)	E_f (GPa)	f_f (MPa)	ε_f (‰)
II	76	197	1000	15	61.8		stirrups	8.0	140	235	4	12.0	500	Sikawrap Hex 230/45					
	77	197	1000	15	61.8			8.0	140	235	4	12.0	500						
	78	197	1000	15	61.8			8.0	140	235	4	12.0	500		1	0.13	238	4300	18.0
	79	197	1000	15	61.8			8.0	140	235	4	12.0	500		1	0.13	238	4300	18.0
	80	197	1000	15	61.8			8.0	140	235	4	12.0	500		3	0.13	238	4300	18.0
	81	197	1000	15	61.8			8.0	140	235	4	12.0	500		3	0.13	238	4300	18.0
III	82	190	570	15	32.0	26.2	spirals							Sikawrap Hex 230 C	0				
	83	190	570	15	32.0	26.2									1	0.13	230	3500	15.0
	84	190	570	15	32.0	26.2									2	0.13	230	3500	15.0
	85	190	570	15	32.0	26.2		5.0	50	756	6	8.0	554.8						
	86	190	570	15	35.2			5.0	25	756	6	8.0	554.8						
	87	190	570	15	32.0	26.2		5.0	50	756	6	8.0	554.8		1	0.13	230	3500	15.0
	88	190	570	15	35.2			5.0	25	756	6	8.0	554.8		1	0.13	230	3500	15.0
	89	190	570	15	32.0	26.2		5.0	50	756	6	8.0	554.8		2	0.13	230	3500	15.0
	90	190	570	15	35.2			5.0	25	756	6	8.0	554.8		2	0.13	230	3500	15.0
IV	91	150	750	25	38.0	26.4								Replark 30					
	92	150	750	25	38.0	26.4													
	93	150	750	25	38.0	26.4													
	94	150	750	25	38.0	26.4									2	0.167	230	3400	15.0
	95	150	750	25	38.0	26.4									2	0.167	230	3400	15.0
	96	150	750	25	38.0	26.4									2	0.167	230	3400	15.0
	97	150	750	25	38.0	26.4									3	0.167	230	3400	15.0
	98	150	750	25	38.0	26.4	stirrups	3.0	100	323	6	6.0	391						
	99	150	750	25	38.0	26.4		3.0	100	323	6	6.0	391						
	100	150	750	25	38.0	26.4		3.0	100	323	6	6.0	391						
	101	150	750	25	38.0	26.4		3.0	150	323	6	6.0	391						

* concrete compressive strength measured in the specimen of plane concrete in the same dimensions of the column

Table 4.2 - Characteristics of the specimens in the compiled database (continued).

Paper	Geometry				Concrete		Transversal Steel				Longitudinal Steel			FRP Details			Fiber properties		
	Specimen	D (mm)	H (mm)	c (mm)	f'_c (MPa)	$f_{c0\,exp}$* (MPa)	Type	diameter ϕ_t (mm)	spacing s (mm)	f_{yw} (MPa)	# of bars	diameter ϕ_L(mm)	f_{yL} (MPa)	FRP type	# of plies	ply thickness t (mm)	E_f (GPa)	f_f (MPa)	ε_f(‰)
IV	102	150	750	25	38.0	26.4	stirrups	3.0	150	323	6	6.0	391	Replark 30					
	103	150	750	25	38.0	26.4		3.0	50	323	6	6.0	391						
	104	150	750	25	38.0	26.4		3.0	50	323	6	6.0	391						
	105	150	750	25	38.0	26.4		3.0	100	323	6	6.0	391		2	0.167	230	3400	15.0
	106	150	750	25	38.0	26.4		3.0	100	323	6	6.0	391		2	0.167	230	3400	15.0
	107	150	750	25	38.0	26.4		3.0	150	323	6	6.0	391		2	0.167	230	3400	15.0
	108	150	750	25	38.0	26.4		3.0	50	323	6	6.0	391		2	0.167	230	3400	15.0
	109	250	750	25	35.2	34.9								Mbrace C1-30					
	110	250	750	25	35.2	34.9									2	0.176	240	3800	15.5
	111	250	750	25	35.2	34.9		6.0	150	391	6	12.0	458						
	112	250	750	25	35.2	34.9		6.0	150	391	6	12.0	458		1	0.176	240	3800	15.5
	113	250	750	25	35.2	34.9		6.0	150	391	6	12.0	458		2	0.176	240	3800	15.5
	114	250	750	25	35.2	34.9		6.0	150	391	6	12.0	458		3	0.176	240	3800	15.5
	115	250	750	25	35.2	34.9		6.0	150	391	6	12.0	458		4	0.176	240	3800	15.5
V	116	303	1200	25	29.4		stirrups	9.5	150	602	6	16.0	423	-	2	0.128	230	3450	15.0
	117	303	1200	25	31.7			9.5	70	602	6	16.0	550		2	0.128	230	3450	15.0
	118	303	1200	25	31.7			9.5	45	602	6	16.0	486.5		2	0.128	230	3450	15.0
	119	303	1200	25	31.7		spirals	11.3	100	456	6	16.0	423						
	120	303	1200	25	36.0			11.3	100	456	6	16.0	423						
	121	303	1200	25	31.7			11.3	100	456	6	16.0	423		2	0.128	230	3450	15.0
	122	303	1200	25	36.0			11.3	100	456	6	16.0	423		2	0.128	230	3450	15.0
	123	303	1200	25	31.7			11.3	100	456	6	16.0	423		4	0.128	230	3450	15.0
	124	303	1200	25	50.8			11.3	100	456	6	16.0	423						
	125	303	1200	25	50.8			11.3	100	456	6	16.0	423		2	0.128	230	3450	15.0
	126	303	1200	25	31.7			11.3	65	456	6	16.0	423						

* concrete compressive strength measured in the specimen of plane concrete in the same dimensions of the column

Table 4.2 - Characteristics of the specimens in the compiled database (continued).

Paper	Geometry				Concrete		Transversal Steel				Longitudinal Steel			FRP Details			Fiber properties		
	Specimen	D (mm)	H (mm)	c (mm)	f'_c (MPa)	$f_{c0\,exp}$* (MPa)	Type	diameter ϕ_t (mm)	spacing s (mm)	f_{yw} (MPa)	# of bars	diameter ϕ_L(mm)	f_{yL} (MPa)	FRP type	# of plies	ply thickness t (mm)	E_f (GPa)	f_f (MPa)	ε_f(‰)
V	127	303	1200	25	36.0		spirals	11.3	65	456	6	16.0	423	-					
	128	303	1200	25	31.7			11.3	65	456	6	16.0	423		2	0.128	230	3450	15.0
	129	303	1200	25	36.0			11.3	65	456	6	16.0	423		2	0.128	230	3450	15.0
	130	303	1200	25	36.0			11.3	65	456	6	16.0	423		4	0.128	230	3450	15.0
	131	253	1200	0	36.0			11.3	65	456	6	16.0	423		2	0.128	230	3450	15.0
	132	303	1200	25	50.8			11.3	65	456	6	16.0	423		0				
	133	303	1200	25	50.8			11.3	65	456	6	16.0	423		2	0.128	230	3450	15.0
	134	303	1200	25	50.8			11.3	65	456	6	16.0	423		4	0.128	230	3450	15.0
	135	253	1200	0	50.8			11.3	65	456	6	16.0	423		2	0.128	230	3450	15.0
VI	136	250	500	25	15.1		stirrups	8.0	145	476	6	10.0	367	-	1	0.165	230	3430	15.0
	137	250	500	25	15.5			8.0	145	476	6	10.0	367		1	0.165	230	3430	15.0
	138	250	500	25	15.6			8.0	145	476	6	10.0	367		3	0.165	230	3430	15.0
	139	250	500	25	15.9			8.0	145	476	6	10.0	367		3	0.165	230	3430	15.0
	140	250	500	25	15.1			8.0	145	476	6	10.0	367		5	0.165	230	3430	15.0
	141	250	500	25	15.9			8.0	145	476	6	10.0	367		5	0.165	230	3430	15.0
	142	250	500	25	27.6			8.0	50	476	6	10.0	367		3	0.165	230	3430	15.0
	143	250	500	25	27.6			8.0	100	476	6	10.0	367		3	0.165	230	3430	15.0
	144	250	500	25	27.6			8.0	145	476	6	10.0	367		3	0.165	230	3430	15.0
	145	250	500	25	27.6			8.0	145	476	6	10.0	367		5	0.165	230	3430	15.0
VII	146	400	2000	15	31.8		stirrups	8.0	140	560	10	12.0	620	S&P C Sheet					
	147	400	2000	15	34.3			8.0	140	560	10	12.0	620		5	0.117	240	3800	15.5
	148	400	2000	15	34.3			8.0	140	560	10	12.0	620		4	0.235	640	2650	4.0
VIII	149	200	1600	15	15.5		stirrups	5.0	100	616	8	10.0	539	S&P C Sheet					
	150	200	1600	15	15.5			5.0	100	616	8	10.0	539		1	0.117	240	3800	15.5
	151	200	1600	15	15.5			5.0	100	616	8	10.0	539		4	0.117	240	3800	15.5

* concrete compressive strength measured in the specimen of plane concrete in the same dimensions of the column

Of special interest, the experimental confined concrete compressive strength in the column, $f_{cc\ exp}$, was obtained as the ratio of the load resisted by the concrete (total load minus the contribution of the longitudinal steel) and the net concrete area of the cross-section. The strain $\varepsilon_{cc\ exp}$ is the experimental value measured in the test. These quantities, $f_{cc\ exp}$, and $\varepsilon_{cc\ exp}$ are presented in the second and third columns in Table 4.3, respectively. Other information in this table will be discussed in section 4.3.

Figure 4.1-a) illustrates the normalized gains to concrete strength ($f_{cc\ exp}$ / f'_c) relative to strength and Fig 4.1-b) the normalized gain to concrete strain, $\varepsilon_{cc\ exp}$ / ε'_c, with respect the confinement ratio: ($f_{\ell F}$ + $f_{\ell s}$) / f'_c, for the 70 columns confined by both CFRP and steel.

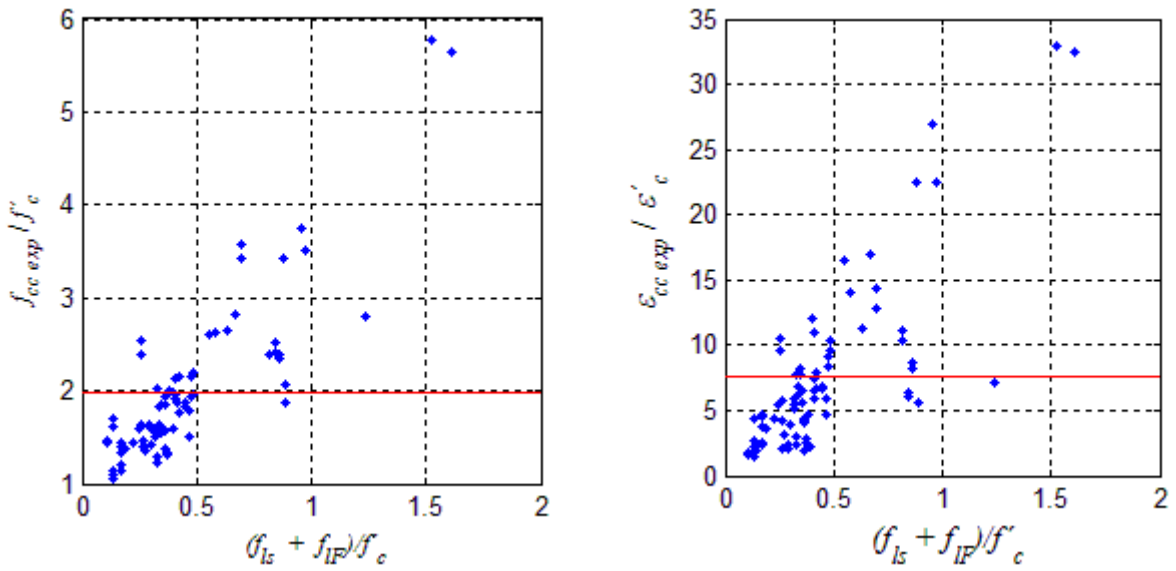

Figure 4.1 - Normalized gains with respect the confinement ratio: a) strength; and b) ultimate strain.

The strength normalized gain is in the range 1.05 - 5.77, with a mean of 1.99, and coefficient of variation (COV) of 0.43; the normalized gain to strain is in the range 1.46 - 33.0, with a mean of 7.53, and COV of 0.84. It can be observed from this figure that normalized gain to strength and strain increases almost linearly when FRP confinement ratio increases as expected.

Table 4.3 - Model predictions and model errors (ultimate stress and ultimate strain) according to C&S, P&M, Lee, SH and Ilki models.

Specimen	Experimental Results		Model Predictions																			
			C&S				P&M				Lee				SH				Ilki			
	$f_{cc\ exp}$ (MPa)	$\varepsilon_{cc\ exp}$ (‰)	$f_{cc\ calc}$ (MPa)	$\varepsilon_{cc\ calc}$ (‰)	ξ_f	ξ_ε	$f_{cc\ calc}$ (MPa)	$\varepsilon_{cc\ calc}$ (‰)	ξ_f	ξ_ε	$f_{cc\ calc}$ (MPa)	$\varepsilon_{cc\ calc}$ (‰)	ξ_f	ξ_ε	$f_{cc\ calc}$ (MPa)	$\varepsilon_{cc\ calc}$ (‰)	ξ_f	ξ_ε	$f_{cc\ calc}$ (MPa)	$\varepsilon_{cc\ calc}$ (‰)	ξ_f	ξ_ε
1	37.0	0.6	35.1	**	1.05	**	40.1	4.0	0.92	0.16	40.1	3.5	0.92	0.18	44.1	4.0	0.84	0.16	37.0	2.0	1.00	0.32
2	55.1	2.0	72.2	12.6	0.76	0.16	47.3	11.6	1.17	0.17	54.1	12.6	1.02	0.16	86.7	68.5	0.64	0.03	98.0	18.5	0.56	0.11
3	51.0	2.3	42.9	4.9	1.19	0.47	41.5	5.8	1.23	0.40	44.2	5.5	1.15	0.42	42.1	4.0	1.21	0.58	43.4	11.2	1.18	0.20
4	62.3	4.1	80.0	15.0	0.78	0.27	46.3	12.4	1.35	0.33	58.2	13.0	1.07	0.31	85.5	70.8	0.73	0.06	104.4	27.7	0.60	0.15
5	25.9	2.9	25.9	**	1.00	**	25.9	4.0	1.00	0.72	25.9	3.5	1.00	0.82	28.5	4.0	0.91	0.72	25.9	2.0	1.00	1.43
6	26.1	2.6	25.9	**	1.01	**	25.9	4.0	1.01	0.65	25.9	3.5	1.01	0.74	28.5	4.0	0.92	0.65	25.9	2.0	1.01	1.30
7	25.7	*	25.9	-	0.99	-	25.9	4.0	0.99	-	25.9	3.5	0.99	-	28.5	4.0	0.90	-	25.9	2.0	0.99	-
8	39.6	12.8	48.1	9.5	0.82	1.35	35.1	10.2	1.13	1.25	39.9	11.1	0.99	1.15	28.5	4.0	1.39	3.20	41.0	19.6	0.97	0.65
9	66.1	15.2	92.5	20.4	0.72	0.74	58.4	22.6	1.13	0.67	67.9	26.3	0.97	0.58	28.5	4.0	2.32	3.79	71.2	33.6	0.93	0.45
10	19.2	3.9	32.8	4.2	0.59	0.93	26.0	4.5	0.74	0.86	28.5	6.3	0.67	0.61	38.0	24.6	0.51	0.16	28.9	3.1	0.67	1.23
11	18.1	3.7	32.8	4.2	0.55	0.88	26.0	4.5	0.70	0.82	28.5	6.3	0.64	0.58	38.0	24.6	0.48	0.15	28.9	3.1	0.63	1.17
12	40.2	15.9	55.0	11.4	0.73	1.39	27.5	7.4	1.47	2.14	42.5	12.5	0.95	1.27	39.1	25.3	1.03	0.63	44.0	20.8	0.92	0.77
13	38.8	14.8	55.0	11.4	0.71	1.29	27.5	7.4	1.41	1.98	42.5	12.5	0.91	1.18	39.1	25.3	0.99	0.58	44.0	20.8	0.88	0.71
14	61.0	22.2	99.3	21.9	0.61	1.02	43.7	23.7	1.40	0.94	70.5	27.7	0.87	0.80	40.7	26.0	1.50	0.85	74.1	34.7	0.82	0.64
15	62.0	23.7	99.3	21.9	0.62	1.09	43.7	23.7	1.42	1.00	70.5	27.7	0.88	0.86	40.7	26.0	1.52	0.91	74.1	34.7	0.84	0.68
16	20.0	3.8	34.0	4.1	0.59	0.93	27.2	4.4	0.73	0.85	29.7	6.2	0.67	0.61	39.7	24.1	0.50	0.16	30.1	3.1	0.66	1.23
17	20.4	4.0	34.0	4.1	0.60	0.97	27.2	4.4	0.75	0.90	29.7	6.2	0.69	0.64	39.7	24.1	0.51	0.17	30.1	3.1	0.68	1.29
18	64.6	20.7	100.6	21.5	0.64	0.96	44.6	22.8	1.45	0.91	71.7	26.6	0.90	0.78	42.3	25.4	1.53	0.82	75.4	33.9	0.86	0.61
19	64.8	22.2	100.6	21.5	0.64	1.03	44.6	22.8	1.45	0.97	71.7	26.6	0.90	0.83	42.3	25.4	1.53	0.87	75.4	33.9	0.86	0.65
20	48.0	1.9	49.5	**	0.97	**	49.5	4.0	0.97	0.47	49.5	3.5	0.97	0.53	54.4	4.0	0.88	0.47	49.5	2.0	0.97	0.93
21	51.0	1.5	49.5	**	1.03	**	49.5	4.0	1.03	0.38	49.5	3.5	1.03	0.44	54.4	4.0	0.94	0.38	49.5	2.0	1.03	0.77
22	49.5	*	49.5	-	1.00	-	49.5	4.0	1.00	-	49.5	3.5	1.00	-	54.4	4.0	0.91	-	49.5	2.0	1.00	-
23	52.8	2.5	71.6	7.4	0.74	0.34	57.8	7.2	0.91	0.35	63.4	7.5	0.83	0.34	54.4	4.0	0.97	0.63	64.5	14.5	0.82	0.17
24	82.9	7.3	116.0	15.9	0.71	0.46	78.9	13.7	1.05	0.53	91.4	15.5	0.91	0.47	54.4	4.0	1.52	1.82	94.7	24.4	0.88	0.30
25	48.5	2.5	56.3	3.2	0.86	0.77	49.5	4.2	0.98	0.59	52.1	5.0	0.93	0.50	70.3	18.5	0.69	0.13	52.4	2.6	0.92	0.96
26	47.7	3.5	56.3	3.2	0.85	1.09	49.5	4.2	0.96	0.83	52.1	5.0	0.92	0.71	70.3	18.5	0.68	0.19	52.4	2.6	0.91	1.36
27	66.1	7.4	78.5	8.9	0.84	0.83	50.6	5.8	1.30	1.27	66.0	8.2	1.00	0.90	71.0	18.8	0.93	0.39	67.5	15.1	0.98	0.49
28	69.5	9.4	78.5	8.9	0.89	1.05	50.6	5.8	1.37	1.61	66.0	8.2	1.05	1.14	71.0	18.8	0.98	0.50	67.5	15.1	1.03	0.62
29	92.3	13.7	122.9	17.0	0.75	0.81	63.2	14.3	1.46	0.96	94.0	16.2	0.98	0.85	71.9	19.1	1.28	0.72	97.7	25.0	0.95	0.55
30	90.1	13.4	122.9	17.0	0.73	0.79	63.2	14.3	1.43	0.94	94.0	16.2	0.96	0.83	71.9	19.1	1.25	0.70	97.7	25.0	0.92	0.54

* Not measured during the test; ** Not applicable for prediction of ultimate strain in unconfined columns.

Table 4.3 - Model predictions and model errors (ultimate stress and ultimate strain) according to C&S, P&M, Lee, SH and Ilki models (cont.).

Specimen	Experimental Results		Model Predictions																				
			C&S				P&M				Lee				SH				Ilki			
	$f_{cc\ exp}$ (MPa)	$\varepsilon_{cc\ exp}$ (‰)	$f_{cc\ calc}$ (MPa)	$\varepsilon_{cc\ calc}$ (‰)	ξ_f	ξ_ε	$f_{cc\ calc}$ (MPa)	$\varepsilon_{cc\ calc}$ (‰)	ξ_f	ξ_ε	$f_{cc\ calc}$ (MPa)	$\varepsilon_{cc\ calc}$ (‰)	ξ_f	ξ_ε	$f_{cc\ calc}$ (MPa)	$\varepsilon_{cc\ calc}$ (‰)	ξ_f	ξ_ε	$f_{cc\ calc}$ (MPa)	$\varepsilon_{cc\ calc}$ (‰)	ξ_f	ξ_ε
31	62.4	3.2	61.8	**	1.01	**	61.8	4.0	1.01	0.79	61.8	3.5	1.01	0.91	68.0	4.0	0.92	0.79	61.8	2.0	1.01	1.59
32	66.7	2.5	61.8	**	1.08	**	61.8	4.0	1.08	0.63	61.8	3.5	1.08	0.72	68.0	4.0	0.98	0.63	61.8	2.0	1.08	1.26
33	56.4	*	61.8	-	0.91	-	61.8	4.0	0.91	-	61.8	3.5	0.91	-	68.0	4.0	0.83	-	61.8	2.0	0.91	-
34	62.7	3.3	84.0	6.7	0.75	0.48	69.9	6.6	0.90	0.50	75.8	6.7	0.83	0.49	68.0	4.0	0.92	0.82	76.9	13.1	0.82	0.25
35	93.2	10.5	128.3	14.6	0.73	0.72	90.3	11.8	1.03	0.89	103.7	13.1	0.90	0.81	68.0	4.0	1.37	2.64	107.1	21.9	0.87	0.48
36	54.7	2.4	68.7	3.0	0.80	0.82	61.9	4.2	0.88	0.58	64.4	4.7	0.85	0.52	87.0	16.9	0.63	0.14	64.8	2.5	0.84	0.98
37	51.2	3.0	68.7	3.0	0.75	1.00	61.9	4.2	0.83	0.71	64.4	4.7	0.80	0.63	87.0	16.9	0.59	0.18	64.8	2.5	0.79	1.19
38	68.3	4.6	90.9	8.1	0.75	0.56	62.9	5.4	1.09	0.84	78.4	7.3	0.87	0.63	87.5	17.1	0.78	0.27	79.9	13.6	0.86	0.34
39	64.6	2.9	90.9	8.1	0.71	0.36	62.9	5.4	1.03	0.53	78.4	7.3	0.82	0.40	87.5	17.1	0.74	0.17	79.9	13.6	0.81	0.21
40	85.6	3.9	135.2	15.6	0.63	0.25	74.4	12.3	1.15	0.32	106.3	13.7	0.80	0.28	88.3	17.3	0.97	0.22	110.0	22.4	0.78	0.17
41	85.4	8.5	135.2	15.6	0.63	0.54	74.4	12.3	1.15	0.69	106.3	13.7	0.80	0.62	88.3	17.3	0.97	0.49	110.0	22.4	0.78	0.38
42	16.1	1.1	29.6	4.8	0.54	0.23	27.2	4.4	0.59	0.25	29.8	6.3	0.54	0.18	39.2	23.6	0.41	0.05	25.9	3.2	0.62	0.35
43	14.3	1.2	29.6	4.8	0.48	0.26	27.2	4.4	0.53	0.28	29.8	6.3	0.48	0.20	39.2	23.6	0.37	0.05	25.9	3.2	0.55	0.38
44	68.1	12.2	98.3	25.1	0.69	0.49	44.8	23.0	1.52	0.53	73.1	27.4	0.93	0.44	42.0	25.0	1.62	0.49	72.6	37.4	0.94	0.33
45	65.5	12.8	98.3	25.1	0.67	0.51	44.8	23.0	1.46	0.56	73.1	27.4	0.90	0.47	42.0	25.0	1.56	0.51	72.6	37.4	0.90	0.34
46	15.2	1.1	28.6	4.9	0.53	0.22	26.0	4.4	0.58	0.24	28.6	6.4	0.53	0.17	37.5	24.1	0.41	0.04	24.9	3.3	0.61	0.33
47	12.7	1.2	28.6	4.9	0.44	0.24	26.0	4.4	0.49	0.27	28.6	6.4	0.44	0.18	37.5	24.1	0.34	0.05	24.9	3.3	0.51	0.36
48	33.6	5.9	51.5	13.4	0.65	0.44	27.5	7.4	1.22	0.79	43.1	12.8	0.78	0.46	38.7	24.8	0.87	0.24	40.4	22.8	0.83	0.26
49	32.1	4.7	51.5	13.4	0.62	0.35	27.5	7.4	1.17	0.62	43.1	12.8	0.74	0.36	38.7	24.8	0.83	0.19	40.4	22.8	0.79	0.20
50	48.4	11.1	97.3	25.6	0.50	0.43	43.9	23.9	1.10	0.46	71.9	28.5	0.67	0.39	40.4	25.6	1.20	0.43	71.6	38.3	0.68	0.29
51	53.7	11.1	97.3	25.6	0.55	0.43	43.9	23.9	1.22	0.46	71.9	28.5	0.75	0.39	40.4	25.6	1.33	0.43	71.6	38.3	0.75	0.29
52	33.8	1.2	48.1	3.8	0.70	0.32	49.5	4.2	0.68	0.29	52.2	5.0	0.65	0.24	69.5	18.2	0.49	0.07	44.9	2.7	0.75	0.45
53	33.8	1.8	48.1	3.8	0.70	0.46	49.5	4.2	0.68	0.42	52.2	5.0	0.65	0.35	69.5	18.2	0.49	0.10	44.9	2.7	0.75	0.66
54	56.3	4.8	71.0	10.4	0.79	0.47	50.7	5.8	1.11	0.83	66.6	8.4	0.85	0.58	70.2	18.5	0.80	0.26	60.4	16.6	0.93	0.29
55	59.6	5.0	71.0	10.4	0.84	0.49	50.7	5.8	1.18	0.87	66.6	8.4	0.90	0.60	70.2	18.5	0.85	0.27	60.4	16.6	0.99	0.30
56	88.8	11.9	116.8	19.9	0.76	0.60	63.3	14.4	1.40	0.82	95.4	16.6	0.93	0.71	71.2	18.8	1.25	0.63	91.6	27.5	0.97	0.43
57	74.2	9.2	116.8	19.9	0.64	0.46	63.3	14.4	1.17	0.64	95.4	16.6	0.78	0.55	71.2	18.8	1.04	0.49	91.6	27.5	0.81	0.33
58	44.8	1.7	58.3	3.5	0.77	0.49	61.9	4.2	0.72	0.41	64.5	4.7	0.69	0.36	86.0	16.6	0.52	0.10	55.4	2.5	0.81	0.68
59	39.6	1.8	58.3	3.5	0.68	0.52	61.9	4.2	0.64	0.43	64.5	4.7	0.61	0.38	86.0	16.6	0.46	0.11	55.4	2.5	0.71	0.71
60	70.0	4.7	81.2	9.5	0.86	0.49	62.9	5.4	1.11	0.85	78.9	7.4	0.89	0.63	86.6	16.8	0.81	0.28	70.9	14.9	0.99	0.31

* Not measured during the test; ** Not applicable for prediction of ultimate strain in unconfined columns.

Table 4.3 - Model predictions and model errors (ultimate stress and ultimate strain) according to C&S, P&M, Lee, SH and Ilki models (cont.).

Specimen	Experimental Results		Model Predictions																				
			C&S				P&M				Lee				SH				Ilki			
	$f_{cc\ exp}$ (MPa)	$\varepsilon_{cc\ exp}$ (‰)	$f_{cc\ calc}$ (MPa)	$\varepsilon_{cc\ calc}$ (‰)	ξ_f	ξ_ε	$f_{cc\ calc}$ (MPa)	$\varepsilon_{cc\ calc}$ (‰)	ξ_f	ξ_ε	$f_{cc\ calc}$ (MPa)	$\varepsilon_{cc\ calc}$ (‰)	ξ_f	ξ_ε	$f_{cc\ calc}$ (MPa)	$\varepsilon_{cc\ calc}$ (‰)	ξ_f	ξ_ε	$f_{cc\ calc}$ (MPa)	$\varepsilon_{cc\ calc}$ (‰)	ξ_f	ξ_ε
31	62.4	3.2	61.8	**	1.01	**	61.8	4.0	1.01	0.79	61.8	3.5	1.01	0.91	68.0	4.0	0.92	0.79	61.8	2.0	1.01	1.59
32	66.7	2.5	61.8	**	1.08	**	61.8	4.0	1.08	0.63	61.8	3.5	1.08	0.72	68.0	4.0	0.98	0.63	61.8	2.0	1.08	1.26
33	56.4	*	61.8	-	0.91	-	61.8	4.0	0.91	-	61.8	3.5	0.91	-	68.0	4.0	0.83	-	61.8	2.0	0.91	-
34	62.7	3.3	84.0	6.7	0.75	0.48	69.9	6.6	0.90	0.50	75.8	6.7	0.83	0.49	68.0	4.0	0.92	0.82	76.9	13.1	0.82	0.25
35	93.2	10.5	128.3	14.6	0.73	0.72	90.3	11.8	1.03	0.89	103.7	13.1	0.90	0.81	68.0	4.0	1.37	2.64	107.1	21.9	0.87	0.48
36	54.7	2.4	68.7	3.0	0.80	0.82	61.9	4.2	0.88	0.58	64.4	4.7	0.85	0.52	87.0	16.9	0.63	0.14	64.8	2.5	0.84	0.98
37	51.2	3.0	68.7	3.0	0.75	1.00	61.9	4.2	0.83	0.71	64.4	4.7	0.80	0.63	87.0	16.9	0.59	0.18	64.8	2.5	0.79	1.19
38	68.3	4.6	90.9	8.1	0.75	0.56	62.9	5.4	1.09	0.84	78.4	7.3	0.87	0.63	87.5	17.1	0.78	0.27	79.9	13.6	0.86	0.34
39	64.6	2.9	90.9	8.1	0.71	0.36	62.9	5.4	1.03	0.53	78.4	7.3	0.82	0.40	87.5	17.1	0.74	0.17	79.9	13.6	0.81	0.21
40	85.6	3.9	135.2	15.6	0.63	0.25	74.4	12.3	1.15	0.32	106.3	13.7	0.80	0.28	88.3	17.3	0.97	0.22	110.0	22.4	0.78	0.17
41	85.4	8.5	135.2	15.6	0.63	0.54	74.4	12.3	1.15	0.69	106.3	13.7	0.80	0.62	88.3	17.3	0.97	0.49	110.0	22.4	0.78	0.38
42	16.1	1.1	29.6	4.8	0.54	0.23	27.2	4.4	0.59	0.25	29.8	6.3	0.54	0.18	39.2	23.6	0.41	0.05	25.9	3.2	0.62	0.35
43	14.3	1.2	29.6	4.8	0.48	0.26	27.2	4.4	0.53	0.28	29.8	6.3	0.48	0.20	39.2	23.6	0.37	0.05	25.9	3.2	0.55	0.38
44	68.1	12.2	98.3	25.1	0.69	0.49	44.8	23.0	1.52	0.53	73.1	27.4	0.93	0.44	42.0	25.0	1.62	0.49	72.6	37.4	0.94	0.33
45	65.5	12.8	98.3	25.1	0.67	0.51	44.8	23.0	1.46	0.56	73.1	27.4	0.90	0.47	42.0	25.0	1.56	0.51	72.6	37.4	0.90	0.34
46	15.2	1.1	28.6	4.9	0.53	0.22	26.0	4.4	0.58	0.24	28.6	6.4	0.53	0.17	37.5	24.1	0.41	0.04	24.9	3.3	0.61	0.33
47	12.7	1.2	28.6	4.9	0.44	0.24	26.0	4.4	0.49	0.27	28.6	6.4	0.44	0.18	37.5	24.1	0.34	0.05	24.9	3.3	0.51	0.36
48	33.6	5.9	51.5	13.4	0.65	0.44	27.5	7.4	1.22	0.79	43.1	12.8	0.78	0.46	38.7	24.8	0.87	0.24	40.4	22.8	0.83	0.26
49	32.1	4.7	51.5	13.4	0.62	0.35	27.5	7.4	1.17	0.62	43.1	12.8	0.74	0.36	38.7	24.8	0.83	0.19	40.4	22.8	0.79	0.20
50	48.4	11.1	97.3	25.6	0.50	0.43	43.9	23.9	1.10	0.46	71.9	28.5	0.67	0.39	40.4	25.6	1.20	0.43	71.6	38.3	0.68	0.29
51	53.7	11.1	97.3	25.6	0.55	0.43	43.9	23.9	1.22	0.46	71.9	28.5	0.75	0.39	40.4	25.6	1.33	0.43	71.6	38.3	0.75	0.29
52	33.8	1.2	48.1	3.8	0.70	0.32	49.5	4.2	0.68	0.29	52.2	5.0	0.65	0.24	69.5	18.2	0.49	0.07	44.9	2.7	0.75	0.45
53	33.8	1.8	48.1	3.8	0.70	0.46	49.5	4.2	0.68	0.42	52.2	5.0	0.65	0.35	69.5	18.2	0.49	0.10	44.9	2.7	0.75	0.66
54	56.3	4.8	71.0	10.4	0.79	0.47	50.7	5.8	1.11	0.83	66.6	8.4	0.85	0.58	70.2	18.5	0.80	0.26	60.4	16.6	0.93	0.29
55	59.6	5.0	71.0	10.4	0.84	0.49	50.7	5.8	1.18	0.87	66.6	8.4	0.90	0.60	70.2	18.5	0.85	0.27	60.4	16.6	0.99	0.30
56	88.8	11.9	116.8	19.9	0.76	0.60	63.3	14.4	1.40	0.82	95.4	16.6	0.93	0.71	71.2	18.8	1.25	0.63	91.6	27.5	0.97	0.43
57	74.2	9.2	116.8	19.9	0.64	0.46	63.3	14.4	1.17	0.64	95.4	16.6	0.78	0.55	71.2	18.8	1.04	0.49	91.6	27.5	0.81	0.33
58	44.8	1.7	58.3	3.5	0.77	0.49	61.9	4.2	0.72	0.41	64.5	4.7	0.69	0.36	86.0	16.6	0.52	0.10	55.4	2.5	0.81	0.68
59	39.6	1.8	58.3	3.5	0.68	0.52	61.9	4.2	0.64	0.43	64.5	4.7	0.61	0.38	86.0	16.6	0.46	0.11	55.4	2.5	0.71	0.71
60	70.0	4.7	81.2	9.5	0.86	0.49	62.9	5.4	1.11	0.85	78.9	7.4	0.89	0.63	86.6	16.8	0.81	0.28	70.9	14.9	0.99	0.31

* Not measured during the test; ** Not applicable for prediction of ultimate strain in unconfined columns.

Table 4.3 - Model predictions and model errors (ultimate stress and ultimate strain) according to C&S, P&M, Lee, SH and Ilki models (cont.).

Specimen	Experimental Results		Model Predictions																				
			C&S				P&M				Lee				SH				Ilki			
	$f_{cc\ exp}$ (MPa)	$\varepsilon_{cc\ exp}$ (‰)	$f_{cc\ calc}$ (MPa)	$\varepsilon_{cc\ calc}$ (‰)	ξ_f	ξ_ε	$f_{cc\ calc}$ (MPa)	$\varepsilon_{cc\ calc}$ (‰)	ξ_f	ξ_ε	$f_{cc\ calc}$ (MPa)	$\varepsilon_{cc\ calc}$ (‰)	ξ_f	ξ_ε	$f_{cc\ calc}$ (MPa)	$\varepsilon_{cc\ calc}$ (‰)	ξ_f	ξ_ε	$f_{cc\ calc}$ (MPa)	$\varepsilon_{cc\ calc}$ (‰)	ξ_f	ξ_ε
61	70.3	3.9	81.2	9.5	0.87	0.41	62.9	5.4	1.12	0.72	78.9	7.4	0.89	0.53	86.6	16.8	0.81	0.23	70.9	14.9	0.99	0.26
62	82.9	5.7	127.0	18.2	0.65	0.31	74.5	12.3	1.11	0.46	107.8	14.0	0.77	0.41	87.5	17.0	0.95	0.34	102.1	24.6	0.81	0.23
63	81.4	5.2	127.0	18.2	0.64	0.29	74.5	12.3	1.09	0.42	107.8	14.0	0.76	0.37	87.5	17.0	0.93	0.31	102.1	24.6	0.80	0.21
64	39.8	5.5	27.3	3.9	1.45	1.41	26.1	4.6	1.53	1.20	28.0	5.7	1.42	0.97	41.2	28.1	0.97	0.20	25.5	3.6	1.56	1.55
65	33.5	3.8	27.3	3.9	1.22	0.97	26.1	4.6	1.28	0.83	28.0	5.7	1.20	0.66	41.2	28.1	0.81	0.13	25.5	3.6	1.31	1.07
66	61.8	19.3	45.4	11.0	1.36	1.75	27.4	7.4	2.25	2.61	39.3	10.8	1.57	1.79	41.9	28.6	1.48	0.67	37.7	20.8	1.64	0.93
67	65.8	20.9	45.4	11.0	1.45	1.90	27.4	7.4	2.40	2.83	39.3	10.8	1.67	1.94	41.9	28.6	1.57	0.73	37.7	20.8	1.74	1.01
68	92.7	28.8	81.4	21.2	1.14	1.36	42.4	22.7	2.19	1.27	62.0	23.1	1.50	1.24	43.0	29.1	2.16	0.99	62.2	34.4	1.49	0.84
69	88.9	25.6	81.4	21.2	1.09	1.21	42.4	22.7	2.10	1.13	62.0	23.1	1.43	1.11	43.0	29.1	2.07	0.88	62.2	34.4	1.43	0.74
70	54.7	2.9	47.3	3.0	1.16	0.96	49.6	4.3	1.10	0.68	51.5	4.7	1.06	0.63	75.6	21.0	0.72	0.14	45.5	2.8	1.20	1.04
71	57.5	2.9	47.3	3.0	1.22	0.94	49.6	4.3	1.16	0.67	51.5	4.7	1.12	0.62	75.6	21.0	0.76	0.14	45.5	2.8	1.27	1.02
72	80.0	5.3	65.3	8.6	1.22	0.61	50.6	5.8	1.58	0.91	62.8	7.3	1.27	0.72	76.1	21.2	1.05	0.25	57.7	15.0	1.39	0.35
73	84.1	8.6	65.3	8.6	1.29	1.01	50.6	5.8	1.66	1.49	62.8	7.3	1.34	1.18	76.1	21.2	1.11	0.41	57.7	15.0	1.46	0.57
74	96.3	8.9	101.4	16.5	0.95	0.54	62.2	13.8	1.55	0.64	85.5	13.8	1.13	0.64	76.7	21.4	1.26	0.41	82.2	24.7	1.17	0.36
75	91.2	8.3	101.4	16.5	0.90	0.50	62.2	13.8	1.47	0.60	85.5	13.8	1.07	0.60	76.7	21.4	1.19	0.39	82.2	24.7	1.11	0.33
76	70.9	3.0	57.8	2.8	1.23	1.06	61.9	4.2	1.15	0.70	63.8	4.4	1.11	0.67	93.3	19.1	0.76	0.16	56.0	2.7	1.27	1.12
77	69.3	2.9	57.8	2.8	1.20	1.03	61.9	4.2	1.12	0.68	63.8	4.4	1.09	0.65	93.3	19.1	0.74	0.15	56.0	2.7	1.24	1.09
78	89.4	3.5	75.8	7.8	1.18	0.45	62.9	5.4	1.42	0.65	75.2	6.6	1.19	0.54	93.7	19.2	0.95	0.18	68.2	13.5	1.31	0.26
79	90.9	3.3	75.8	7.8	1.20	0.42	62.9	5.4	1.45	0.60	75.2	6.6	1.21	0.50	93.7	19.2	0.97	0.17	68.2	13.5	1.33	0.24
80	100.8	4.1	111.8	15.1	0.90	0.27	73.4	11.8	1.37	0.35	97.9	11.7	1.03	0.35	94.2	19.4	1.07	0.21	92.7	22.1	1.09	0.19
81	99.3	4.8	111.8	15.1	0.89	0.32	73.4	11.8	1.35	0.40	97.9	11.7	1.01	0.41	94.2	19.4	1.05	0.25	92.7	22.1	1.07	0.22
82	26.2	2.0	29.3	**	0.89	**	32.0	4.0	0.82	0.51	32.0	3.5	0.82	0.58	35.2	4.0	0.74	0.51	26.2	2.0	1.00	1.01
83	38.8	11.2	44.5	7.1	0.87	1.57	37.8	7.4	1.03	1.50	41.6	7.4	0.93	1.51	35.2	4.0	1.10	2.80	36.5	16.4	1.06	0.68
84	53.2	17.5	59.7	11.6	0.89	1.51	44.8	10.9	1.19	1.60	51.2	11.3	1.04	1.55	35.2	4.0	1.51	4.37	46.8	22.8	1.14	0.77
85	26.3	3.3	49.0	8.5	0.54	0.38	34.4	8.0	0.76	0.41	39.4	9.5	0.67	0.34	53.6	53.3	0.49	0.06	55.6	13.2	0.47	0.25
86	40.1	15.2	71.5	13.3	0.56	1.14	42.0	12.0	0.95	1.27	50.0	14.5	0.80	1.05	61.5	87.9	0.65	0.17	94.1	23.4	0.43	0.65
87	46.8	11.6	64.2	12.7	0.73	0.92	36.6	10.5	1.28	1.11	49.0	10.4	0.96	1.12	55.6	54.1	0.84	0.22	65.9	27.6	0.71	0.42
88	54.3	16.5	86.7	16.7	0.63	0.98	44.8	14.2	1.21	1.16	59.6	14.5	0.91	1.14	65.3	88.9	0.83	0.19	104.4	36.8	0.52	0.45
89	60.2	15.8	79.4	16.4	0.76	0.97	43.1	16.1	1.40	0.98	58.6	14.3	1.03	1.11	57.1	54.6	1.05	0.29	76.2	34.0	0.79	0.47
90	68.8	19.2	101.9	19.9	0.68	0.96	52.1	19.3	1.32	0.99	69.2	16.1	0.99	1.19	68.1	89.6	1.01	0.21	114.7	42.8	0.60	0.45

* Not measured during the test; ** Not applicable for prediction of ultimate strain in unconfined columns.

Table 4.3 - Model predictions and model errors (ultimate stress and ultimate strain) according to C&S, P&M, Lee, SH and Ilki models (cont.).

Specimen	Experimental Results		Model Predictions																				
			C&S				P&M				Lee				SH				Ilki			
	$f_{cc\ exp}$ (MPa)	$\varepsilon_{cc\ exp}$ (‰)	$f_{cc\ calc}$ (MPa)	$\varepsilon_{cc\ calc}$ (‰)	ξ_f	ξ_ε	$f_{cc\ calc}$ (MPa)	$\varepsilon_{cc\ calc}$ (‰)	ξ_f	ξ_ε	$f_{cc\ calc}$ (MPa)	$\varepsilon_{cc\ calc}$ (‰)	ξ_f	ξ_ε	$f_{cc\ calc}$ (MPa)	$\varepsilon_{cc\ calc}$ (‰)	ξ_f	ξ_ε	$f_{cc\ calc}$ (MPa)	$\varepsilon_{cc\ calc}$ (‰)	ξ_f	ξ_ε
91	23.0	1.4	32.3	**	0.71	**	38.0	4.0	0.61	0.35	38.0	3.5	0.61	0.40	41.8	4.0	0.55	0.35	26.4	2.0	0.87	0.70
92	24.2	*	32.3	-	0.75	-	38.0	4.0	0.64	-	38.0	3.5	0.64	-	41.8	4.0	0.58	-	26.4	2.0	0.92	-
93	31.9	2.2	32.3	**	0.99	**	38.0	4.0	0.84	0.55	38.0	3.5	0.84	0.63	41.8	4.0	0.76	0.55	26.4	2.0	1.21	1.10
94	75.8	12.8	80.4	15.7	0.94	0.82	59.1	13.2	1.28	0.97	68.3	13.9	1.11	0.92	41.8	4.0	1.81	3.20	59.0	28.4	1.28	0.45
95	69.0	9.9	80.4	15.7	0.86	0.63	59.1	13.2	1.17	0.75	68.3	13.9	1.01	0.71	41.8	4.0	1.65	2.48	59.0	28.4	1.17	0.35
96	83.8	12.5	80.4	15.7	1.04	0.80	59.1	13.2	1.42	0.95	68.3	13.9	1.23	0.90	41.8	4.0	2.01	3.13	59.0	28.4	1.42	0.44
97	107.8	18.7	104.4	20.9	1.03	0.90	71.6	17.7	1.50	1.05	83.4	19.0	1.29	0.98	41.8	4.0	2.58	4.68	75.4	34.7	1.43	0.54
98	22.2	2.0	34.7	1.9	0.64	1.03	38.0	4.1	0.59	0.49	38.9	4.1	0.57	0.48	43.9	23.7	0.51	0.08	27.5	2.4	0.81	0.82
99	26.8	2.0	34.7	1.9	0.77	1.03	38.0	4.1	0.71	0.49	38.9	4.1	0.69	0.48	43.9	23.7	0.61	0.08	27.5	2.4	0.98	0.82
100	20.6	2.3	34.7	1.9	0.59	1.19	38.0	4.1	0.54	0.56	38.9	4.1	0.53	0.56	43.9	23.7	0.47	0.10	27.5	2.4	0.75	0.95
101	22.2	2.0	33.9	1.5	0.65	1.37	38.0	4.0	0.58	0.50	38.6	3.9	0.58	0.51	43.8	18.0	0.51	0.11	26.6	2.1	0.84	0.96
102	26.2	1.7	33.9	1.5	0.77	1.17	38.0	4.0	0.69	0.42	38.6	3.9	0.68	0.43	43.8	18.0	0.60	0.09	26.6	2.1	0.99	0.82
103	26.7	1.9	37.1	3.1	0.72	0.60	38.1	4.4	0.70	0.44	39.8	4.7	0.67	0.40	44.3	39.2	0.60	0.05	31.3	3.9	0.85	0.49
104	29.1	2.2	37.1	3.1	0.78	0.70	38.1	4.4	0.77	0.50	39.8	4.7	0.73	0.46	44.3	39.2	0.66	0.06	31.3	3.9	0.93	0.57
105	81.1	13.1	82.8	16.3	0.98	0.81	58.3	20.5	1.39	0.64	69.2	14.2	1.17	0.92	44.5	24.0	1.82	0.55	60.2	28.8	1.35	0.46
106	74.8	11.8	82.8	16.3	0.90	0.73	58.3	20.5	1.28	0.57	69.2	14.2	1.08	0.83	44.5	24.0	1.68	0.49	60.2	28.8	1.24	0.41
107	80.8	15.0	82.0	16.1	0.99	0.93	58.2	20.5	1.39	0.73	68.9	14.1	1.17	1.07	44.1	18.2	1.83	0.82	59.2	28.4	1.36	0.53
108	81.5	13.5	85.2	16.8	0.96	0.80	58.8	20.8	1.39	0.65	70.1	14.5	1.16	0.93	45.4	39.7	1.80	0.34	64.0	30.2	1.27	0.45
109	34.9	2.2	32.3	**	1.08	**	35.2	4.0	0.99	0.55	35.2	3.5	0.99	0.63	38.7	4.0	0.90	0.55	34.9	2.0	1.00	1.10
110	67.8	11.1	66.2	12.0	1.02	0.92	49.5	11.0	1.37	1.01	56.6	11.5	1.20	0.96	38.7	4.0	1.75	2.78	58.0	20.9	1.17	0.53
111	33.2	2.7	36.2	2.6	0.92	1.02	35.3	4.3	0.94	0.63	36.7	4.6	0.90	0.59	48.3	27.2	0.69	0.10	37.7	2.8	0.88	0.96
112	50.7	9.1	53.1	8.6	0.95	1.06	36.4	6.3	1.39	1.43	47.4	8.1	1.07	1.13	48.7	27.4	1.04	0.33	49.3	15.9	1.03	0.57
113	70.9	15.5	70.1	13.0	1.01	1.19	40.7	10.9	1.74	1.42	58.1	12.1	1.22	1.28	49.0	27.6	1.45	0.56	60.8	21.7	1.17	0.71
114	75.5	16.6	87.1	16.8	0.87	0.99	49.3	17.4	1.53	0.95	68.8	16.1	1.10	1.03	49.2	27.7	1.53	0.60	72.4	26.2	1.04	0.63
115	93.3	22.5	104.1	20.3	0.90	1.11	62.8	25.7	1.49	0.87	79.5	20.1	1.17	1.12	49.5	27.8	1.89	0.81	83.9	30.1	1.11	0.75
116	39.7	6.3	56.2	12.3	0.71	0.51	31.8	8.3	1.25	0.76	45.6	10.6	0.87	0.59	48.4	35.2	0.82	0.18	48.5	22.7	0.82	0.28
117	51.7	12.4	71.8	15.5	0.72	0.80	37.0	11.2	1.40	1.11	53.0	12.2	0.98	1.01	56.0	60.7	0.92	0.20	74.3	30.6	0.70	0.41
118	56.2	15.1	85.9	18.9	0.65	0.80	40.9	14.7	1.37	1.03	58.4	15.8	0.96	0.96	59.4	86.0	0.95	0.18	99.8	40.1	0.56	0.38
119	34.1	2.2	46.9	8.7	0.73	0.25	33.8	7.8	1.01	0.28	38.9	9.4	0.88	0.23	51.9	45.3	0.66	0.05	54.7	12.3	0.62	0.18
120	38.4	2.4	50.7	8.2	0.76	0.29	38.0	7.3	1.01	0.33	43.2	8.7	0.89	0.28	58.4	42.6	0.66	0.06	58.3	11.1	0.66	0.22

* Not measured during the test; ** Not applicable for prediction of ultimate strain in unconfined columns.

Table 4.3 - Model predictions and model errors (ultimate stress and ultimate strain) according to C&S, P&M, Lee, SH and Ilki models (cont.).

Specimen	Experimental Results		Model Predictions																				
			C&S				P&M				Lee				SH				Ilki			
	$f_{cc\ exp}$ (MPa)	$\varepsilon_{cc\ exp}$ (‰)	$f_{cc\ calc}$ (MPa)	$\varepsilon_{cc\ calc}$ (‰)	ξ_f	ξ_ε	$f_{cc\ calc}$ (MPa)	$\varepsilon_{cc\ calc}$ (‰)	ξ_f	ξ_ε	$f_{cc\ calc}$ (MPa)	$\varepsilon_{cc\ calc}$ (‰)	ξ_f	ξ_ε	$f_{cc\ calc}$ (MPa)	$\varepsilon_{cc\ calc}$ (‰)	ξ_f	ξ_ε	$f_{cc\ calc}$ (MPa)	$\varepsilon_{cc\ calc}$ (‰)	ξ_f	ξ_ε
121	45.0	7.7	65.4	13.9	0.69	0.55	36.1	10.3	1.25	0.75	50.6	11.2	0.89	0.68	54.2	46.2	0.83	0.17	67.3	28.0	0.67	0.27
122	50.6	8.4	69.2	13.2	0.73	0.64	40.1	9.5	1.26	0.88	54.9	10.3	0.92	0.81	60.5	43.3	0.84	0.19	70.9	25.7	0.71	0.33
123	69.9	20.8	83.9	18.4	0.83	1.13	42.4	15.9	1.65	1.31	62.2	16.0	1.12	1.30	55.9	46.7	1.25	0.45	79.9	35.0	0.88	0.59
124	48.0	3.1	63.6	7.2	0.76	0.43	52.6	6.3	0.91	0.49	58.0	7.2	0.83	0.43	80.6	36.0	0.60	0.09	70.9	8.4	0.68	0.37
125	69.4	8.8	82.1	11.6	0.85	0.76	54.4	7.9	1.28	1.11	69.7	8.3	1.00	1.06	82.2	36.5	0.84	0.24	83.5	20.7	0.83	0.43
126	35.1	2.8	57.2	11.7	0.61	0.24	36.1	10.3	0.97	0.27	42.8	12.6	0.82	0.22	53.4	63.3	0.66	0.04	73.2	19.2	0.48	0.15
127	42.0	3.0	61.0	11.1	0.69	0.27	40.1	9.5	1.05	0.31	47.1	11.5	0.89	0.26	60.1	59.4	0.70	0.05	76.9	17.1	0.55	0.18
128	49.7	13.2	75.7	16.5	0.66	0.80	38.7	12.8	1.28	1.03	54.5	12.8	0.91	1.03	57.0	64.5	0.87	0.20	85.8	34.9	0.58	0.38
129	56.3	10.3	79.5	15.7	0.71	0.66	42.6	11.7	1.32	0.88	58.8	11.7	0.96	0.88	63.3	60.4	0.89	0.17	89.4	31.8	0.63	0.32
130	69.8	18.4	98.0	19.7	0.71	0.93	49.3	16.7	1.42	1.10	70.4	15.9	0.99	1.15	65.7	61.0	1.06	0.30	102.0	38.3	0.68	0.48
131	67.0	15.5	82.4	16.8	0.81	0.92	45.9	14.3	1.46	1.09	61.1	12.6	1.10	1.23	130.1	53.1	0.52	0.29	91.9	33.3	0.73	0.47
132	49.0	2.5	73.9	9.7	0.66	0.26	54.4	7.9	0.90	0.32	61.9	9.2	0.79	0.27	82.9	50.0	0.59	0.05	89.4	12.7	0.55	0.20
133	73.0	10.4	92.4	13.7	0.79	0.76	56.6	9.5	1.29	1.10	73.6	9.3	0.99	1.11	85.3	50.6	0.86	0.21	102.0	24.9	0.72	0.42
134	92.4	16.4	110.9	17.2	0.83	0.95	62.4	13.0	1.48	1.26	85.2	12.3	1.08	1.33	87.2	51.0	1.06	0.32	114.6	30.4	0.81	0.54
135	81.4	12.9	95.0	14.7	0.86	0.88	59.4	11.3	1.37	1.14	75.9	9.9	1.07	1.30	173.0	44.5	0.47	0.29	104.5	26.2	0.78	0.49
136	29.1	22.0	38.2	12.0	0.76	1.83	17.4	10.8	1.67	2.04	27.5	14.1	1.06	1.56	23.9	43.2	1.22	0.51	29.2	27.5	1.00	0.80
137	30.6	24.0	38.6	11.9	0.79	2.01	17.8	10.6	1.72	2.26	27.8	13.9	1.10	1.73	24.4	42.7	1.25	0.56	29.5	27.1	1.04	0.89
138	54.7	45.0	67.5	20.9	0.81	2.15	38.0	37.4	1.44	1.20	46.1	28.9	1.19	1.56	26.7	43.8	2.05	1.03	49.2	42.8	1.11	1.05
139	59.7	54.0	67.8	20.7	0.88	2.60	38.1	36.8	1.57	1.47	46.4	28.4	1.29	1.90	27.1	43.4	2.20	1.24	49.4	42.3	1.21	1.28
140	85.2	65.0	95.7	28.8	0.89	2.25	74.6	72.8	1.14	0.89	63.7	45.3	1.34	1.44	28.0	45.7	3.04	1.42	68.3	54.9	1.25	1.18
141	91.9	66.0	96.5	28.3	0.95	2.34	74.2	69.3	1.24	0.95	64.5	43.2	1.43	1.53	28.9	44.4	3.18	1.49	69.0	53.3	1.33	1.24
142	77.6	34.0	96.0	20.3	0.81	1.67	51.0	27.0	1.52	1.26	64.3	20.8	1.21	1.63	48.5	73.6	1.60	0.46	88.1	43.6	0.88	0.78
143	72.6	28.0	83.3	17.6	0.87	1.59	46.6	23.9	1.56	1.17	59.5	18.6	1.22	1.51	43.7	43.0	1.66	0.65	65.8	34.1	1.10	0.82
144	72.0	33.0	79.4	16.7	0.91	1.97	45.4	22.9	1.59	1.44	58.0	17.9	1.24	1.85	41.9	32.6	1.72	1.01	59.3	31.3	1.21	1.05
145	94.5	45.0	108.2	22.8	0.87	1.97	74.4	41.7	1.27	1.08	76.2	26.4	1.24	1.70	43.1	33.1	2.19	1.36	78.9	39.5	1.20	1.14
146	32.0	2.8	32.8	3.8	0.98	0.74	32.2	5.1	0.99	0.55	34.0	5.3	0.94	0.53	65.3	42.3	0.49	0.07	33.8	4.5	0.95	0.62
147	54.3	11.1	70.2	14.6	0.77	0.76	45.6	15.7	1.19	0.71	58.7	12.9	0.92	0.86	71.1	41.3	0.76	0.27	59.9	25.5	0.91	0.43
148	54.5	4.3	73.2	15.4	0.74	0.28	53.8	21.3	1.01	0.20	61.4	9.2	0.89	0.47	71.2	64.6	0.77	0.07	62.8	26.8	0.87	0.16
149	15.3	3.4	20.1	6.3	0.76	0.54	16.0	6.0	0.96	0.57	18.4	8.3	0.83	0.41	26.3	46.9	0.58	0.07	20.1	7.2	0.76	0.47
150	31.1	9.5	34.3	13.1	0.91	0.72	17.0	8.9	1.82	1.07	27.3	13.5	1.14	0.71	27.6	47.9	1.13	0.20	29.7	27.1	1.05	0.35
151	43.3	14.4	76.6	28.1	0.57	0.51	37.2	36.8	1.17	0.39	53.9	36.1	0.80	0.40	30.2	49.6	1.43	0.29	58.5	48.6	0.74	0.30

4.2. Prediction of the Stress-Strain Curve

In order to investigate the concrete stress-strain behavior according to the models described previously (C&S, P&M, Lee, P&M, and Ilki models), 10 columns were selected in the database for comparison between experimental and the corresponding analytical stress-strain curve. Table 4.4 presents the selected columns and their main parameters related to confinement. In this table, the first column corresponds to the specimen identification used in this study (specimens 1 through 151, see Table 4.2), and the second column corresponds to the original identification of the specimen. Due to the upper limit for the ratio, $f_{\ell F} / f_{\ell s}$, in the Lee model, all columns in Table 4.4 have ratios, $f_{\ell F} / f_{\ell s} < 5$.

Table 4.4 - Confinement parameters associated to the selected columns.

Spec. ID	Original ID	f'_c (MPa)	ρ_{sL} (%)	s (mm)	ρ_{sw} (%)	ρ_F (%)	$f_{\ell s}$ (MPa)	$f_{\ell F}$ (MPa)	$f_{\ell F}/f_{\ell s}$	$f_{\ell s}/f'_c$	$f_{\ell F}/f'_c$	f_{cc}/f'_c
04	C-FRP	38.3	2.54	50	2.97	0.17	7.01	2.94	0.42	0.18	0.08	1.63
87	C1S50	32.0	1.06	50	0.98	0.27	3.71	4.79	1.29	0.12	0.15	1.46
90	C2S25	35.2	1.06	25	1.96	0.48	7.42	9.58	1.29	0.21	0.27	1.95
118	A1NP2C	31.7	1.67	45	2.49	0.34	7.50	5.83	0.78	0.24	0.18	1.77
123	C4NP4C	31.7	1.67	100	1.59	0.68	3.62	11.66	3.22	0.11	0.37	2.21
128	C2NP2C	31.7	1.67	65	1.59	0.34	5.56	5.82	1.05	0.18	0.18	1.57
130	C2N1P4C	36.0	1.67	65	2.44	0.68	2.56	11.66	4.55	0.07	0.32	1.94
134	C2MP4C	50.8	1.67	65	2.44	0.68	5.56	11.66	2.10	0.11	0.23	1.82
136	LSR-C-1-a	15,1	0.96	145	0.69	0.26	1.65	4.53	2.75	0.11	0.30	1.93
150	PC01S'0	15.5	2.00	100	0.46	0.23	1.42	4.44	3.13	0.09	0.29	2.00

An important issue in the prediction of stress-strain curve f_c-ε_c is the unconfined concrete strength f_{c0}. Usually, it is assumed as the concrete strength of standard cylinders, ignoring size effects. Regarding to the four models considered herein, that presented stress-strain curves, only C&S model considers size effects, introducing a factor α for correction of the strength given by standard cylinders, i.e. $f_{c0} = \alpha f'_c$.; in all other models, it is assumed $f_{c0} = f'_c$. In the absence of further directions given in the model, the strain ε_{c0} corresponding to f_{c0} is adopted as 0.002.

Figures 4.2 - 4.11 show the comparison of f_c- ε_c curves according to the selected models and the corresponding experimental curve of columns C-FRP (I) C1S50 (III) C2S25 (III) A1NP2C (V), C4NP4C (V), C2NP2C (V), C2N1P4C (V), C2MP4C (V), LSR-C-1-a (VI) and PC01S'0 (VIII), respectively. For better visualization of the resulting stress-strain diagram, the horizontal axis in each figure has been truncated. This is due to the behavior of the SH model that largely overestimates the ultimate strain; this can be seen in the insert that accompanies each plot.

From these figures, it can be observed that, as already mentioned, SH model largely overestimates ultimate strain. Regarding the other three models: (i) with exception of column column R-CFRP (Fig. 4.2) and column PC01S'0 (Fig. 4.11), C&S model always overestimates column resistance; (ii) a comparison between Lee model and P&M model shows that the former best represents the experimental results for both the shape of the stress-strain curve and ultimate conditions, displaying a very accurate fit, as in the A1NP2C and C2MP4C A1NP2C, C2NP2C, C2N1P4C and C2MP4C columns, Figs. 4.5, 4.7, 4.8 and 4.9, respectively.

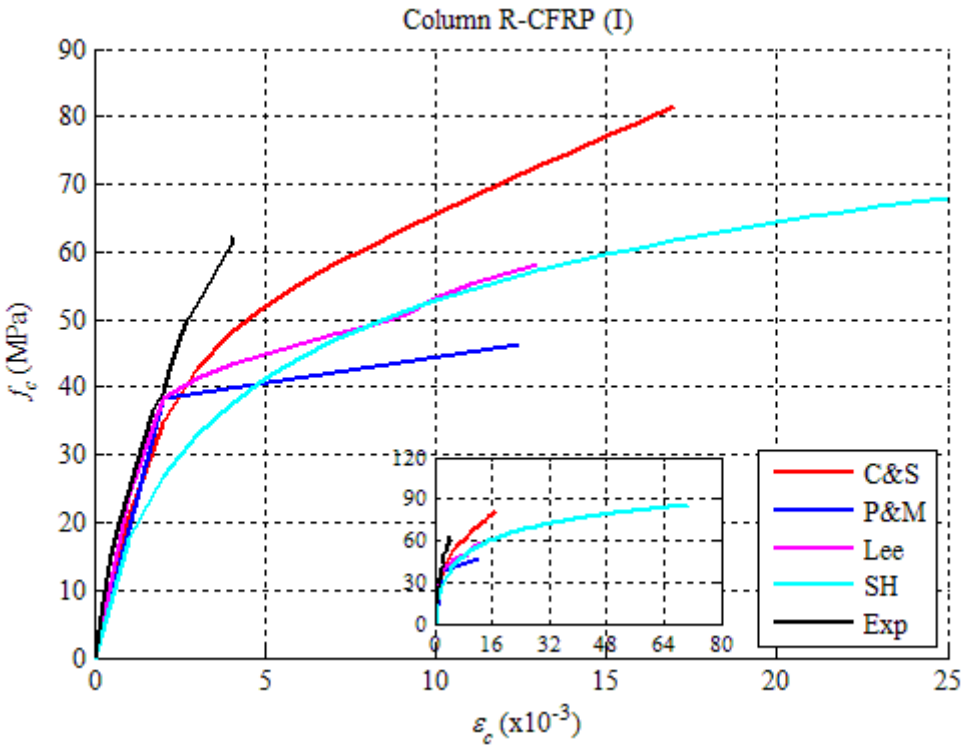

Figure 4.2 - Comparison of f_c-ε_c curves according to the selected models and the experimental curve of column R-CFRP (I).

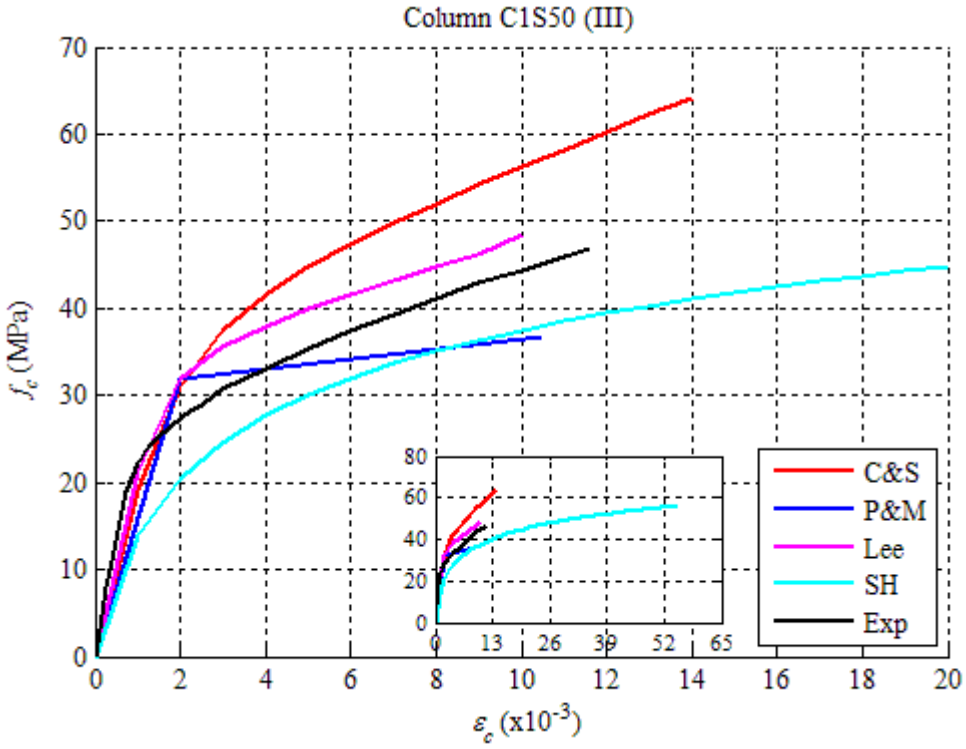

Figure 4.3 - Comparison of f_c-ε_c curves according to the selected models and experimental curve of column C1S50 (III).

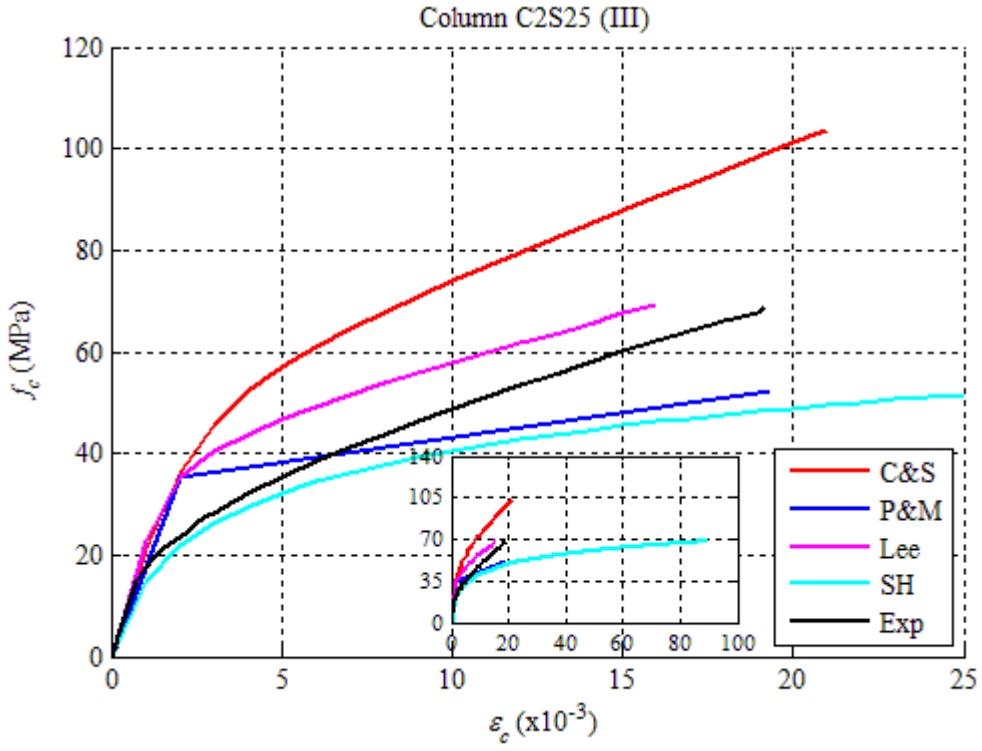

Figure 4.4 - Comparison of f_c-ε_c curves according to the selected models and experimental curve of column C2S25 (III).

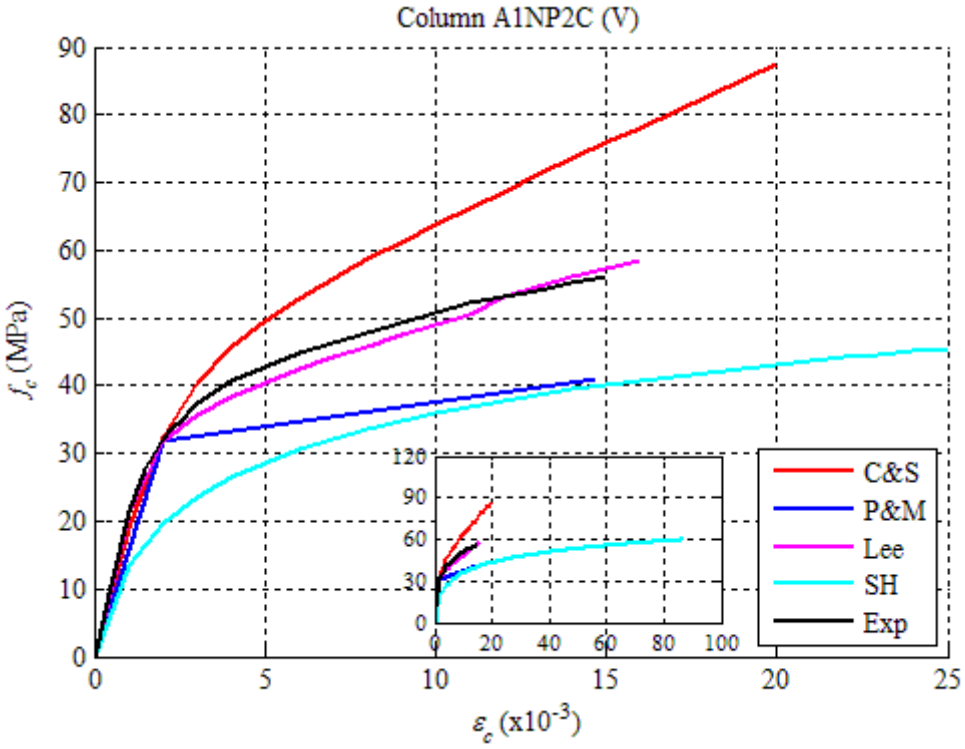

Figure 4.5 - Comparison of f_c-ε_c curves according to the selected models and experimental curve of column A1NP2C (V).

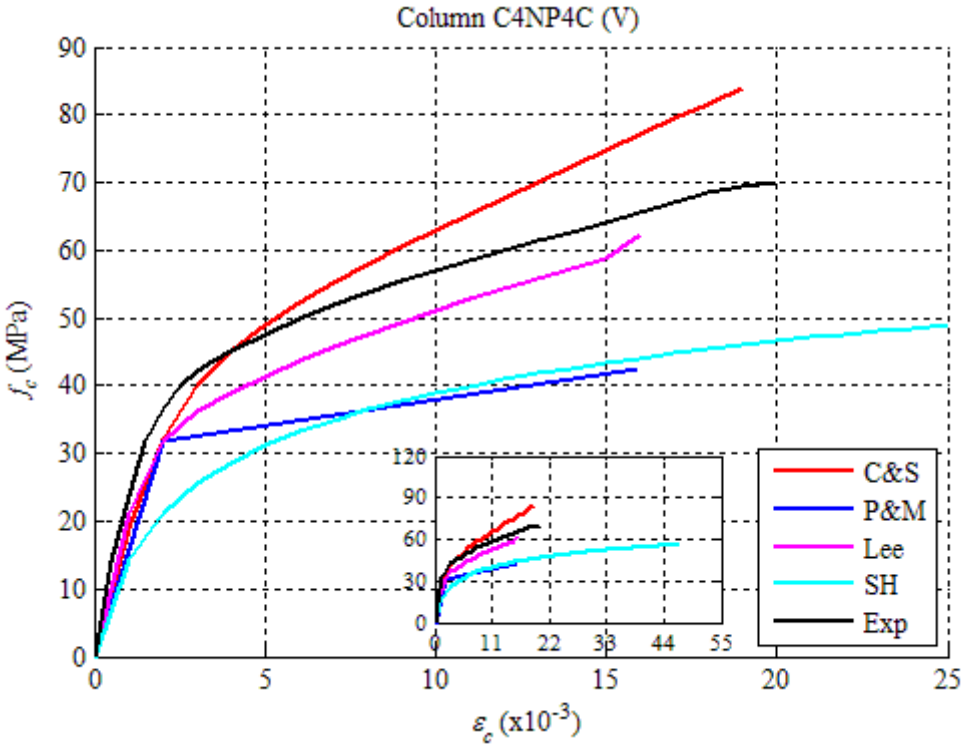

Figure 4.6 - Comparison of f_c-ε_c curves according to the selected models and the experimental curve of column C4NP4C (V).

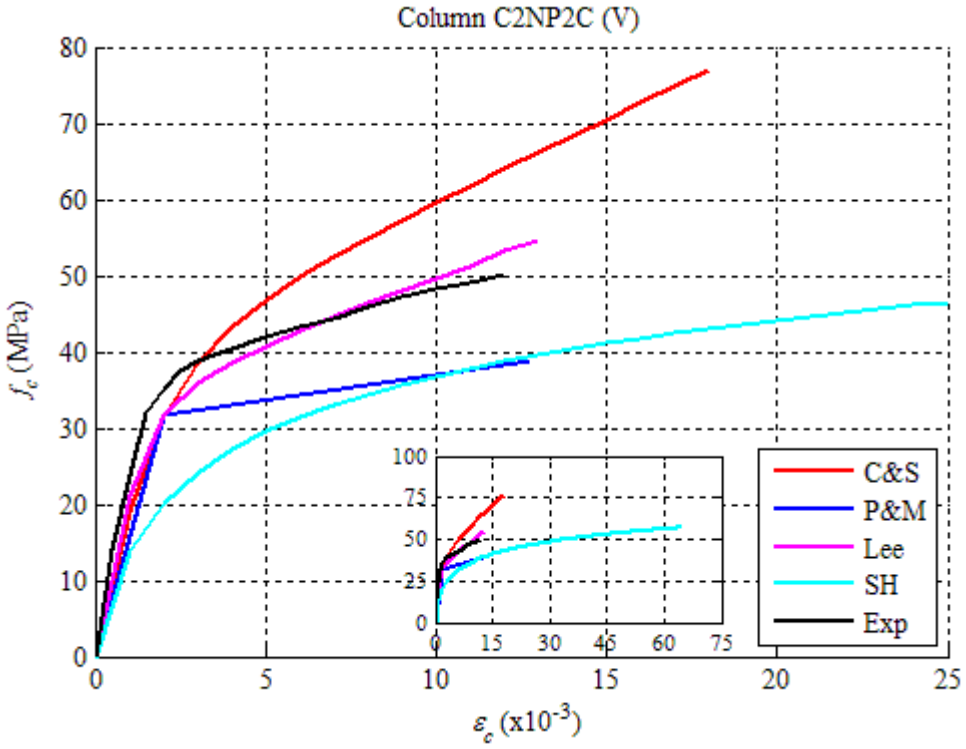

Figure 4.7 - Comparison of f_c-ε_c curves according to the selected models and experimental curve of column C2NP2C (V).

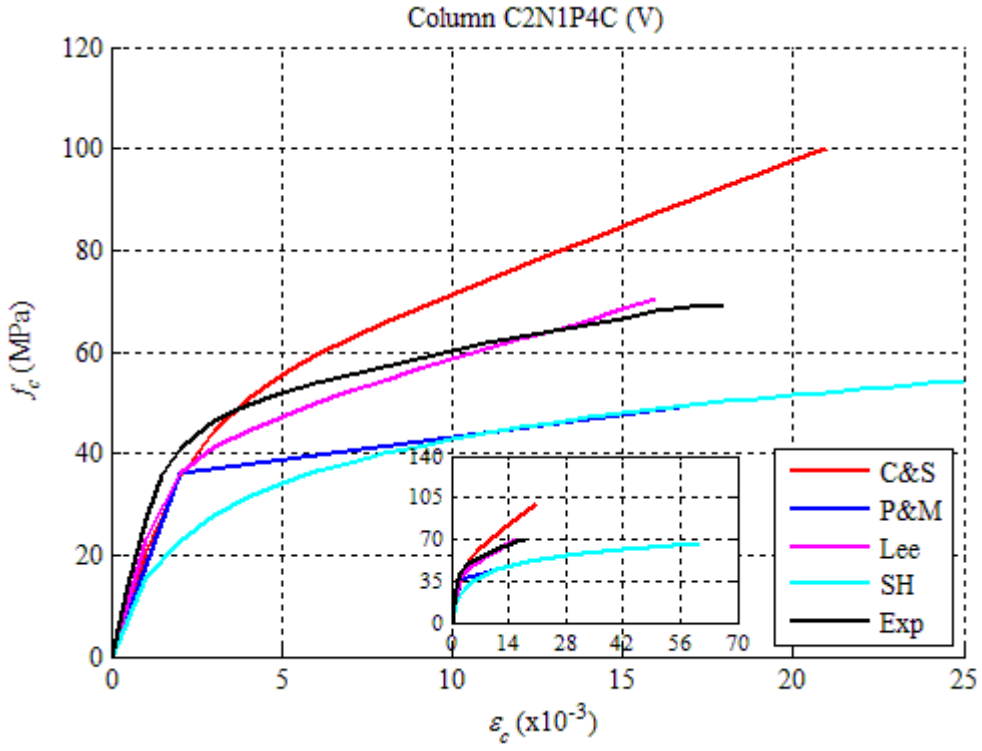

Figure 4.8 - Comparison of f_c-ε_c curves according to the selected models and the experimental curve of column C2N1P4C (V).

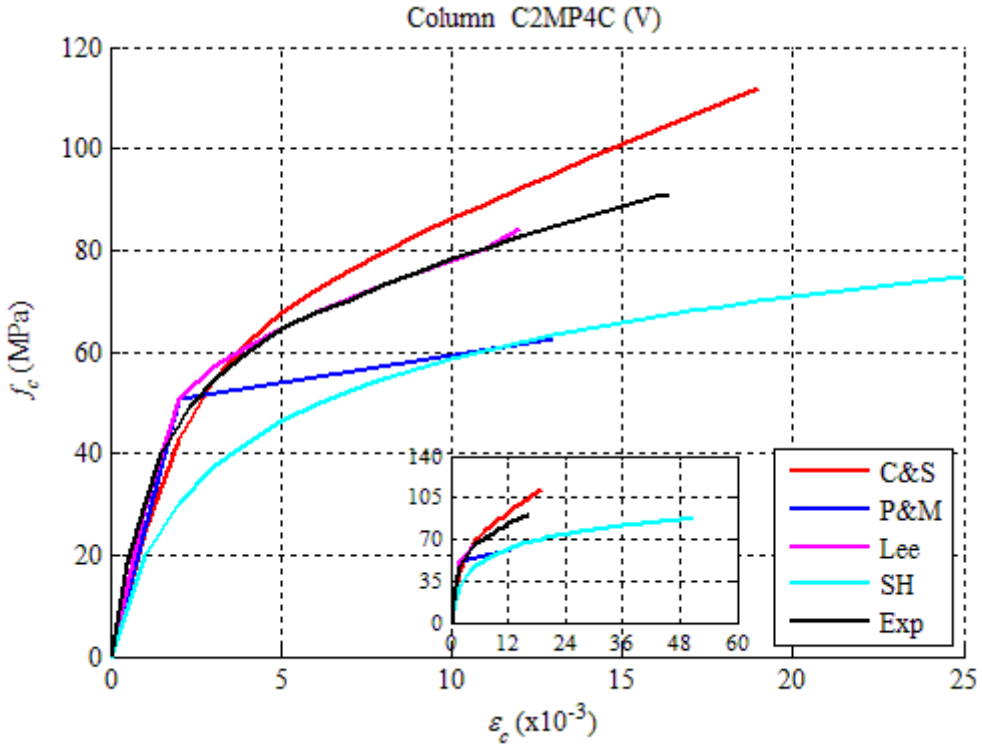

Figure 4.9 - Comparison of f_c-ε_c curves according to the selected models and the experimental curve of column C2MP4C (V).

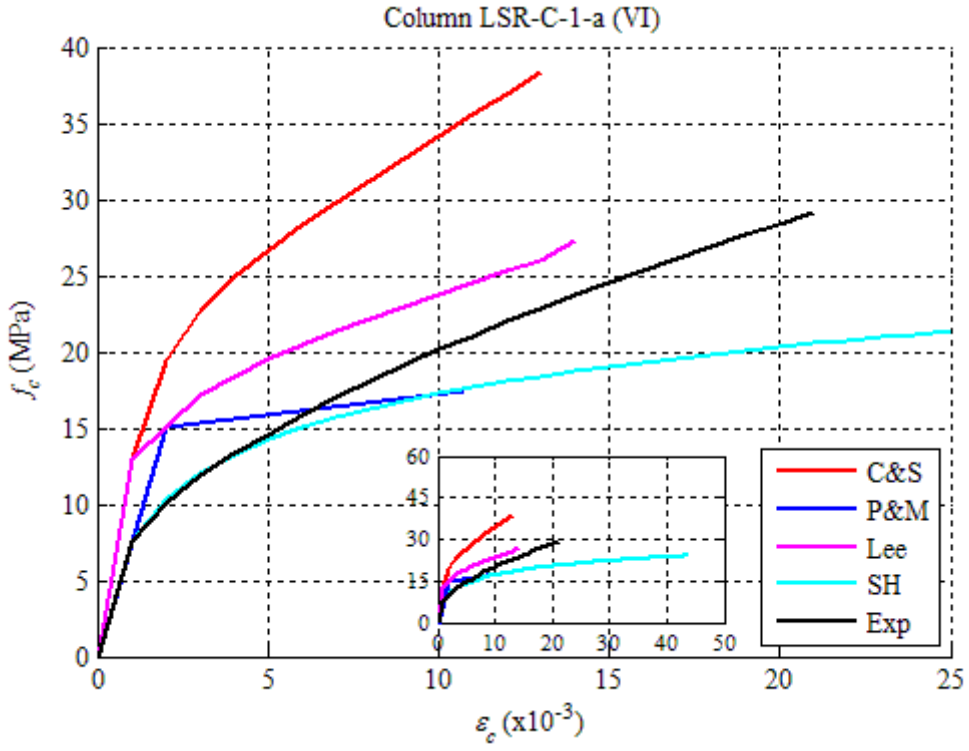

Figure 4.10 - Comparison of f_c-ε_c curves according to the selected models and the experimental curve of column LSR-C-1-a (VI).

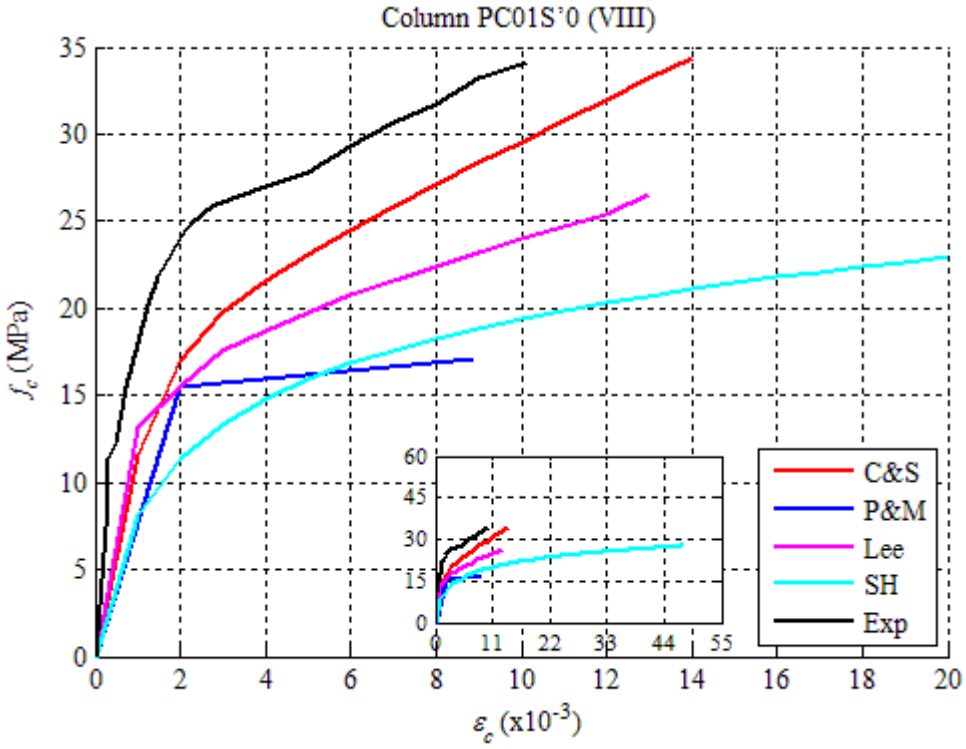

Figure 4.11 - Comparison of f_c-ε_c curves according to the selected models and the experimental curve of column PC01S'0 (VIII).

4.3. Predictions of the Ultimate Conditions

The determination of the ultimate conditions is important to define the stress-strain curve for FRP confined concrete. For this reason, the equations to predict the ultimate stress and strain of the presented models were assessed through the database presented previously.

Figures 4.12 - 4.16 (a) show the relationship between the ultimate theoretical stress $f_{cc\ calc}$ calculated according to each of the four selected models and the ultimate experimental stress $f_{cc\ exp}$ for the 151 columns in the compiled experimental database. The data displayed in these figures corroborate that C&S model overestimates peak stress f_{cc}; additionally, the model that best describes the compressive strength of CFRP confined RC columns is Lee model, with data points with less dispersion along the 45^o line, representing the ideal model. Figures. 4.12 - 4.16 (b) show the relationship between the ultimate theoretical strain $\varepsilon_{cc\ calc}$ and the ultimate experimental strain $\varepsilon_{cc\ exp}$. These figures show that SH model, as already observed in the context of the stress-strain behavior, overestimates ultimate strains. To a lesser extent, this is

also the case of C&S model and Ilki *et al.* model. P&M model and Lee model show similar results, with the former displaying slightly better results.

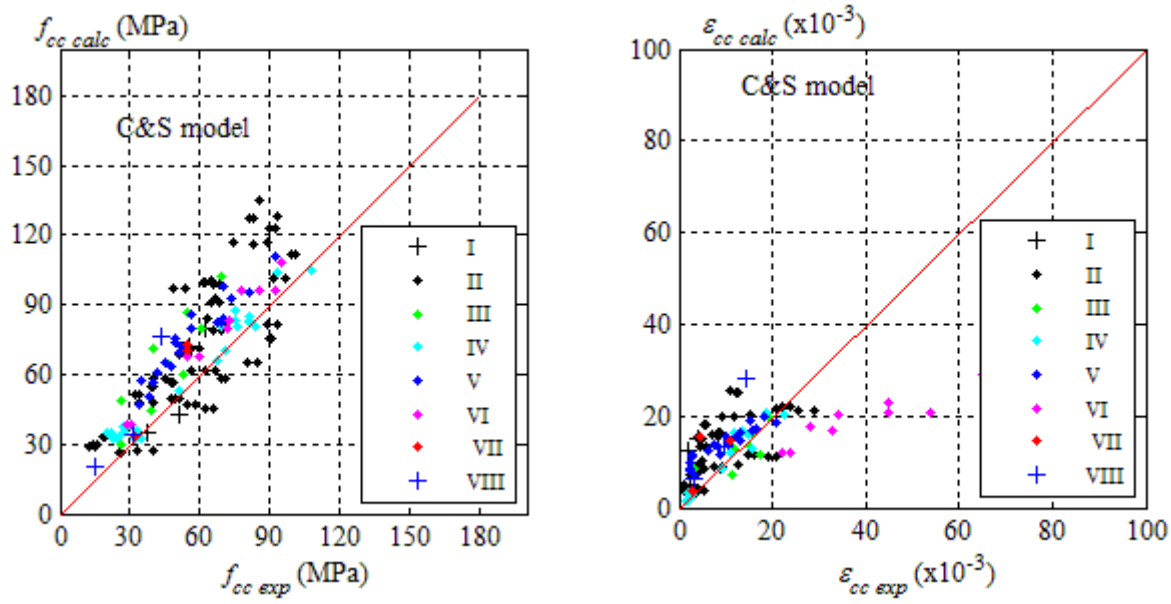

Figure 4.12 - Comparison of C&S model predictions with experimental data: a) strength; and b) ultimate strain.

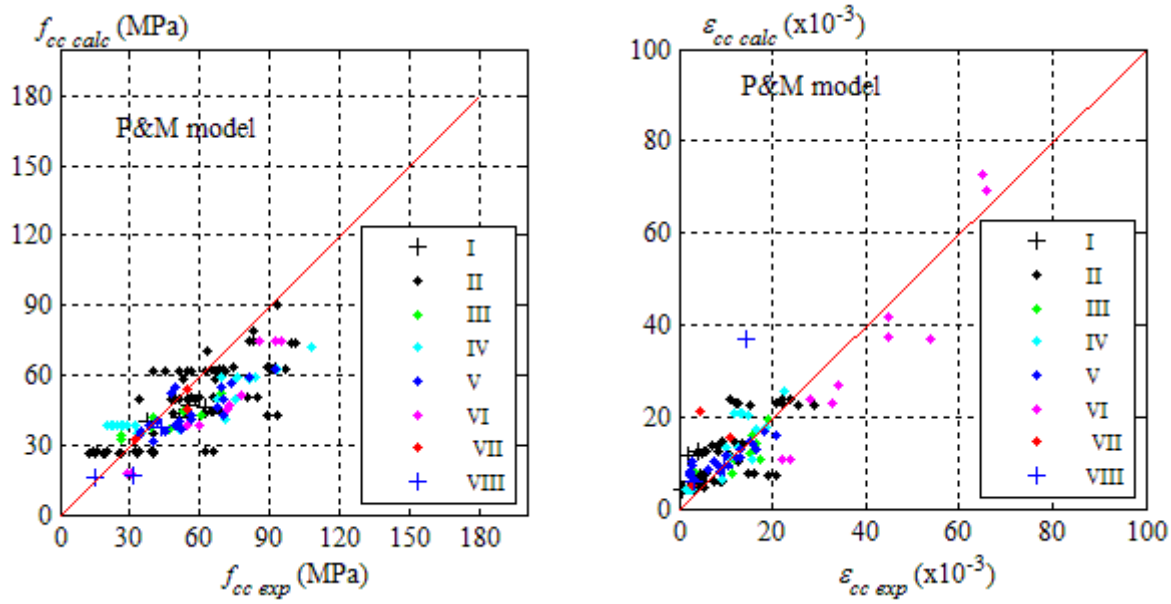

Figure 4.13 - Comparison of P&M model predictions with experimental data: a) strength; and b) ultimate strain.

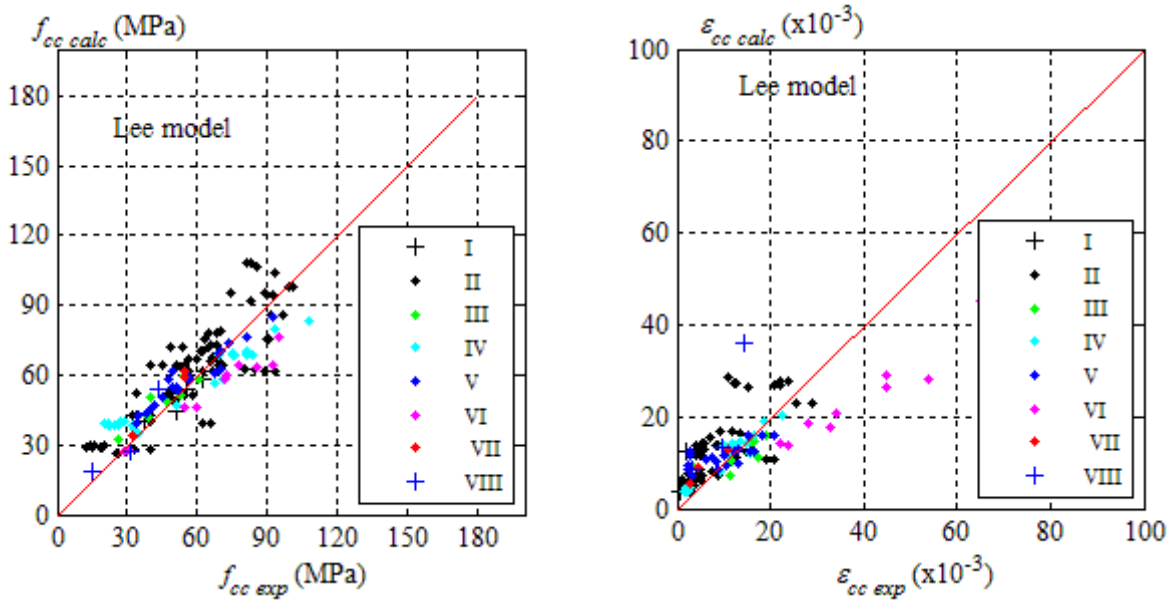

Figure 4.14 - Comparison of Lee model predictions with experimental data: a) strength; and b) ultimate strain.

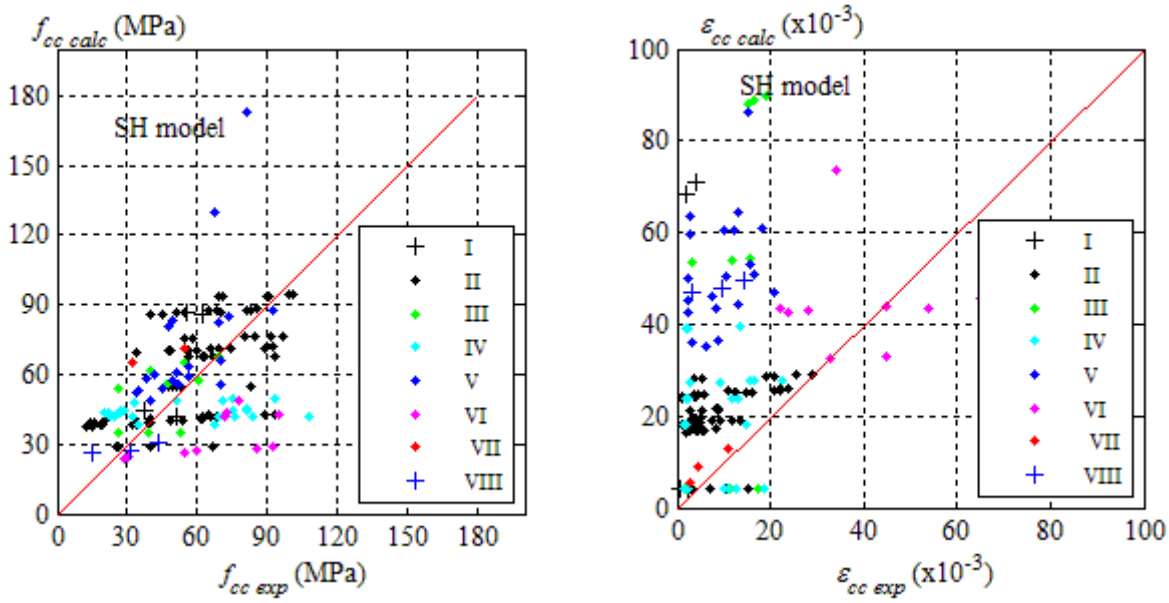

Figure 4.15 - Comparison of SH model predictions with experimental data: a) strength; and b) ultimate strain.

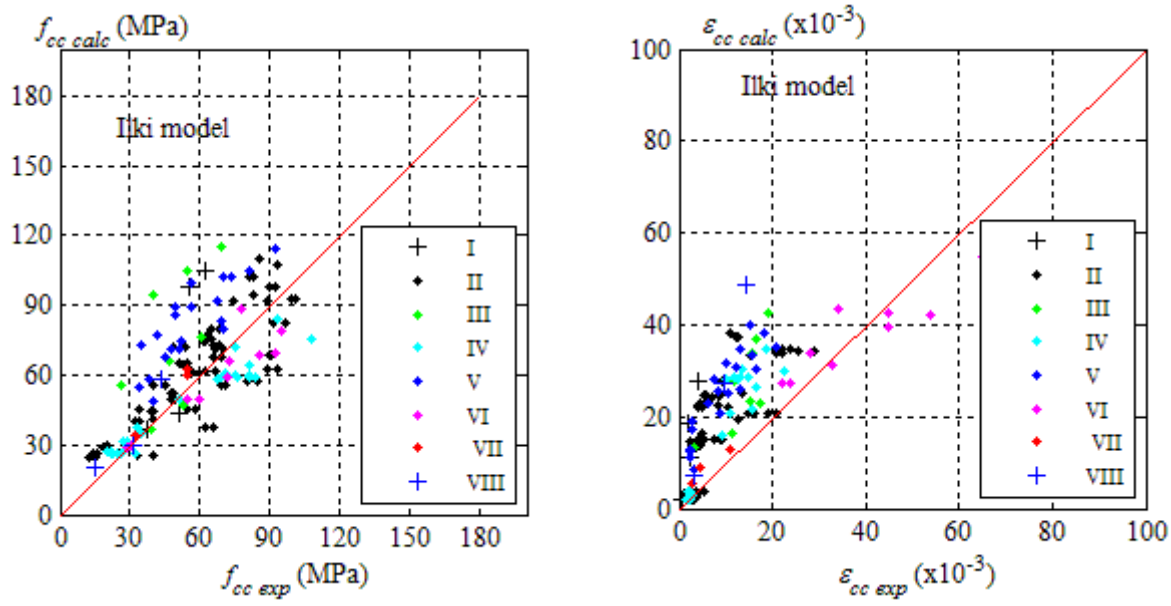

Figure 4.16 - Comparison of Ilki model predictions with experimental data: a) strength; and b) ultimate strain.

4.4. Model Error for the Ultimate Conditions

As clearly seen from the previous sections, ultimate conditions for FRP-confined RC columns, i.e. ultimate stress and ultimate strain, cannot be predicted with certainty. Of particular interest in a reliability analysis and code calibrations, the random variable "model error" (model uncertainty) ξ, shall be described. The model error associated to the calculation of the concrete confined strength ξ_f is obtained by the ratio between experimental and predicted values, $f_{cc\ exp}/f_{cc\ calc}$. Analogously, the model error associated to the calculation of the ultimate strain ξ_ε is given by the ratio $\varepsilon_{cc\ exp}/\varepsilon_{cc\ calc}$ for each model. Table 4.3 presents the corresponding model errors, ξ_f and ξ_ε, for each of the 151 columns in the experimental database. To further investigate the behavior of each model with respect to the ratio H/D, f'_c and confinement ratio f_ℓ / f'_c, plots of the model error as a function of these variables are presented.

Figures 4.17 - 4.19 illustrate the model errors (ξ_f and ξ_ε) as a function of the ratio H/D, f'_c and f_ℓ / f'_c, respectively, for the five analyzed models.

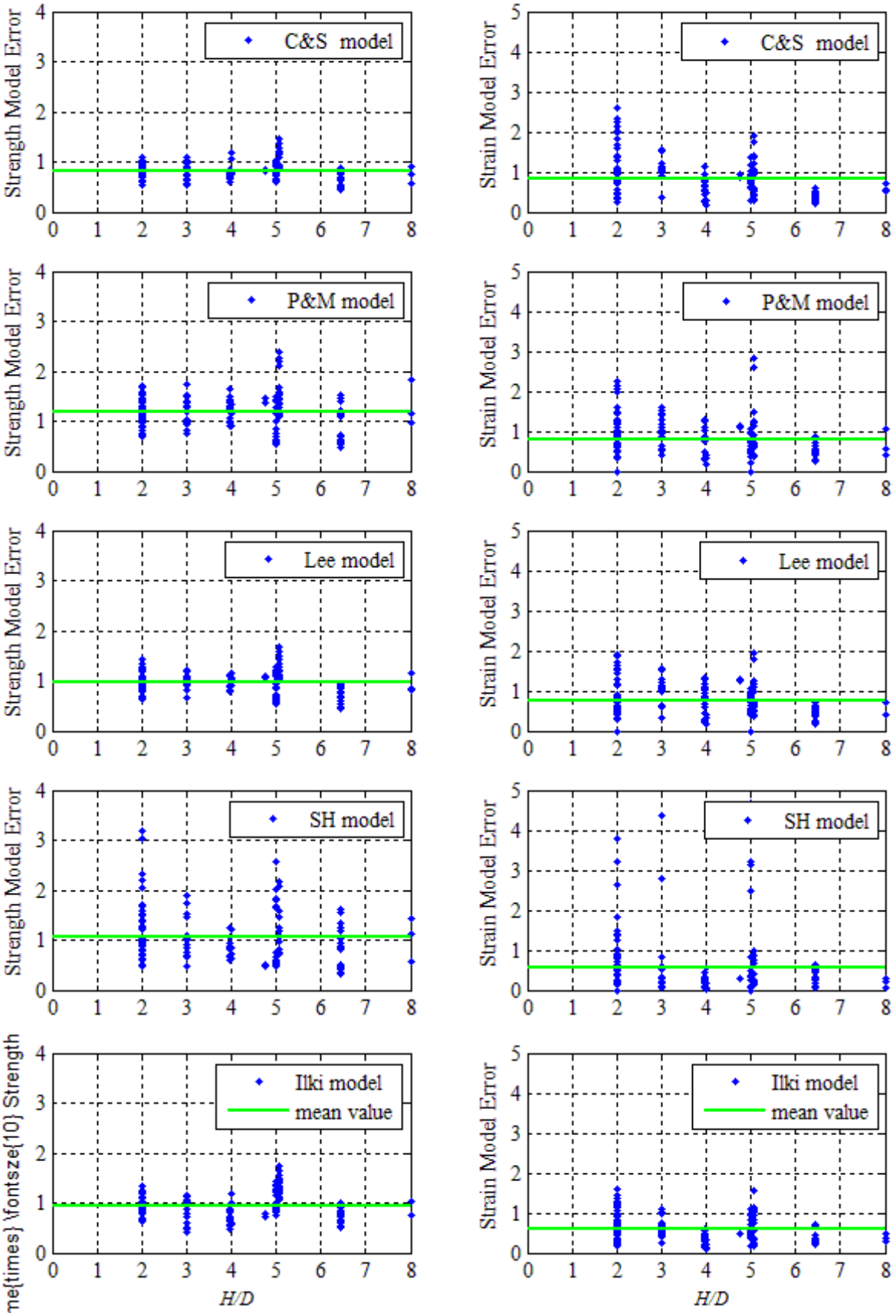

Figure 4.17 - Model error as a function of the ratio *H/D*: a) strength; and b) ultimate strain.

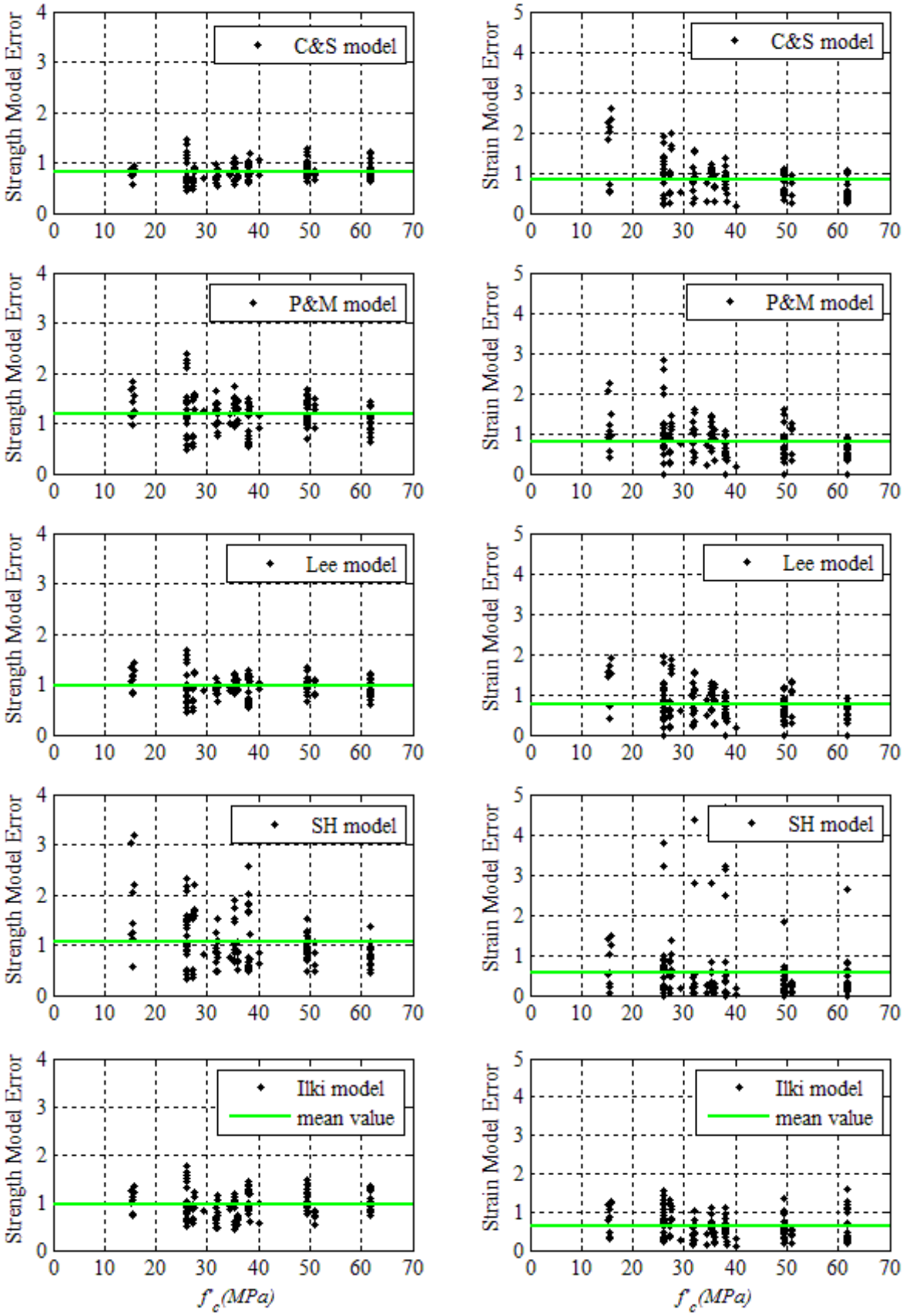

Figure 4.18 - Model error as a function of f'_c: a) strength; and b) ultimate strain.

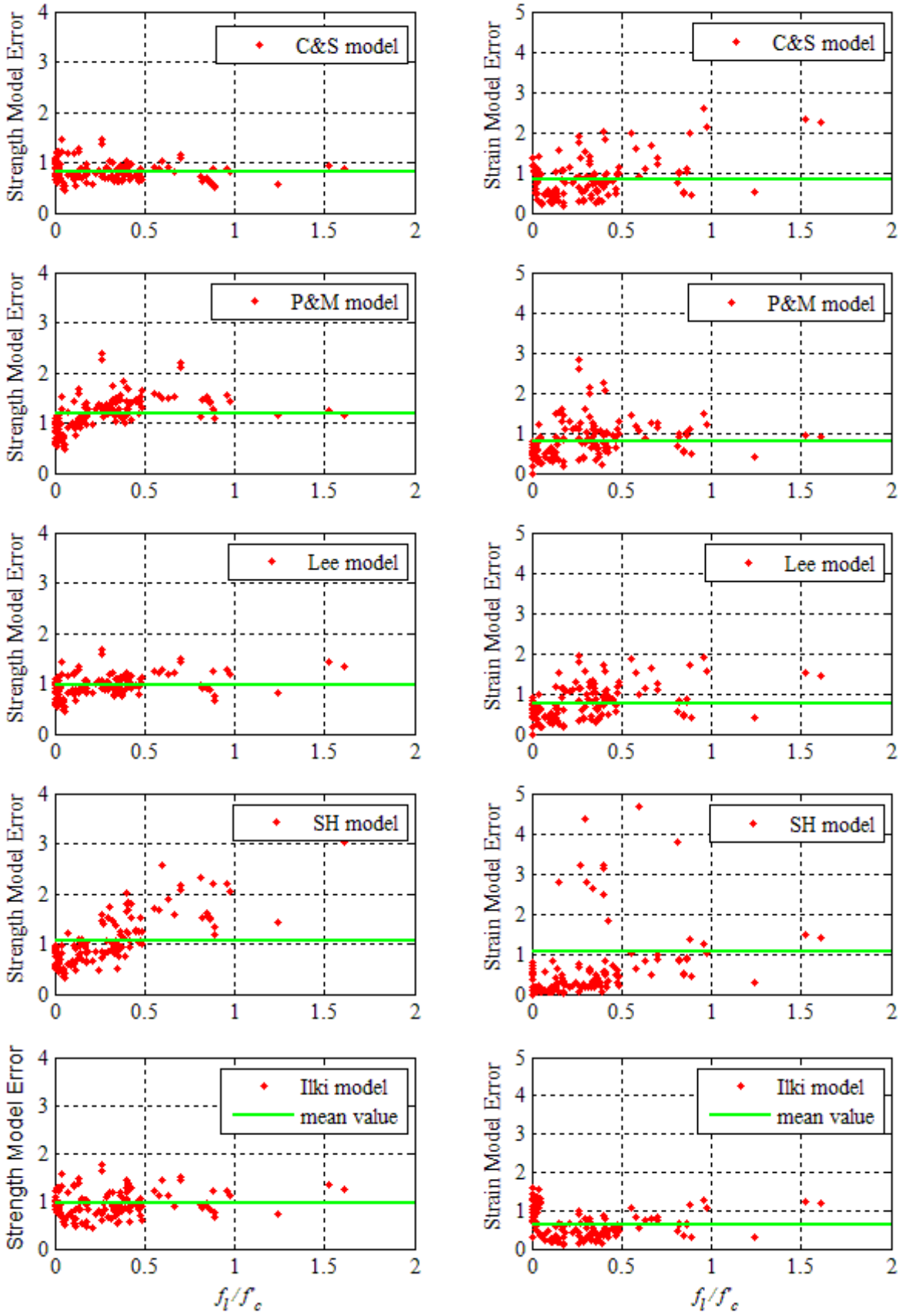

Figure 4.19 - Model error as a function of the ratio f_ℓ / f'_c: a) strength; and b) ultimate strain.

Statistics of the random variable model error (mean, median, standard deviation (SD), coefficient of variation (COV), minimum and maximum) for both ξ_f and ξ_ε are presented in Table 4.5. Regarding the model error associated to the prediction of the ultimate stress, ξ_f, it can be observed that mean values are in the range 0.83-1.18, with C&S and P&M models displaying the smallest and the largest mean, respectively; and COV in the range 0.23-0.49 (or 0.23-0.29 if SH model is excluded), with the smallest value corresponding to Lee model and the largest to SH model (or the largest to P&M, if SH model is excluded). The model with a bias closer to the unity and smaller COV is Lee model. Regarding ξ_ε, it can be observed that the predictions of the ultimate strain are not as accurate as those related to ultimate stresses. Mean values of ξ_ε are in the range 0.58-0.85, with C&S and P&M models displaying the smallest and the largest mean, respectively; COVs are in the range 0.54-1.43 (or 0.54-0.58 if SH model is excluded), with the smallest value corresponding to Lee model.

Table 4.5 - Statistics of the model error for the ultimate stress (ξ_f) and strain (ξ_ε).

Model	C&S		P&M		Lee		SH		Ilki	
	ξ_f	ξ_ε	ξ_f	ξ_ε	ξ_f	ξ_ε	ξ_f	ξ_ε	ξ_f	ξ_ε
Mean	0.83	0.85	1.18	0.82	0.96	0.77	1.06	0.58	0.94	0.61
Median	0.78	0.80	1.17	0.73	0.94	0.64	0.92	0.29	0.91	0.49
SD	0.20	0.49	0.34	0.46	0.22	0.41	0.52	0.83	0.26	0.35
COV	0.24	0.58	0.29	0.56	0.23	0.54	0.49	1.43	0.27	0.58
Min	0.44	0.16	0.49	0.16	0.44	0.16	0.34	0.03	0.43	0.11
Max	1.45	2.60	2.40	2.83	1.67	1.94	3.18	4.68	1.74	1.59

In addition to satisfying the features related to not displaying a trend with respect to the variables *H/D*, f'_c and f_ℓ / f'_c, the model error associated to Lee model has a bias close to the unity and the smallest COV (0.23 for ξ_f and 0.54 for ξ_ε). It can be concluded that among the five selected models, Lee model is the best model for the estimation of both ultimate stress and ultimate strain.

In order to define the probability distribution function that describes the random variable ξ_f associated to Lee model, Chi-Square goodness-of-fit tests were performed. The tests have shown that at a significance level of 5%, both Normal and Lognormal distributions (Fig. 4.20) are acceptable probabilistic models. However, a further analysis of the probability plots corresponding to the strength model error shows that a Normal distribution results in a better

fit of the data in the lower tail of the distribution (Fig. 4.21). Then, Lee model error for strength can be represented by a Normal distribution (mean equal to 0.96 and 0.23 for the COV).

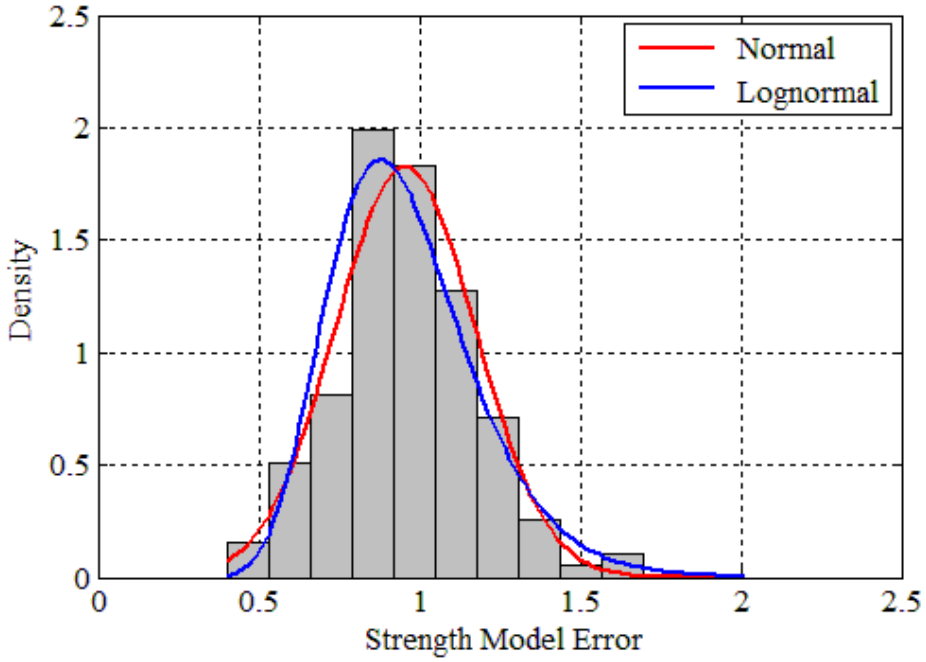

Figure 4.20- Frequency diagram of Lee model error for strength.

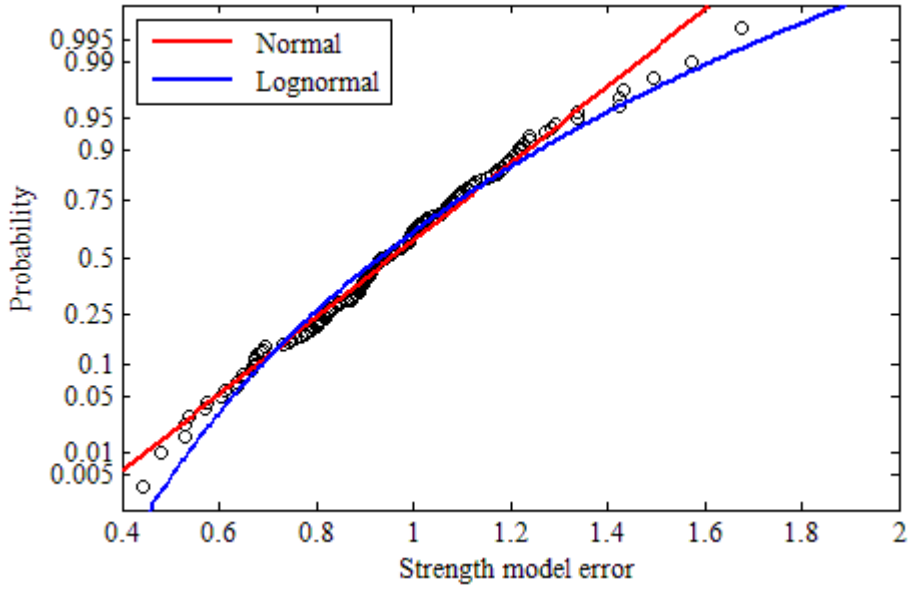

Figure 4.21 - Probability plot of the Lee model error associated to strength.

Regarding ξ_{ε}, at a significance level of 5%, a lognormal distribution is acceptable but not a normal distribution (Fig. 4.22). Analysis of the probability plot associated to ξ_{ε} confirms the

good fitting of the Lognormal distribution to ξ_{ε}, at the lower tail of the distribution (Fig. 4.23).

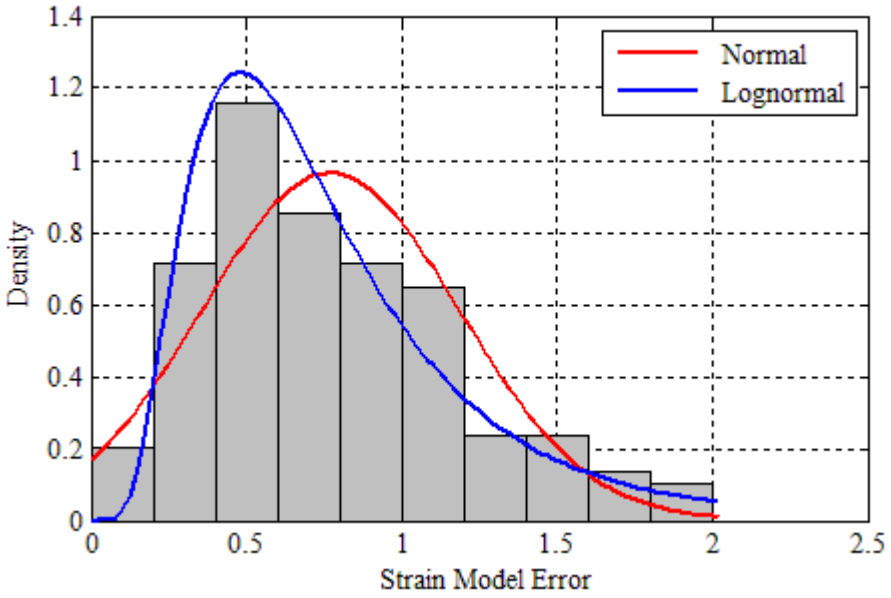

Figure 4.22- Frequency diagram of Lee model error for strain.

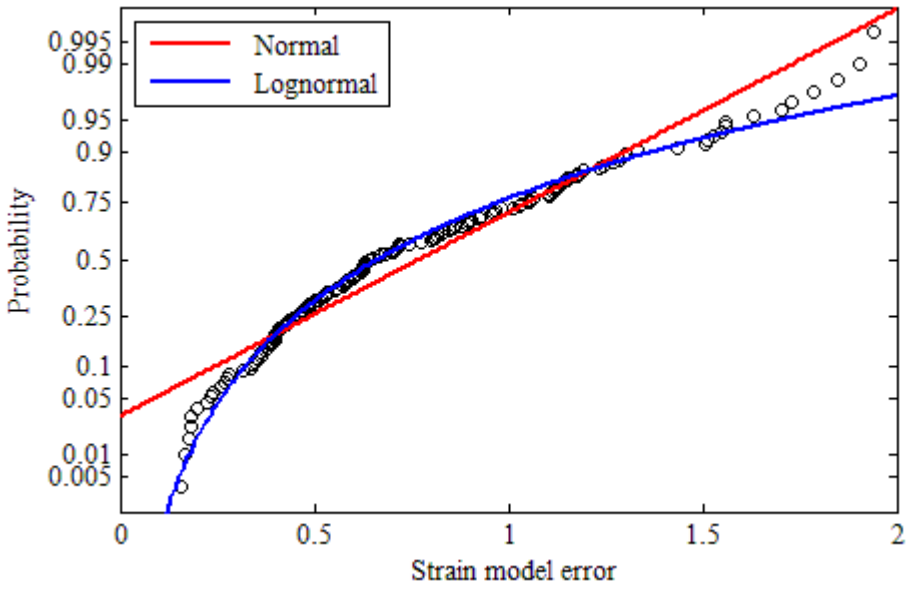

Figure 4.23 - Probability plot of the Lee model error associated to strain.

Figure 4.24 shows a plot of the model error ξ_{ε} *versus* ξ_f for Lee model. As expected it can be observed a statistical dependence between these variables with a moderate positive correlation (correlation coefficient equal to 0.68).

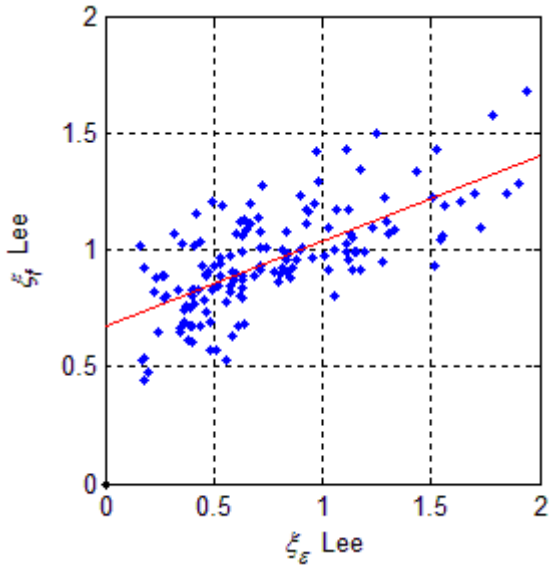

Figure 4.24 - Correlation between the variables ξ_ε versus ξ_f to Lee model.

4.5. Summary of the Chapter

Different models with different levels of conservatism have been proposed in an attempt to describe FRP confinement. In this chapter, the performance of five representative models (C&S, Lee, P&M, SH, and Ilki) addressing the behavior of circular RC columns confined by CFRP was analyzed with respect to the corresponding stress-strain curve and the prediction of the ultimate stress and strain. Such predictions were checked against an experimental database encompassing 151 CFRP-confined RC columns with longitudinal and transversal steel (spirals or circular hoops). The details of the columns in this database are presented, namely: specimen geometric properties (D, H and concrete cover c), concrete properties (f'_c), mechanical properties of the fibers in the CFRP composite (type, elastic modulus E_f, tensile strength f_f and ultimate strain ε_f as provided by the manufacturer), and details of the confinement (ply thickness t and number of plies n).

Regarding the stress-strain curve, it is observed that SH model largely overestimates the ultimate strain. C&S model always overestimates column resistance; a comparison between Lee model and P&M model has shown that the former best represents the experimental results for both the shape of the stress-strain curve and ultimate conditions.

Of particular interest in a reliability analysis and code calibrations, the statitistical description of the random variable “model error” (model uncertainty) ξ is sought. Mean, median, standard

deviation (SD), coefficient of variation (COV), minimum and maximum values for both ξ_f and ξ_ε are presented. Considering the desirable features for a model, i.e. bias close to unit and a smaller COV, it is concluded that among the five selected models, Lee model is the one that best combines these features for the estimation of both ultimate stress and ultimate strain. The probability distribution that best describes the random variable, ξ_f, associated to Lee model, is the Normal distribution, with mean equal to 0.96 and 0.23 for the COV; similarly, the model error related to the ultimate strain, ξ_ε, may be described by a Lognormal distribution, with mean equal to 0.77 and 0.54 for the COV.

5

STRUCTURAL RELIABILITY

5.1. General

The concepts and methods embodied in the Structural Reliability theory provide a proper framework for dealing with problems related to uncertainty in the pertaining variables. In this work, the assessment of the reliability levels corresponding to RC columns strengthened by FRP wrapping is aimed. In such a problem a number of the variables involved in the estimation of both column resistance (concrete compressive strength, steel yield strength, FRP tensile strength, column dimensions, and model error in the prediction of column capacity) and column loading (dead load, live load, etc.) are uncertain and may be modeled as random variables. Considering that the probabilistic description (mean, standard deviation, and type of distribution) of each variable is known, methods for the computation of the corresponding probability of failure (or the reliability index) are needed. A large body of knowledge has already been attained in the field of Structural Reliability translated in a number of textbooks (Ang & Tang, 1984; Melchers, 1999; Haldar & Mahadevan; Nowak & Collins, 2012). Such methods are briefly reviewed in this Chapter.

The great variety of idealizations in reliability models of structures, and the numerous ways in which it is possible to combine these idealizations to suit a particular problem, make it desirable to have a classification. Reliability methods are divided into levels, characterized by the extent of information about the structural problem that is used and provided (Diniz, 2008)

- Level 0: methods that use the allowable stress design format;
- Level 1: methods that employ only one “characteristic” value of each uncertain parameter (also known as semi-probabilistic methods). Load and resistance factor formats are examples of level 1 methods;

- Level 2: methods that employ two values of each uncertain parameter (commonly mean and variance), supplemented with a measure of the correlation between the parameters (usually covariance). These methods use the reliability index as a reference and are consistent with First Order Second Moment (FOSM);
- Level 3: methods that employ probability of failure as a measure, and which therefore require the knowledge of the probability distribution of all uncertain parameters. These methods are consistent with First Order Reliability Method (FORM or SORM) and Monte Carlo Simulation.
- Level 4: methods that explicitly account for risks (i.e., the product of probabilities of failure and consequences for all potential failure modes) in the assessment of life-cycle costs. The goal is the "Minimization of Life-Cycle Costs" or "Maximization of Net Benefits".

5.2. The Basic Reliability Problem

Reliability of a structural component may be formulated as a problem of capacity versus demand. The capacity may be the resistance of the structural component and the demand may be the load effects. In this way, the safety of the component is ensured when its resistance is sufficient to withstand the load effects throughout its service life. Due to uncertainties in the determination of resistance R and load effects S, reliability can only be established in probabilistic terms. A limit state function G, in this case, can be defined as $G = R - S$, and the failure probability P_F is: $P_F = P\,(R < S) = P\,(G < 0)$

Mathematically the failure probability is represented by the following expression:

$$P_F = \iint_F f_{RS}\,(r,s)\;dr\;ds \tag{5.1}$$

where:

- $f_{RS}(\,)$ is the joint probability density function of the random variables R and S;
- F is the failure domain, G < 0.

For R and S statistically independent variables, failure probability P_F is given by:

$$P_F = P(R<S) = \int_0^{\infty}\int_0^{S} f_R(r)\;f_S(s)\,dr\,ds \tag{5.2}$$

where $f_R(r)$ and $f_S(s)$ are the probability density functions (PDF) of the variables R and S, respectively.

Figure 5.1 illustrates the marginal probability density function of each variable, $f_R(\ )$ and $f_S(\ )$; the joint probability density function, $f_{RS}(\ )$; and the failure domain, $G \leq 0$.

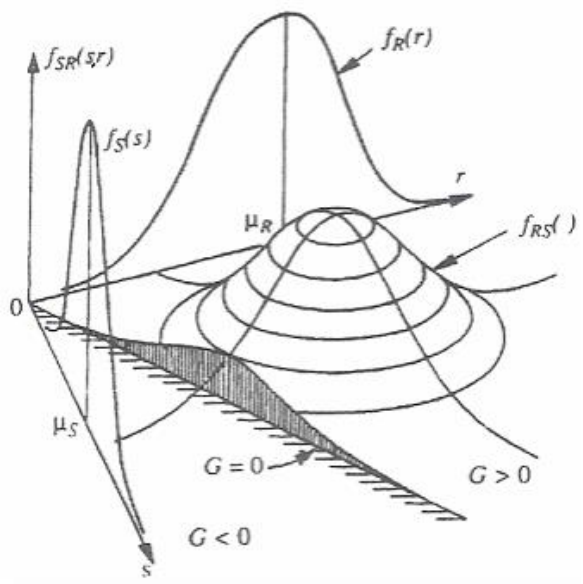

Figure 5.1 - Representation of the failure domain (Melchers, 1999).

In Eq. 5.2, the integral $\int_{-\infty}^{s} f_R(r)$ defines the cumulative distribution function (CDF) of the random variable R, $F_R(s)$. Then the failure probability is given by:

$$P_F = P(R<S) = \int_0^{\infty} F_R(s)\, f_S(s)\, ds \tag{5.3}$$

This integral is known as "convolution integral", were $F_R(s)$ represents the probability of $R \leq s$ that would lead to failure; and $f_S(s)ds$ represents the probability of S take on a value between (s) and ($s+ds$), with ds tending to zero, as illustrated in Fig. 5.2:

The calculation of the failure probability by Eq. 5.2 (statistically independent random variables) requires the information about the probability density function $f_S(s)$ and $f_R(r)$. In practice, R and S are functions of other random variables and only in a few cases, the failure probability is obtained directly from the integration of this equation.

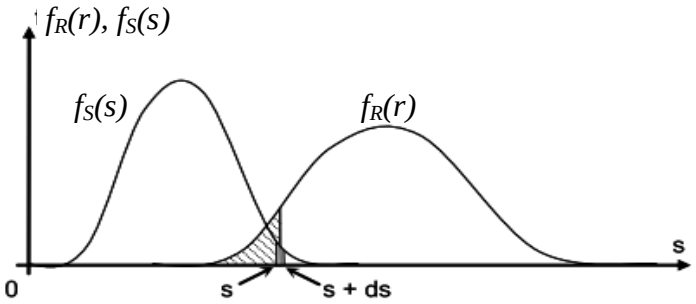

Figure 5.2 - Convolution integral (Melchers, 1999).

5.3. Methods of Structural Reliability

Computation of failure probability of a structural element requires knowledge of the probability density function $f_R(r)$ and $f_S(s)$ or the joint probability density function $f_{RS}(r, s)$. If the probability distributions are known, the First Order Reliability Method (FORM) and the Monte Carlo simulation may be used. When there is no information on the probability distributions of the variables, reliability can be measured entirely as a function of the mean and variance (and covariance in the case of statistically dependent variables) by the First Order Second Moment (FOSM) reliability method (Ang & Tang, 1984).

5.3.1. First Order Second Moment method (FOSM)

First Order Second Moment method (FOSM) is based on the first order Taylor series approximation of the performance function linearized at the mean values of the random variables. FOSM uses only second moment statistics (mean and variance) of the random variables.

The performance function is defined as $g(\boldsymbol{X}) = g(X_1, X_2, ..., X_n)$, where $\boldsymbol{X} = (X_1, X_2, ..., X_n)$ is the vector of the basic variables. The function $g(X) = 0$ defines the limit state, being $g(\boldsymbol{X}) > 0$ the safety state and $g(\boldsymbol{X}) < 0$ the failure state. Geometrically, the limit state function, $g(\boldsymbol{X}) = 0$ is an n-dimensional surface (or hypersurface) called failure surface.

Considering a problem defined by n statistically independent variables X_i, then the reduced variables X'_i (transformed into standard normal variables) are represented by Eq. 5.4 and the limit state function $g(X') = 0$, given by Eq. 5.5:

$$X'_i = \frac{X_i - \mu_{X_i}}{\sigma_{X_i}}; \text{ with } i = 1, 2, ..., n. \tag{5.4}$$

$$g\left(\sigma_{X_1} X'_1 + \mu_{X_1}, ..., \sigma_{X_n} X'_n + \mu_{X_n}\right) = 0 \tag{5.5}$$

Figure 5.3 shows the safety state and the failure state of the reduced variables X'_1 and X'_2 (i.e. n = 2). It can be observed that when the failure surface moves away from the origin in the space of reduced variables, the safety (failure) region increases (decreases). The point on the failure surface with the shortest distance to the origin in the space of reduced variables is the most likely point of failure (design point). This shortest distance d_{min} can be taken as a reliability index β.

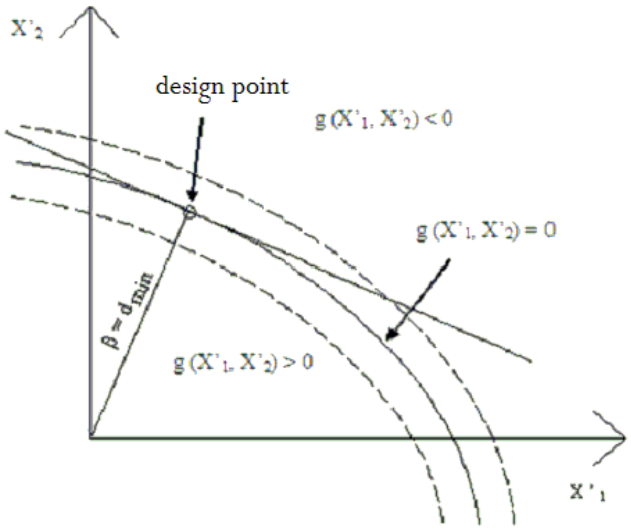

Figure 5.3 - Limit state and failure state in the space of reduced variabeles

The reliability index β is the distance from design point, $x^{*'} = x_1^{*'}, x_2^{*'} ... x_n^{*'}$, to the origin in the space of reduced variables, subject to the restriction $g(\boldsymbol{X}) = 0$, (i.e. the design point is on the failure surface). According to Ang & Tang (1990), the realibility index β is given by Eqs. 5.6 and 5.7, in the matrix and scalar forms, respectively:

$$\beta = \frac{-G^{*T} X'^{*}}{\left(G^{*T} G^{*}\right)^{1/2}} \tag{5.6}$$

$$\beta = \frac{-\sum x_i'^{*}\left(\frac{\partial g}{\partial X'_i}\right)_*}{\sqrt{\sum\left(\frac{\partial g}{\partial X'_i}\right)_*^2}} \tag{5.7}$$

where:

$\mathbf{G}^*$ is the gradient vector in the design point, given by Eq. 5.8:

$$G = \left(\frac{\partial g}{X_1'^*}, \frac{\partial g}{X_2'^*}, \ldots, \frac{\partial g}{X_n'^*}\right) \tag{5.8}$$

Derivatives $\partial g / \partial X^{*'}$ are evaluated in the design point $x^{*'} = (x_1^{*'}, x_2^{*'} \ldots x_n^{*'})$

Eqs. 5.6 (matrix form) or Eq. 5.7 (scalar form) correspond to a linearization of the performance function on the design point. By the linearization performance function and the use of information only to the second momento of the variables involved, this formulation is called First Order Second Moment method. The measure of reliability obtained is the reliability index β, than this method corresponds to a level 2.

5.3.2. First Order Reliability Method (FORM)

In general, it is unpractical to integrate Eq. 5.3 to find the failure probability due to the high dimensionality in most engineering applications. To this end, approximation methods, such as the First Order Reliability Method (FORM), are used.

The name First Order Reliability Method comes from the fact that the performance function $g(\boldsymbol{X})$ is approximated by the first order Taylor expansion (linearization). The simplification is achieved through transforming the random variables from their original random space into a standard normal space

The basic principle of FORM method consists in transforming the random variables of a group $\boldsymbol{X} = (X_1, X_2, ..., X_n)$ with any probability distributions, correlated or not, in a group $\boldsymbol{U} = (U_1, U_2, ..., U_n)$ of random variables, independent statistically and standard equivalent normal. The failure probability is obtained utilizing probability distributions of the random variables by the minimum distance from the point on the failure surface to the origin, in the space of

reduced variables. This minimum distance is obtained through the procedures presented in the previous section and FORM corresponds to a level 3 Method.

5.3.3. Linear limit state functions

In case of linear limit state functions, for example, the safety margin $M = R - S$, the failure probability can be obtained by Eq. 5.9, since R and S are random variables, M also is a random variable with probability density function $f_M(m)$.

$$P_F = \int_{-\infty}^{0} f_M(m)\, dm = F_M(0) \tag{5.9}$$

When the resistance R and the effect of the load S are statistically independent Gaussian variables, the safety margin will be also a Gaussian variable. The mean μ_M and standard deviation σ_M of the safety margin are given by Eqs. 5.10 and 5.11, respectively.

$$\mu_M = \mu_R - \mu_s \tag{5.10}$$

$$\sigma_M = \sqrt{\sigma_R^2 + \sigma_S^2} \tag{5.11}$$

where:

- μ_R and μ_S are the mean of the resistance and the loading, respectively;
- σ_R and σ_S are the standard deviation of the resistance and the loading, respectively;

The failure probability can be obtained by Eq. 5.12, where Φ is the cumulative distribution function of the standard Normal distribution.

$$P_F = F_M(0) = \Phi\left(\frac{-\mu_M}{\sigma_M}\right) = 1 - \Phi\left(\frac{\mu_M}{\sigma_M}\right) \tag{5.12}$$

Failure probability is a function of the ratio μ_M / σ_M , i.e the realibility index β., according to Eq. 5.13. Graphically, the failure probability is given by the area under the curve $f_M(m)$ for values of M lesser than zero (Fig. 5.4).

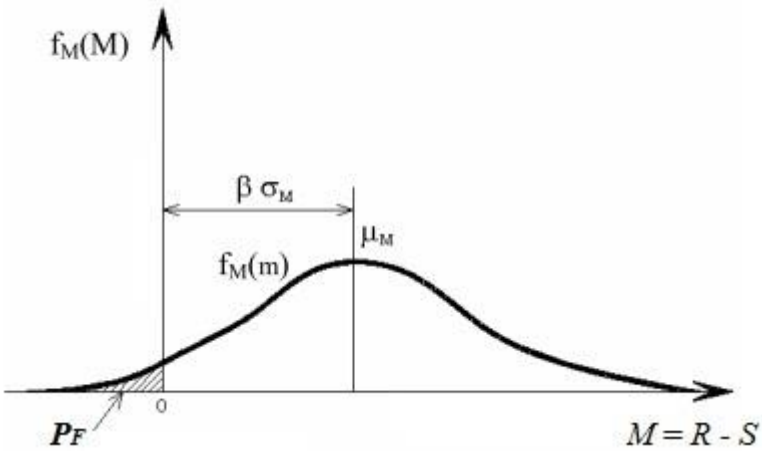

Figure 5.4 - Probability density function of the safety margin (Ang & Tang, 1990).

$$\beta = \frac{\mu_R - \mu_S}{\sqrt{\sigma_R^2 + \sigma_S^2}} = \frac{\mu_M}{\sigma_M} \tag{5.13}$$

5.3.4. Monte Carlo simulation

Simulation is a technique for conducting experiments in a laboratory or on a digital computer in order to model the behavior of a system. Usually simulation models result in 'simulated' data that must be treated statistically in order to predict the future behavior of the system. Monte Carlo simulation is usually used for problems involving random variables of known or assumed probability distribution. Using statistical sampling techniques, a set of values of the random variables is generated in accordance with the corresponding probability distributions. These values are treated as being similar to a sample of experimental observations and are used to obtain a "sample" solution. By repeating the process and generating several sets of sample data, many sample solutions can be determined. Statistical analysis of the sample solutions is then performed.

First, the variability of the main parameters that influence the behavior of the structure must be represented by defined probability distributions. Second, one must have a mathematical model that relates the main parameters of structural behavior with its performance under given load. With known parameters values (design variables), the simulation process provides a specific measure of performance. Through repeated simulations, the performance evaluation of the structure becomes more precise (Ang & Tang, 1990).

Generally, the solutions obtained by Monte Carlo simulation are asymptotically exact as sample size is infinitely large. Since the results from the Monte Carlo technique depend on the number of samples used, they are not exact and are subject to sampling errors. In this way, the accuracy increases as the sample size increases. According to Ang & Tang (1990), the error (in percentage) can be calculated by Eq. 5.14, where P_F is the failure probability and n is the number of simulations used:

$$\% \text{ error} = 200\sqrt{\frac{1 - P_F}{n\ P_F}} \tag{5.14}$$

6

RELIABILITY BASES FOR FRP-RC COLUMNS

In this study, Monte Carlo simulation is used in the probabilistic description of FRP-RC column strength and the computation of the corresponding probability of failure (and attendant reliability index). As highlighted in the previous chapter, for the utilization of Monte Carlo simulation, the following information is required: (i) the probability distributions of all random variables involved in the problem, and (ii) the deterministic relationship that defines failure of the column. As such, in this chapter the reliability bases for the safety assessment of FRP-RC columns are presented. The chapter starts with a brief presentation of both ACI 318-14 (2014) and ACI 440.2R (2008) recommendations for column strengthening, followed by a description of the selected 48 FRP-RC confined columns. In the sequence, the relevant random variables are identified (column diameter, concrete cover, concrete compressive strength, FRP tensile strength, model errors, mechanical properties of steel, dead and live loads), a summary of the corresponding statistics is presented and a performance function is established.

6.1. Designed Columns

One hundred forty-four circular FRP-RC columns were selected for analysis. These columns were designed complying with the prescriptions of ACI 440.2R (2008) and ACI 318 (2014).

6.1.1. Design of FRP-Confined RC Columns by ACI 440.2R

ACI 440 2R (2008) provides guidance for the selection, design, and installation of FRP systems for externally strengthened concrete structures. Information on material properties, design, installation, quality control, and maintenance of FRP systems is also presented.

ACI 440 2R recommendations are based on: (i) traditional RC design principles, as incorporated in ACI 318-05; (ii) knowledge of the specific mechanical behavior of FRP reinforcement; and (iii) limit-states design format. According to ACI 440 2R, strength of the existing structure shall be sufficient to resist the load as defined by:

$$(\phi R_n)_{existing} \geq (1.1 S_{DL} + 0.75 S_{LL})_{new} \tag{6.1}$$

The rationale in ACI 440 2R for smaller load factors, as compared to those recommended by ACI 318-14 is as follows. The dead load factor of 1.1 is used because the dead load acting on the existing structure can be more accurately assessed than in the case of design of new structures; a live load factor of 0.75 is used to exceed the statistical mean of yearly maximum live load factor of 0.5, as given in ASCE 7-05 (2005).

FRP properties reported by manufacturers typically do not consider long-term exposure to environmental conditions and shall be considered as initial properties. Because long-term exposure to various types of environments can reduce the tensile properties and creep-rupture and fatigue endurance of FRP laminates, the ultimate tensile strength and strain used in design equations should be reduced by the environmental reduction factor C_E according to Eqs. 6.2 and 6.3, respectively. Table 6.1 presents values of the environmental reduction factor C_E according to the fiber type and exposure condition.

Table 6.1- Environmental reduction factor for various FRP systems and exposure conditions.

Exposure conditions	Fiber type	Environmental reduction factor (C_E)
Interior exposure	Carbon	0.95
	Glass	0.75
	Aramid	0.85
Exterior exposure (bridges, piers, and unenclosed parking garages)	Carbon	0.85
	Glass	0.65
	Aramid	0.75
Aggressive environment (chemical plants and wastewater treatment plants)	Carbon	0.85
	Glass	0.50
	Aramid	0.70

$$f_{Fu} = C_E \, f_F^* \tag{6.2}$$

$$\varepsilon_{Fu} = C_E \, \varepsilon_F^* \tag{6.3}$$

where:

f_{Fu} and ε_{Fu} are the design ultimate tensile strength and design rupture strain of FRP, respectively;

f^*_F and ε^*_F are ultimate tensile strength and ultimate rupture strain of FRP, respectively, as reported by the manufacturer.

Because FRP materials are linear elastic until failure, the design modulus of elasticity for unidirectional FRP can be determined from Hooke's law, being unaffected by environmental conditions, according to Eq. 6.4:

$$E_F = \frac{f^*_F}{\varepsilon^*_F} = \frac{f_{Fu}}{\varepsilon_{Fu}} \tag{6.4}$$

Manufacturers should report an ultimate tensile strength defined by Eq. 6.5:

$$f^*_F = \mu f_F - 3\,\sigma \tag{6.5}$$

where μf_F and σ are the means tensile strength and standard deviation, respectively, of a tests sample;

Due to the primary role of the fibers and methods of application, the properties of an FRP repair system may be reported based on the net-fiber area, calculated using the known area of fibers, neglecting the total width and thickness of the cured system. The net-fiber area is typically used for reporting properties of wet layup systems that use manufactured fiber sheets and field-installed resins. The wet layup installation process leads to a controlled fiber content and a variable resin content.

In other instances, the reported properties are based on the gross-laminate area, calculated using the total cross-sectional area of the cured FRP system, including all fibers and resin. The gross-laminate area is typically used for reporting precured laminate properties where the cured thickness is constant and the relative proportion of fiber and resin is controlled.

Regardless of the basis for the reported values, the load-carrying strength ($f_{fu}\,A_f$) and stiffness ($A_f\,E_f$) remain constant. It is important, however, that any design calculations consistently use

material properties based on only one of the two methods (for example, if the net-fiber area is used in any calculation, the strength based on net-fiber area area should be used in the calculations as well).

The nominal axial force acting on an FRP-strengthened column, P_n, can be calculated by Eqs. 6.6 and 6.7, for members with existing steel spirals and stirrups, respectively:

$$\phi P_n = 0.85\,\phi \left[0.85\ f_{cc}\left(A_g - A_{sL}\right) + f_y\, A_{sL}\right] \tag{6.6}$$

$$\phi P_n = 0.80\,\phi \left[0.85\ f_{cc}\left(A_g - A_{sL}\right) + f_y\, A_{sL}\right] \tag{6.7}$$

where:

ϕ is the strength reduction factor. In the case of compression controlled sections, ϕ is adopted as 0.70 for members with spiral reinforcement, and 0.65 for other reinforced members;

A_g is the gross area of concrete section;

A_{sL} is the total area of longitudinal reinforcement;

f_y is the specified yield strength of longitudinal steel reinforcement.

The stress-strain model by Lam & Teng (2003) for FRP-confined concrete has been adopted by ACI 440-2R and it is shown in Fig.6.1 and defined by the following expressions:

$$f_c = \begin{cases} E_c\,\varepsilon_c - \dfrac{\left(E_c - E_2\right)^2}{4 f'_c}\,\varepsilon^2{}_c & 0 \le \varepsilon_c \le \varepsilon'_t \\ f'_c + E_2\,\varepsilon_c & \varepsilon'_t \le \varepsilon_c \le \varepsilon_{cc} \end{cases} \tag{6.8}$$

$$E_2 = \frac{f_{cc} - f'_c}{\varepsilon_{cc}} \tag{6.9}$$

$$\varepsilon'_t = \frac{2 f'_c}{E_c - E_2} \tag{6.10}$$

where:

f'_c is the unconfined cylinder concrete compressive strength;

E_2 is the slope of linear portion of stress-strain curve for FRP-confined concrete;

ε'_t is the transition strain in stress-strain curve of FRP confined concrete;

ε'_c is the strain of unconfined concrete corresponding to f'_c; may be taken as 0.002.

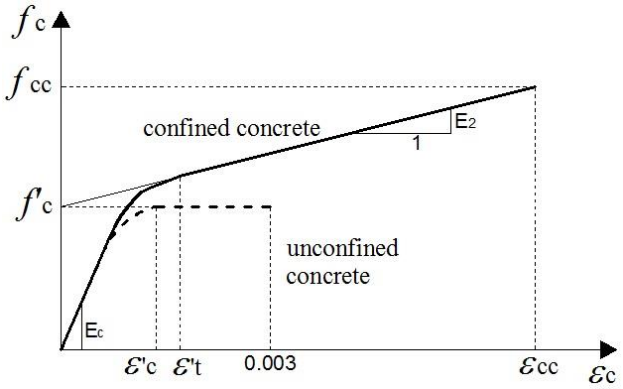

Figure 6.1 - Lam and Teng's stress-strain model for FRP confined concrete.

It shall be emphasized that in Section 12.1 "Pure Axial Compression", the symbol f'_c is used to represent the unconfined cylinder compressive strength of concrete in a given column, while in Section 2 of the same document (ACI 440, 2008) f'_c is used to represent the specified compressive strength of concrete, what is based on statistics of a concrete population. In an attempt to clarify these matters, Section 27.3.1.3 in ACI 318 (2014) prescribes that "If required, an estimated equivalent f'_c shall be based on analysis of results of cylinder tests from the original construction or tests of cores removed from the part of the structure where strength is in question."

The maximum confined concrete compressive strength f_{cc} calculated using the equation proposed by Lam & Teng (2003) with the inclusion of an additional reduction factor ψ_f = 0.95, is obtained by:

$$f_{cc} = f'_c + 3.3\psi_f \kappa_a f_\ell \tag{6.11}$$

The efficiency factor κ_a is based on geometry of cross section and in the case of circular sections κ_a is unity. The confinement pressure f_ℓ provided by the FRP is calculated by Eq. 6.12, with effective strain level in FRP reinforcement attained at failure, i. e., $\varepsilon_{Fe} = k_F \varepsilon_{Fu}$, where k_F = 0.55. (Note: Eq. 6.12 is the same as Eq. 3.12; it is reapresented here with the same notation as used in ACI 440 (2008)).

$$f_\ell = \frac{2 E_F n t \varepsilon_{Fe}}{D} \tag{6.12}$$

According to Lam & Teng (2003), the ratio f_ℓ / f'_c should not be less than 0.08. This is the minimum level of confinement required to assure a non-descending second branch in the stress-strain curve.

The maximum compressive strain in the FRP confined concrete ε_{cc} can be found using Eq. 6.13. This strain should be limited to the value 0.01 to prevent excessive cracking and the resulting loss of concrete integrity. When this limit is applicable, the corresponding maximum value of f_{cc} should be recalculated from the stress-strain curve.

$$\varepsilon_{cc} = \varepsilon'_c \left(1.50 + 12 \frac{f_\ell}{f'_c} \left(\frac{\varepsilon_{Fe}}{\varepsilon'_c} \right)^{0.45} \right) \leq 0.01 \tag{6.13}$$

6.1.2. Design limits by ACI 318 (2014)

According to ACI, the required strength U is expressed in terms of factored loads, or related internal moments and forces. Factored loads are the loads specified multiplied by appropriate load factors. The required strength shall be at least equal to the effects of factored loads. In this work it is assumed that the column is subject only to dead load (D) and live load (L):

$$U = 1.2\ D + 1.6\ L \tag{6.14}$$

Design strength of a member shall be taken as the nominal strength S_n multiplied by the applicable strength reduction factor ϕ. Structural members shall have design strength at all sections greater than or equal to the required strength U calculated for the factored loads. The basic requirement for design strength may be expressed as follows:

$$\phi S_n \geq U \tag{6.15}$$

Second-order effects in many structures are negligible depending on the slenderness ratio of the member. Slenderness effects shall be permitted to be neglected if the following conditions are satisfied:

For columns not braced against sidesway:

$$\frac{k\ell_u}{r} \leq 22 \tag{6.16}$$

For columns braced against sidesway:

$$\frac{k\ell_u}{r} \leq 34+12\left(M_1/M_2\right) \tag{6.17}$$

and

$$\frac{k\ell_u}{r} \leq 40 \tag{6.18}$$

where:

k is the effective length factor for compression members;

l_u is the unsupported length of compression member;

r is the radius of gyration of cross section of a compression member;

M_1 is the smaller factored end moment on a compression member, to be taken as positive if member is bent in single curvature, and negative if bent in double curvature;

M_2 is the larger factored end moment on compression member, always positive.

Regarding reinforcement limits, a minimum of 0.01 is placed on the longitudinal reinforcement ratio ρ_{sL}; a minimum of six longitudinal bars shall be adopted, for circular columns. For the transverse reinforcement, in the case of ties, the center-to-center spacing shall not exceed the least of 16 times the longitudinal bar diameter, 48 times the tie bar diameter and the smallest dimension of the member. The diameter of tie bar shall be at least No. 10 (9.525mm). Furthermore, in the case of spirals, a volumetric spiral reinforcement ratio ρ_s shall satisfy the Eq. 6.19:

$$\rho_s \geq 0.45\left(\frac{A_g}{A_{ch}}-1\right)\frac{f'_c}{f_{yt}} \tag{6.19}$$

where:

A_g is the gross area of concrete section;

A_{ch} is the cross-sectional measured to the outside edges of transverse reinforcement;
f'_c is the specified concrete compressive strength;
f_{yt} is the specified yield strength of transverse steel reinforcement (≤ 700 MPa).

Spirals shall consist of evenly spaced continuous bar or wire with clear spacing greater than 25 mm and (4/3) of nominal maximum size of coarse aggregate and not exceeding 75 mm. For cast-in-place construction, spiral bar diameter shall be at least 9.5 mm.

The limits related to the specified concrete cover for nonprestressed cast-in-place concrete members are given in Table 6.2.

Table 6.2 - Specified concrete cover for cast-in-place of RC members (ACI 318, 2014).

Concrete exposure	**Member**	**Reinforcement**	**Specified cover, mm**
Cast against and permanently in contact with ground	All	All	75
Exposed to weather or in contact with ground	All	No. 19 through No. 57 bars	50
		No. 16 bar, MW200, or MD 200 wire and smaller.	40
Not exposed to weather or in contact with ground	Slabs, joists, and walls	No. 43 and No. 57 bars	40
		No. 36 and smaller	20
	Beams, columns, pedestals, and tension ties	Primary reinforcement, stirrups, ties, spirals, and hoops	40

6.1.3. Column details

In this study, the reliability analysis considers 144 columns corresponding to 3 different load ratios and 48 column cross-section details (Table 6.3); they have been initially designed following recommendations of ACI 318 and strengthened by ACI 440.2R (2008). All columns are confined by CFRP and have height of 3000 mm, diameter of 300 mm or 400 mm and concrete cover of 40 mm, and are exposed to weather or in contact with ground. Two specified concrete strengths f'_c were adopted: 20 MPa and 35 MPa. Regarding reinforcements, steel bars Grade 420 MPa, with Young modulus of 200 GPa were adopted. For the longitudinal reinforcement bars No. 13 (12.7mm) and No. 16 (15.875 mm), uniformly distributed over the column perimeter were used. The number of longitudinal steel bars was defined in order to provide longitudinal steel ratios around 1% (minimum prescribed by ACI 318) and 2%.

Table 6.3 - Details of the designed columns.

Column		H (mm)	c (mm)	D (mm)	f'_c (MPa)*	Long. Steel **	Transversal Steel **		CFRP plies
#	ID						type	s (mm)	
1	D1F1L1T1C1	3000	40	300	20	6 #4	ties	#3 @ 200	1
2	D1F1L1T1C2	3000	40	300	20	6 #4	spirals	#3 @ 200	2
3	D1F1L1T2C1	3000	40	300	20	6 #4	ties	#3 @ 100	1
4	D1F1L1T2C2	3000	40	300	20	6 #4	spirals	#3 @ 100	2
5	D1F1L1T3C1	3000	40	300	20	6 #4	ties	#3 @ 50	1
6	D1F1L1T3C2	3000	40	300	20	6 #4	spirals	#3 @ 50	2
7	D1F1L2T1C1	3000	40	300	20	7 #5	ties	#3 @ 200	1
8	D1F1L2T1C2	3000	40	300	20	7 #5	spirals	#3 @ 200	2
9	D1F1L2T2C1	3000	40	300	20	7 #5	ties	#3 @ 100	1
10	D1F1L2T2C2	3000	40	300	20	7 #5	spirals	#3 @ 100	2
11	D1F1L2T3C1	3000	40	300	20	7 #5	ties	#3 @ 50	1
12	D1F1L2T3C2	3000	40	300	20	7 #5	spirals	#3 @ 50	2
13	D1F2L1T1C1	3000	40	300	35	6 #4	ties	#3 @ 110	2
14	D1F2L1T1C2	3000	40	300	35	6 #4	spirals	#3 @ 110	4
15	D1F2L1T2C1	3000	40	300	35	6 #4	ties	#3 @ 60	2
16	D1F2L1T2C2	3000	40	300	35	6 #4	spirals	#3 @ 60	4
17	D1F2L1T3C1	3000	40	300	35	6 #4	ties	#3 @ 30	2
18	D1F2L1T3C2	3000	40	300	35	6 #4	spirals	#3 @ 30	4
19	D1F2L2T1C1	3000	40	300	35	7 #5	ties	#3 @ 110	2
20	D1F2L2T1C2	3000	40	300	35	7 #5	spirals	#3 @ 110	4
21	D1F2L2T2C1	3000	40	300	35	7 #5	ties	#3 @ 60	2
22	D1F2L2T2C2	3000	40	300	35	7 #5	spirals	#3 @ 60	4
23	D1F2L2T3C1	3000	40	300	35	7 #5	ties	#3 @ 30	2
24	D1F2L2T3C2	3000	40	300	35	7 #5	spirals	#3 @ 30	4
25	D2F1L1T1C1	3000	40	400	20	7 #5	ties	#3 @ 140	2
26	D2F1L1T1C2	3000	40	400	20	7 #5	spirals	#3 @ 140	3
27	D2F1L1T2C1	3000	40	400	20	7 #5	ties	#3 @ 70	2
28	D2F1L1T2C2	3000	40	400	20	7 #5	spirals	#3 @ 70	3
29	D2F1L1T3C1	3000	40	400	20	7 #5	ties	#3 @ 30	2
30	D2F1L1T3C2	3000	40	400	20	7 #5	spirals	#3 @ 30	3
31	D2F1L2T1C1	3000	40	400	20	12 #5	ties	#3 @ 140	2
32	D2F1L2T1C2	3000	40	400	20	12 #5	spirals	#3 @ 140	3
33	D2F1L2T2C1	3000	40	400	20	12 #5	ties	#3 @ 70	2
34	D2F1L2T2C2	3000	40	400	20	12 #5	spirals	#3 @ 70	3
35	D2F1L2T3C1	3000	40	400	20	12 #5	ties	#3 @ 30	2
36	D2F1L2T3C2	3000	40	400	20	12 #5	spirals	#3 @ 30	3
37	D2F2L1T1C1	3000	40	400	35	7 #5	ties	#4 @ 140	3
38	D2F2L1T1C2	3000	40	400	35	7 #5	spirals	#4 @ 140	5
39	D2F2L1T2C1	3000	40	400	35	7 #5	ties	#4 @ 70	3
40	D2F2L1T2C2	3000	40	400	35	7 #5	spirals	#4 @ 70	5
41	D2F2L1T3C1	3000	40	400	35	7 #5	ties	#4 @ 30	3
42	D2F2L1T3C2	3000	40	400	35	7 #5	spirals	#4 @ 30	5
43	D2F2L2T1C1	3000	40	400	35	12 #5	ties	#4 @ 140	3
44	D2F2L2T1C2	3000	40	400	35	12 #5	spirals	#4 @ 140	5
45	D2F2L2T2C1	3000	40	400	35	12 #5	ties	#4 @ 70	3
46	D2F2L2T2C2	3000	40	400	35	12 #5	spirals	#4 @ 70	5
47	D3F2L2T3C1	3000	40	400	35	12 #5	ties	#4 @ 30	3
48	D4F2L2T3C2	3000	40	400	35	12 #5	spirals	#4 @ 30	5

*f'_c = specified concrete strength; ** #3 = No. 10; #4 = No. 13; #5 = No. 16

For the transversal steel, the diameter and the spacing of the bars were calculated in order to attend three confinement indexes $I_{se} = f_{\ell se} / f_{cm}$ according to classification presented by Cusson & Paultre (1995). The concrete cylinder strength f'_c is assumed as the required average concrete strength f_{cm} (details of the calculation of f_{cm} will be presented in section 6.2.2). The first index represents low confinement ($0 < I_{se} < 0.05$); the second is medium confinement ($0.05 < I_{se} < 0.20$), and third is high confinement ($I_{se} > 0.20$). In this way, bars No. 10 (9.525 mm) and No. 13 (12.7 mm), with spacing ranging from 35 mm to 200 mm were necessary.

Relative to CFRP, two confinement ratios $I_{Fe} = f_{\ell Fe} / f_{cm}$ were targeted at: 0.08 and 0.16. The first value is the minimum level of confinement recommended by ACI 440.2R, in order to assure a non-descending second branch in the stress-strain curve. These ratios were assumed as low and high confinement levels, respectively. In order to satisfy the target values, up to 5 plies of FRP were required.

In Table 6.4, for each of the 48 columns, the following information is presented: concrete cylinder strength ($f'_c = f_{cm}$), slenderness ratio λ, longitudinal (ρ_s) and transversal steel (ρ_{sw}) ratios, volumetric spiral ratio (as given by Eq. 6.19), ratio of CFRP fibers (ρ_F), FRP confinement indexes ($I_{Fe} = f_{\ell F} / f'_c$ and $I_{Fe} = f_{\ell Fe} / f'_c$), steel confinement indexes ($I_s = f_{\ell s} / f'_c$ and $I_{se} = f_{\ell se} / f'_c$) and the ratio ($f_{\ell F}/f_{\ell s}$). It can be observed that all columns have ratios $f_{\ell F}/f_{\ell s} < 5$, (attending the upper limit in Lee model). It should be noted that for all columns the corresponding slenderness ratio is less than or equal to 40, and can be considered as short columns (according to Eq.6.18 for braced columns).

Each column was identified by a group of five letters and numbers. The first group is related to the column diameter, where D1 corresponds to 300 mm and D2 to 400 mm. The second group stands for the specified compressive strength of concrete, with F1 and F2 corresponding to 20 MPa and 35 MPa, respectively. The third group is related to longitudinal reinforcement, with L1 and L2 corresponding to 1% and 2% ratios, respectively. The fourth group is related to transversal reinforcement, with T1, T2, and T3, corresponding to low, median, and high confinement ratios, respectively. Finally, the fifth group is related to the CFRP confinement, with C1 and C2 representing low and high confinement levels, respectively.

Table 6.4 - Main parameters of the designed columns.

Column		f_{cm} (MPa)	λ [A]	$\rho_{s/}$ (%)	ρ_{sw} (%)	$\rho_{s\,min}$ (%)	ρ_F (%)	I_F	I_{Fe} [B]	I_s	I_{se} [C]	$(f_{\ell F}/f_{\ell s})$
#	ID											
1	D1F1L1T1C1	23.1	40	1.09	0.65	1.84	0.17	0.13	0.07	0.07	0.02	1.86
2	D1F1L1T1C2	23.1	40	1.08	0.65	1.84	0.34	0.25	0.14	0.07	0.04	3.73
3	D1F1L1T2C1	23.1	40	1.08	1.30	1.84	0.17	0.13	0.07	0.14	0.09	0.93
4	D1F1L1T2C2	23.1	40	1.08	1.30	1.84	0.34	0.25	0.14	0.14	0.11	1.86
5	D1F1L1T3C1	23.1	40	1.08	2.59	1.84	0.17	0.13	0.07	0.27	0.23	0.47
6	D1F1L1T3C2	23.1	40	1.08	2.59	1.84	0.34	0.25	0.14	0.27	0.25	0.93
7	D1F1L2T1C1	23.1	40	1.96	0.65	1.84	0.17	0.13	0.07	0.07	0.02	1.86
8	D1F1L2T1C2	23.1	40	1.96	0.65	1.84	0.34	0.25	0.14	0.07	0.04	3.73
9	D1F1L2T2C1	23.1	40	1.96	1.30	1.84	0.17	0.13	0.07	0.14	0.09	0.93
10	D1F1L2T2C2	23.1	40	1.96	1.30	1.84	0.34	0.25	0.14	0.14	0.11	1.86
11	D1F1L2T3C1	23.1	40	1.96	2.59	1.84	0.17	0.13	0.07	0.27	0.23	0.47
12	D1F1L2T3C2	23.1	40	1.96	2.59	1.84	0.34	0.25	0.14	0.27	0.26	0.93
13	D1F2L1T1C1	41.1	40	1.08	1.08	3.22	0.34	0.14	0.08	0.06	0.04	2.24
14	D1F2L1T1C2	41.1	40	1.08	1.08	3.22	0.68	0.29	0.16	0.06	0.05	4.47
15	D1F2L1T2C1	41.1	40	1.08	2.16	3.22	0.34	0.14	0.08	0.13	0.10	1.12
16	D1F2L1T2C2	41.1	40	1.08	2.16	3.22	0.68	0.29	0.16	0.13	0.12	2.24
17	D1F2L1T3C1	41.1	40	1.08	4.32	3.22	0.34	0.14	0.08	0.26	0.24	0.56
18	D1F2L1T3C2	41.1	40	1.08	4.32	3.22	0.68	0.29	0.16	0.26	0.25	1.12
19	D1F2L2T1C1	41.1	40	1.96	1.08	3.22	0.34	0.14	0.08	0.06	0.04	2.24
20	D1F2L2T1C2	41.1	40	1.96	1.08	3.22	0.68	0.29	0.16	0.06	0.05	4.47
21	D1F2L2T2C1	41.1	40	1.96	2.16	3.22	0.34	0.14	0.08	0.13	0.10	1.12
22	D1F2L2T2C2	41.1	40	1.96	2.16	3.22	0.68	0.29	0.16	0.13	0.12	2.24
23	D1F2L2T3C1	41.1	40	1.96	4.32	3.22	0.34	0.14	0.08	0.26	0.24	0.56
24	D1F2L2T3C2	41.1	40	1.96	4.32	3.22	0.68	0.29	0.16	0.26	0.25	1.12
25	D2F1L1T1C1	23.1	30	1.10	0.64	1.21	0.26	0.19	0.11	0.07	0.04	2.85
26	D2F1L1T1C2	23.1	30	1.10	0.64	1.21	0.38	0.29	0.16	0.07	0.05	4.27
27	D2F1L1T2C1	23.1	30	1.10	1.27	1.21	0.26	0.19	0.11	0.13	0.11	1.42
28	D2F1L1T2C2	23.1	30	1.10	1.27	1.21	0.38	0.29	0.16	0.13	0.12	2.14
29	D2F1L1T3C1	23.1	30	1.10	2.54	1.21	0.26	0.19	0.11	0.27	0.25	0.71
30	D2F1L1T3C2	23.1	30	1.10	2.54	1.21	0.38	0.29	0.16	0.27	0.26	1.07
31	D2F1L2T1C1	23.1	30	1.89	0.64	1.21	0.26	0.19	0.11	0.07	0.04	2.85
32	D2F1L2T1C2	23.1	30	1.89	0.64	1.21	0.38	0.29	0.16	0.07	0.06	4.27
33	D2F1L2T2C1	23.1	30	1.89	1.27	1.21	0.26	0.19	0.11	0.13	0.11	1.42
34	D2F1L2T2C2	23.1	30	1.89	1.27	1.21	0.38	0.29	0.16	0.13	0.13	2.14
35	D2F1L2T3C1	23.1	30	1.89	2.54	1.21	0.26	0.19	0.11	0.27	0.26	0.71
36	D2F1L2T3C2	23.1	30	1.89	2.54	1.21	0.38	0.29	0.16	0.27	0.27	1.07
37	D2F2L1T1C1	41.1	30	1.10	1.13	2.11	0.38	0.16	0.09	0.07	0.04	2.35
38	D2F2L1T1C2	41.1	30	1.10	1.13	2.11	0.64	0.27	0.15	0.07	0.06	3.92
39	D2F2L1T2C1	41.1	30	1.10	2.26	2.11	0.38	0.16	0.09	0.14	0.12	1.18
40	D2F2L1T2C2	41.1	30	1.10	2.26	2.11	0.64	0.27	0.15	0.14	0.13	1.96
41	D2F2L1T3C1	41.1	30	1.10	4.52	2.11	0.38	0.16	0.09	0.27	0.26	0.59
42	D2F2L1T3C2	41.1	30	1.10	4.52	2.11	0.64	0.27	0.15	0.27	0.27	0.98
43	D2F2L2T1C1	41.1	30	1.89	1.13	2.11	0.38	0.16	0.09	0.07	0.05	2.35
44	D2F2L2T1C2	41.1	30	1.89	1.13	2.11	0.64	0.27	0.15	0.07	0.06	3.92
45	D2F2L2T2C1	41.1	30	1.89	2.26	2.11	0.38	0.16	0.09	0.14	0.12	1.18
46	D2F2L2T2C2	41.1	30	1.89	2.26	2.11	0.64	0.27	0.15	0.14	0.13	1.96
47	D3F2L2T3C1	41.1	30	1.89	4.52	2.11	0.38	0.16	0.09	0.27	0.26	0.59
48	D4F2L2T3C2	41.1	30	1.89	4.52	2.11	0.64	0.27	0.15	0.27	0.27	0.98

[A] k = 1; [B] k_F = 0.55; [C] k_s = Eqs. 3.6 and 3.7;

6.2. Statistical Description of the Random Variables

In this study, the following variables related to the column performane were assumed as deterministic: height of the column H, number of longitudinal bars n_L, diameter of longitudinal ϕ_L and transversal steel ϕ_w bars, transversal steel spacing s, FRP number of plies n, FRP elastic modulus E_f and thickness t of each FRP ply. The other variables are assumed as random: diameter of the column $D_{\_R}$, concrete cover $c_{\_R}$, concrete compressive strength f'_{c_R}, mechanical properties of steel (Young's modulus E_{s_R}, yield strength f_{y_R}, ultimate strength f_{su_R}, strain at the onset of the strain-hardening ε_{sh_R}, and ultimate strain ε_{su_R}), ultimate tensile strength of fibers in the FRP composite f_{F_R}, model errors ξ_f and ξ_ε (see Section 4.4), dead load DL and the live load LL. In some cases where confusion might happen, distinction between random variables and their deterministic counterparts, is made by using the subscript "$_R$" in the corresponding random variable.

6.2.1. Variability in dimensions of the cross section

Based on an extensive study on the variations in dimensions of RC members from field data, Mirza & MacGregor (1979) have recommended normal distributions as probability models for all geometric deviations. The mean and standard deviation of the variable "deviation from the nominal value of the diameter" (Δ_D) are suggested as +1.52 mm and 6.35 mm, respectively; relative to the variable "deviation from the nominal value of the concrete cover" (Δ_C), the mean and standard deviation are 8.13 mm and 4.32 mm, respectively. It should be noted that column diameter $D_{\_R}$ and concrete cover $c_{\_R}$ are derived Gaussian random variables, ($D_{\_R} = D_n + \Delta_D$; $c_{\_R} = c_n + \Delta_C$). The same observation is valid for the steel confined core $D_{c\_R} = D_{\_R} - 2\, c_{\_R}$.

6.2.2. Variability in concrete compressive strength

The major sources of variation in concrete strength are the variation in materials properties and proportions of concrete mix, the variations in mixing, transporting, placing and curing methods, the variations in testing procedures, and variations due to concrete being in a structure rather than in control specimens. The average coefficient of variation (COV) can be

taken as roughly constant at 10, 15, and 20% for strength levels below 27.6 MPa for excellent, average, and poor control, respectively (Mirza *et al.*, 1979).

More recent studies indicate that the development of quality controls worldwide leads to variation coefficients close to 0.10 for a wide range of resistances (Azevedo & Diniz, 2008; Szerszen & Nowak, 2003). In this study, the lognormal distribution is assumed as the probabilistic model to describe the variability of the concrete compressive strength f'_{c_R}. The specified compressive strength of concrete f'_c is taken as 20 MPa and 35MPa and COV equal to 0.10. It should be noted that this information may be considered either the specified compressive strength for new structures or the equivalent specified compressive strength for existing structures.

According to ACI 318 (2005) the mean value of the unconfined cylinder strength f_{cm} (required average compressive strength), in MPa, can be obtained as the largest of Eq. 6.20:

$$f_{cm} = \frac{f'_c}{1 - 1.34\ COV} \qquad \text{for } f'_c \leq 35 \text{ MPa}$$
$$f_{cm} = \frac{f'_c - 3.5}{1 - 2.33\ COV} \qquad (6.20)$$

From these equations, the mean values of 23.1 MPa and 41.1 MPa are obtained, for f'_c equal to 20 MPa and 35MPa, respectively.

6.2.3. Variability in mechanical properties of steel

In this study, reinforcing bars 420 MPa grade were adopted for both the longitudinal and transversal steel. In the case of transversal steel, the only required information is the steel yield strength; on the other hand, the main parameters used in the representation of the stress-strain curve of the longitudinal steel bars are required. A Lognormal distribution was assumed as the probabilistic model to describe the variability of the steel yield strength. According to Nowak & Szerszen (2010), the recommended COV is 0.05, and the bias factor (ratio of mean strength to nominal value) is 1.145, that implies a mean value of 480.9 MPa.

The steel stress-strain curve (f_s-ε_s) proposed by Park & Paulay (1975), illustrated in Fig. 6.2, is given by the following expressions:

$$f_s = E_s\,\varepsilon_s\,; \quad \text{for} \quad \varepsilon_s \le \varepsilon_y \tag{6.21}$$

$$f_s = f_y; \quad \text{for} \quad \varepsilon_y < \varepsilon_s \le \varepsilon_{sh} \tag{6.22}$$

$$f_s = f_y\left[\frac{m(\varepsilon_s-\varepsilon_{sh})+2}{60(\varepsilon_s-\varepsilon_{sh})+2}+\frac{(\varepsilon_s-\varepsilon_{sh})(60-m)}{2(30r+1)^2}\right]; \quad \text{for} \quad \varepsilon_{sh} < \varepsilon_s \le \varepsilon_{su} \tag{6.23}$$

with $m=\dfrac{(f_{su}/f_y)(30r+1)^2 - 60r - 1}{15r^2}$ and $r=\varepsilon_{su} - \varepsilon_{sh}$

where E_s is the Young's modulus of steel; f_y is the yield strength; f_{su} is the ultimate strength; ε_y is the yield strain ($\varepsilon_y = f_y / E_s$); ε_{sh} is the strain at the onset of the strain-hardening; and ε_{su} is the ultimate strain.

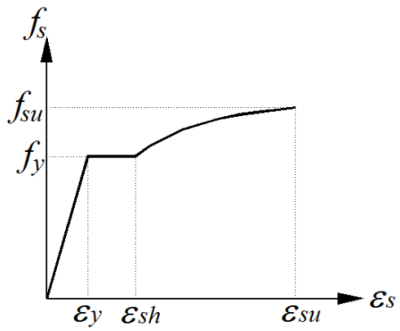

Figure 6.2 - Stress-strain curve for the steel (Park & Paulay, 1975).

In this study, the parameters f_y, f_{su}, ε_{sh}, ε_{su} and E_s that describe the stress-strain curve of steel are assumed as random variables. Their corresponding statistics are presented in Table 6.6.

6.2.4. Variability in mechanical properties of FRP

The Weibull (Extreme value type III) distribution is widely used to predict the strength of composite materials (Plevris, *et al.* 1995; Jun Jin, 2008; Wang & Yang, 2010). In this study the ultimate tensile strength of fibers f_{f_R} is assumed as a random variable following Weibull

distribution with COV of 0.05 (Wang & Yang, 2010). The mean ultimate tensile strength μf_f is taken as 3,500 MPa and the ultimate tensile strength as reported by the manufacturer f^*_F can be obtained by Eq. 6.5 ($f^*_F = \mu f_F - 3\sigma$). The fiber thickness t_f and FRP fiber elastic modulus E_f are taken as deterministic (E_f = 230 GPa; t_f = 0.128 mm); these values are consistent with CFRP Sikawrap Hex 230. Due to the linear elastic behavior of FRP, the tensile ultimate strain ε_{f_R} is also a random variable, since $\varepsilon_{f\_R} = f_{f\_R} / E_f$.

6.2.5. Model Uncertainty

A reliability analysis of FRP-RC columns requires the use of an adequate resistance model for the confined concrete and the corresponding statistics of the model error. From the results presented in Chapter 5, Lee model is adopted in this study for the simulation of the column resistance. The model error associated to the prediction of the ultimate stress ξ_f can be represented by a Normal distribution, with mean equal to 0.96 and COV equal to 0.23. Regarding the ultimate strain, the model error ξ_ε can be represented by a Lognormal distribution, with mean equal to 0.77 and COV equal to 0.54.

Model errors ξ_f and ξ_ε, as noted in the Fig. 4.24, present a moderate positive correlation, indicating a possible statistical dependence. However, in this study it was assumed that these variables are statistically independent, since, with this consideration it is possible to express a greater variability of the ultimate confined stress and the corresponding strain.

6.2.6. Variability in load effects

According to Diniz & Frangopol (1997), the load effect statistics may be computed in two different ways. The first way is to design a column for a given load combination. In this case, the nominal loads are known a priori, and the column is designed to withstand these loads. Different load combinations are analyzed (dead load, live load, etc.) and the design load is obtained as the sum of the factored nominal loads. If the relationship between nominal and mean values of a given load type is known the mean value corresponding to an assumed nominal value is computed.

In the second way, the column characteristics (materials, geometry, etc.) are chosen a priori, and the maximum nominal load acting on the column is required. In this process the design strength R_d is assumed as the same as the design load S_d, i.e:

$$R_d = \phi P_n = S_d \tag{6.24}$$

Here, the nominal strength of the column is computed by the ACI 440 approach, using either Eq. 6.7 (spirals) or Eq. 6.8 (circular ties). In these equations the confinement lateral pressure provided by FRP is calculated using the net-fiber area of the FRP, neglecting the total width and thickness of the cured system.

In this study it is considered that only dead and live loads are acting on the column. For this load combination, ACI 318 (2014) provides the Eq. 6.25 for design load, where F^*_{DL} and F^*_{LL} are the nominal dead and live loads, respectively:

$$S_d = 1.2F^*_{DL} + 1.6F^*_{LL} \tag{6.25}$$

The values of dead and live loads used for designing a structure, the so called nominal values, may differ from the corresponding mean values. Moreover, the design load is obtained by applying load factors to each load type. In a reliability analysis, the load descriptors, i.e., mean value, COV, and type of probability distribution are required. (COV and probability distribution for dead and live loads are listed in Table 6.6). Galambos *et al.* (1982) provide the values 1.05 and 1.0, for the ratio mean to nominal load μ / F^* (dead and live loads, respectively). From these data, Eq. 6.25 can be rewriten as:

$$S_d = 1.143\ \mu_{DL} + 1.6\mu_{LL} \tag{6.26}$$

Now, the mean values μ_{DL} and μ_{LL} can be easily found by, first computing the design load S_d corresponding to a given column, and then assuming the ratio between μ_{DL} and μ_{LL}. Three load ratios ($r = \mu_{DL}/\mu_{LL}$ = 0.5, 1.0, and 2.0) have been selected. Table 6.5 presents column design load, mean dead and live load obtained from the utilization of the above procedure for the 48 designed columns in this study.

Table 6.5 - Column design strength, mean dead and live loads for the designed columns.

Columns		S_d **(kN)**	**Load Ratio = 0.5**		**Load Ratio = 1.0**		**Load Ratio = 2.0**	
#	ID		μ_{DL} **(kN)**	μ_{LL} **(kN)**	μ_{DL} **(kN)**	μ_{DL} **(kN)**	μ_{LL} **(kN)**	μ_{DL} **(kN)**
1	D1F1L1T1C1	994.5	229.0	458.0	362.6	362.6	511.9	255.9
2	D1F1L1T1C2	1269.1	292.2	584.5	462.7	462.7	653.2	326.6
3	D1F1L1T2C1	994.5	229.0	458.0	362.6	362.6	511.9	255.9
4	D1F1L1T2C2	1269.1	292.2	584.5	462.7	462.7	653.2	326.6
5	D1F1L1T3C1	994.5	229.0	458.0	362.6	362.6	511.9	255.9
6	D1F1L1T3C2	1269.1	292.2	584.5	462.7	462.7	653.2	326.6
7	D1F1L2T1C1	1123.7	258.7	517.5	409.7	409.7	578.4	289.2
8	D1F1L2T1C2	1415.8	326.0	652.0	516.2	516.2	728.7	364.4
9	D1F1L2T2C1	1123.7	258.7	517.5	409.7	409.7	578.4	289.2
10	D1F1L2T2C2	1415.8	326.0	652.0	516.2	516.2	728.7	364.4
11	D1F1L2T3C1	1123.7	258.7	517.5	409.7	409.7	578.4	289.2
12	D1F1L2T3C2	1415.8	326.0	652.0	516.2	516.2	728.7	364.4
13	D1F2L1T1C1	1664.7	383.3	766.6	606.9	606.9	856.8	428.4
14	D1F2L1T1C2	2167.3	499.0	998.1	790.1	790.1	1115.5	557.8
15	D1F2L1T2C1	1664.7	383.3	766.6	606.9	606.9	856.8	428.4
16	D1F2L1T2C2	2167.3	499.0	998.1	790.1	790.1	1115.5	557.8
17	D1F2L1T3C1	1664.7	383.3	766.6	606.9	606.9	856.8	428.4
18	D1F2L1T3C2	2167.3	499.0	998.1	790.1	790.1	1115.5	557.8
19	D1F2L2T1C1	1787.9	411.7	823.4	651.8	651.8	920.2	460.1
20	D1F2L2T1C2	2305.9	531.0	1061.9	840.7	840.7	1186.8	593.4
21	D1F2L2T2C1	1787.9	411.7	823.4	651.8	651.8	920.2	460.1
22	D1F2L2T2C2	2305.9	531.0	1061.9	840.7	840.7	1186.8	593.4
23	D1F2L2T3C1	1787.9	411.7	823.4	651.8	651.8	920.2	460.1
24	D1F2L2T3C2	2305.9	531.0	1061.9	840.7	840.7	1186.8	593.4
25	D2F1L1T1C1	1877.0	432.2	864.4	684.3	684.3	966.1	483.0
26	D2F1L1T1C2	2322.6	534.8	1069.6	846.8	846.8	1195.5	597.7
27	D2F1L1T2C1	1877.0	432.2	864.4	684.3	684.3	966.1	483.0
28	D2F1L1T2C2	2322.6	534.8	1069.6	846.8	846.8	1195.5	597.7
29	D2F1L1T3C1	1877.0	432.2	864.4	684.3	684.3	966.1	483.0
30	D2F1L1T3C2	2322.6	534.8	1069.6	846.8	846.8	1195.5	597.7
31	D2F1L2T1C1	2080.6	479.1	958.2	758.5	758.5	1070.9	535.4
32	D2F1L2T1C2	2554.2	588.1	1176.3	931.2	931.2	1314.7	657.3
33	D2F1L2T2C1	2080.6	479.1	958.2	758.5	758.5	1070.9	535.4
34	D2F1L2T2C2	2554.2	588.1	1176.3	931.2	931.2	1314.7	657.3
35	D2F1L2T3C1	2080.6	479.1	958.2	758.5	758.5	1070.9	535.4
36	D2F1L2T3C2	2554.2	588.1	1176.3	931.2	931.2	1314.7	657.3
37	D2F2L1T1C1	3017.2	694.7	1389.5	1100.0	1100.0	1553.0	776.5
38	D2F2L1T1C2	3802.2	875.5	1751.0	1386.2	1386.2	1957.0	978.5
39	D2F2L1T2C1	3017.2	694.7	1389.5	1100.0	1100.0	1553.0	776.5
40	D2F2L1T2C2	3802.2	875.5	1751.0	1386.2	1386.2	1957.0	978.5
41	D2F2L1T3C1	3017.2	694.7	1389.5	1100.0	1100.0	1553.0	776.5
42	D2F2L1T3C2	3802.2	875.5	1751.0	1386.2	1386.2	1957.0	978.5
43	D2F2L2T1C1	3211.7	739.5	1479.1	1170.9	1170.9	1653.1	826.5
44	D2F2L2T1C2	4022.0	926.1	1852.2	1466.4	1466.4	2070.1	1035.1
45	D2F2L2T2C1	3211.7	739.5	1479.1	1170.9	1170.9	1653.1	826.5
46	D2F2L2T2C2	4022.0	926.1	1852.2	1466.4	1466.4	2070.1	1035.1
47	D2F2L2T3C1	3211.7	739.5	1479.1	1170.9	1170.9	1653.1	826.5
48	D2F2L2T3C2	4022.0	926.1	1852.2	1466.4	1466.4	2070.1	1035.1

6.2.7. Summary of the statistics of the basic variables

Table 6.6 summarizes the statistics of random variables considered in this study; all symbols have been previously defined.

Table 6.6 - Statistics of the basic variables related to column performance

Random variables associated with column Resistance						
Variable		Mean Value	*SD*	*COV*	Distribution	Reference
Dimensions	Δ_D (mm)	+1.52*	6.35	-	Normal	Mirza & McGregor (1979)
	Δ_C (mm)	+ 8.13*	4.32	-	Normal	Mirza & McGregor (1979)
Concrete compressive strength	f'_{c_R} (f'_c = 20 MPa)	23.1	2.31	0.10	Lognormal	Diniz & Frangopol (1997); Nowak & Szerszen (2010)
	f'_{c_R} (f'_c = 35 MPa)	41.1	4.11	0.10	Lognormal	
Longitudinal steel properties	f_{y_R} (f_{yk} = 420 MPa)	489.3	24.47	0.05	Lognormal	Nowak & Szerszen (2010)
	f_{su_R} (MPa)	714	59.3	0.083	Lognormal	Mirza & McGregor (1979)
	ε_{sh_R}	0.015	0.004	0.266	Normal	Mirza & Skrabek (1991)
	ε_{su_R}	0.15	0.03	0.20	Normal	Mirza & Skrabek (1991)
	E_{s_R} (GPa)	200	6.6	0.033	Normal	Mirza & Skrabek (1991)
Transversal steel yield strength	f_{yw} (f_{yk} = 420 MPa)	489.3	24.47	0.05	Lognormal	Nowak & Szerszen (2010)
CFRP fibers tensile strength	f_{F_R} (MPa)	3,500	175	0.05	Weibull	Plevris, *et al.* 1995; Jun Jin, 2008; Wang & Yang, 2010
Model Errors	ξ_f	0.94	0.22	0.23	Normal	see chapter 5
	ξ_ε	0.77	0.41	0.54	Lognormal	see chapter 5
Random variables associated with Loads						
Variable		Mean Value	*SD*	*COV*	Distribution	Reference
Dead Load	F_{DL} (kN)	see Table 6.6		0.10	Normal	Galambos *et al.* (1982)
Live Load	F_{LL} (kN)	see Table 6.6		0.25	Type I	Galambos *et al.* (1982)

* mean deviation from the nominal value.

6.3. Performance Function

The safety margin is given by $g(\boldsymbol{X}) = R - S$, where in the case of axially-loaded FRP-RC columns, the resistance corresponds to the maximum axial load P_R and S corresponds to the load effects, i.e, the acting load P_A. Then, the performance function is:

$$g(P_R, P_A) = P_R - P_A \tag{6.27}$$

where the resistance P_R of the confined column, is given by:

$$P_R = f_{cc\_up}\left(A_{g\_R} - A_{sL}\right) + f_{sL\_R}\, A_{sL} \tag{6.28}$$

with:

f_{cc_up} is the random variable corresponding to the confined compressive strength of the column (see Chapter 7);

A_{g_R} is the random variable corresponding to the gross area of the cross-section;

A_{sL} is the total cross-sectional area of the longitudinal steel bars (deterministic);

f_{sL_R} is the random variable corresponding to the stress in the steel longitudinal reinforcement, as given by Park & Paulay stress-strain model.

The acting load P_A is the sum of dead and live loads (see section 6.2.5):

$$P_A = F_{DL} + F_{LL} \tag{6.29}$$

where F_{DL} is the dead load and F_{LL} is the live load.

The limit state that separates the safe and the failure regions is given by the condition:

$$g(P_R, F_{DL}, F_{LL}) = P_R - F_{DL} - F_{LL} = 0 \tag{6.30}$$

where P_R is given by Eq. 6.28. The procedure for obtaining the column resistance P_R is presented in the next chapter.

7

RESISTANCE AND RELIABILITY OF FRP-RC COLUMNS

In this chapter the procedures involved in the column resistance simulation and the reliability evaluation of FRP-RC columns are presented. The chapter starts with the description of the deterministic procedure for the computation of column resistance, followed by the generation of the statistics of the column resistance. Next, a reliability analysis is performed for the 144 columns described in 6.1.3. The influence of some parameters on the resulting safety levels are investigated. Monte Carlo simulation was used to obtain the statistics of the column resistance for each of of 48 FRP-RC column cross-sections and probabilities of failure of the corresponding 144 columns. A computational procedure, program RACOL-FRP, was implemented for this purpose.

7.1. Column Resistance Simulation

7.1.1. Deterministic procedure for the computation of column resistance

The adopted deterministic procedure for column resistance calculation is based on Eq. 6.28, which is a function of the random variables: concrete confined strength $f_{cc\text{-}up}$, gross area A_{g_R}, and stress in the longitudinal steel f_{sL_R} (the area of longitudinal reinforcement A_{sL} is taken as deterministic). These variables, in their turn, are a function of other random variables. The adopted procedure is presented in Fig. 7.1; this procedure corresponds to a module in the program RACOL-FRP. The code corresponding to this program is presented in Annex B.

The procedure starts with the calculation of the random variables confined concrete ultimate conditions (f_{cc_R} and ε_{cc_R}) according to Lee *et al.* model and these values are adjusted by the corresponding model errors (ξ_f and ξ_ε), resulting in f_{cc_A} and ε_{cc_A}. In the sequence, the strain compatibility between confined concrete and longitudinal steel is verified. In the case ε_{cc_A} is

less than ε_{su}, steel strain is taken as the confined concrete strain ε_{cc_A} and the corresponding steel stress value is updated from the corresponding stress-strain curve, thus providing f_{sL_R}. In the case ε_{cc_A} is larger than ε_{su}, steel stress f_{sL_R} is the ultimate stress f_{su}, concrete strain is taken as the ultimate steel strain ε_{su}, and the corresponding confined concrete stress value is updated from the Lee stress-strain curve. The updated compatible values for confined concrete strength, f_{cc_up}, and for stress in the longitudinal steel are then used in Eq. 6.28. In the computation of confined concrete strength $f_{cc\text{-}up}$, the confinement lateral pressure provided by FRP is obtained using the net-fiber area of the FRP, neglecting the total width and thickness of the cured system. This procedure is consistent with the calculation of mean loads (section 6.2.5) and with the estimation of the model errors (Chapter 4).

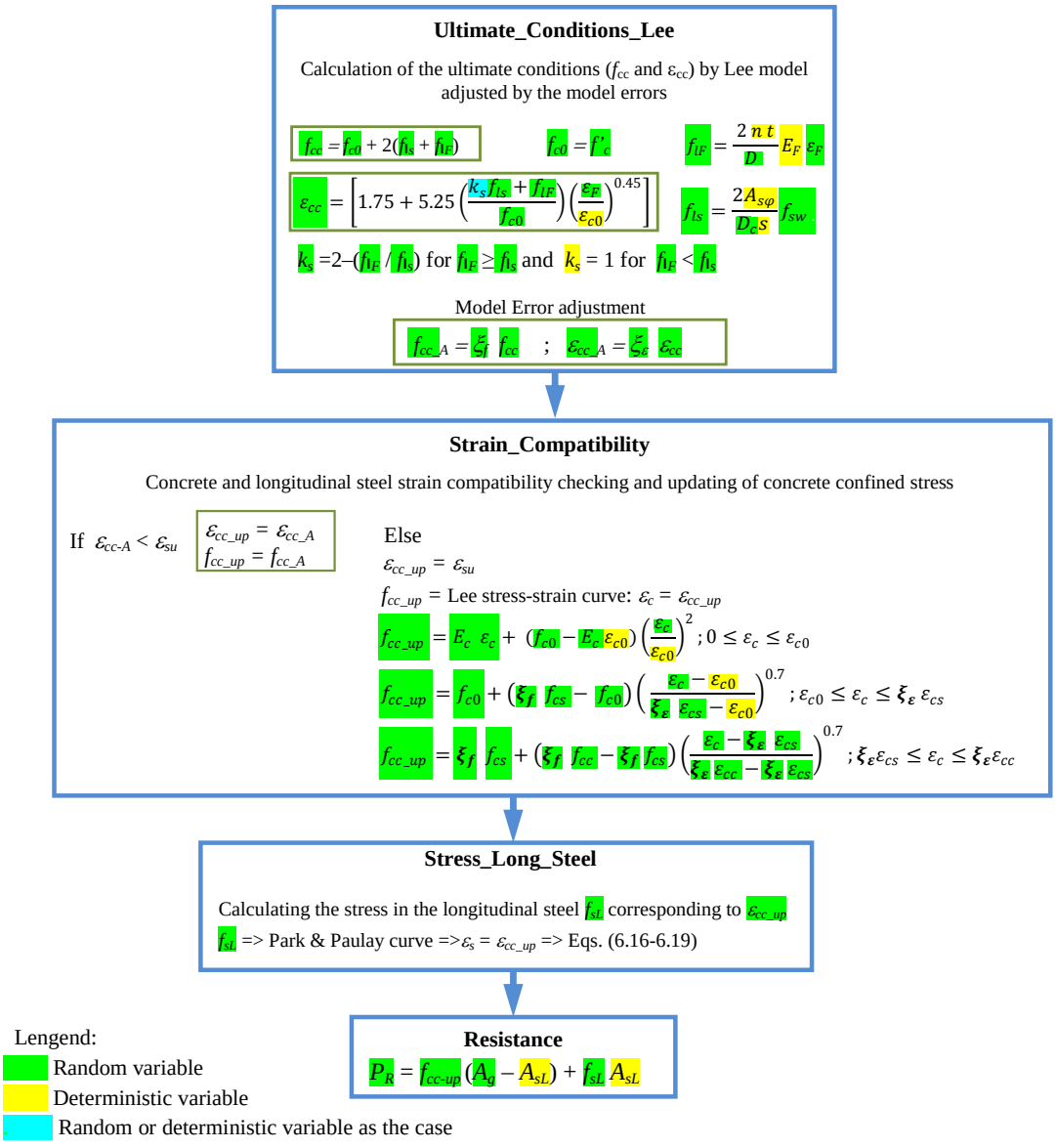

Figure 7.1 - Flowchart of the deterministic procedure for computation of column resistance

7.1.2. Statistics of column resistance

In this study, Monte Carlo simulation is used in the generation of 1,000,000 realizations of the column resistance. Statistics of the resistance P_R of the 48 FRP-confined RC columns described in Section 6.1.3 were obtained. Table 7.1 presents the statistics of the column resistance (mean, standard deviation, COV, minimum, and maximum), nominal resistance P_n, and ratio $\mu P_R / P_n$ for the 48 analyzed columns. The nominal resistance P_n is calculated according to Eq. 6.5 (spirals) or Eq. 6.6 (hoops). The ratios $\mu P_R / P_n$ are displayed in graphical form in Fig. 7.2. It can be observed that the ratios $\mu P_R / P_n$ are in the range 4.79-7.33, demonstrating that for all analyzed columns the simulated mean resistance μP_R is much higher than the corresponding nominal resistance P_n. Regarding the coefficient of variation, it is in the range 0.22-0.24.

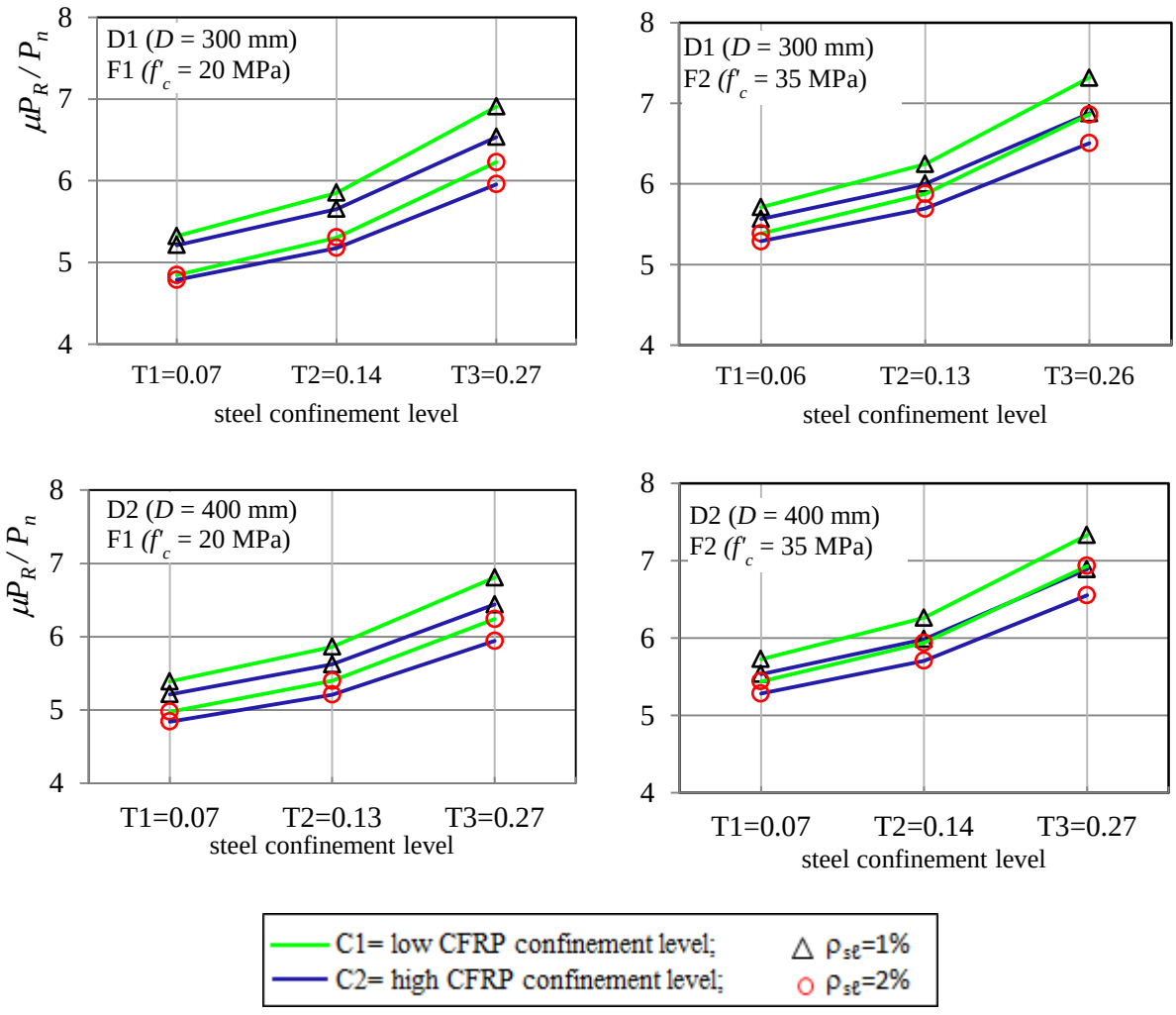

Figure 7.2 - Ratio between the mean simulated column resistance μP_R and nominal resistance P_n for the 48 analysed columns.

Table 7.1 - Statistics of the column resistance P_R and the nominal resistance $P_{n.}$

Column		Mean	SD	COV	Min (kN)	Max	P_n	$\mu P_R/P_n$
#	ID	μP_R	(kN)			(kN)	(kN)	
1	D1F1L1T1C1	7360.4	1700.4	0.23	364.2	16267.4	1382.8	5.32
2	D1F1L1T1C2	8635.2	1985.8	0.23	369.9	18893.0	1656.7	5.21
3	D1F1L1T2C1	8090.4	1862.6	0.23	367.4	17722.0	1382.8	5.85
4	D1F1L1T2C2	9365.2	2149.6	0.23	373.0	20347.5	1656.7	5.65
5	D1F1L1T3C1	9550.4	2193.2	0.23	373.7	20631.2	1382.8	6.91
6	D1F1L1T3C2	10825.2	2481.8	0.23	379.4	23256.7	1656.7	6.53
7	D1F1L2T1C1	7669.3	1696.0	0.22	638.6	16523.9	1582.9	4.85
8	D1F1L2T1C2	8940.5	1980.6	0.22	644.2	19142.6	1867.6	4.79
9	D1F1L2T2C1	8397.3	1857.8	0.22	641.8	17974.7	1582.9	5.31
10	D1F1L2T2C2	9668.4	2143.9	0.22	647.4	20593.4	1867.6	5.18
11	D1F1L2T3C1	9853.2	2187.4	0.22	648.1	20876.3	1582.9	6.22
12	D1F1L2T3C2	11124.3	2475.2	0.22	653.7	23494.9	1867.6	5.96
13	D1F2L1T1C1	12979.6	3068.8	0.24	388.1	29066.1	2272.5	5.71
14	D1F2L1T1C2	15529.1	3641.2	0.23	398.6	34317.2	2789.5	5.57
15	D1F2L1T2C1	14196.3	3339.2	0.24	392.4	31490.4	2272.5	6.25
16	D1F2L1T2C2	16745.7	3914.2	0.23	402.9	36741.5	2789.5	6.00
17	D1F2L1T3C1	16629.6	3889.4	0.23	401.1	36339.0	2272.5	7.32
18	D1F2L1T3C2	19179.0	4467.5	0.23	411.6	41590.0	2789.5	6.88
19	D1F2L2T1C1	13272.7	3060.2	0.23	663.3	29289.2	2464.6	5.39
20	D1F2L2T1C2	15815.1	3631.1	0.23	674.5	34526.6	2990.2	5.29
21	D1F2L2T2C1	14486.0	3329.9	0.23	668.6	31707.2	2464.6	5.88
22	D1F2L2T2C2	17028.3	3903.4	0.23	679.8	36944.5	2990.2	5.69
23	D1F2L2T3C1	16912.5	3878.7	0.23	679.1	36543.1	2464.6	6.86
24	D1F2L2T3C2	19454.8	4455.2	0.23	690.4	41780.4	2990.2	6.51
25	D2F1L1T1C1	14151.2	3241.3	0.23	667.4	30649.8	2626.1	5.39
26	D2F1L1T1C2	15848.6	3623.1	0.23	675.0	34116.1	3040.1	5.21
27	D2F1L1T2C1	15393.3	3518.5	0.23	672.8	33091.7	2626.1	5.86
28	D2F1L1T2C2	17090.6	3901.9	0.23	680.4	36558.1	3040.1	5.62
29	D2F1L1T3C1	17877.4	4080.7	0.23	683.6	37975.6	2626.1	6.81
30	D2F1L1T3C2	19574.8	4466.0	0.23	691.2	41441.9	3040.1	6.44
31	D2F1L2T1C1	14637.2	3233.6	0.22	1101.6	31050.3	2941.4	4.98
32	D2F1L2T1C2	16330.4	3614.5	0.22	1109.1	34508.4	3373.2	4.84
33	D2F1L2T2C1	15876.2	3510.2	0.22	1107.0	33486.4	2941.4	5.40
34	D2F1L2T2C2	17569.3	3892.7	0.22	1114.5	36944.5	3373.2	5.21
35	D2F1L2T3C1	18354.1	4071.1	0.22	1117.7	38358.7	2941.4	6.24
36	D2F1L2T3C2	20047.2	4455.4	0.22	1125.2	41816.8	3373.2	5.94
37	D2F2L1T1C1	23653.6	5553.3	0.23	708.2	52059.9	4128.9	5.73
38	D2F2L1T1C2	27048.3	6314.6	0.23	722.2	58992.6	4886.8	5.53
39	D2F2L1T2C1	25861.7	6045.0	0.23	716.1	56401.1	4128.9	6.26
40	D2F2L1T2C2	29256.4	6809.8	0.23	730.2	63333.8	4886.8	5.99
41	D2F2L1T3C1	30277.9	7043.0	0.23	732.0	65083.5	4128.9	7.33
42	D2F2L1T3C2	33672.6	7812.0	0.23	746.1	72016.2	4886.8	6.89
43	D2F2L2T1C1	24115.9	5539.3	0.23	1143.5	52409.6	4432.3	5.44
44	D2F2L2T1C2	27502.1	6298.8	0.23	1158.6	59325.9	5205.1	5.28
45	D2F2L2T2C1	26318.5	6029.9	0.23	1153.1	56740.5	4432.3	5.94
46	D2F2L2T2C2	29704.7	6792.8	0.23	1168.1	63656.8	5205.1	5.71
47	D2F2L2T3C1	30723.7	7025.5	0.23	1172.2	65402.4	4432.3	6.93
48	D2F2L2T3C2	34109.9	7792.7	0.23	1187.3	72318.7	5205.1	6.55

7.2. Reliability Analysis

In this section the reliability of the 144 designed FRP-RC columns, corresponding to 3 different load ratios ($r = \mu_{DL}/\mu_{LL}$ = 0.5, 1.0, and 2.0), for the ultimate limit state, is investigated. The safety levels implicit in the design procedures recommended by ACI 440 2R (2008) are evaluated. Monte Carlo simulation is used in the estimation of the probability of failure (and corresponding reliability indexes) of the analyzed columns. As already mentioned in the previous section, a sample size of 1,000,000 elements is used in the simulation of the column resistance and in the calculation of the corresponding probability of failure.

The results obtained via Monte Carlo simulation are affected by sampling errors (see Section 5.3.3). In the estimation of the percentage error associated to a given sample size via Eq. 5.10, an initial guess for the resulting probability of failure is required. Szerszen & Nowak (2003) recommend for RC columns, a target reliability index β = 4.0, which corresponds to a failure probability P_f = 3.2 x 10^{-5}. For this failure probability, and assuming 1,000,000 simulations, the resulting percentage error is aproximately 35%. Considering the nonlinear relationship between β and P_f , this percentage error will translate in terms of a range in the reliability index (3.9 - 4.1) similar to the range observed by Szerszen & Nowak (2003) in the selection of the target reliability for RC columns.

For each column, the load statistics presented in section 6.2.6, together with column resistance statistics generated in the previous section are used in Eq. 6.30 for the computation of the corresponding probability of failure. In the calculation of the failure probability, a sample of the possible outcomes (realizations) of the safety margin is simulated according to the corresponding performance function. Program RACOL-FRP uses the flowchart shown in Fig. 7.3; the number of unsatisfactory performances ($g(\boldsymbol{X}) < 0$), n_u, is counted, and the failure probability P_f is obtained by the ratio n_u / n_s, where n_s is the number of simulations (1,000,000 in this study). For comparative purposes, the reliability index β is also obtained:

$$\beta = -\Phi^{-1}(P_f) \tag{7.1}$$

where Φ^{-1} is the inverse standard Normal distribution.

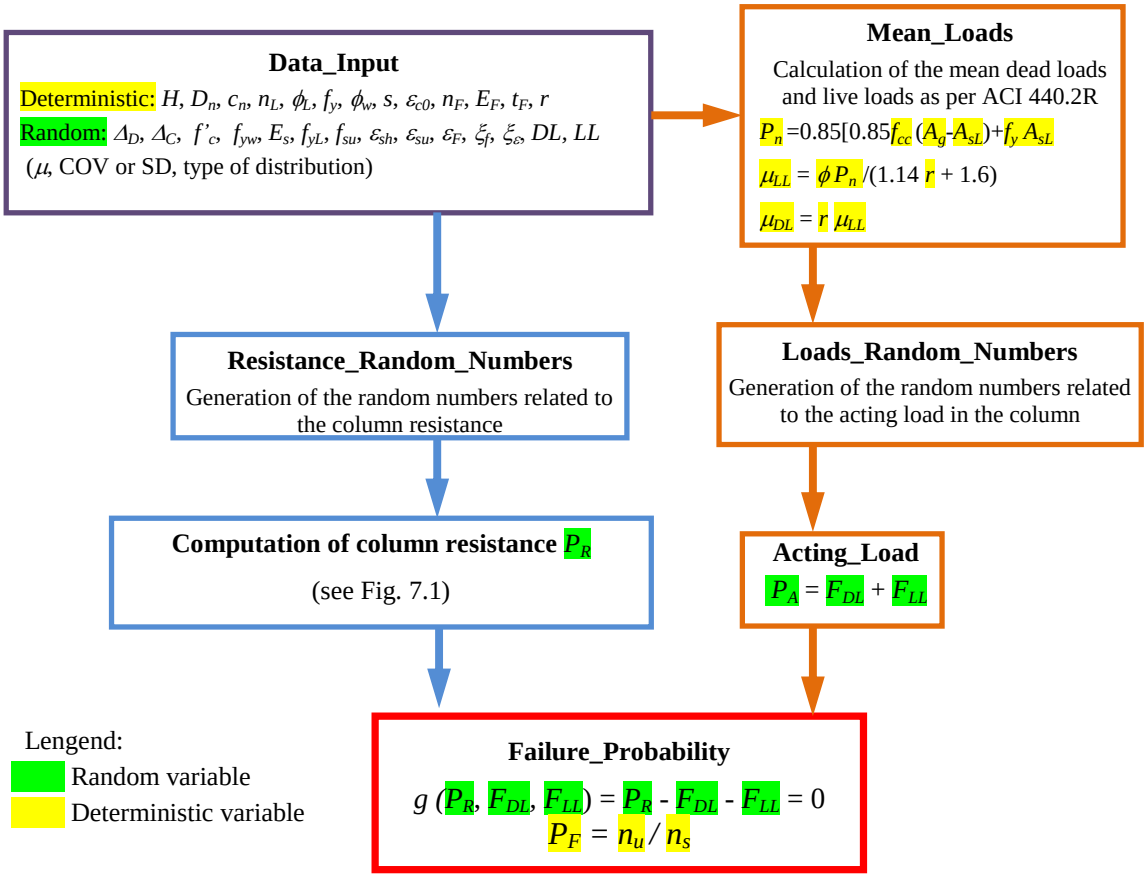

Figure 7.3 - Flowchart of the reliability assessment of FRP-RC columns, program RACOL-FRP.

Statistics of the column resistances, acting loads, and corresponding failure probabilities (and attendant reliability indexes), associated to the analyzed columns are presented in tables 7.2, 7.3 and 7.4, for the load ratios equal to 0.5, 1.0, and 2.0, respectively. This information is also presented in graphical form in Figs. 7.4 and 7.5 for the probability of failure and reliability index, respectively. From the results shown in tables 7.2 – 7.4, the values of the reliability index are in the range 4.132 (P_f = 1.8 x 10^{-5}) to 4.753 (P_f = 10^{-6}). These β values are above the target reliability index suggested by Szerszen & Nowak (2003), β_T = 4.0. It should also be noted that, while the largest probability of failure is about 18 times the smallest, this does translate into a reasonably small range in terms of the reliability index. In the sequence, the influences of some selected parameters on the resulting reliability levels are discussed.

Table 7.2 - Statistics of the column resistance, acting load, failure probability and reliability index associated to the 48 analyzed columns, load ratio = 0.5.

Columns		Resistance P_R		Acting load P_A				P_F	β
#	ID	Mean (kN)	COV	Mean (kN)	COV	Min (kN)	Max (kN)		
1	D1F1L1T1C1	7360.4	0.23	620.9	0.17	316.3	1678.6	5.0E-6	4.42
2	D1F1L1T1C2	8635.2	0.23	801.1	0.17	411.1	2126.3	8.0E-6	4.31
3	D1F1L1T2C1	8090.4	0.23	620.9	0.17	320.9	1697.5	4.0E-6	4.47
4	D1F1L1T2C2	9365.2	0.23	801.1	0.17	418.7	2178.8	8.0E-6	4.31
5	D1F1L1T3C1	9550.4	0.23	620.9	0.17	328.3	1657.1	4.0E-6	4.47
6	D1F1L1T3C2	10825.2	0.23	801.1	0.17	435.2	2149.7	7.0E-6	4.34
7	D1F1L2T1C1	7669.3	0.22	710.7	0.17	372.1	1905.1	2.0E-6	4.61
8	D1F1L2T1C2	8940.5	0.22	903.1	0.17	480.7	2454.2	6.0E-6	4.38
9	D1F1L2T2C1	8397.3	0.22	710.7	0.17	361.7	1907.0	2.0E-6	4.61
10	D1F1L2T2C2	9668.4	0.22	903.1	0.17	430.8	2408.3	4.0E-6	4.47
11	D1F1L2T3C1	9853.2	0.22	710.7	0.17	374.2	1909.1	1.0E-6	4.75
12	D1F1L2T3C2	11124.3	0.22	903.1	0.17	473.2	2432.1	4.0E-6	4.47
13	D1F2L1T1C1	12979.6	0.24	1020.4	0.17	545.8	2719.3	1.0E-5	4.26
14	D1F2L1T1C2	15529.1	0.23	1348.8	0.17	695.4	3674.7	1.3E-5	4.21
15	D1F2L1T2C1	14196.3	0.24	1020.3	0.17	562.9	2746.2	8.0E-6	4.31
16	D1F2L1T2C2	16745.7	0.23	1348.8	0.17	718.0	3604.9	1.2E-5	4.22
17	D1F2L1T3C1	16629.6	0.23	1020.3	0.17	522.5	2756.8	9.0E-6	4.29
18	D1F2L1T3C2	19179.0	0.23	1348.8	0.17	732.0	3631.2	1.1E-5	4.24
19	D1F2L2T1C1	13272.7	0.23	1106.6	0.17	564.7	2985.2	5.0E-6	4.42
20	D1F2L2T1C2	15815.1	0.23	1445.9	0.17	721.1	3951.6	8.0E-6	4.31
21	D1F2L2T2C1	14486.0	0.23	1106.6	0.17	553.3	3000.8	4.0E-6	4.47
22	D1F2L2T2C2	17028.3	0.23	1445.9	0.17	766.4	3884.2	9.0E-6	4.29
23	D1F2L2T3C1	16912.5	0.23	1106.6	0.17	599.0	2994.5	4.0E-6	4.47
24	D1F2L2T3C2	19454.8	0.23	1445.9	0.17	763.6	3914.1	6.0E-6	4.38
25	D2F1L1T1C1	14151.2	0.23	1179.1	0.17	639.4	3193.4	6.0E-6	4.38
26	D2F1L1T1C2	15848.6	0.23	1470.2	0.17	777.3	3955.4	9.0E-6	4.29
27	D2F1L1T2C1	15393.3	0.23	1179.1	0.17	646.6	3222.7	5.0E-6	4.42
28	D2F1L1T2C2	17090.6	0.23	1470.0	0.17	783.8	3934.9	8.0E-6	4.31
29	D2F1L1T3C1	17877.4	0.23	1179.2	0.17	634.3	3173.6	4.0E-6	4.47
30	D2F1L1T3C2	19574.8	0.23	1470.0	0.17	796.9	3957.0	7.0E-6	4.34
31	D2F1L2T1C1	14637.2	0.22	1320.7	0.17	636.1	3504.2	2.0E-6	4.61
32	D2F1L2T1C2	16330.4	0.22	1631.0	0.17	854.5	4408.7	6.0E-6	4.38
33	D2F1L2T2C1	15876.2	0.22	1320.8	0.17	684.0	3613.7	2.0E-6	4.61
34	D2F1L2T2C2	17569.3	0.22	1631.1	0.17	874.4	4414.1	4.0E-6	4.47
35	D2F1L2T3C1	18354.1	0.22	1320.7	0.17	718.9	3553.5	2.0E-6	4.61
36	D2F1L2T3C2	20047.2	0.22	1631.2	0.17	894.3	4343.9	3.0E-6	4.53
37	D2F2L1T1C1	23653.6	0.23	1854.0	0.17	965.8	5139.4	9.0E-6	4.29
38	D2F2L1T1C2	27048.3	0.23	2363.0	0.17	1277.5	6380.2	1.2E-5	4.22
39	D2F2L1T2C1	25861.7	0.23	1853.8	0.17	1000.2	4944.5	9.0E-6	4.29
40	D2F2L1T2C2	29256.4	0.23	2362.9	0.17	1259.3	6420.0	1.2E-5	4.22
41	D2F2L1T3C1	30277.9	0.23	1853.8	0.17	998.9	5024.2	8.0E-6	4.31
42	D2F2L1T3C2	33672.6	0.23	2363.0	0.17	1248.0	6363.7	1.0E-5	4.26
43	D2F2L2T1C1	24115.9	0.23	1990.1	0.17	1056.3	5484.7	6.0E-6	4.38
44	D2F2L2T1C2	27502.1	0.23	2516.8	0.17	1310.2	6844.4	8.0E-6	4.31
45	D2F2L2T2C1	26318.5	0.23	1990.1	0.17	1039.8	5350.2	4.0E-6	4.47
46	D2F2L2T2C2	29704.7	0.23	2516.9	0.17	1356.1	6959.8	8.0E-6	4.31
47	D2F2L2T3C1	30723.7	0.23	1990.1	0.17	1043.4	5363.4	4.0E-6	4.47
48	D2F2L2T3C2	34109.9	0.23	2516.8	0.17	1326.8	6735.7	6.0E-6	4.38

Table 7.3 - Statistics of the column resistance, acting load, failure probability and reliability index associated to the 48 analyzed columns, load ratio = 1.0.

Columns		Resistance P_R		Acting load P_A				P_F	β
#	ID	Mean (kN)	COV	Mean (kN)	COV	Min (kN)	Max (kN)		
1	D1F1L1T1C1	7360.4	0.23	655.4	0.13	368.3	1780.2	6.0E-6	4.38
2	D1F1L1T1C2	8635.2	0.23	845.6	0.13	541.7	2317.1	1.0E-5	4.26
3	D1F1L1T2C1	8090.4	0.23	655.4	0.13	435.1	1755.1	5.0E-6	4.42
4	D1F1L1T2C2	9365.2	0.23	845.7	0.13	549.8	2293.2	9.0E-6	4.29
5	D1F1L1T3C1	9550.4	0.23	655.4	0.13	423.3	1775.7	4.0E-6	4.47
6	D1F1L1T3C2	10825.2	0.23	845.6	0.13	558.4	2314.5	8.0E-6	4.31
7	D1F1L2T1C1	7669.3	0.22	750.3	0.13	481.1	2021.8	3.0E-6	4.53
8	D1F1L2T1C2	8940.5	0.22	953.3	0.13	621.9	2651.3	5.0E-6	4.42
9	D1F1L2T2C1	8397.3	0.22	750.2	0.13	486.7	2065.7	2.0E-6	4.61
10	D1F1L2T2C2	9668.4	0.22	953.3	0.13	613.1	2589.9	4.0E-6	4.47
11	D1F1L2T3C1	9853.2	0.22	750.3	0.13	485.3	1998.2	2.0E-6	4.61
12	D1F1L2T3C2	11124.3	0.22	953.2	0.13	577.0	2639.4	3.0E-6	4.53
13	D1F2L1T1C1	12979.6	0.24	1077.1	0.13	695.9	2990.0	1.1E-5	4.24
14	D1F2L1T1C2	15529.1	0.23	1423.8	0.13	932.9	4062.2	1.6E-5	4.16
15	D1F2L1T2C1	14196.3	0.24	1077.1	0.13	702.9	3079.8	1.1E-5	4.24
16	D1F2L1T2C2	16745.7	0.23	1423.7	0.13	941.9	4006.9	1.4E-5	4.19
17	D1F2L1T3C1	16629.6	0.23	1077.1	0.13	680.6	3167.8	1.0E-5	4.26
18	D1F2L1T3C2	19179.0	0.23	1423.8	0.13	897.3	4074.1	1.1E-5	4.24
19	D1F2L2T1C1	13272.7	0.23	1168.1	0.13	728.2	3335.2	8.0E-6	4.31
20	D1F2L2T1C2	15815.1	0.23	1526.4	0.13	1018.2	4230.4	1.0E-5	4.26
21	D1F2L2T2C1	14486.0	0.23	1168.2	0.13	791.4	3248.3	4.0E-6	4.47
22	D1F2L2T2C2	17028.3	0.23	1526.3	0.13	1012.0	4261.1	9.0E-6	4.29
23	D1F2L2T3C1	16912.5	0.23	1168.0	0.13	794.6	3196.3	3.0E-6	4.53
24	D1F2L2T3C2	19454.8	0.23	1526.2	0.13	1001.5	4224.6	8.0E-6	4.31
25	D2F1L1T1C1	14151.2	0.23	1244.5	0.13	754.5	3510.1	6.0E-6	4.38
26	D2F1L1T1C2	15848.6	0.23	1551.7	0.13	1032.5	4316.4	1.1E-5	4.24
27	D2F1L1T2C1	15393.3	0.23	1244.6	0.13	802.6	3434.2	6.0E-6	4.38
28	D2F1L1T2C2	17090.6	0.23	1551.7	0.13	1023.8	4277.3	1.0E-5	4.26
29	D2F1L1T3C1	17877.4	0.23	1244.6	0.13	811.1	3491.3	4.0E-6	4.47
30	D2F1L1T3C2	19574.8	0.23	1551.7	0.13	996.8	4225.4	1.0E-5	4.26
31	D2F1L2T1C1	14637.2	0.22	1394.2	0.13	849.6	3762.8	3.0E-6	4.53
32	D2F1L2T1C2	16330.4	0.22	1721.7	0.13	1052.5	4641.9	5.0E-6	4.42
33	D2F1L2T2C1	15876.2	0.22	1394.1	0.13	850.4	3776.2	2.0E-6	4.61
34	D2F1L2T2C2	17569.3	0.22	1721.6	0.13	1098.3	4694.2	6.0E-6	4.38
35	D2F1L2T3C1	18354.1	0.22	1394.1	0.13	922.8	3827.8	2.0E-6	4.61
36	D2F1L2T3C2	20047.2	0.22	1721.7	0.13	1122.4	4725.3	3.0E-6	4.53
37	D2F2L1T1C1	23653.6	0.23	1957.0	0.13	1255.2	5333.7	1.1E-5	4.24
38	D2F2L1T1C2	27048.3	0.23	2494.2	0.13	1688.4	7014.1	1.5E-5	4.17
39	D2F2L1T2C1	25861.7	0.23	1957.0	0.13	1279.5	5700.4	9.0E-6	4.29
40	D2F2L1T2C2	29256.4	0.23	2494.4	0.13	1714.3	7114.0	1.4E-5	4.19
41	D2F2L1T3C1	30277.9	0.23	1956.7	0.13	1247.2	5490.0	8.0E-6	4.31
42	D2F2L1T3C2	33672.6	0.23	2494.4	0.13	1679.0	6940.8	1.1E-5	4.24
43	D2F2L2T1C1	24115.9	0.23	2100.6	0.13	1360.9	5879.9	7.0E-6	4.34
44	D2F2L2T1C2	27502.1	0.23	2656.7	0.13	1819.9	7508.5	1.2E-5	4.22
45	D2F2L2T2C1	26318.5	0.23	2100.6	0.13	1346.1	5863.8	6.0E-6	4.38
46	D2F2L2T2C2	29704.7	0.23	2656.9	0.13	1750.4	7531.9	1.1E-5	4.24
47	D2F2L2T3C1	30723.7	0.23	2100.6	0.13	1379.7	5713.8	5.0E-6	4.42
48	D2F2L2T3C2	34109.9	0.23	2656.4	0.13	1661.0	7148.9	7.0E-6	4.34

Table 7.4 - Statistics of the column resistance, acting load, failure probability and reliability index associated to the 48 analyzed columns, load ratio = 2.0.

Columns		Resistance P_R		Acting load P_A				P_F	β
#	ID	Mean (kN)	COV	Mean (kN)	COV	Min (kN)	Max (kN)		
1	D1F1L1T1C1	7360.4	0.23	694.0	0.11	413.3	1329.9	7.0E-6	4.34
2	D1F1L1T1C2	8635.2	0.23	895.3	0.11	516.3	1790.3	1.4E-5	4.19
3	D1F1L1T2C1	8090.4	0.23	694.0	0.11	404.9	1332.1	7.0E-6	4.34
4	D1F1L1T2C2	9365.2	0.23	895.4	0.11	515.8	1705.9	1.2E-5	4.22
5	D1F1L1T3C1	9550.4	0.23	694.0	0.11	413.9	1359.9	3.0E-6	4.53
6	D1F1L1T3C2	10825.2	0.23	895.4	0.11	524.9	1699.1	8.0E-6	4.31
7	D1F1L2T1C1	7669.3	0.22	794.4	0.11	464.2	1500.6	3.0E-6	4.53
8	D1F1L2T1C2	8940.5	0.22	1009.2	0.11	560.6	1871.0	6.0E-6	4.38
9	D1F1L2T2C1	8397.3	0.22	794.3	0.11	478.2	1486.6	2.0E-6	4.61
10	D1F1L2T2C2	9668.4	0.22	1009.3	0.11	593.6	1909.0	6.0E-6	4.38
11	D1F1L2T3C1	9853.2	0.22	794.3	0.11	449.4	1478.3	2.0E-6	4.61
12	D1F1L2T3C2	11124.3	0.22	1009.3	0.11	597.5	1912.1	3.0E-6	4.53
13	D1F2L1T1C1	12979.6	0.24	1140.4	0.11	647.8	2083.7	1.2E-5	4.22
14	D1F2L1T1C2	15529.1	0.23	1507.6	0.11	881.7	2862.4	1.8E-5	4.13
15	D1F2L1T2C1	14196.3	0.24	1140.3	0.11	614.5	2260.8	1.1E-5	4.24
16	D1F2L1T2C2	16745.7	0.23	1507.4	0.11	860.9	2861.5	1.5E-5	4.17
17	D1F2L1T3C1	16629.6	0.23	1140.5	0.11	646.8	2169.2	1.1E-5	4.24
18	D1F2L1T3C2	19179.0	0.23	1507.6	0.11	851.1	2937.3	1.4E-5	4.19
19	D1F2L2T1C1	13272.7	0.23	1236.8	0.11	744.7	2414.4	9.0E-6	4.29
20	D1F2L2T1C2	15815.1	0.23	1616.1	0.11	954.6	2955.2	1.5E-5	4.17
21	D1F2L2T2C1	14486.0	0.23	1236.9	0.11	724.3	2322.9	7.0E-6	4.34
22	D1F2L2T2C2	17028.3	0.23	1615.9	0.11	860.9	3030.1	1.1E-5	4.24
23	D1F2L2T3C1	16912.5	0.23	1236.8	0.11	715.4	2476.5	3.0E-6	4.53
24	D1F2L2T3C2	19454.8	0.23	1615.9	0.11	942.5	2980.8	1.3E-5	4.21
25	D2F1L1T1C1	14151.2	0.23	1317.9	0.11	763.0	2525.8	9.0E-6	4.29
26	D2F1L1T1C2	15848.6	0.23	1642.6	0.11	960.3	3009.6	1.3E-5	4.21
27	D2F1L1T2C1	15393.3	0.23	1318.0	0.11	749.7	2557.0	8.0E-6	4.31
28	D2F1L1T2C2	17090.6	0.23	1643.1	0.11	955.4	3125.7	1.1E-5	4.24
29	D2F1L1T3C1	17877.4	0.23	1318.0	0.11	782.7	2448.9	6.0E-6	4.38
30	D2F1L1T3C2	19574.8	0.23	1643.1	0.11	931.0	3142.2	1.0E-5	4.26
31	D2F1L2T1C1	14637.2	0.22	1476.1	0.11	866.2	2823.7	3.0E-6	4.53
32	D2F1L2T1C2	16330.4	0.22	1823.3	0.11	1074.1	3382.8	6.0E-6	4.38
33	D2F1L2T2C1	15876.2	0.22	1476.1	0.11	842.7	2814.8	3.0E-6	4.53
34	D2F1L2T2C2	17569.3	0.22	1823.0	0.11	1108.7	3370.5	7.0E-6	4.34
35	D2F1L2T3C1	18354.1	0.22	1476.0	0.11	844.7	2838.6	3.0E-6	4.53
36	D2F1L2T3C2	20047.2	0.22	1822.9	0.11	1105.0	3438.6	6.0E-6	4.38
37	D2F2L1T1C1	23653.6	0.23	2072.1	0.11	1157.2	3861.8	1.2E-5	4.22
38	D2F2L1T1C2	27048.3	0.23	2641.1	0.11	1447.6	5067.5	1.7E-5	4.14
39	D2F2L1T2C1	25861.7	0.23	2072.1	0.11	1229.4	3831.6	1.3E-5	4.21
40	D2F2L1T2C2	29256.4	0.23	2641.0	0.11	1544.5	4793.5	1.6E-5	4.16
41	D2F2L1T3C1	30277.9	0.23	2072.2	0.11	1148.4	3913.4	1.0E-5	4.26
42	D2F2L1T3C2	33672.6	0.23	2640.8	0.11	1400.4	4892.3	1.3E-5	4.21
43	D2F2L2T1C1	24115.9	0.23	2224.1	0.11	1335.9	4147.1	9.0E-6	4.29
44	D2F2L2T1C2	27502.1	0.23	2812.6	0.11	1676.1	5367.1	1.3E-5	4.21
45	D2F2L2T2C1	26318.5	0.23	2224.4	0.11	1312.9	4024.3	8.0E-6	4.31
46	D2F2L2T2C2	29704.7	0.23	2813.2	0.11	1696.0	5534.6	1.3E-5	4.21
47	D2F2L2T3C1	30723.7	0.23	2224.4	0.11	1315.4	4266.8	4.0E-6	4.47
48	D2F2L2T3C2	34109.9	0.23	2813.0	0.11	1705.0	5242.2	1.0E-5	4.26

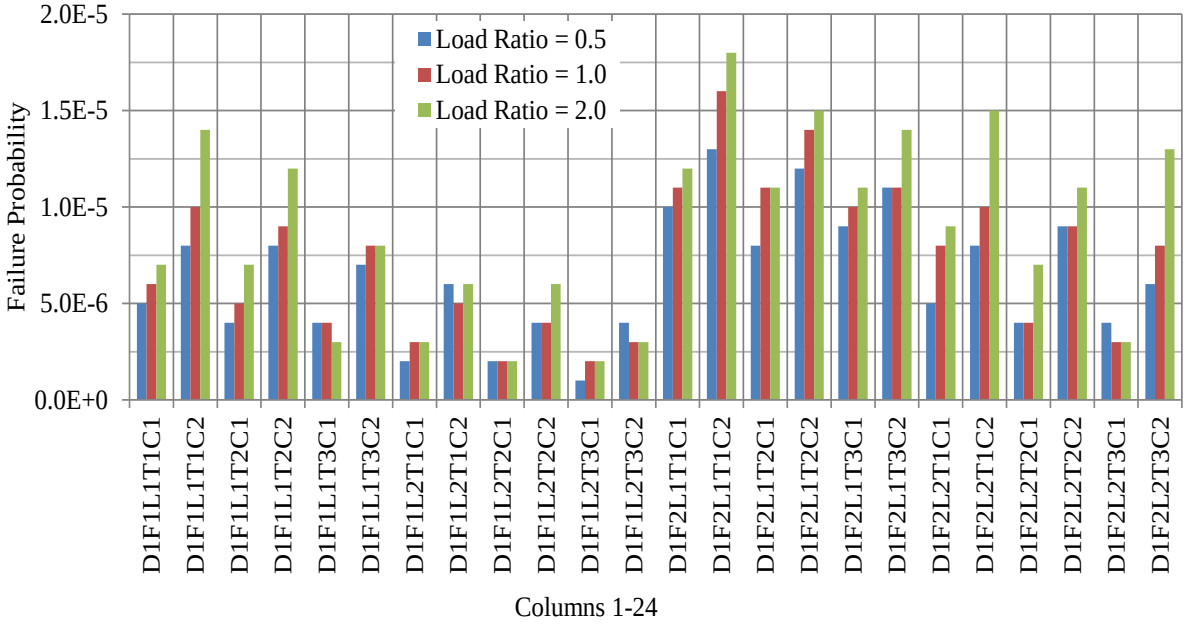

(a)

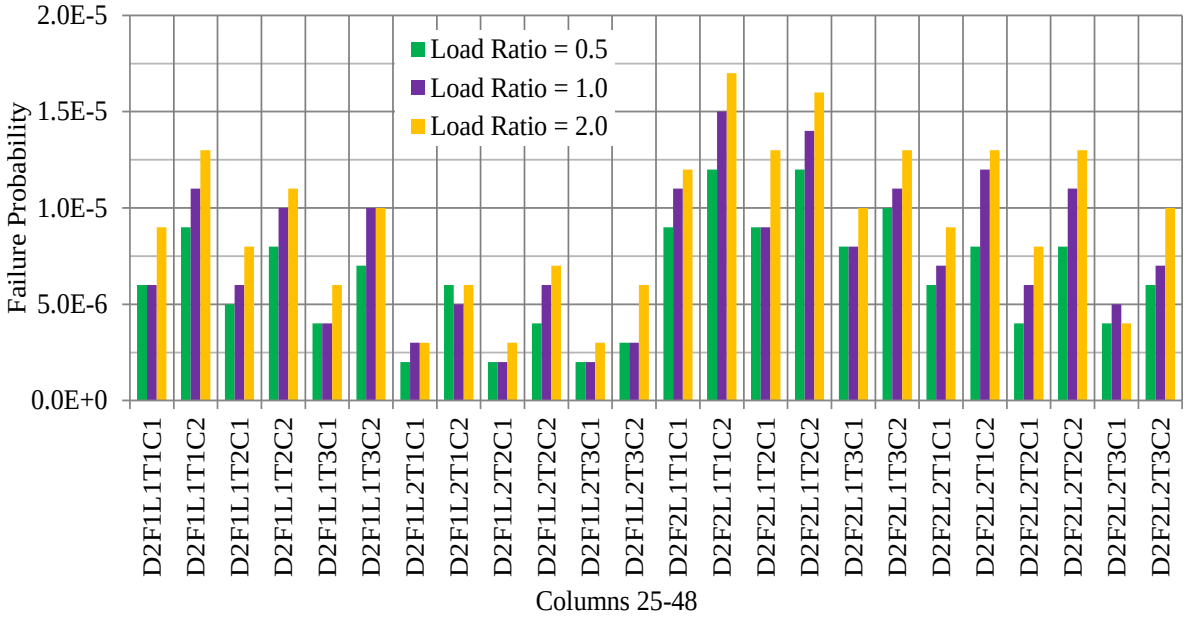

(b)

Figure 7.4 - Failure probability of FRP-RC columns: a) columns 1-24, b) columns 25-48.

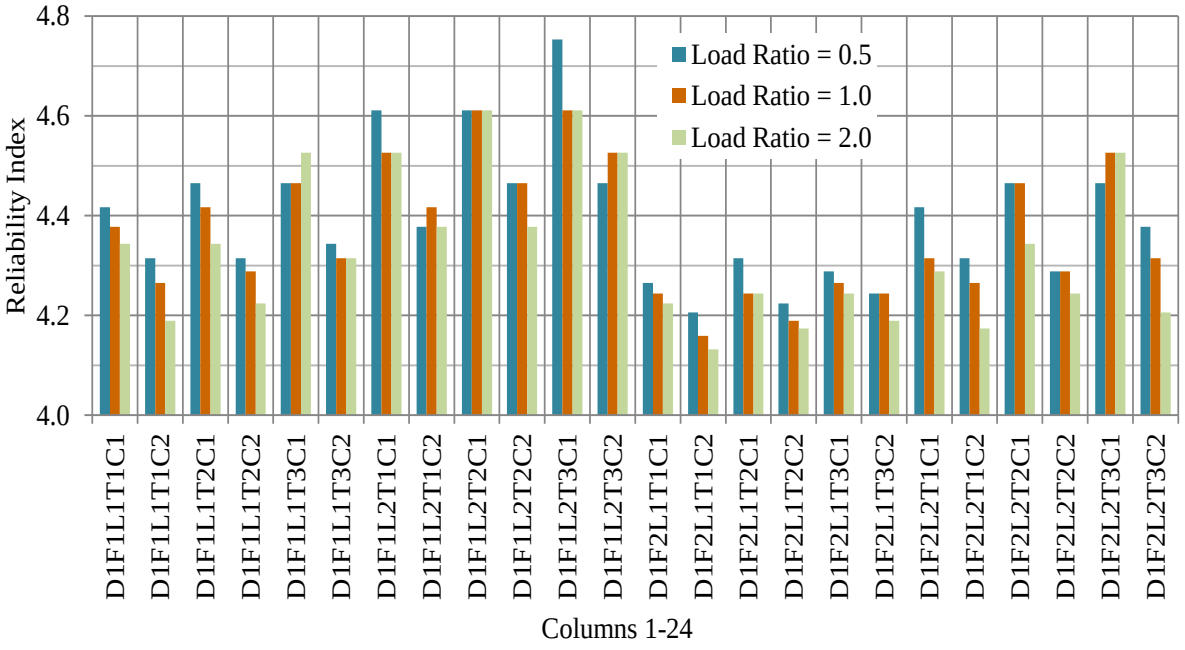

(a)

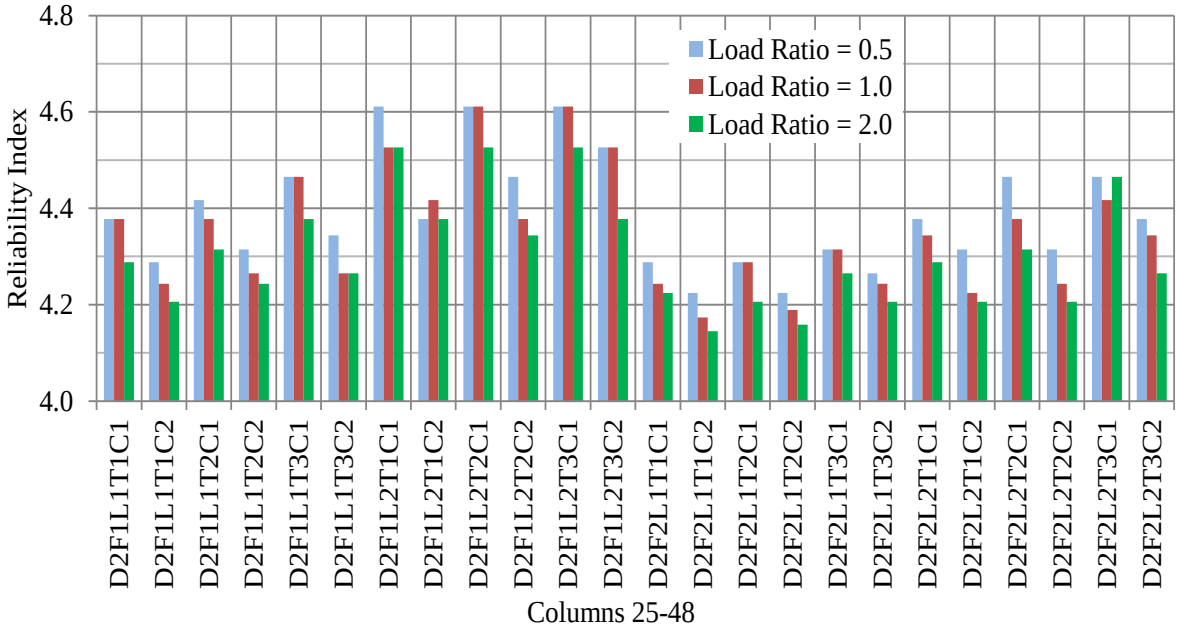

(b)

Figure 7.5 - Reliability index of FRP-RC columns: a) columns 1-24 b) columns 25-48.

Table 7.5 presents a summary of the statistics of the failure probability and reliability index of the analyzed columns. Columns 14-D1F2L1T1C2 and 11-D1F1L2T3C1 present the smallest and the largest values of β (and consequently, the largest and smallest failure probability), respectively.

Table 7.5 - Summary of the statistics of the failure probability P_F and reliability index β.

statistics	Failure Probability P_F			Reliability Index β		
	r = 0.5	r = 1.0	r = 2.0	r = 0.5	r = 1.0	r = 2.0
mean	6.42E-06	7.50E-06	9.06E-06	4.392	4.360	4.318
min	1.00E-06	2.00E-06	2.00E-06	4.206	4.159	4.132
max	1.30E-05	1.60E-05	1.80E-05	4.753	4.611	4.611

7.3. Influence of the selected variables on FRP-RC column reliability

The influence of the variables: load ratio r, diameter D, specified concrete strength f'_c, longitudinal steel ratio ρ_{sL}, steel confinement level $f_{\ell se}/f_{cm}$, and FRP confinement level $f_{\ell Fe}/f_{cm}$, on FRP-RC column reliability, is evaluated. Figures 7.6, 7.7 and 7.8 depict the influence of these selected variables on the failure probabilities P_F of FRP-RC analyzed columns for the load ratios r = 0.5, r = 1.0 and r = 2.0, respectively.

From these figures, it can be observed for the columns considered in this work an increase in the failure probability P_F as the load ratio r increases. Furthermore, the cases where this observation does not apply, are associated to the smallest failure probabilities. It is submitted that these exceptions are related to the the fact that larger samples would be required in order to capture best estimates of the failure probability.

The analysis of the results of each load ratio isolated shows that regarding to diameter D, a slight variability in the failure probability is observed, when the diameter varies, inferring that the diameter was not a significant variable in this case. With respect to the concrete compressive strength, the columns with smallest compressive strength (f'_c = 20 MPa) resulted in smallest failure probabilities. The influence of the longitudinal steel ratio ρ_{sL} on the failure probability was positive: the failure probability decreases as longitudinal steel ratio ρ_{sL} increases.

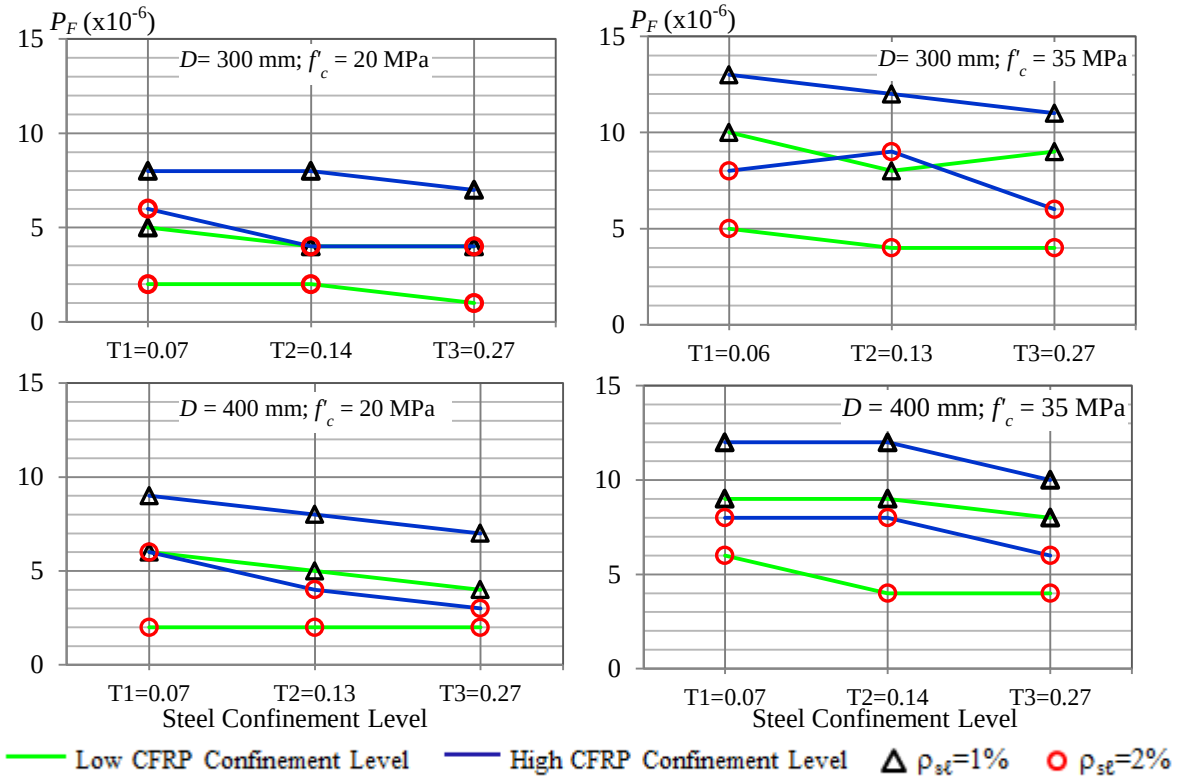

Figure 7.6 - Influence of the selected variables on the failure probability for load ratio r = 0.5.

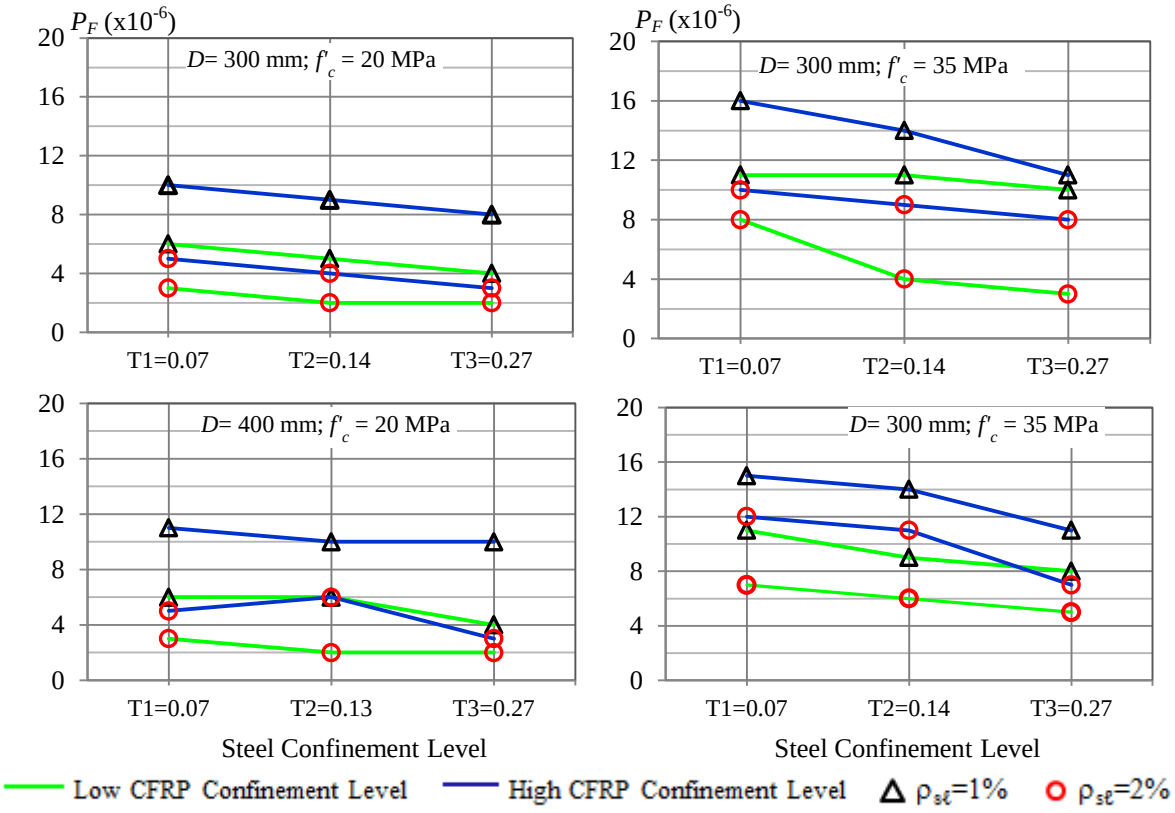

Figure 7.7 - Influence of the selected variables on the failure probability for load ratio r = 1.0.

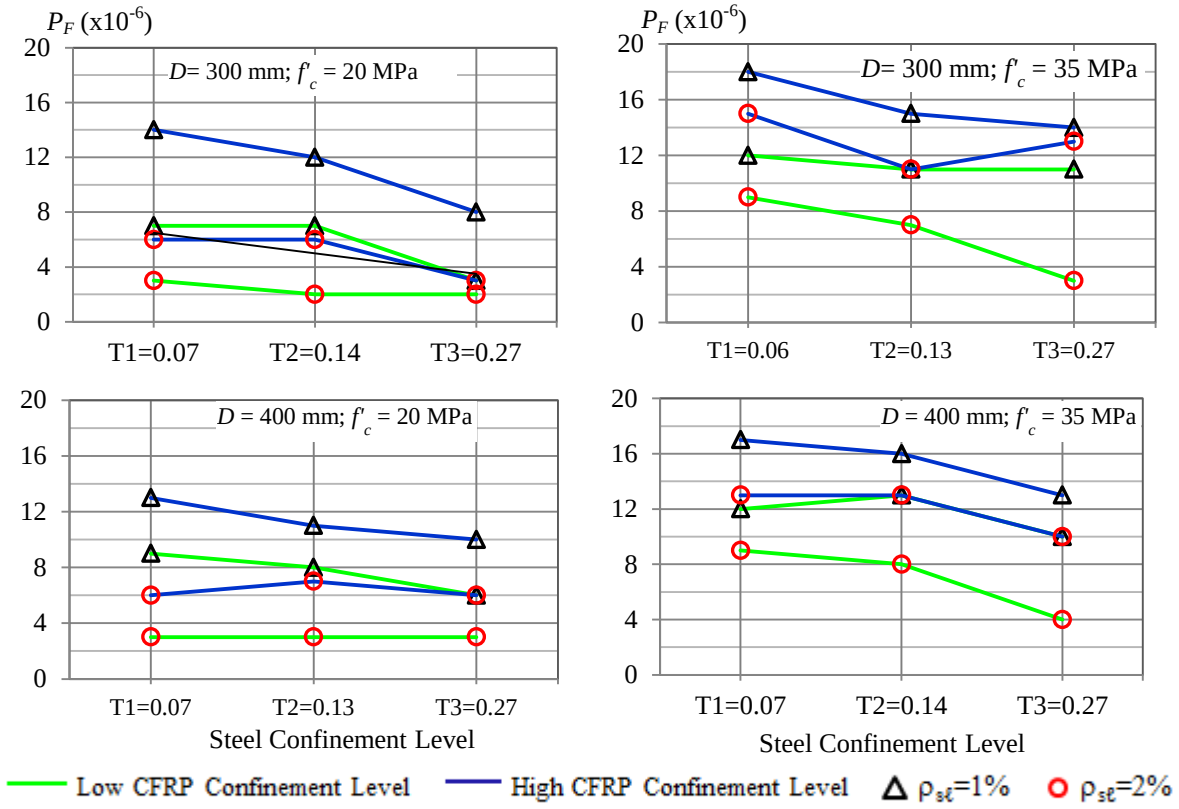

Figure 7.8 - Influence of the selected variables on the failure probability for load ratio r = 2.0.

Regarding to confinement level, the influence of the steel confinement in the failure probability reveal, in the most cases, a slight tendency of an decrease of the failure probability with an increase of the steel confinement level. This result could be expected, since: (i) the levels of steel confinement used in the designed columns is either less or at most equal to the minimum suggested by ACI 318, (ii) the confinement effect provided by the transversal steel is smaller than the effect of the FRP confinement, (iii) ACI 440 confinement model for FRP-RC columns does not consider steel confinement effects (see Eqs. 6.11 and 6.12), while this effect is incorporated in the Lee model, used herein for the computation of the column resistance. Relative to the FRP confinement level, the failure probability increases with an increase of the FRP confinement level. This is an interesting result because it is largely known that an increase in the FRP confinement level should result in a higher confined concrete compressive strength. However, the acting loads suggested by ACI 440 procedures overestimate the increase in concrete strength due to confinement effects. This is confirmed by the results presented in Table 7.1, where the ratio $\mu P_R/P_n$ always decreases as the FRP confinement level increases.

Similar results are presented in Figs. 7.9, 7.10 and 7.11 that depict the influence of these selected variables relative to the realibility index β of the FRP-RC analyzed columns for the load ratios 0.5, 1.0 and 2.0, respectively.

From these figures, analogous conclusions those presented before can be made: an increase in the load ratio *r* has resulted in a slight decrease in the reliability index; the diameter have no influence in the realiability index; smaller concrete compressive strengths and larger longitudinal steel ratios resulted in largest reliability indexes; there is a slight tendency of an increase of the reliability index with an increase of the steel confinement ratio and decreasing when the CFRP confinement level increasing. In summary, for the recommendations of ACI 440.2R (2008), the most significant variables in the reliability for the analyzed columns herein were f'_c, ρ_{sL}, and $f_{\ell Fe}/f'_c$.

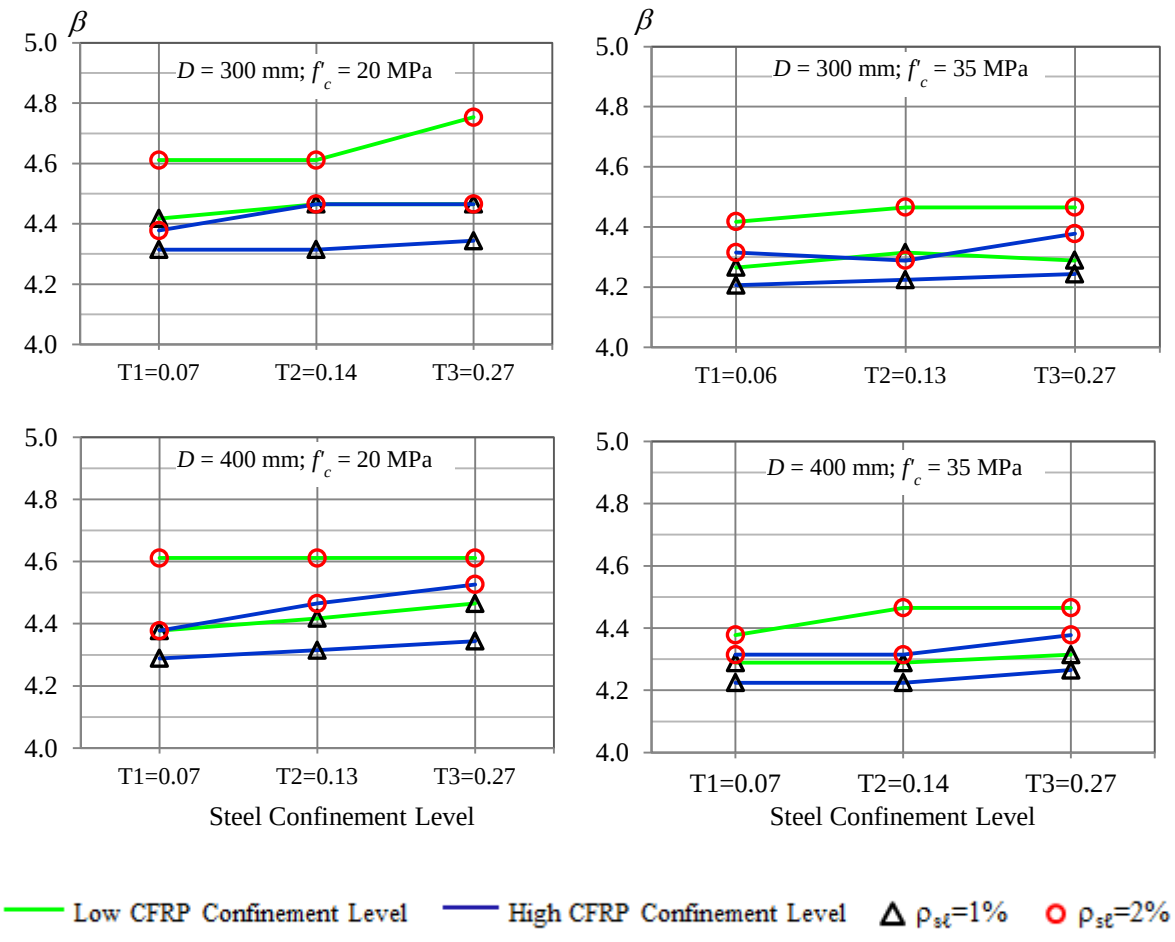

Figure 7.9 - Influence of the selected variables on the reliability index for load ratio *r* = 0.5.

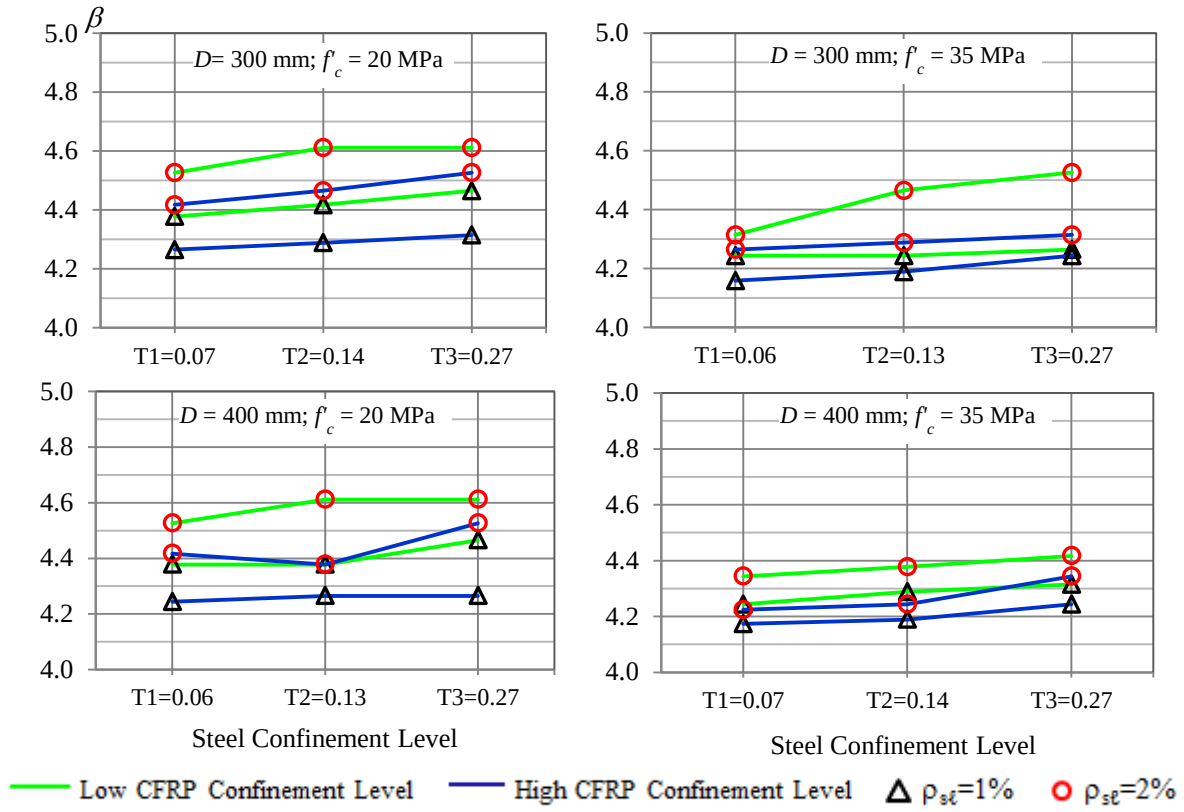

Figure 7.10 - Influence of the selected variables on the reliability index load ratio r = 1.0.

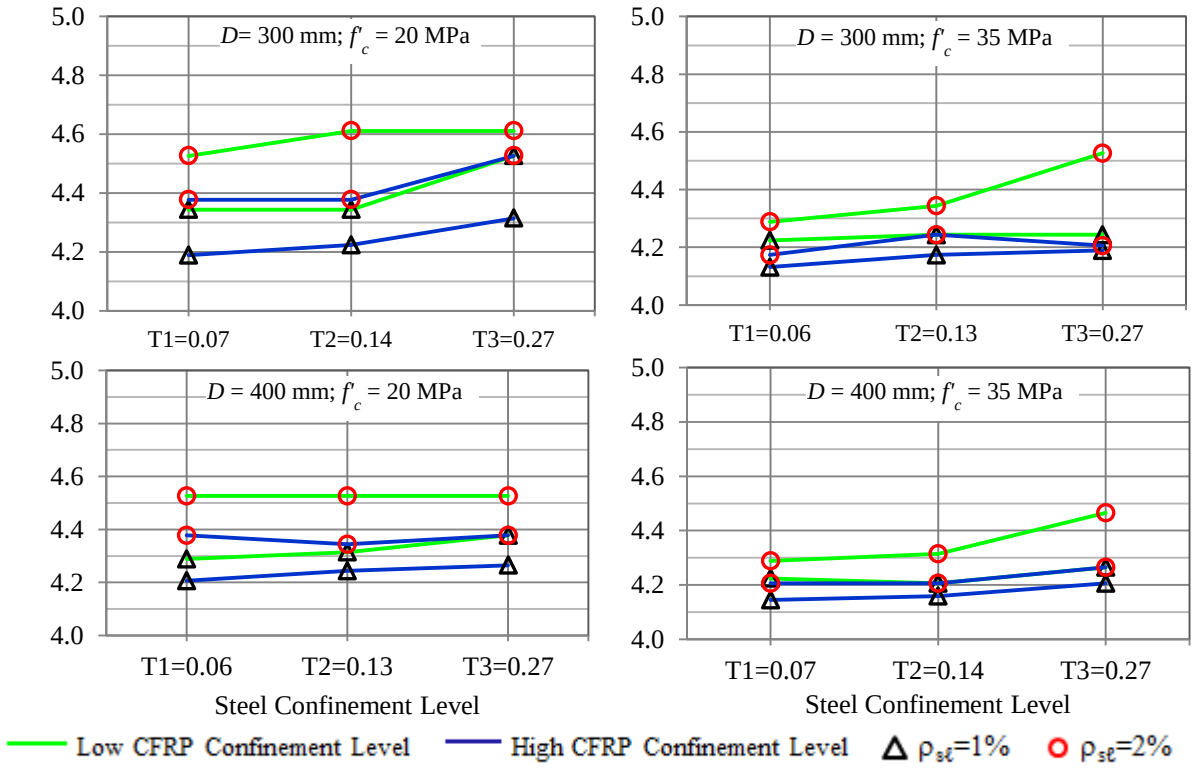

Figure 7.11 - Influence of the selected variables on the failure probability for load ratio r = 2.0

8.

SUMMARY, CONCLUSIONS AND SUGESTIONS FOR FURTHER RESEARCHES

8.1. Summary

In this study, the performance of five representative models, C&S (Chastre & Silva, 2010); P&M (Pellegrino & Modena, 2010); Lee (Lee *et al.*, 2010); SH (Shirmohamadi *et al.*, 2015); and Ilki (Ilki *et al.*, 2008), addressing the behavior of circular RC columns confined by FRP and transversal steel was discussed. In order to support this discussion, a database of 151 CFRP confined RC columns with longitudinal and transversal steel (spirals or circular hoops) was compiled from the available literature. This investigation addressed the stress-strain curve of confined concrete and prediction of the ultimate stress and strain. The predictions according to the selected models were checked against the experimental database results. A statistical analysis was performed in order to describe the random variables "model error" associated to ultimate stress, ξ_f, and ultimate strain, ξ_ε, that are required information in a reliability analysis of FRP-RC columns. Based on the results of these statistics the best model has been selected.

The reliability assessment of short circular RC columns confined by CFRP, with respect to the ultimate limit state, has been performed. One hundred forty-four axially-loaded FRP-RC short columns, designed according to the recommendations of ACI 440.2R (2008) and ACI 318 (2014), were considered in the analysis. All columns have height of 3000 mm, diameter of 300 mm or 400 mm, specified concrete strength of 20 MPa or 35 MPa, and longitudinal steel ratios around 1% or 2%. Three confinement indexes (I_{se}) for transversal steel were adopted, representing low, medium and high confinement, and two confinement indexes (I_{Fe}) for FRP jacketing were adopted, representing low and high confinement. These columns were subjected to three different load ratios (0.5, 1.0, and 2.0). A computational procedure for the

simulation of column resistance and reliability analysis, program RACOL-FRP, was implemented in the Matlab software. Finally, the influence of the variables diameter *D*, specified concrete strength f'_c, longitudinal steel ratio ρ_{sL}, steel confinement level $f_{\ell se} / f_{cm}$, FRP confinement level $f_{\ell Fe}/f_{cm}$, and load ratio on the reliability of FRP-RC columns has been evaluated.

8.2. Conclusions

Relative to the existing confinement models for FRP-RC columns, several confinement models have been suggested, most of them have been validated by experimental results of cylinders of plain concrete. However, in the confinement of existing RC columns by FRP, concrete, longitudinal steel, tranversal steel and FRP are involved. As such, a database of experimental results of columns confined by FRP and transversal steel was required to validate suggested models. In this study, a comprehensive database comprising 151 CFRP confined RC columns was compiled. For the 151 columns in the database, the normalized gain, with respect to concrete strength ($f_{cc\ exp} / f'_c$) is in the range 1.05-5.77, with a mean of 1.99, and COV of 0.43; the normalized gain with respect to concrete ultimate strain ($\varepsilon_{cc\ exp} / \varepsilon_{c0}$), is in the range 1.46-33.0, with a mean of 7.53, and COV of 0.84.

For the performance of the analyzed models:

- Regarding the stress-strain curve, it was observed that SH model largely overestimates the ultimate strain; C&S model always overestimates stresses; a comparison between Lee and P&M model shows that the former best represents experimental results for both the shape of the stress-strain curve and ultimate conditions, displaying a very accurate fit, in many cases;
- Regarding the prediction of the ultimate conditions, C&S and Ilki model overestimate both ultimate stress and strain; additionally, the model that best describes the compressive strength of FRP-RC columns is Lee model, with data points with less dispersion along the 45^o line, representing the ideal model. SH model, as already observed in the context of the stress-strain behavior, overestimates ultimate strains; to a lesser extent, this is also the case of C&S model. P&M model and Lee model show similar results, with the former displaying slightly better results;

- Regarding the model error associated to the prediction of the ultimate stress, ξ_f, mean values are in the range 0.83-1.18, with C&S and P&M models displaying the smallest and the largest mean, respectively; and COV in the range 0.23-0.49, with the smallest value corresponding to Lee model and the largest to SH model;
- Regarding ξ_ε, predictions of the ultimate strain are not as accurate as those related to ultimate stresses. Mean values of ξ_ε are in the range 0.58-0.85, with C&S and P&M models displaying the smallest and the largest mean, respectively; COVs are in the range 0.54-1.43, with the smallest value corresponding to Lee model;
- It is also interesting to note that the COV of the model error,--for both ultimate stress and strain--, in all confinement models considered in this work, are considerably high; this information has a large impact on the reliability of FRP-RC columns;
- In addition to satisfying the features related to a bias closer to the unity and smaller COV, for both ultimate stress and ultimate strain, Lee model does not display a trend with respect to the variables *H/D*, f'_c and f_l / f'_c; as a result, this model and the corresponding statistics of the model error has been selected to be used in the simulation of the column resistance. For Lee model, the model error, ξ_f , can be represented by a Normal distribution (mean equal to 0.96 and 0.23 for the COV), and the model error, ξ_ε, by a Lognormal distribution (mean equal to 0.77 and 0.54 for the COV).

The reliability evaluation of 144 FRP-RC short axially-loaded columns for the ultimate limit state was performed; all considered columns have been designed according to ACI 440.2R (2008) and ACI 318 (2014). For the results obtained, the following conclusions can be drawn:

- A computational procedure using Monte Carlo simulation, program RACOL-FRP, has been developed as part of this research. In this tool, a sample size of 1,000,000 has proved to be effective for the probabilities of failure associated to the columns considered in this work. This program incorporates a module for the simulation of the statistics of the column resistance and a module for the generation of the statistics of the acting loads (which depends on the selected strengthening design procedure, e.g. ACI 440.2R (2008));
- The reliability indexes β associated to the columns considered in this work are above the target reliability index suggested by Szerszen & Nowak (2003), β_T = 4.0, for the design of new RC columns. It is largely accepted that the target values for existing

structures may be smaller than those of new structures; in this light, the safety of the strengthened RC columns considered in this research has been verified;

- The reliability indexes obtained herein are in the range 4.132 – 4.753; in terms of the failure probabilities, the largest ($1.8x10^{-5}$) is about 18 times the smallest (10^{-6}). This is a limitation of the semiprobabilistic design formats currently in use;

The influence of the variables diameter D, specified concrete strength f'_c, longitudinal steel ratio ρ_{sL}, steel confinement level $f_{\ell se}/f_{cm}$, and FRP confinement level $f_{\ell Fe}/f_{cm}$, and load ratio on the resulting reliability levels of FRP-RC columns was evaluated. It was concluded that:

- An increase in the load ratio r has resulted in a slight increase in the failure probability;
- Smaller concrete compressive strengths and larger longitudinal steel ratios have a positive effect on column reliability;
- There is a slight tendency of an increase of the reliability index (and consequently a decrease of the failure probability) with an increase of the steel confinement ratio. While this increase may not be significant in the case of new structures, this may have an important impact on the decision about the performance of an existing structure;
- ACI 440 procedures overestimate the increase in concrete strength due to confinement effects; this translates into reliability indexes decreasing (and consequently the failure probability increases) as FRP confinement levels increase;
- In summary, for the analyzed columns, and the recommendations of ACI 440.2R (2008) the most influential variables are f'_c, ρ_{sL}, and $f_{\ell Fe}/f'_c$;
- Even though, in this study, the reliability assessment of the safety levels implicit in current design procedures has been limited to ACI 440.2R (2008) recommendations, the modular structure used in the program RACOL-FRP can be easily modified in order to accommodate different design requirements.

It may be envisioned that FRP jacketing of RC columns may be used for both new and existing structures; however, the most important application of this technique has been in the strengthening of existing columns. As pointed out by Melchers (1999), the safety evaluation of existing structures is distinct from that related to the safety implementation in the design of new ones. While design codes for new structures allow for uncertainties in the design and

construction processes, much of what was initially uncertain are no longer in the finished structure.

This would translate into the challenge of obtaining statistics that would describe material properties in the existing structure, e.g. concrete compressive strength. In this study this difficulty was dealt with using ACI 440 (2008) recommendation in which f'_c represents either: (i) the specified compressive strength of concrete (based on statistics of a concrete population of new structures), or (ii) an estimated equivalent f'_c based on analysis of results of cylinder tests from the original construction, or tests of cores removed from the part of the structure where strength is in question. The statistics of mechanical properties of materials to be used in the reliability analysis of FRP-RC columns, as well as, the target reliability index, --from the viewpoint of existing structures--, are still open and controversial issues that must be addressed by normative committees.

8.3. Sugestions for Further Researches

This work focused of reliability assessment of short circular FRP-RC columns for ultimate limit state of pure axial compression. The implicity . A number of further studies may be a follow up of the present study:

This study has been limited to the reliability assessment of short circular axially-loaded FRP-RC columns, for the ultimate limit state, designed according to ACI 440.2R (2008) recommendations. A number of further studies may be a follow up of the present study:

(1) With respect to confinement models:
   - This study has been limited to circular FRP-RC columns. This limitation is related to the efficiency of lateral confinement for circular cross-section configurations. Other geometries should be investigated in both experimental and theoretical studies;
   - This study has been limited to short axially-loaded columns. This limitation was the result of: (i) FRP confinement is more effective when there is no strain gradient along the cross-section; and (ii) in the cases when there is a strain gradient along the cross-section, this effect should be accounted for in the analysis. More

research should be addressed to the evaluation of the influence of strain gradients on the FRP confinement effects.

(2) With respect to the reliability assessment:

- Evaluate the reliability levels implicit in the design of FRP-RC columns for recommendations from different documents such as: CNR DT 200 (2004); CSA S806 (2002); fib (2001); ISIS (2001); JSCE (2001). This can be easily performed for the case of short axially-loaded circular FRP columns, by adjusting the load statistics module in program RACOL-FRP;
- Perform reliability analyses for FRP-RC columns with square or rectangular cross-sections (provided adequate FRP confinement models exist for such geometries);
- Provided that models that account for the presence of strain gradients along the cross-section are available, the reliability assessment of both short and slender eccentrically-loaded FRP-RC columns may be performed.

(3) With respect to the reliability assessment of existing structures, this is a challenging problem that would require the definition of:

- statistics to be used for the in situ mechanical properties of the materials (concrete and steel), geometry (concrete dimensions, area of longitudinal steel, area of transversal steel);
- adequate treatment of resistance deterioration (e.g. chemical attacks and long-term effects);
- load statistics must be defined in such a way to be compatible to the use of the structure and updated intended service life;
- target values of the reliability index for existing structures, that must be reached by consensus in normative bodies.

REFERENCES

ABDELRAHMAN, K.; EL HACHA, R. Behavior of large-scale concrete columns wrapped with CFRP and SFRP sheets. *Journal of Composites for Construction*. Vol. 16, nº 4, pp. 30-43, 2012.

AMERICAN SOCIETY OF CIVIL ENGINEERS ASCE 7-05. *Minimum design loads for buildings and other structures*, Virginia, 388p. 2005.

AMERICAN CONCRETE INSTITUTE - ACI 318: *Building code requirements for reinforced concrete and commentary.* Farmington Hills, Michigan, USA, 430p. 2005

AMERICAN CONCRETE INSTITUTE - ACI 318: *Building code requirements for reinforced concrete and commentary.* Farmington Hills, Michigan, USA, 519p. 2014

AMERICAN CONCRETE INSTITUTE - ACI 440.2R: G*uide for the design and construction of externally bonded FRP systems for strengthening concrete structures*, Farmington Hills, Michigan, USA, 45p., 2002.

AMERICAN CONCRETE INSTITUTE - ACI 440.2R: G*uide for the design and construction of externally bonded FRP systems for strengthening concrete structures*, Farmington Hills, Michigan, USA, 76p., 2008.

AMERICAN CONCRETE INSTITUTE – ACI 440.R: S*tate-of-the-art report on fiber reinforced plastic (FRP) reinforcement for concrete structures*, Detroit, USA, 68 p., 1996.

ANG, A. H .S.; TANG, W. H. *Probability Concepts in Engineering Planning and Design: Decision, Risk, and Reliability*. Xª Ed. Nova York: John Wiley & Sons, Xxx p., 1984.

AZEVEDO, C.P.B.; DINIZ, S.M.C. Estudo probabilístico da resistência à compressão de concretos utilizados em fundações (in Portuguese). *50º Congresso Brasileiro do Concreto*, Salvador, 2008.

BENZAID, R.; MESBAH, H.; CHIKH, N. FRP-confined concrete cylinders: axial compression experiments and strength model. *Journal of Reinforced Plastics and Composites*, Vol. 29, nº 16, pp. 2469-2488, 2010.

BENZAID, R. (2010). Contribution à l'étude des matériaux composite dans le renforcement et la réparation des éléments structuraux linéaires en béton (In Franch) PhD Thesis. Mentouri University of Constantine, Algeria.

BISBY, A. L.; DENT, A. J. S.; GREEN M. F. Comparison of confinement models for fiber reinforced polymer-wrapped concrete. *ACI Structural Journal.* Vol. 102, nº 1, pp. 62-72, 2005.

CANADIAN STANDARDS ASSOCIATION - CSA S806: D*esign and construction of building components with fiber reinforced polymers*, Ottawa, Canadá, 2002.

CARRAZEDO, R. *Mecanismos de confinamento e suas implicações no reforço de pilares de concreto por encamisamento com compósito de fibras de carbono* (in Portuguese). Master's thesis. 2002. 173p. Engineering School of the University of São Carlos, São Carlos, Brasil.

CARRAZEDO, R.; HANAI, J. B. Efeitos do confinamento em pilares de concreto armado encamisados com compósito de fibras de carbono. *Cadernos de Engenharia de Estruturas*, São Carlos, Vol. 8, nº 30, pp. 59-77, 2006.

CHASTRE, C., SILVA, M. A. G. Monotonic axial behavior and modelling of RC circular columns confined with CFRP. *Engineering Structures*, ELSEVIER. Vol. 2, nº1, pp. 2268-2277, 2010.

CHOWDHURY, E. U. Behaviour of fibre reinforced polymer confined reinforced concrete columns under fire condition. PhD Thesis. 235p. 2006. Queen's University Kingston, Ontario, Canada

CUSSON, D. AND PAULTRE, P. Stress-Strain Model for Confined High-Strength Concrete. *Journal of Structural Engineering*, ASCE, Vol. 121, nº 3, 468-477, 1995.

DE LORENZIS, L.; TEPFERS, R. Comparative study of models on confinement of concrete cylinders with fiber reinforced polymer composites. *Journal of Composites for Construction*, ASCE. Vol. 7, nº.3, pp. 219-237, 2003.

DINIZ, S. M. C.; FRANGOPOL, D. M. Reliability bases for high-strength concrete columns. *Journal of Structural Engineering*, 123:1375-81, 1997.

DINIZ, S.M.C. Structural reliability: Rational tools for design code development, *Structures 2008:* Crossing Borders, 2008

EDWARDS, K. L. An overview of the technology of fibre reinforced plastics for design purposes. *Materials and Design.* Vol. 19, pp.1-10, 1998.

EID, R., ROY, N., PAULTRE, P. Normal and high-strength concrete circular elements wrapped with FRP composites. *Journal of Composite for Construction*. ASCE. 13 (2):113-124, 2009.

EL-HACHA , R.; GREEN, M.; WIGHT, G. R. Effect of severe environmental exposures on CFRP wrapped concrete columns. *Journal of Composites for Construction,* ASCE, Vol. 14, nº 1, pp. 83-93, 2010.

ESCOBAR, C. J. *Avaliação do desempenho estrutural de vigas de concreto armado reforçadas com lâminas de CFRP tensionadas* (in Portuguese). Master's thesis. 2003, 183p. Federal University of Paraná. Curitiba, Brasil.

EUROPEAN STANDARD- *Eurocode 2: design of concrete structures: part 1–1: general rules and rules for buildings*. CEN. Brussels, 226p. 2004.

FAHMY, M.; WU, Z. Evaluating and proposing models of circular concrete columns confined with different FRP composites. *Composites Part B: Engeneering*, ELSEVIER. Vol. 41, nº 3, pp. 199-213, 2010.

FARDIS, M. N.; KHALILI H. FRP encased concrete as a structural material. *Magazine Concrete Research.* Vol. 34, Nº 121, pp. 191-202, 1982.

GREEN, M. F.; BISBY, L. A.; FAM, A. Z.; KODUR, V. K. R. FRP confined concrete columns: Behaviour under extreme conditions. *Cement e Concrete Composites,* ELSEVIER, Vol. 28, nº 1, pp. 928-937, 2006.

HALDAR, A.; MAHADEVAN, S. Probability, reliability, and statistical methods in engineering design. John Wiley, 304 p. 2000.

ILKI, A.; KUMBASAR, N.; KOC, V. Low strength concrete members externally confined with FRP sheets. *Structural Engineering Mechanics*. Vol. 18, nº 2, pp. 167-194, 2004.

ILKI, A.; PEKER, O.; KARAMUK, E.; DEMIR, C.; KUMBASAR, N. FRP retrofit of low and medium strength circular and rectangular reinforced concrete columns. *Journal of Materials in Civil Engineering*, ASCE. Vol. 20, nº 2, pp. 169-188, 2008.

INTELLIGENT SENSING FOR INNOVATE STRUCTURES - ISIS: Manual de Projeto nº4: S*trengthening reinforced concrete structures with externally bonded fiber reinforced polymers*, Winnipeg, Manitoba, Canada, 209 p., 2001.

INTERNATIONAL FEDERATION FOR STRUCTURAL CONCRETE – *fib Bulletin 14:* E*xternally bonded FRP reinforcement for RC structures*, Lausanne, Switzerland, 130 p., 2001.

JAPAN SOCIETY OF CIVIL ENGINEERS - JSCE: Concrete Engineering Series 41: *Recommendations for the upgrading of concrete structures with use of continuous fiber sheets*, Japão, 41p., 2001.

JIANG, T.; TENG, J. G. Strengthening of short circular RC columns with FRP jackets: a design proposal. In: Proceedings of *Third international conference on FRP composites in civil engineering*. Miami, Florida, USA; 2006.

JONES, M. R. Mechanics of composite materials. 2ª Ed. Taylor & Francis, 1999.

JUVANDES, L. F. P. Reforço e reabilitação de estruturas de betão usando materiais compósitos de CFRP. Tese. 1999. 360p. Faculdade de Engenharia da Universidade do Porto, Porto, Portugal.

LAM, L.; TENG, J.G. Design-oriented stress-strain model for FRP-confined concrete. *Construction and Building Materials*, ELSEVIER. Vol. 17, pp. 471-489, 2003.

LAM, L.; TENG, J.G. Strength Models for Fiber-Reinforced Plastic-Confined Concrete. *Journal of Structural Engineering*, ASCE. Vol. 128, nº5 pp. 612-623, 2002.

LEE, J. Y.; YI, C. K.; JEONG, H. S.; KIM, S. W.; KIM, J. K. Compressive response of concrete confined with steel spirals and FRP composites. *Journal of Composite Materials.*Vol. 44, nº4, pp. 481-504, 2010.

LI, Y. F.; LIN, C. T.; SUNG, Y. Y. A constitutive model for concrete confined with carbono fiber reinforced plastics. Mechanics of Materials, ELSEVIER. Vol. 35, nº 3, pp. 603-619, 2003.

LIGNOLA, G.P.; PROTA, A.; MANFREDI, G.; COSENZA, E. Effective strain in FRP jackets on circular RC columns. *Fourth International Conference on FRP Composites in Civil Engineering* (CICE). Zurich, Switzerland, 2008.

MACHADO, A. P. *Reforço de estruturas de concreto armado com fibras de carbono.* 1st ed. São Paulo: Pini, 282p. 2002.

MANDELL, J. F.; MEIER, U. Effect of stress ratio, frequency, and loading time on the tensile fatigue of glass-reinforced epoxy. *Long-Term Behavior of Composites, ASTM STP 813,* pp. 55-77, 1983.

MANDER, J. B.; PRIESTLEY, M. J. N.; PARK, R. Theoretical stress strain model for confined concrete.*Journal of Structural Engineering,* ASCE. Vol. 114, nº 8, pp. 1804-1826, 1988.

MARQUES, S. P. C.; MARQUES, D. C. S. C.; SILVA, J. L.; CAVALCANTE, M. A. A. Model for analysis of short columns of concrete confined by fiber-reinforced polymer. Journal of Composites for Construction, ASCE. Vol. 8, nº4, pp. 332-340, 2004.

MATTHYS, S.; TOUTANJI, H.; TAERWE, L. Stress-strain behavior of large-scale circular columns confined with FRP composites. *Journal of Structural Engineering,* ASCE.Vol. 132, nº 1, pp. 123-133, 2006.

MEIER, U.; KAISER, H., Strengthening of Structures with CFRP Laminates. *Advanced Composite Materials in Civil Engineering Structures,* ASCE, pp. 224-232, 1991.

MELCHERS, R. E. Assessment of existing structures-approaches and research needs. *Journal of Structural Engineering,* ASCE. Vol. 127, nº. 4, pp. 406-411, 2001

MELCHERS, R. E. *Structural Reliability Analysis and Prediction*. Xª Ed. Cidade: John Wiley & Son, 1999.

MIYAUCHI, K.; NISHIBAYASHI, S.; INOUE, S. Estimation of strengthening effects with carbon fiber sheet for concrete column. *Third International symposium of non-metallic reinforcement for concrete structures*, 1997.

MUGURUMA, H., WATANABE, F. Ductility improvement of high-strength concrete columns with lateral confinement. *Highstrength Concrete, SP-121, American Concrete Institute*, Detroit, Mich., pp. 47-60, 1990.

NACIONAL RESEARCH COUNCIL - CNR DT 200: G*uide for the design and construction of externally bonded FRP systems for strengthening existing structures*, Roma, Itália, 144 p., 2004.

NOWAK, A. S.; COLLINS, K. R. *Reliability of Structures***,** CRC Press, 2nd edition, 407p. 2012.

OZBAKKALOGLU, T., LIM, J. C. Axial compressive behavior of FRP-confined concrete: Experimental test database and a new design-oriented model. *Engineering Structures*. ELSEVIER. 49(1): 1068-1088, 2013.

OZBAKKALOGLU, T.; LIM, J. C.; VINCENT, T. FRP confined concrete in circular sections: review and assessment of stress–strain models. *Engineering Structures*, ELSEVIER. Vol 49, nº 1, pp. 1068-1088, 2013.

PELLEGRINO C., MODENA C. Analytical model for FRP confinement of concrete columns with and without internal steel reinforcement. *Journal of Composites for Construction*, ASCE. 14 (6): 693-705, 2010

PESSIKI, S.; HARRIES, K. A; KESTNER, J.; SAUSE, R.; RICLES, J. M. The axial behavior of concrete confined with fiber reinforced composite jackets. *Journal of Composites for Construction*, ASCE. Vol. 5, nº 4, pp. 237-245, 2001.

POPOVICS, S. a numerical approach to the complete stress-strain curve of concrete. *Cement and Concrete Research*. Vol. 3, nº 5, pp. 583-599, 1973.

RAZVI, S. R., SAATCIOGLU, M. Strength and ductility of confined concrete. *Journal of Structural Engineering*, ASCE, 118(6), 1590-1607, 1992.

RICHARD, R. M.; ABBOTT, B. J. Versatile elastic-plastic stress-strain formula. *Journal of Engeneering Mechanics Div*, ASCE. Vol. 101, nº 4, pp. 511-515, 1975

RICHART, F. E; BRANDTZAEG, A.; BROWN, R. L. A study of the failure of concrete under combined compressive stresses. In: Bulletin no. 185, Univ. of Illinois, Engineering Experimental Station: Champaign; 1928.

RICHART, F. E; BRANDTZAEG, A.; BROWN, R. L. The failure of plain and spirally reinforced concrete in compression. *Bulletin nº 190*, Univ. of Illinois, Engineering. Experimental Station, Urbana, 77p. 1929.

RIGAZZO, A. O., MORENO JR, A. L. (2006) Design parameters for reinforced concrete columns strengthening with CFRP. *IBRACON Structural Journal*. 2 (2):178-186.

ROYLANCE, M. E. The effect of moisture on the properties of an aramid/epoxy composite. *Army Materials and mechanics research center*, Massachussets, PhD Thesis. 147p, 1983.

SARGIN M. *Stress-strain relationship for concrete and the analysis of structural concrete section*. PhD Thesis. 1971. 167p. University of Waterloo: Ontario, Canada.

SAADATMANESH, H.; EHSANI, M. R.; LI, M. W. Strength and ductility of concrete columns externally reinforced with fiber composite straps. *ACI Structural Journal.* Vol. 91, nº 4, pp. 434-447, 1994.

SAATCIOGLU, M.; RAZVI, S. R. Strength and ductility of confined concrete. *Journal of Structural Engineering*, ASCE. Vol. 118, nº.6, pp. 1590-1607, 1992.

SAMAAN, M.; MIRMIRAM, A.; SHAHAWY, M. Model of concrete confined by fiber composites. *Journal of structural engineering*, ASCE. Vol. 124, nº9, pp. 1025-1031, 1998.

SHEHATA, I. A. E. M.; CARNEIRO, L. A. V.; SHEHATA; L. C. D. Strength of short concrete columns confined with CFRP sheets. *Materials Structural* Vol. 35, pp. 50-58, 2002.

SHEHATA, I. A. E. M.; CARNEIRO, L. A. V.; SHEHATA; L. C. D. Strength of confined short concrete columns. *Proc. 8th int. symp. on fiber reinforced polymer reinforcement for concrete structures*. Patras, Greece: University of Patras, 2007.

SHEIKH, S. A., UZUMERI, S. M. Analytical model for concrete confinement in tied columns. *Journal of Structural Division*, ASCE, 108(12), 2703-2722, 1982.

SHIN, M.; ANDRAWES, B. Experimental investigation of actively confined concrete using shape memory alloys, *Engineering Structures*, ELSEVIER. Vol. 32 (3), pp. 656-664, 2010.

SHIRMOHAMMADI, F., ESMAEILY A., KIAEIPOUR Z. Stress-strain model for circular concrete columns confined by FRP and conventional lateral steel. *Engineering Structures*, ELSEVIER. Vol. 84, pp.395-405, 2015.

SILVA, A. S. *Comportamento de pilares curtos confinados por compósitos de fibras de vidro e carbono* (in Portuguese) Master's Thesis. 2002. 167p. Polytechnic School of the University of São Paulo, São Paulo, Brasil.

STRONG, A. B.; *Fundaments of composites manufacturing, material, methods, and applications* . 2th Edition. USA. Society of manufacturing engineers, 625p., 2008.

SZERSZEN, M.; NOWAK, A. Calibration of design code for buildings (ACI 318): part 2 - reliability analysis and resistance factors. *ACI Structural Journal*, American Concrete Institute, 100 (3), pp 383-391, 2003.

TAMUZS, V.; TEPFERS, R.; SPARNINS, E. Behavior of concrete cylinders confined by carbon composite II: prediction of strength. *Mechanics of Composite Materials.* Vol. 42, nº 2, pp. 109-118, 2006.

TASDEMIR, M. A; TASDEMIR, C.; JEFFERSON, A. D.; LYDON, F. D.; BARR, B. I G. Evaluation of strains at peak stresses in concrete: a three-phase composite model approach. *Cement and Concrete Research.* Vol. 20, nº 4, pp. 301-318, 1998.

TENG ,J. G.; JIANG, T.; LAM, L., LUO, Y. Refinement of a design-oriented stress–strain model for FRP-confined concrete. *Journal of Composites for Construction,* ASCE. Vol. 13, nº 4, pp. 269-278, 2009.

TENG, J. G.; LAM, L. Behavior and modeling of fiber reinforced polymer confined concrete. *Journal of Structural Engineering*, ASCE. Vol. 130, nº 11, pp. 1713-1723, 2004.

TOUTANJI, H. A. Stress strain characteristics of concrete columns externally confined with advanced fiber composite sheets. *ACI Materials Journal*. Vol. 96, nº 3, pp. 397-404, 1999.

TRAPKO, T. The effect of high temperature on the performance of CFRP and FRCM confined concrete elements. *Composites: Part B,* ASCE, Vol. 54, nº 1, pp.138-145, 2013.

XIAO, Y.; WU, H. Compressive behavior of concrete confined by carbon fiber composite jackets. *Journal of Materials in Civil Engineering*, ASCE. Vol. 12, nº 2, pp. 139-146, 2000.

.

ANNEX A:

EXAMPLE: RELIABILITY ANALYSIS OF COLUMN 32 - D2F1L2T1C2

This annex presents a complete worked example of the reliability analysis procedure adopted in this research, featuring the analysis of column 32 (D2F1L2T1C2). Program RACOL-FRP is used for both the simulation of FRP-RC column resistance and computation of the corresponding probability of failure.

A.1. Geometric characteristics and mechanical properties of materials

Column 32 (D2F1L2T1C2) is used for illustrative purposes; the details of this column are:

1. Heigth: H = 3000 mm;
2. Diameter: D = 400 mm;
   - gross area of concrete section: A_g = 125,663.7 mm²
3. Concrete cover: c = 40 mm;
4. Specified concrete compressive strength: f'_c = 20 MPa;
5. Longitudinal reinforcement: Reinforcing bars 420 MPa grade
   - 12 #5 (15.875 mm)
   - total area of longitudinal reinforcement: A_{sL} = 2,375.2 mm²
   - volumetric ratio of longitudinal steel reinforcement: ρ_{sL} = 0.019
6. Specified yield strength of the longitudinal steel: f_y = 420 MPa
7. Transversal reinforcement: Reinforcing bars 420 MPa
   - spirals: #3 (9.525 mm) @ 140mm
   - spiral area: $A_{s\phi}$ =
   - volumetric ratio of transversal steel reinforcement: ρ_{sw} =
8. Specified yield strength of the transversal steel: f_{yw} = 420 MPa
9. Young's modulus of the reinforcement steel: E_{sw} = 200 GPa;
10. Number of CFRP plies: n = 2;
11. Elasticity modulus of CFRP: E_F = 230 GPa;
12. Fiber thickness: t_f = 0.128 mm.

A.2. Calculation of nominal resistance of the column

The nominal resistance of the column, ϕP_n, is calculated using ACI 440.2R(2008). For columns with spirals, this strength is given by Eq. 6.6 ($\phi P_n = 0.85\phi \left[0.85 f_{cc}\left(A_g - A_{s\ell}\right) + f_y A_{s\ell}\right]$). The strength reduction factor ϕ is adopted as 0.70 for members with spiral reinforcement.

The maximum confined concrete compressive strength f_{cc} is calculated using Eq. 6.11: $f_{cc} = f'_c + 3.3\psi_f \kappa_a f_\ell$, where κ_a = 1.00 for circular sections, and ψ_f = 0.95. The term f'_c (unconfined cylinder concrete compressive strength) is adopted as the specified concrete strength, f'_c = 20 MPa. The confinement pressure f_ℓ is calculated by $f_\ell = \frac{2 \; n \; t \; k_F f_{fu}}{D}$, where k_F is 0.55. The mechanical properties of the fibers are adopted in the calculation of the confinement pressure. The design ultimate tensile strength of fibers f_{fu} is obtained using the environmental reduction factor C_E, i. e. $f_{fu} = C_E \; f^*_f$. Considering CFRP jacket and exterior exposure (bridges, piers, and unenclosed parking garages), C_E is equal to 0.85 (Table 6.1). Assuming mean ultimate tensile strength μf_f as 3500 MPa and the standard deviation as 175 MPa, it comes from Eq. 6.5 ($f^*_f = \mu f_f - 3\sigma$) that the ultimate tensile strength of fibers, f^*_f, is 2975 MPa.

The nominal resistance P_n, of column 32, is calculated by Eq. 6.6 resulting in 3373.2 kN. The design strength R_d is obtained including the strength reduction factor ϕ, (equal to 0.7 for spirals)resulting in $R_d = \phi P_n$ = 2361.2 kN.

A.3 Simulation of the column axial resistance

Monte Carlo simulation was used to obtain the column axial resistance. In the simulation of column resistance, the following information is required: (i) the statistics of all random variables associated with resistance, (ii) a deterministic procedure for calculating the column resistance.

The statistics of all random variables associated with resistance are described in section 6.2 and summarized in Table 6.6. The deterministic procedure for column resistance P_R simulation is described in section 7.1.1 and illustrated in Fig. 7.1. In this way, a key task in

the Monte Carlo simulation is the generation of random numbers associated to the assumed random variables. The histograms of the random variables associated to the simulation of FRP-RC column resistance are presented below.

Considering that deviation from nominal values of the diameter Δ_D and of the concrete cover Δ_C were assumed as Gaussian random variables, column diameter ($D_{\_R} = D_n + \Delta_D$), concrete cover D ($D = D_n + \Delta_D$) and concrete cover ($c_{\_R} = c_n + \Delta_C$) are also Gaussian random variables. The same observation is valid for the diameter of the steel confined core ($D_{c\_R} = D_{\_R} - 2\ c_{\_R}$). Figures 0.1 and 0.2 show the histograms (and superimposed normal distribution) for column diameter $D_{\_R}$ and steel confined core D_{c_R}, respectively.

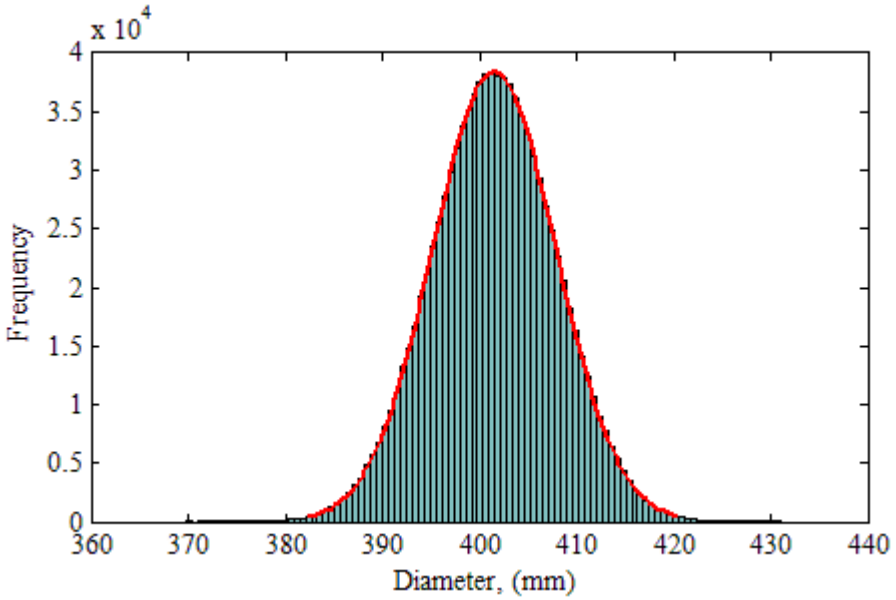

Figure A.1 - Histogram of the column diameter (nominal diameter D_n = 400 mm) with a superimposed normal distribution.

Figure 0.3 shows the histogram of the concrete compressive strength, for the concrete compressive strength f'_c = 20 MPa (standard cylinders). This variable is assumed as following a lognormal distribution, with mean 23.1 MPa and COV of 0.10.

The variability of the ultimate tensile strength of CFRP fibers is illustrated in Fig. 0.4. It is assumed as a random variable following Weibull distribution with mean of 3500 MPa and COV of 0.05.

Reinforcing bars 420 MPa grade were adopted, for both the transversal and longitudinal steel. The yield strength was assumed as random variable with lognormal distribution, mean of 489.3 MPa and COV of 0.05, as illustrated in Fig. 0.5.

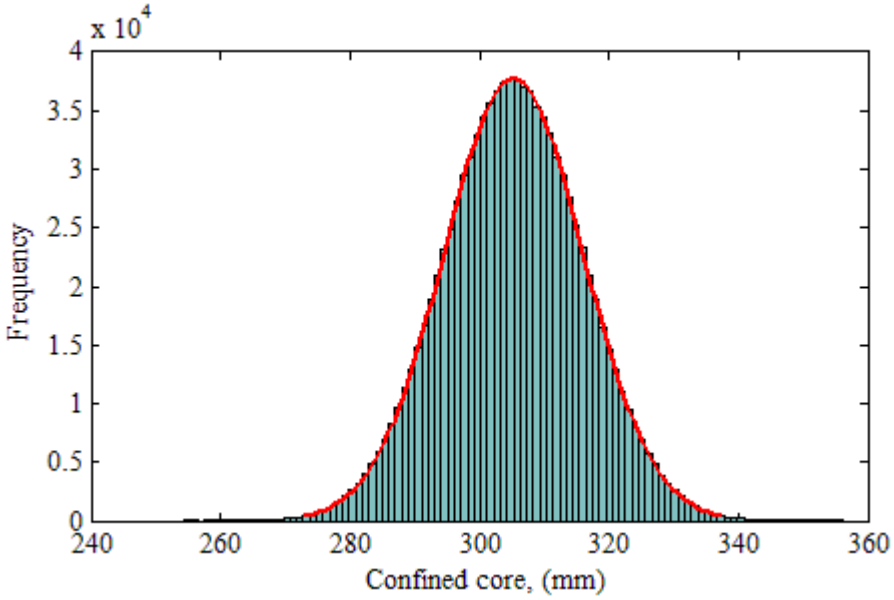

Figure A.2 - Histogram of the diameter of steel confined core (nominal diameter D_n = 400mm and nominal cover c_n = 40mm) with a superimposed normal distribution.

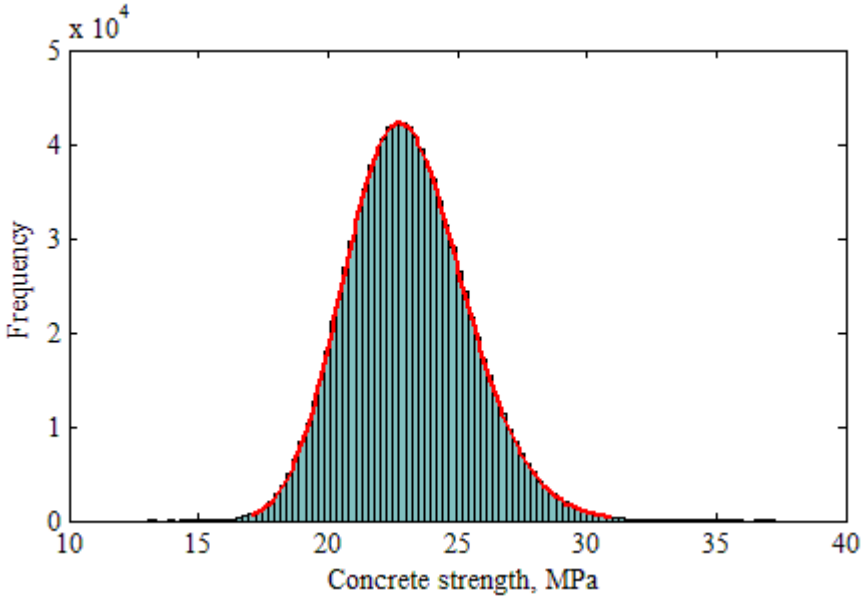

Figure A.3 - Histogram of the concrete compressive strength (f_{cm} =23,1 MPa) with a superimposed lognormal distribution.

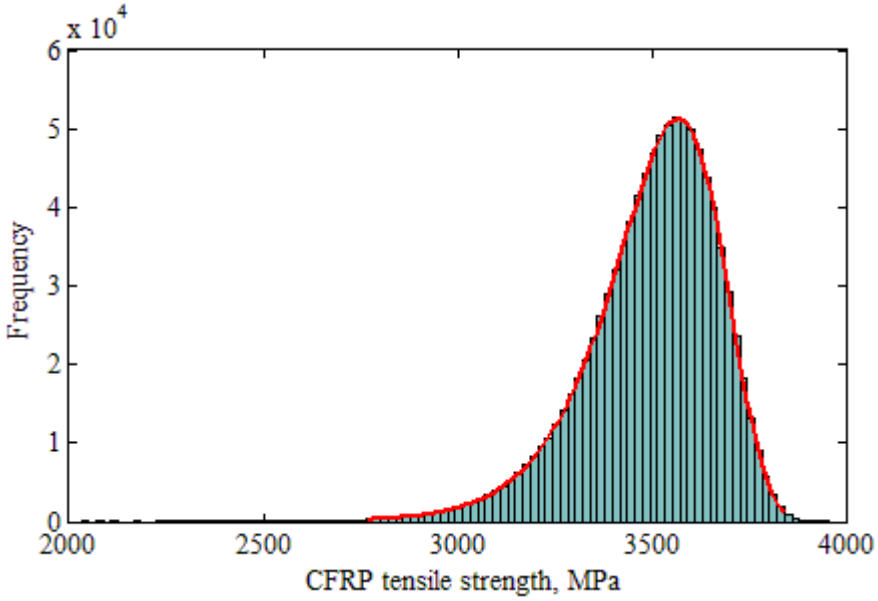

Figure A.4 - Histogram of the CFRP tensile strength with a superimposed Gumbell distribution.

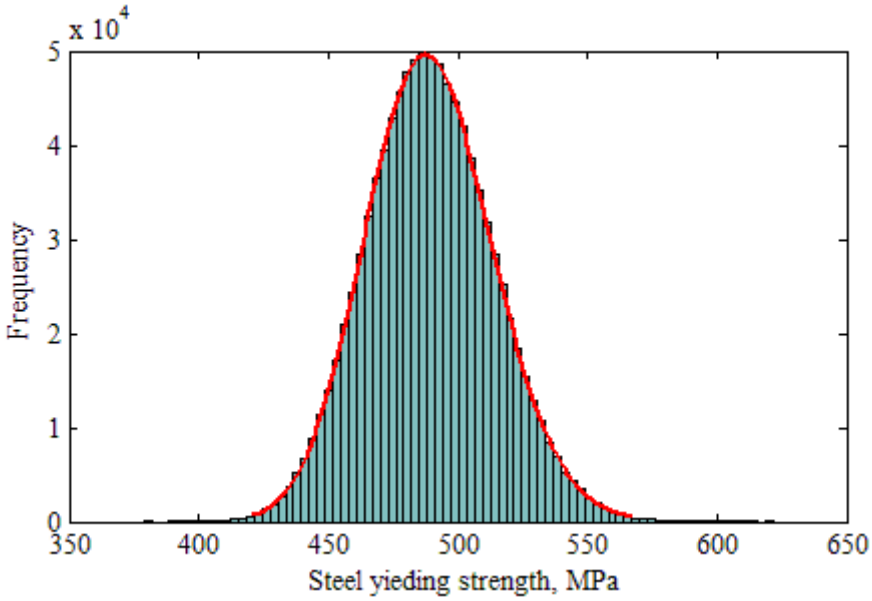

Figure A.5 - Histogram of the steel yield strength of the transversal steel and longitudinal steel with a superimposed lognormal distribution.

The stress-strain curve proposed by Park & Paulay (1975) was adopted to calculate the random variable associated with the actual stress in the longitudinal steel f_{sL_R}. The parameters f_y, f_{su}, ε_{sh}, ε_{su} and E_s that describe the stress-strain curve of longitudinal steel are also assumed as random variables. The corresponding statistics and probability distributions were presented in section 6.2.3 and summarized in Table 6.6. Figures A.6 - A.10 presents the histograms with

the corresponding superimposed distributions of the random variables f_{y_R}, f_{su_R}, ε_{sh_R}, ε_{su_R} and E_{s_R}, respectively. 0.6, 0.7, 0.8, 0.9, 0.10

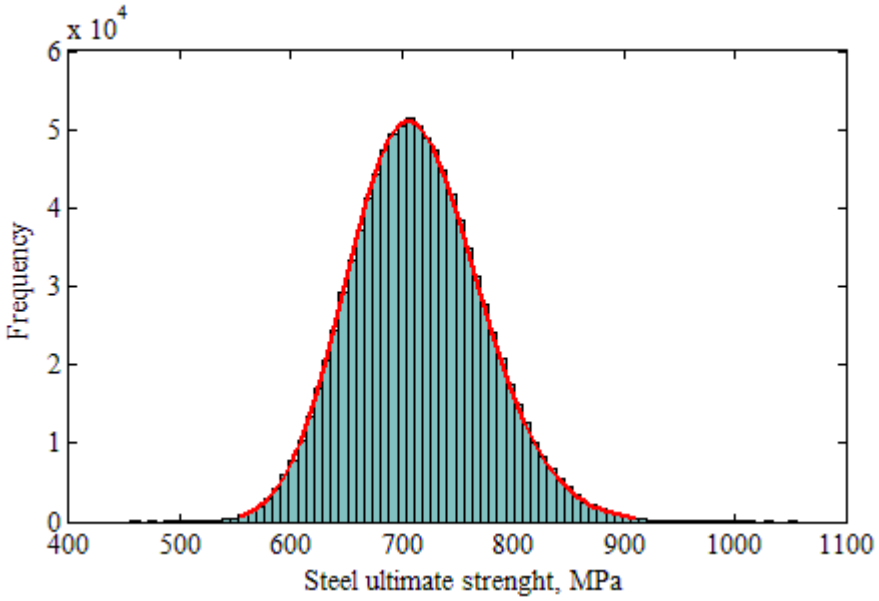

Figure A.6 - Histogram of the steel yield strain of the transversal steel and longitudinal steel with a superimposed lognormal distribution.

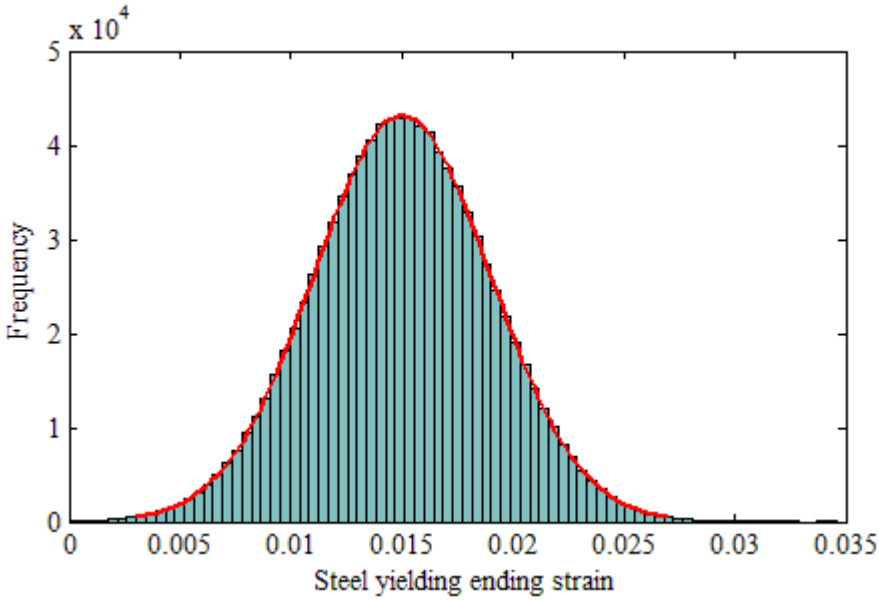

Figure A.7 - Histogram of the the strain at the onset of the strain-hardening of the longitudinal steel with a superimposed lognormal distribution.

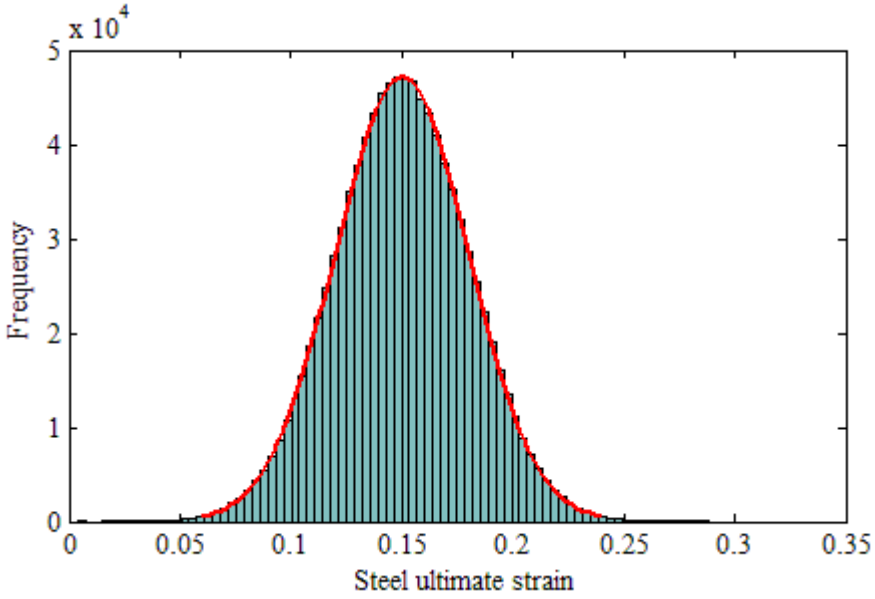

Figure A.8 - Histogram of the longitudinal steel ultimate strain with a superimposed lognormal distribution.

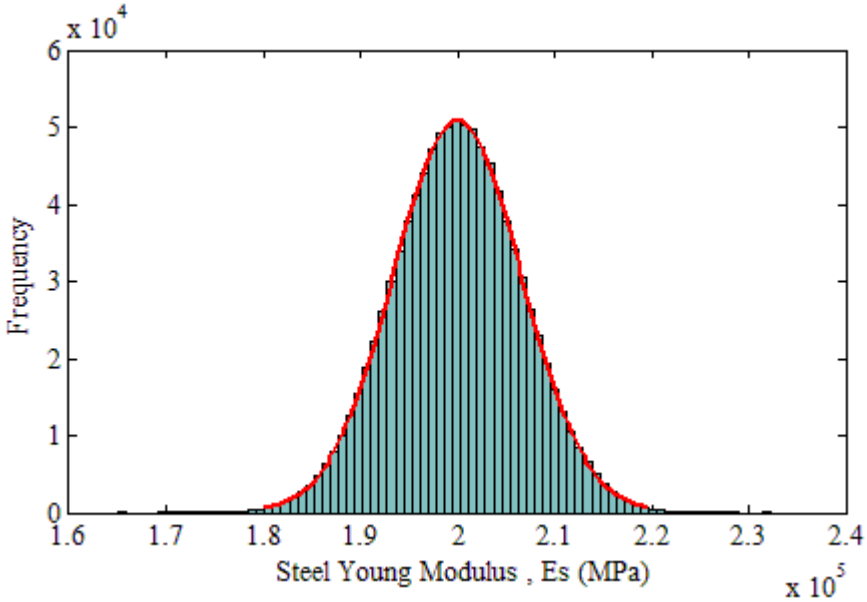

Figure A.9 - Histogram of the longitudinal steel Young modulus with a superimposed normal distribution.

The histogram with the stress in the longitudinal steel f_{sL_R}, obtained by Park & Paulay stress-strain curve is presented in Fig. 0.11.

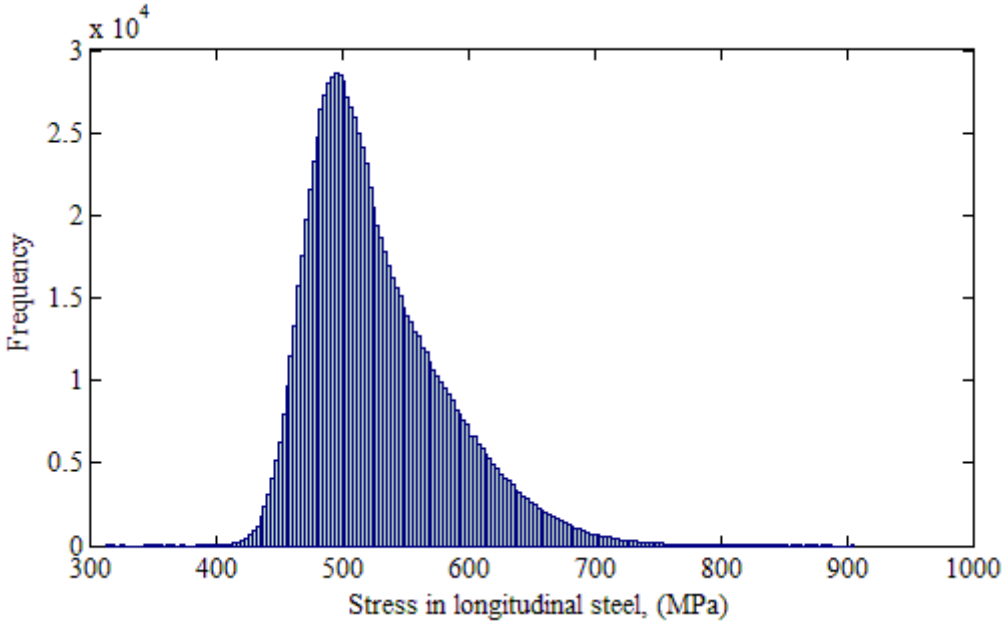

Figure A.10 - Histogram of the stress in the longitudinal steel of the column 32.

By the deterministic procedure described in section 7.1.1, the column resistance is simulated. Figure 0.12 presented the histogram of the resistance the column 32, with a superimposed normal distribution.

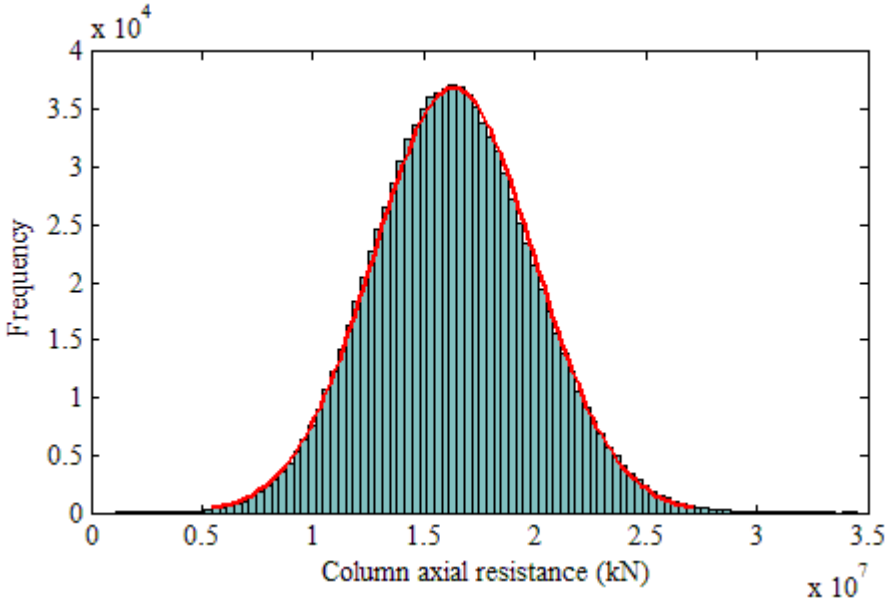

Figure A.11 - Histogram of the colum axial resistance P_R of the column 32 with a superimposed normal distribution.

A.4. Simulation of the acting load

In this study it is considered that only dead and live loads are acting on the column. Then, the acting load in the columns is the sum of the random variables dead load F_{DL} and live load F_{LL}, for each load ratio. The procedure to calculate mean values μ_{DL} and μ_{LL} was described in section 6.2.5. The histograms corresponding to acting load to column 32, for load ratios of 0.5, 1.0 and 2.0 are presented in the Figs. 0.13, 0.14, 0.15, respectively.

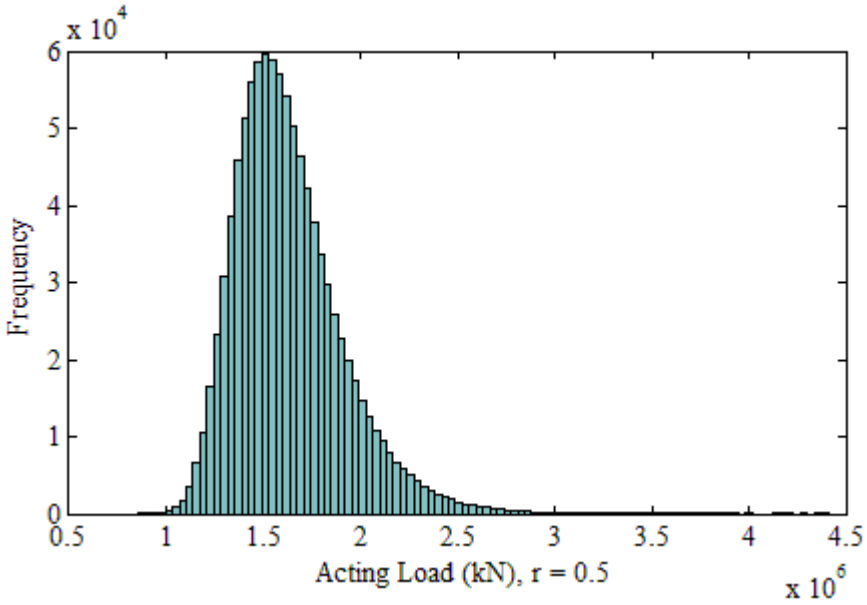

Figure A.12 - Histogram of acting load P_A of the column 32 for the load ratio of 0.5.

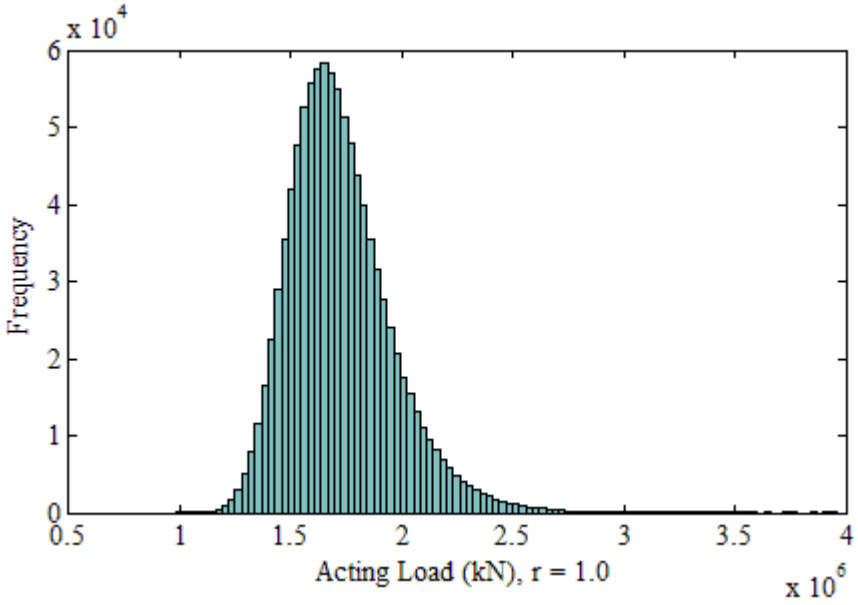

Figure A.13 - Histogram of acting load P_A of the column 32 for the load ratio of 1.0.

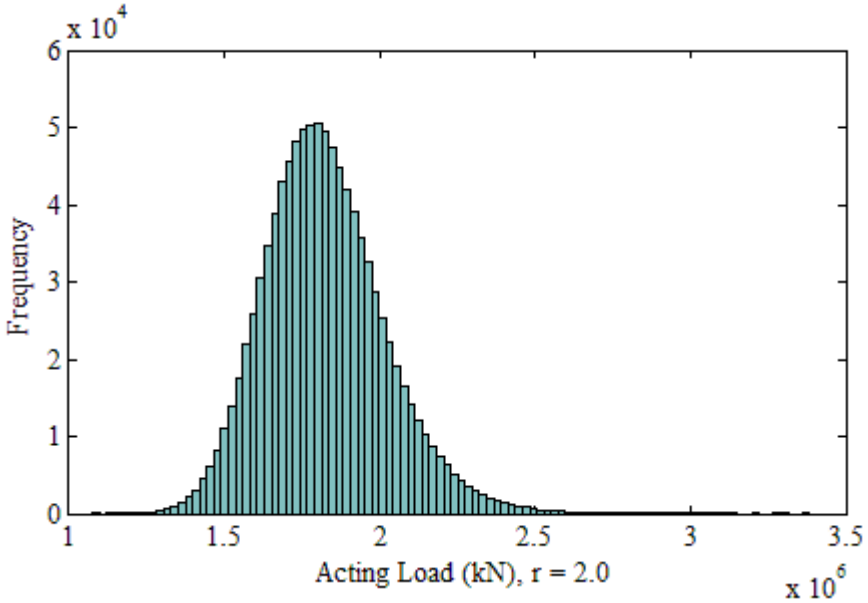

Figure A.14 - Histogram of acting load P_A of the column 32 for the load ratio of 2.0.

A.5. Calculation of the failure probability

The number of unsatisfactory performances n_u is counted and the failure probability P_f is obtained, $P_f = n_u / n_s$, where n_s is the number of simulations. For the column 32, the failure probability is 6.0E-6 and the reliability index is 4.38. Fig. 0.16 displays the histogram of the safety margin with a superimposed normal distribution, for load ratio of 2.0.

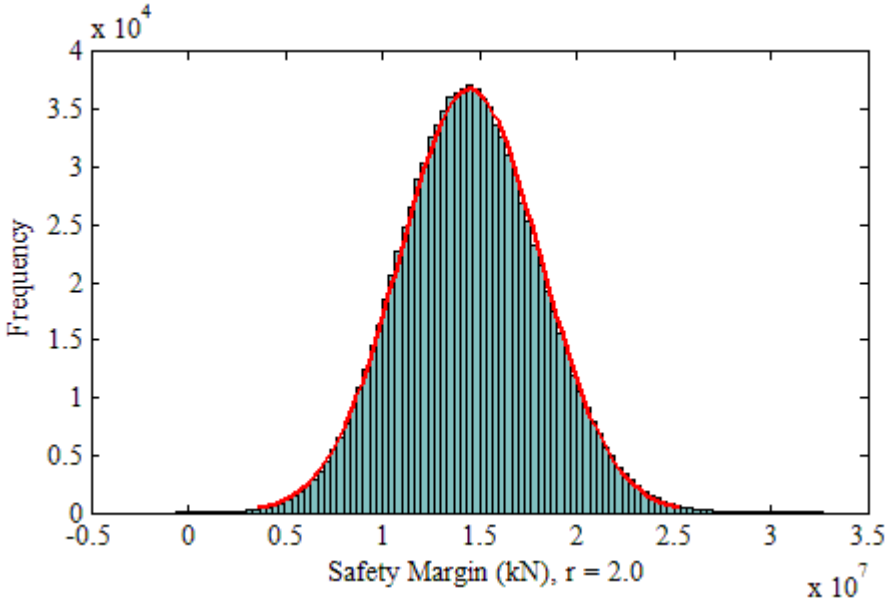

Figure A.15 - Histogram of the safety margin of column 32 for the load ratio of 2.0 with a superimposed normal distribution.

ANNEX B:

SOURCE OF THE SOFTWARE "RACOL-FRP"

RACOL_FRP.m

```
% program for reliability analysis of CFRP-RC confined columns, designed
% according to ACI 440.2R (2008)

clear all
clc

Data_Input;

% Resistance_Simulation
Resistance_Random_Numbers;
Ultimate_Conditions_Lee;
Strain_Compability;
Steel_Longitudinal_Stress;
Resistance;

% Loading Simulation
Mean_Loads;
Loads_Random_Numbers;
Acting_Load;

Reliability;
```

Data_Input.m

```
%Data input file

%************************************************
%                    General                     *
%************************************************%
cycles = 1000000; % Number of Simulations
columns = 48; % number of selected columns

% LateralSteelType = Vector with the type of transvesal reinforcemenet
(1=stirrups, 0=spiral)
LateralSteelType = [1 0 1 0 1 0 1 0 1 0 1 0 1 0 1 0 1 0 1 0 1 0 1 0 1 0
1 0 1 0 1 0 1 0 1 0 1 0 1 0 1 0 1 0 1 0];

%************************************************
%            DETERMINISTIC VARIABLES             *
%************************************************
% mi=mean; SD=Standard Deviation; COV= coefficient of variation

h = 3000; % Height of the column in mm

% n_D = Vector with the Nominal Diameter  of the columns;
%(Columns 1-24, Dn = 300 mm; Columns 35-48, Dn = 400 mm
n_D1=linspace(300, 300, columns/2); n_D2=linspace(400, 400, columns/2);% in
mm, nominal diameter
n_D=[n_D1 n_D2];
```

```
% n_C = Vector with the Nominal cover of the columns, in mm.
n_C=linspace(40, 40 ,columns);

%_____________________________________
%LONGITUDINAL STEEL
% nL = vector with the number of Longitudinal steel
nL = [6 6 6 6 6 6 7 7 7 7 7 7 6 6 6 6 6 6 7 7 7 7 7 7 7 7 7 7 7 12 12 12
12 12 12 7 7 7 7 7 7 12 12 12 12 12 12]; % quantity of longitudinal bars

% fiL = vector with the diameter of longitudinal bars
%Columns: 1-6, 13-18: longitudinal bar = #4(12.7 mm); Columns: 7-12, 19-
48:longitudinal bar = #5(15.875 mm);
fiL1 = 12.7*[1 1 1 1 1 1]; fiL2=15.875*[1 1 1 1 1 1];
fiL=[fiL1 fiL2 fiL1 fiL2 fiL2 fiL2 fiL2 fiL2];

% fyL = Specified Yielding Strengh of Longitudinal Steel, in MPa
fyL = 420;

%_____________________________________
%TRANSVERSAL STEEL
% fiT = Vector with the diameter of Transversal steel
% Columns: 1-36 => diameter transversal bar = #3 (9.525mm); Columns: 37-48
= #4 (12.7mm)
fiT = [linspace(9.525,9.525,36) 12.7 12.7 12.7 12.7 12.7 12.7 12.7 12.7
12.7 12.7 12.7 12.7];

% S_s = vector with the spacement of stirrups or spirals, in mm.
S_s1 = [200 200 100 100 50 50]; % columns 1-6 = columns 7-12
S_s2 = [120 120 60 60 30 30]; % columns 13-18 = columns 19-24
S_s3=[140 140 70 70 35 35]; % columns 25-32 = columns 33-38 = columns 39-42
= columns 43-48
S_s = [S_s1 S_s1 S_s2 S_s2 S_s3 S_s3 S_s3 S_s3];

% fyT = Specified yielding strength of Transversal Steel
fyT = 420;

%_____________________________________
% CONCRETE
% fc = Vector with the Specified compressive strength of each column.
% columns 1-12 (fc=20);  columns 13-24 (fc=35); columns 25-36
(fc=20);columns 37-48 (fc=35); in MPa
fc1=linspace(20,20,12); fc2=linspace(35,35,12);
fc=[fc1 fc2 fc1 fc2];

% strain corresponding to strength fc0 of the concrete
ec0 = 0.002;

%_____________________________________
%CFRP
% CFRP_NumberOfPlies = Vector with the number of plies of CFRP in each
column
CFRP_NumberOfPlies = [1 2 1 2 1 2 1 2 1 2 1 2 2 4 2 4 2 4 2 4 2 4 2 4 2 3 2
3 2 3 2 3 2 3 2 3 3 5 3 5 3 5 3 5 3 5 3 5];

% CFRP_Thickness = thickness of each ply of CFRP fibers, in mm, as reported
by the fabricator
CFRP_Thickness = 0.128;
```

```
% CFRP_Elasticity_modulus = Elasticity modulus of CFRP, in MPa, as reported
by the fabricator
CFRP_Elastic_modulus = 230000;

ff_CFRP = 2975; % Assuming mean ultimate tensile strength mi_fCFRP as 3500
MPa
% and the standard deviation as 175 MPa, the ultimate tensile strength of
fibers, ff_CFRP, is 2975 MPa.

ef_CFRP = 0.0129; % ef_CFRP = ff_CFRP / CFRP_Elastic_modulus

%***********************************************
%            RANDON VARIABLES                  *
%***********************************************
% mi=mean; SD=Standard Deviation; COV= coefficient of variation

%_____________________________________________________
% Statistics of the deviations of the diameter
% DISTRIBUTION = NORMAL
% mi_delta_d = mean deviations from the nominal value of diameter
mi_delta_d = +1.52; % mean in mm

% SD_D = Standard deviation of the nominal diameter column, in mm
SD_d=6.35;

%_____________________________________________________
% Statistics of the deviations of the diameter
% DISTRIBUTION = NORMAL
% mi_delta_c = mean deviations from the nominal value of cover, in mm
mi_delta_c = +8.13;

% SD_C = Standard deviation of the nominal cover, in mm
SD_c = 4.32;

%_____________________________________________________
% Statistics of the Concrete strength
% DISTRIBUTION = LOGNORMAL

% COV_fcm = Coeficient of variation of Specified compressive strength
COV_fcm = 0.10; %

% mi_fcm = Required average compressive strength
mi_fcm1 = fc/(1-1.34*COV_fcm); % VECTOR % ACI 318 (2014)
mi_fcm2 = (fc-3.5)/(1-2.33*COV_fcm);
mi_fcm = max(mi_fcm1, mi_fcm2);

% SD_fcm = Standard Deviation of Specified compressive strength
SD_fcm = COV_fcm*mi_fcm; % VECTOR % concrete compressive strength (fcm)

%_____________________________________________________
%Statistics of the YOUNG MODULUS of LONGITUDINAL STEEL
% DISTRIBUTION = NORMAL
% mi_EsL = mean of Young Modulus of Longitudinal Steel
mi_EsL = 200000; % in MPa

% COV_esL = Coeficient of variation of the Young Modulus of Longitudinal
Steel
COV_EsL = 0.033;
```

```
% SD_EsL = Standard Deviation of the Young Modulus of Longitudinal Steel
SD_EsL = COV_EsL*mi_EsL;

%_____________________________________________________
%Statistics of the YIELD STRENGTH of LONGITUDINAL STEEL
% DISTRIBUTION = LOGNORMAL
% mi_fy = mean value of Longitudinal Steel yielding strength (Nowak &
Szerszen, 2010)
mi_fyL = 1.165*fyL;

% COV_esL = Coeficient of variation of the Yielding Strengh Longitudinal
Steel
COV_fyL = 0.050;

% SD_fyL = Standard Deviation of Longitudinal Steel yielding strength
SD_fyL = COV_fyL*mi_fyL;

%_____________________________________________________
%Statistics of the ULTIMATE STRENGTH of LONGITUDINAL STEEL
% DISTRIBUTION = LOGNORMAL
% mi_fsu = mean of Ultimate Strengh of Longitudinal Steel, in MPa
mi_fsu = 714;

% COV_fsu = coeficient of variation of Ultimate Strengh of Longitudinal
Steel
COV_fsu = 0.083;

% SD_fsu = Standard Deviation of Longitudinal Steel Ultimate strength
SD_fsu = COV_fsu*mi_fsu; % Steel Ultimate Strength (fsu)

%_____________________________________________________
%Statistics of the STRAIN HARDENING of LONGITUDINAL STEEL
% DISTRIBUTION = NORMAL
% mi_esh = mean of the Strain hardening
mi_esh = 0.015;

% COV_esh = coeficient of variation of strain hardening of Longitudinal
Steel
COV_esh = 0.2667;

% SD_esh = Standard deviation of strain hardening of Longitudinal Steel
SD_esh = COV_esh*mi_esh;

%_____________________________________________________
%Statistics of the ULTIMATE STRAIN of LONGITUDINAL STEEL
% DISTRIBUTION = NORMAL
% mi_esu = mean of the strain of the yielding ending
mi_esu = 0.15;

% COV_esu = Coefient of variation of the strain of the yielding ending
COV_esu = 0.2;

% SD_esu = Standard deviation of Ultimate strain of Longitudinal Steel
SD_esu = COV_esu*mi_esu;

%_____________________________________________________
%Statistics of the YIELD STRENGTH of TRANSVERSAL STEEL
% mi_fyT = mean value of transversal Steel yielding strength (Nowak &
Szerszen, 2010)
```

```
% DISTRIBUTION = LOGNORMAL
mi_fyT = 1.165*fyT; % Transversal steel

%COV_fyT = Coeficient of variation of the Specified yielding strength of
Transversal Steel
COV_fyT = 0.05; %

%Standard deviation of Transversal Steel yielding strength
SD_fyT = mi_fyT*COV_fyT;


%Statistics of the ULTIMATE TENSILE STRENGTH OF CFRP
% DISTRIBUTION = weibull
% COV_eCFRP = Coeficient of variation of CFRP ultimate Tensile Strain
COV_fCFRP = 0.05;

% mi_eCFRP = mean of CFRP ultimate Tensile Strain
mi_fCFRP = 3500; % MPa

%Standard deviation of CFRP ultimate Tensile Strain
SD_fCFRP = COV_fCFRP*mi_fCFRP;

%_____________________________________________________
%Statistics of the DEAD LOADS
% DISTRIBUTION = NORMAL
% Mean values will be obtained in Loads-Calculations

% COV_DL = Coefficient of variation of Dead Load
COV_DL=0.10; %Dead Load - Normal Distribution

%_____________________________________________________
%Statistics of the LIVE LOADS
% DISTRIBUTION = Extreme Value Type I (Gumbel)
% Mean values will be obtained in Loads-Calculations

% COV_LL = Coefficient of variation of Live Load
COV_LL=0.25; %Live Load - Valores extremos Tipo I

%_____________________________________________________
%Statistics of the STRENGTH MODEL ERROR
% DISTRIBUTION = NORMAL
% mi_error = mean of Strength Model Error
mi_error=0.96;

% COV_error = Coefficient of variation of Strength Model Error
COV_error=0.23;

% SD_error = Standard deviation of Strength Model Error
SD_error = COV_error*mi_error;

%_____________________________________________________
%Statistics of the STRAIN MODEL ERROR
% DISTRIBUTION = LOGNORMAL
% mi_error_ec = mean of Strain Model Error
mi_error_ec=0.77;

% COV_error_ec = Coefficient of variation of Strain Model Error
COV_error_ec=0.54;
```

```
 % SD_error_ec = Standard deviation of Strain Model Error
SD_error_ec = COV_error_ec*mi_error_ec;
```

Resistance_Random_Numbers.m;

```
% program that generates the random numbers for Resistance

% rgn produce the same random numbers as if you restarted MATLAB
rng('default');

%_____________________________________________________________________
% Geometric Properties =>  Normal distribution
% 48 vetores [1x1,000,000]

for k=1:columns

% Diameter
rng(1);
D{1,k} = n_D(1,k)+ normrnd(mi_delta_d, SD_d, 1,cycles);

% Cover
rng(2);
C{1,k} = n_C(1,k)+ normrnd(mi_delta_c, SD_c, 1,cycles);

% Dc - confined diameter
Dc{1,k} = D{1,k}-2*C{1,k};
end

%_____________________________________________________________
% Compressive concrete strength => LogNormal Distribution
% Parameters of Lognormal Distribution => Mean (mi_log) and Standard
Deviation (sigma)
mi_log_fcm = log((mi_fcm.^2)./sqrt(SD_fcm.^2+mi_fcm.^2));%
sigma_fcm = sqrt(log((SD_fcm.^2)./(mi_fcm.^2)+1));

% 48 vetores [1x1,000,000]
for k=1:columns;
rng(3);
Fcm{1,k} = lognrnd (mi_log_fcm (1,k), sigma_fcm (1,k), 1, cycles);
% Fcm: Compressive Concrete Strength
end

%_____________________________________________________________
% Longitudinal Steel properties - vector [1x1,000,000]

%%%%%%%%% LogNormal distribution
% Yielding Strenght Longitudinal Steel - FyL (Lognormal)
mi_log_fyL = log((mi_fyL^2)/sqrt(SD_fyL^2+mi_fyL^2));
sigma_fyL = sqrt(log(SD_fyL^2/mi_fyL^2+1));

rng(4);
FyL = lognrnd (mi_log_fyL, sigma_fyL, 1, cycles);

% Longitudinal Steel Ultimate Strenght - Fsu (Lognormal)
mi_log_fsu = log((mi_fsu^2)/sqrt(SD_fsu^2+mi_fsu^2));%
sigma_fsu = sqrt(log(SD_fsu^2/mi_fsu^2+1));

rng(5);
Fsu = lognrnd (mi_log_fsu, sigma_fsu, 1, cycles);
```

```
%%%%%%%%  Normal distribution
% Longitudinal Steel Ultimate Strain - Esu (Normal)
rng(6);
Esu = normrnd(mi_esu, SD_esu, 1,cycles);

% strain at the onset of the strain-hardening of Longitudinal Steel - Esh
(Normal)
rng(7);
Esh = normrnd(mi_esh, SD_esh, 1,cycles);

% Longitudinal Steel Young's Modulus - EsL (Normal)
rng(8);
EsL = normrnd(mi_EsL, SD_EsL, 1,cycles);

% Longitudinal Steel Yield Strain - eyL
eyL = (FyL./EsL);

%_____________________________________________________________________
%Transversal Steel Yield Strenght - FyT (Lognormal)
mi_log_fyT = log((mi_fyT^2)/sqrt(SD_fyT^2+mi_fyT^2));%
sigma_fyT = sqrt(log((SD_fyT^2/mi_fyT^2)+1));

rng(9);
FyT = lognrnd (mi_log_fyT, sigma_fyT, 1, cycles);

%_____________________________________________________________________
% CFRP Tensile Strength - e_CFRP (Weibull)
shape_parameter = (SD_fCFRP/mi_fCFRP)^-1.086;
scale_parameter = mi_fCFRP/(gamma(1+1/shape_parameter));

rng(10);
f_CFRP = wblrnd (scale_parameter, shape_parameter, 1, cycles);

e_CFRP = f_CFRP/CFRP_Elastic_modulus;

%_____________________________________________________________________
% Model Error to strength - Normal Distribution
rng(11);
Model_Error = normrnd(mi_error, SD_error, 1, cycles);
Model_Error(Model_Error<=0)=NaN;
%_____________________________________________________________________
%Model Error to strain - Lognormal
mi_log_error_ec = log((mi_error_ec^2)/sqrt(SD_error_ec^2+mi_error_ec^2));
sigma_error_ec = sqrt(log(SD_error_ec^2/mi_error_ec^2+1));

rng(12);
Model_Error_ec = lognrnd (mi_log_error_ec, sigma_error_ec, 1, cycles);
```

Ultimate_Conditions_Lee.m;

```
% program that calculates the ultimate stress and strain (fcc and ecc) of
RC column confined by FRP using the equations proposed by Lee et al. (2010)
and adjusted them  by the model error

%%%% Ultimate Conditions by Lee
for k=1:columns

% confinement pressure due to steel - FLs
```

```
Fls{1,k} = (2*pi*0.25)*(fiT(1,k)^2)*FyT./(Dc{1,k}.*S_s(1,k)); % FyT, Dc =
cell = 1xcolumns[1xcycles]
fls = Fls{1,k};

% confinement pressure due to CFRP - FlF
FlF{1,k} = 2*CFRP_NumberOfPlies(1,k)*CFRP_Thickness*f_CFRP./D{1,k}; %hist
(flF, 100);
flF = FlF{1,k};

% Ultimate Stress of Confined Concrete - FccLee
FccLee{1,k} = Fcm{1,k} + 2*(Fls{1,k}+FlF{1,k});

% Calculating the steel efficiency coefficient - ks
for i=1:cycles;

   if flF(1,i)<=fls(1,i);
     ks(1,i)=(2-flF(1,i)/fls(1,i));
 else
     ks(1,i) = 1.0;
   end
end

% Ultimate Strain of Confined Concrete - EccLee
EccLee{1,k} = ec0*(1.75+5.25*(ks.*fls+flF)./Fcm{1,k}).*(e_CFRP./ec0).^0.45;
end

% Adjustment by the model errors
for k=1:columns
    EccLee_A {1,k} = Model_Error_ec.*EccLee{1,k};

    FccLee_A{1,k} = Model_Error.*FccLee{1,k};
End
```

Strain_Compability.m;

```
%program that verifies the strain compatibility between concrete and
longitudinal steel, and updating of concrete confined stress

for k=1:columns;
         flF = FlF{1,k};
         fls = Fls{1,k};
         fc0 = Fcm{1,k};

        % Vetor with the ultimate strain given by Lee model
         ecc_A = EccLee_A{1,k}; % Vetor with the ultimate strain given by
Lee model, corrected by the model error

fcc_A = FccLee_A{1,k}; % Vetor with the ultimate strain given by Lee model,
corrected by the model error

        % parameters Ec of the Lee stress-strain curve
        Ec = 4700*sqrt(fc0);
         for i=1:cycles;
       % if the strain does not exceeds the ultimate strain of
       % the Longitudinal steel, the stress fcc is given by fccLee adjusted
          if ecc_A(1,i) <= Esu(1,i);
             ecc_up(1,i) = ecc_A(1,i);
             fcc_up(1,i) = fcc_A(1,i);
```

```
      % if the adjusted strain given by Lee model (ecc_A) exceeds the
ultimate strain of Longitudinal steel (Esu)
                  else
                  ecc_up(1,i) = Esu(1,i);

      % Using the Lee stress-strain curve corrected by model error, the
      % confined strength fcc_up corresponding strain to
      % ecc_up = esu (confined strain limited by the ultimate strain in the
      % longitudinal steel Esu)is calculated

      % calculating the parameters ecs and fcs of the Lee stress-strain
curve
                  if flF(1,i)>=fls(1,i);
                  ecs1_A = ecc_A(1,i)*(0.85+0.03*flF(1,i)/fls(1,i));
                  ecs2_A = ecc_A(1,i); % Maximum value for ecs, due to the
upper limit of flF/fls = 5
                  ecs_A(1,i) = min(ecs1_A, ecs2_A);

                  fcs_cor(1,i)=0.95*fcc_A(1,i);
                  else
                  ecs_A(1,i)=0.7*ecc_A(1,i);
                  fcs_cor(1,i)=fcc_A(1,i)*(ecs_A(1,i)/ecc_A(1,i))^0.4;
                  end

      %********First branch of Lee stress-strain curve
              if ecc_up(1,i)<=ec0; %ec0 = 0.002
fcc_up(1,i)=Ec(1,i)*ecc_up(1,i)+(fc0(1,i)-Ec(1,i)*ec0)*(ecc_up(1,i)/ec0)^2;

      %********second branch of Lee stress-strain curve
               else if ecc_up(1,i)<=ecs_A(1,i);
fcc_up(1,i)=fc0(1,i)+(fcs_cor(1,i)-fc0(1,i))*((ecc_up(1,i)-
ec0)/(ecs_A(1,i)-ec0))^0.7;


      %********Third branch of Lee stress-strain curve
                   else if ecc_up(1,i) <= ecc_A(1,i)
                       fcc_up(1,i)= fcs_cor(1,i)+(fcc_A(1,i)-
fcs_cor(1,i))*((ecc_up(1,i)-ecs_A(1,i))/(ecc_A(1,i)-ecs_A(1,i)))^0.7;
                       end
                   end
               end
              end
         end
         Fcc_up{1,k} = fcc_up;
         Ecc_up{1,k} = ecc_up;
end
```

Steel_Longitudinal_Stress.m;

```
% This program calculates the stress in longitudinal steel corresponding to
Ecc_up by the  Park & Paulay stress-strain curve of the steel

 % m,r = parameters of the Park & Paulay stress-strain curve
 r = Esu-Esh;
 m = ((Fsu./FyL).*(30.*r+1).^2-60.*r-1)./(15.*r.^2);

  for k=1:columns;

      Ecc_up{1,k} = ecc_up;
```

```
      for i=1:cycles;
                if ecc_up(1,i) <= eyL(1,i);
                   fs_Long(1,i) = ecc_up(1,i)*EsL(1,i);

                    % Second branch is the yield plateau => fs = fyL
             else if ecc_up(1,i) <= Esh(1,i);
                          fs_Long(1,i) = FyL(1,i);

                     % third branch is the equation given by Park & Paulay
                  else if ecc_up(1,i) <= Esu(1,i);
                             fs_Long(1,i)= FyL(1,i)*((m(1,i)*(ecc_up(1,i)-
Esh(1,i))+2)/(60*(ecc_up(1,i)-Esh(1,i))+2)+(ecc_up(1,i)-Esh(1,i))*(60-
m(1,i))/(2+(30*r(1,i)+1)^2));
                       end
                  end
             end
      end

      Fs_Long{1,k} = fs_Long;
  End
```

Resistance.m;

```
%program that simulates the resistance (axial load) corresponding to Fcc_up

        for k=1:columns;
        % R = Column resistance
R{1,k} = Fcc_up{1,k}.*((pi.*D{1,k}).^2*0.25-
nL(1,k)*pi*fiL(1,k)^2/4)+(nL(1,k)*pi*fiL(1,k)^2/4).*Fs_Long{1,k};

        %****** Statistics of the column resistance
         min_R (1,k) = nanmin(R{1,k});
         mi_R (1,k) = nanmean(R{1,k});
         max_R (1,k) = nanmax(R{1,k});
         SD_R(1,k) = nanstd(R{1,k});
         COV_R(1,k)=SD_R(1,k)/mi_R (1,k);
         end
```

Mean_Loads.m;

```
% program that calculates the design load of RC column confined by FRP
using the ACI 440.2R-2008 and the mean dead and live loads

fc_linha = fc; % fc = specified concrete compressive strength

% efu = design ultimate tensile strain of FRP
efu = 0.85*ef_CFRP; % Exterior exposure (bridges, piers, and unenclosed
parking garages)-CE=0.85

% efe = effective strain level in FRP reinforcement attained at failure
% efe = kF*efu; kF = strain efficiency factor = 0.55 (recommended by ACI
440.2R)
efe = 0.55*efu;

% flFe = vector with the confinement pressure of each column - Eq 12.5 of
ACI 440.2R (2008)

flFe = 2*CFRP_NumberOfPlies.*CFRP_Thickness*CFRP_Elastic_modulus*efe./n_D;
```

```
% fccACI = Vector with the Strength of Confined Concrete (fcc) of each
column % fccACI = 0.95.*(mi_fcm + 3.3*flFe);

fccACI = fc_linha + 0.95*3.3*flFe; % Eq. 12.3 of ACI 440.2R

%_____________________________________________________
%    Ultimate Load of column by ACI
for k=1:columns
    % Pn = nominal resistence given by ACI
    %(Pd=fi*Pn); fi=0.65 for stirrus and fi=0.7 for spiral;
if LateralSteelType(1,k)==1; %1=stirrups, 0=spiral
    Pn(1,k) = 0.80*(0.85*fccACI(1,k)*(pi*n_D(1,k)^2/4-
nL(1,k)*pi*fiL(1,k)^2/4)+ fyL*nL(1,k)*pi*fiL(1,k)^2/4);
% Eq.12.1 of ACI 440.2R

Pd(1,k) = 0.65*Pn(1,k);
    else
    Pn(1,k) = 0.85*(0.85*fccACI(1,k)*(pi*n_D(1,k)^2/4-
nL(1,k)*pi*fiL(1,k)^2/4)+ fyL*nL(1,k)*pi*fiL(1,k)^2/4);
% Eq.12.1 of ACI 440.2R

Pd(1,k) = 0.7*Pn(1,k);
end
end
%_____________________________________________________
% Calculation of mean dead and live loads
% mean dead load = mi_DL

% R=0.5; mi_DL = 0.5*mi_LL;
mi_LL5 = Pd/(1.2*0.5/1.05+1.6);
mi_DL5 = 0.5*mi_LL5;

% R=1.0; mi_DL = mi_LL
mi_LL1 = Pd/(1.2/1.05+1.6);
mi_DL1 = mi_LL1;

%R=2.0; mi_DL = 2*mi_LL
mi_LL2 = Pd/(1.2*2/1.05+1.6);
mi_DL2 = 2*mi_LL2;
```

Loads_Random_Numbers.m;

```
% program that generates the random numbers of Loads

% rgn produce the same random numbers as if you restarted MATLAB
rng('default');

%Dead Loads
SD_DL5=COV_DL*mi_DL5;% VECTOR
SD_DL1=COV_DL*mi_DL1;
SD_DL2=COV_DL*mi_DL2;

%Live Loads
SD_LL5=COV_LL*mi_LL5;% VECTOR
SD_LL1=COV_LL*mi_LL1;
SD_LL2=COV_LL*mi_LL2;

%_____________________________________________________
% Dead Load - Normal Distribution
rng (13);
```

```
for k=1:columns
% 32 vetores [1x100000] => cell {1,32}
DL5{1,k} = normrnd(mi_DL5(1,k),SD_DL5(1,k),1,cycles); % ratio=0.5

DL1{1,k} = normrnd(mi_DL1(1,k),SD_DL1(1,k),1,cycles); % ratio=1.0

DL2{1,k} = normrnd(mi_DL2(1,k),SD_DL2(1,k),1,cycles); % ratio=2.0
end

% _____________________________________________________________
% Live Load - Extreme Value Type I (Gumbel) Distribution
% parameters of Gumbel Distribution; sigma and mi

sigma5 = SD_LL5*sqrt(6)/pi; % Live Load - ratio=0.5
mi5 = mi_LL5-sigma5*0.577215665;

sigma1 = SD_LL1*sqrt(6)/pi; % Live Load - ratio=1.0
mi1 = mi_LL1-sigma1*0.577215665;

sigma2 = SD_LL2*sqrt(6)/pi; % Live Load - ratio=2.0
mi2 = mi_LL2-sigma2*0.577215665;

rng (14); n_LL = rand(1,cycles);% Live Load (LL)

for k=1:columns
    % 32 vetores [1x100000] => cell {1,32}
LL5{1,k} = mi5(1,k) - sigma5(1,k)*(log(-log(n_LL)));

LL1{1,k} = mi1(1,k) - sigma1(1,k)*(log(-log(n_LL)));

LL2{1,k} = mi2(1,k) - sigma2(1,k)*(log(-log(n_LL)));
End
```

Acting_Load.m;

```
% program that calculates the acting Load

% ACTING LOAD - S

     for k=1:columns;
     S5{1,k} = LL5{1,k} + DL5{1,k}; % DL/LL = 0.5;
     S1{1,k} = LL1{1,k} + DL1{1,k}; % DL/LL = 1.0;
     S2{1,k} = LL2{1,k} + DL2{1,k}; % DL/LL = 2.0;

     % Statistics of Acting Load
     % Load ratio = 0.5
     mi_S5(1,k) = nanmean(S5{1,k}); % Mean Acting Load
     SD_S5(1,k) = nanstd(S5{1,k}); % standard deviation
     COV_S5(1,k) = SD_S5(1,k)/mi_S5(1,k); % COV
     min_S5(1,k) = nanmin(S5{1,k}); %minimum
     max_S5(1,k) = nanmax(S5{1,k}); %maximum

     % Statistics of Acting Load
     % Load ratio = 1.0
     mi_S1(1,k) = nanmean(S1{1,k}); % Mean Acting Load
     SD_S1(1,k) = nanstd(S1{1,k}); % standard deviation
     COV_S1(1,k) = SD_S1(1,k)/mi_S1(1,k); % COV
     min_S1(1,k) = nanmin(S1{1,k}); %minimum
     max_S1(1,k) = nanmax(S1{1,k}); %maximum
```

```
    % Statistics of Acting Load
    % Load ratio = 2.0
    mi_S2(1,k) = nanmean(S2{1,k}); % Mean Acting Load
    SD_S2(1,k) = nanstd(S2{1,k}); % standard deviation
    COV_S2(1,k) = SD_S2(1,k)/mi_S2(1,k); % COV
    min_S2(1,k) = nanmin(S2{1,k}); %minimum
    max_S2(1,k) = nanmax(S2{1,k}); %maximum
    end
```

Reliability.m;

```
% program that calculates the probability of failure  and beta
for k=1:columns

% SAFETY MARGIN - M
M5{1,k} = R{1,k} - S5{1,k};% Load ratio = 0.5;
M1{1,k} = R{1,k} - S1{1,k};% Load ratio = 1.0;
M2{1,k} = R{1,k} - S2{1,k};% Load ratio = 2.0;

% mean and standard deviation of Safety Margin to calculated beta
SD_M5(1,k) = nanstd(M5{1,k});
mi_M5(1,k) = nanmean(M5{1,k});

SD_M1(1,k) = nanstd(M1{1,k});
mi_M1(1,k) = nanmean(M1{1,k});

SD_M2(1,k) = nanstd(M2{1,k});
mi_M2(1,k) = nanmean(M2{1,k});

% LOAD RATIO = 0.5
% Probability of Failure
m5=M5{1,k};
Prob_failure5 (1,k) = sum(m5<0)/cycles;
% Reliability Index
beta5s (1,k) = -norminv(Prob_failure5(1,k)); % beta by Monte Carlo
simulation
beta5(1,k) = mi_M5(1,k)/SD_M5(1,k); %beta by Cornell

% LOAD RATIO = 1.0
% Probability of Failure
 m1=M1{1,k};
Prob_failure1 (1,k) = sum (m1<0)/cycles;

% Reliability Index
beta1s (1,k) = -norminv(Prob_failure1(1,k)); % beta by Monte Carlo
simulation
beta1(1,k) = mi_M1(1,k)/SD_M1(1,k); %beta by Cornell

% LOAD RATIO = 2.0
% Probability of Failure
m2=M2{1,k};
Prob_failure2 (1,k) = sum (m2<0)/cycles;

% Reliability Index
beta2s (1,k) = -norminv(Prob_failure2(1,k)); % beta by Monte Carlo
simulation
beta2(1,k) = mi_M2(1,k)/SD_M2(1,k);%beta by Cornell
end
```